Immunogenic Determinants of Coagulation Factor VIII

Dissertation
Karina Winterling

TECHNISCHE
UNIVERSITÄT
DARMSTADT

Immunogenic Determinants of Coagulation Factor VIII

Vom Fachbereich Chemie
der Technischen Universität Darmstadt

zur Erlangung des akademischen Grades
Doktor rerum naturalium (Dr. rer. nat.)
genehmigte Dissertation von

Diplom-Biologin Karina Winterling
aus Hanau

Referent: Prof. Dr. Harald Kolmar
Korreferent: PD Dr. med. Dr. med. habil. Jörg Schüttrumpf

Darmstadt 2018
D17

Zusammenfassung

Hämophilie A ist eine Störung der Blutgerinnung, die weltweit 400 000 Menschen betrifft. Neben verlängerten Blutungszeiten leiden Patienten unter spontanen und inneren Blutungen, die ihr tägliches Leben beeinflussen. Die Behandlung erfolgt mithilfe von therapeutischem FVIII, welcher entweder aus Plasma gewonnen oder rekombinant hergestellt wird. Ob eine Behandlung prophylaktisch oder nur bei Bedarf erfolgt, hängt von der Schwere der Krankheit und den Lebensumständen des Patienten ab. Obwohl die Behandlung den meisten Patienten ein nahezu normales Leben ermöglicht, können Patienten Inhibitoren gegen den therapeutischen FVIII entwickeln, die diesen inaktivieren. In den meisten Fällen kann dies durch eine Immuntoleranztherapie behandelt werden. Diese Therapie ist jedoch lang, strapaziös und sehr teuer. In den vergangenen Jahren wurden verschiedene rekombinante FVIII Produkte mit Modifikationen zur Verlängerung der *in vivo* Halbwertszeit entwickelt. Ein FVIII Produkt mit einer verringerten Immunogenität wurde jedoch noch nicht publiziert. Ein deimmunisierter FVIII könnte die Wahrscheinlichkeit einer Inhibitorentstehung verringern und so eine bessere Therapie für die Patienten ermöglichen.

In dieser Thesis wird eine deimmunisierte FVIII Variante entwickelt. Die Arbeit umfasst die vollständige Entwicklung, begonnen mit den *in silico* Berechnungen, über die Produktion und Reinigung, bis zu den *in vitro* und *in vivo* Analysen. Der Deimmunisierungsansatz beruht auf einer Verringerung der FVIII-Peptidpräsentation auf der Oberfläche von antigenpräsentierenden Immunzellen. Dadurch soll verhindert werden, dass naive T-Zellen aktiviert werden. Ohne FVIII-spezifische T-Helferzellen können wiederum keine naiven B-Zellen aktiviert werden, was zu einem Ausbleiben von hochaffinen Inhibitoren führt. Dadurch wird die Produktion der Antikörper bereits auf der Ebene der T-Zellen unterbunden.

Während der *in silico* Analyse wurden Peptide identifiziert, die mit hoher Affinität an den Haupthistokompatibilitätskomplex II binden, welcher für die Präsentation von Peptiden auf der Zelloberfläche benötigt wird. Anschließend wurden Aminosäureaustausche vorgeschlagen, um diese Bindung zu verringern. Der Einbau der Mutationen in die FVIII Sequenz wurde in drei Runden durchgeführt, begonnen mit dem Einbau von Einzelmutationen, gefolgt von der Kombination mehrerer Mutationen bis zur finalen Kombination aller Mutationen. Nur Mutationen, die zu einem funktionalen FVIII führten, wurden in die nächste Runde transferiert. Final konnten 19 Mutationen in die Sequenz eingebaut werden. Dies führte, basierend auf *in silico* Berechnungen, zu einer Reduzierung des Immunogenitätswerts von 7 auf -11. Eine vollständige Deimmunisierung war jedoch nicht möglich, da besonders aktivitäts-, faltungs- und interaktionsrelevante Regionen des FVIII nicht verändert werden konnten. Funktionale und strukturelle Analysen des mutierten FVIII zeigten Ähnlichkeiten zu einem Kontroll-FVIII und zu kommerziell erwerblichen FVIII Produkten.

Zusätzlich wurde ein *in vitro* DC-T-Zell Test entwickelt, um die reduzierte Immunogenität der deimmunisierten FVIII Variante nachzuweisen, da dies mit den zur Verfügung stehenden *in vivo* Modellen nur begrenzt möglich war. Für diesen Test wurden DCs mit verschiedenen FVIII Produkten vorinkubiert und anschließend zusammen mit $CD4^+$ T-Zellen kultiviert. Final wurde die Proliferation von $CD4^+$ T-Zellen analysiert. Aus der untersuchten $CD4^+$ T-Zell Population wurden vor der Kultivierung die regulatorischen T-Zellen depletiert. Dies wurde durchgeführt, um den Test sowohl mit Zellen von gesunden Spendern als auch von Hämophilie A Patienten durchführen zu können. Mit Zellen von gesunden Spendern bestätigte der Test eine signifikant verringerte Immunogenität des mutierten FVIII im Vergleich zum Kontroll-FVIII. Diese Ergebnisse müssen noch mit Zellen von Hämophilie A Patienten belegt werden. Leider konnte diese verringerte Immunogenität *in vivo* nur begrenzt nachgewiesen werden. Zwei Mausmodelle wurden getestet, jedoch hatten diese entweder ein humanes Immunsystem oder einen FVIII-Knockout. Eine Kombination aus beiden Modellen wäre optimal gewesen, war jedoch nicht verfügbar.

Insgesamt zeigt diese Thesis den ersten deimmunisierten und aktiven FVIII mit 19 Mutationen, der in einem *in vitro* Test mit Zellen von gesunden Spendern eine verringerte Immunogenität aufweist. Wenn diese Ergebnisse *in vivo* bestätigt werden können, kann dieses Molekül die Therapie von Hämophilie A Patienten deutlich verbessern, indem es das Risiko einer Inhibitorentstehung verringert. Diese Verringerung der Inhibitorinzidenz würde zudem auch die Therapiekosten verringern, da Inhibitor-negative Patienten keine teure Immuntoleranztherapie benötigen.

Abstract

Hemophilia A is a bleeding disorder, affecting about 400 000 people worldwide. In addition to prolonged bleeding times, patients suffer from spontaneous and internal bleedings, affecting their everyday life. Patients can be treated by the application of therapeutic FVIII, either derived from plasma or recombinantly produced. Whether the treatment is prophylactic or on-demand depends on the severity of the disease and on the living conditions of the patients. Although treatment allows most of the patients to live a life as normal as possible, patients can develop inhibitory antibodies against the therapeutic FVIII, rendering the molecule inactive. In most cases, this situation can be overcome by an immune-tolerance-induction therapy. However, this therapy is long, strenuous and associated with very high costs. Different recombinant FVIII products evolved within the last years, containing modifications, in order to prolong the *in vivo* half-life of FVIII. However, a FVIII product with a reduced immunogenicity was not yet published. A deimmunized FVIII could reduce the probability of inhibitor development, providing a safer therapy for the patients and lower the costs for therapy.

In this thesis, a deimmunized FVIII molecule is generated. The work comprises the full development, starting with *in silico* calculations of the FVIII sequence, through the production and purification, leading to final analyses *in vitro* and *in vivo*. The deimmunization approach is based on the reduction of FVIII-peptide presentation on antigen-presenting immune cells. This is supposed to lead to a prevention of naïve T cell activation. Without FVIII-specific T helper cells, naïve B cells cannot be activated, leading to the absence of high-affinity inhibitors.

The *in silico* analysis of FVIII was based on the identification of peptides which bind with a high affinity to the major histocompatibility complex class II, which is required for cell surface-presentation of peptides. Amino acid exchanges were proposed, in order to reduce this binding. These mutations were incorporated into the FVIII sequence. This was performed in three rounds, starting with the incorporation of single mutations, followed by the combination of several mutations, to the final combination of all mutations in one molecule. Only mutations still leading to functional FVIII were finally incorporated. Based on this, 19 mutations could be incorporated into the molecule. This led to a reduction of the immunogenicity score of FVIII from 7 to -11, indicating a reduced immunogenicity based on *in silico* calculations. However, a total deimmunization of all epitopes was not possible, as some regions of FVIII, especially those important for activity, folding and binding, could not be altered. Functional and structural analyses of this mutated FVIII variant revealed similarity to a control FVIII as well as to commercially available recombinant FVIII products.

Additionally, an *in vitro* DC-T cell Assay was developed, in order to determine a reduced immunogenicity of the deimmunized FVIII variant, as the available mouse models were limited. The DCs were primed with different FVIII products and the proliferative response of regulatory T cell-depleted $CD4^+$ T cells to these DCs was measured. The regulatory T cells were depleted, in order to be able to perform this assay with cells derived from healthy donors as well as Hemophilia A patients. Using this DC-T cell Assay, cells from healthy donors proved the significantly reduced immunogenicity of the mutated FVIII variant by revealing less proliferation of T helper cells to this variant than to the control FVIII. These results have further to be proven with cells derived from Hemophilia A patients. Unfortunately, the detection of a reduced immunogenicity *in vivo* was limited. Two mouse models were tested but the models had either a FVIII knockout or a human immune system. However, a combination of these two models would have been optimal but was not available.

Finally, this thesis presents the first deimmunized FVIII, containing 19 amino acid mutations, which is still active and proves to be less immunogenic in an *in vitro* assay with cells from healthy donors. Upon confirmation of these results *in vivo*, this molecule can highly improve the therapy of Hemophilia A patients by reducing the risk of inhibitor development in previously treated as well as in previously untreated patients. This reduced inhibitor incidence would also reduce the costs of therapy, as inhibitor-negative patients would not require an expensive immune-tolerance-induction therapy.

Table of contents

1. Introduction

Hemophilia A is a genetic bleeding disorder caused by the absence of sufficient amounts of active Factor VIII (FVIII). The disease is linked to the X-chromosome and occurs in 1 of 5000 newborn males[1]. In females, congenital Hemophilia A is very rare and most women are only carriers of one mutated X-chromosome[2]. However, Hemophilia A can also occur spontaneously, due to an autoimmune response against FVIII. This acquired form of Hemophilia A affects women as well as men and is associated with other autoimmune diseases, increased age and pregnancy[3,4]. Patients with Hemophilia A suffer from longer bleeding durations, spontaneous and internal bleedings, affecting their everyday life[5]. Nowadays many different mutations are known, which lead to congenital Hemophilia A[6]. These include intron inversions, deletions and various point mutations, leading to frameshifts, premature stop-codons or missense mutations in the FVIII gene[1]. These mutations can result in a total absence of endogenous FVIII, in dysfunctional FVIII or in FVIII with reduced activity. Due to the fact that FVIII is one component of the clotting cascade, its absence or non-functionality leads to impaired blood clotting[7]. Although FVIII is not an enzyme, it is a very important co-factor to the activated coagulation Factor IXa (FIXa) and increases its activity dramatically[8].

Based on the amount of functional FVIII left in the patients, compared to a normal plasma level of 1 U/ml, Hemophilia A is subdivided into a mild, a moderate and a severe form. Patients who suffer from severe Hemophilia A have less than 1 % of the normal FVIII plasma level. Compared to that, moderate Hemophilia A covers the range of 1-5 % of FVIII and patients with mild Hemophilia A still have 6-50 % of FVIII[9]. Depending on whether the patients suffer from mild, moderate or severe Hemophilia A, the treatment differs. Patients with mild and moderate forms have a low risk for spontaneous bleedings and are mainly treated on demand, for example after an injury or prior to a surgery. In contrast to that, many patients with severe Hemophilia A, especially children, with a high risk for spontaneous bleedings are treated prophylactically, in order to reduce the risk of internal bleedings and emerging disabilities[10,11]. Nevertheless, Hemophilia A treatment is mainly limited to developed countries, as the therapy is very expensive[12].

The FVIII products used for therapy are either purified from plasma of healthy donors or produced recombinantly in cell culture. Due to that, there are two general FVIII products, plasmatic FVIII (pFVIII) and recombinant FVIII (rFVIII). The main difference is that pFVIII products mostly contain von Willebrand Factor (vWF), the natural partner of FVIII, and other plasma proteins. In contrast to that, rFVIII products contain only FVIII[13]. All recent FVIII products are applied intravenously and suffer from the major drawback that they have a short half-life in the patients with an average of 12 hours, ranging between 6 and 24 hours[14,15]. Due to that, especially patients treated prophylactically, have to receive a FVIII injection every two to three days[16]. Therefore, one focus of ongoing FVIII research is on half-life extension of rFVIII products[17].

Another major drawback in FVIII therapy, next to the short half-life and the intravenous administration, are inhibitory antibodies, occurring in some patients. Antibodies against FVIII are produced when the immune system recognizes FVIII as a foreign protein[18]. Not all antibodies against FVIII affect its function and by that the therapy. Only if the antibodies bind to special regions, for example cleavage sites or binding sites, the FVIII becomes inactive[19]. These antibodies are called inhibitory antibodies or inhibitors. Mainly patients with severe Hemophilia A, up to 30 %, are affected by inhibitory antibodies. Nevertheless, inhibitors also occur in patients with mild or moderate forms but to a lesser extent compared to severe Hemophilia A patients[20,21]. In the case of inhibitor formation, the patients mostly undergo an immune-tolerance-induction (ITI) therapy. During this therapy very high doses of FVIII are applied to the patients, in order to exhaust the immune system and via that to induce tolerance[22]. This therapy is very cost-intensive as well as strenuous for the patients and their caregivers. During ITI, FVIII application occurs daily, in some cases even twice a day. In addition to the strenuous therapy, the number of bleeds are increased when inhibitors are present[23]. The aim to protect the patient from resulting disabilities, due to joint bleeds, impairs the social life of the patient as well as of the whole family[24]. This is why the second focus of FVIII research is on the development of rFVIII molecules, which do not induce an immune response in patients.

1.1. Coagulation Factor VIII

FVIII is an important co-factor in the coagulation cascade. It is mainly produced by liver sinusoidal endothelial cells[25,26] and secreted as a heterodimer[27]. In circulation FVIII is bound to vWF, which protects FVIII from early activation as well as degradation[28]. Normal FVIII plasma concentrations range between 100 and 200 ng/ml[29,30]. Upon activation the heterodimer is cleaved into a heterotrimer, which builds a complex with FIXa and Factor X (FX), the tenase complex[31]. Inactivation of activated FVIII (FVIIIa) occurs either due to dissociation of a FVIII subunit or by activated protein C, a specific inhibitor of the clotting cascade[32].

1.1.1. FVIII gene and protein

The FVIII gene is located on the X chromosome and consists of 26 exons, spanning approximately 186 000 base pairs[33]. The resulting mRNA comprises about 9000 base pairs[34], encoding 2332 amino acids of the FVIII protein plus additional 19 amino acids of the signal sequence[27,35]. The main site of FVIII production is the liver[36] but FVIII production has also been determined in the kidneys, the spleen and endothelial cells[25,37–39]. The protein is synthesized as a single chain and consists of three A domains (A1-A3), one B domain and two C domains (C1 and C2)[35], interrupted by short acidic sequences (a1-a3). The resulting domain structure is A1-a1-A2-a2-B-a3-A3-C1-C2 (Figure 1-1, FVIII pro-protein)[40].

During post-translational modification, FVIII becomes glycosylated, sulfated and proteolytically processed. The whole FVIII protein contains 25 potential N-glycosylation sites. Nineteen of these sites are located in the B domain[35] and six sites are spread along the rest of the protein[29,41]. As not all of these sites become glycosylated, FVIII possesses only 21 N-glycosylations[42]. Additionally, the B domain contains seven O-linked glycosylations[42]. The glycosylation of FVIII is very important for intracellular folding and transport[43,44]. Instead, sulfation is necessary for the extracellular interaction with different proteins, especially thrombin and vWF[45]. It takes place on six tyrosines in the acidic regions a1, a2 and a3 (Figure 1-1, Mature FVIII)[46,47]. Intracellular cleavage, by the serine protease furin, divides FVIII into a heavy chain (A1-a1-A2-a2-B) and a light chain (a3-A3-C1-C2). During this cleavage parts of the B domain can be lost[27,48]. Therefore, the light chain has a molecular weight of 80 kDa, whereas the heavy chain can be slightly heterogeneous, with a molecular weight around 210 kDa. The binding between heavy and light chain is not covalent but mediated by the divalent metal ion Cu^{2+} between the A1 and A3 domain (Figure 1-1, Secreted FVIII)[49–52].

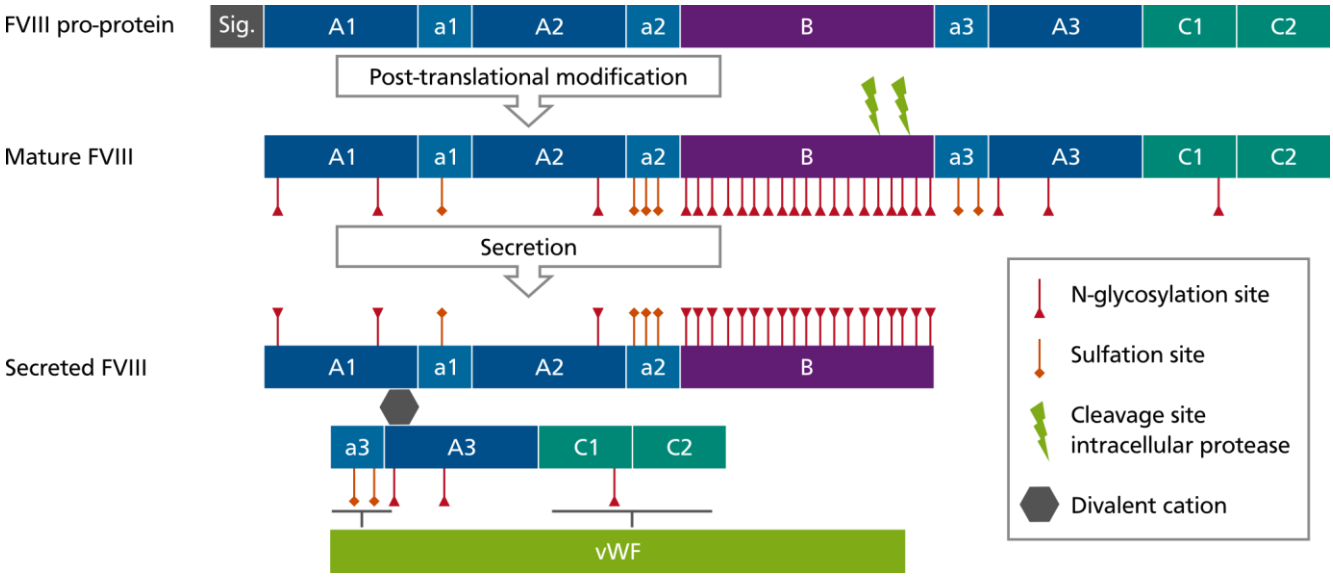

Figure 1-1: Structure of FVIII. The FVIII pro-protein still contains the FVIII signal sequence and is not yet modified. The cleavage of the signal sequence and the post-translational modifications lead to the mature FVIII. Before secretion, FVIII is cleaved by furin. Secreted FVIII is bound to vWF and stabilized by a divalent cation.

Upon secretion into plasma, FVIII complexes with vWF via the a3, C1 and C2 domain (Figure 1-1, Secreted FVIII)[47,53,54]. About 95 % of circulating FVIII is bound to vWF. The interaction stabilizes the heterodimer, protects it from degradation[28,55] and prevents cellular uptake[56]. Due to prevention of uptake and degradation, vWF is important for the prolongation of the FVIII half-life of up to 12 hours[57,58]. Additionally, the binding of vWF to FVIII shields binding sites of FVIII to negatively-charged phospholipids[59,60] and FIXa[61].

1.1.2. FVIII and the coagulation cascade

Coagulation is mainly started upon vascular injury, initiating the extrinsic pathway (Figure 1-2). The damaged cells expose tissue factor (TF) which binds to activated Factor VII (FVIIa), present in blood. This extrinsic tenase complex activates FX and FIX. In the following, the activated FX (FXa) activates prothrombin (FII) to thrombin (FIIa). However, the amounts of generated thrombin are too low to activate fibrinogen. Due to this, thrombin activates Factor V (FV), FVIII and Factor XI (FXI) of the intrinsic pathway, resulting in a positive feedback loop. Activated FXI (FXIa) increases the generation of FIXa. Further on, FIXa, FVIIIa and FX build the intrinsic tenase complex, which generates high amounts of FXa. Afterwards, FXa builds the prothrombinase complex with activated FV (FVa), generating high amounts of thrombin. Thrombin cleaves fibrinogen (FI) to fibrin (FIa) and Factor XIII (FXIII) to activated FXIII (FXIIIa). Fibrin is cross-linked by FXIIIa, in order to build the clot[62,63]. Alternatively, coagulation can be initiated via the intrinsic pathway (Figure 1-2). This cascade is started by contact activation of Factor XII (FXII) to activated FXII (FXIIa) on a charged surface. FXIIa further activates FXI leading to the cascade described above. However, *in vivo* coagulation is mainly triggered by TF exposure[64].

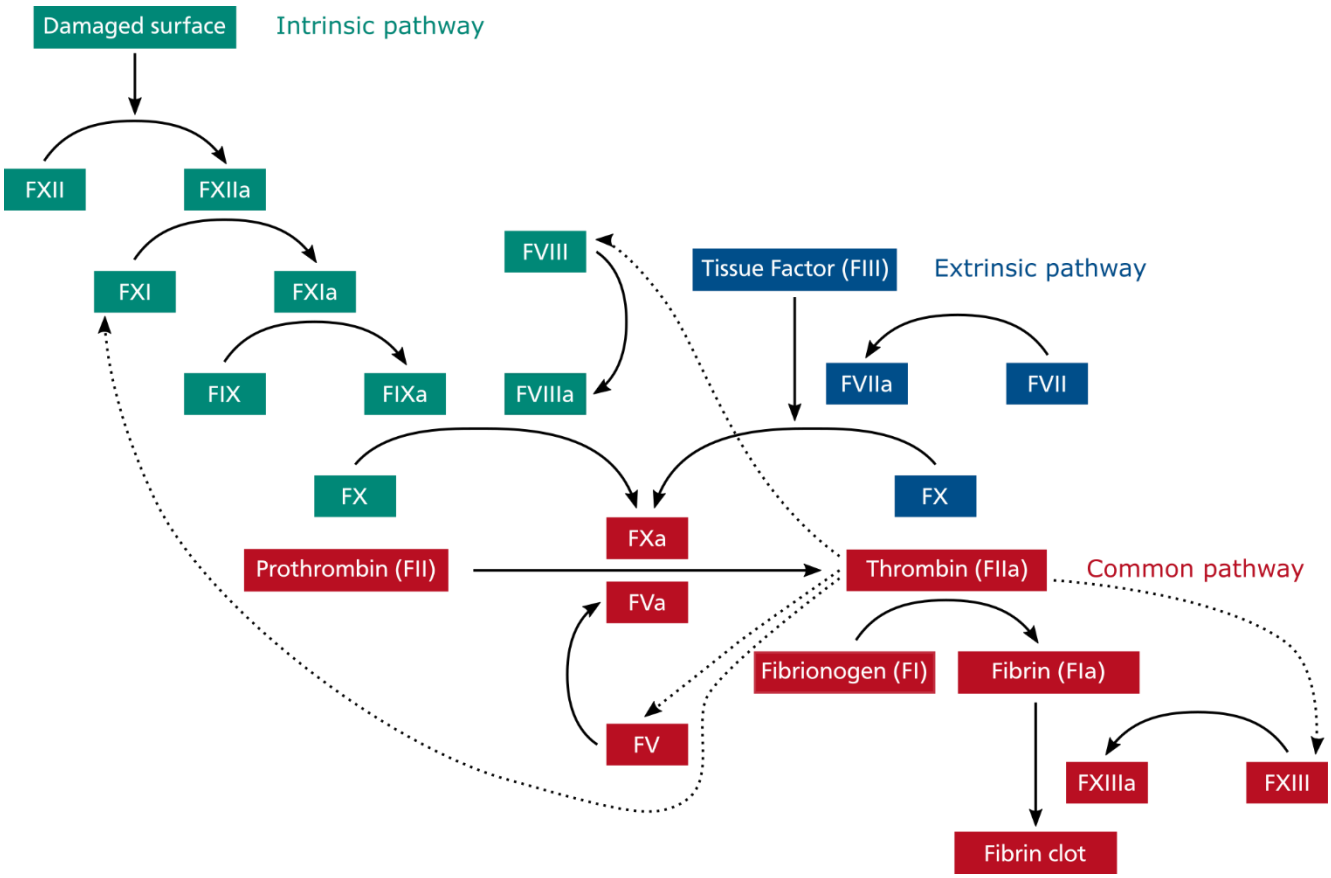

Figure 1-2: Coagulation cascade. The coagulation is initiated either by a damaged surface (intrinsic) or by exposed tissue factor (extrinsic). Both pathways lead to the activation of FX. Further on FXa generates thrombin. In the beginning, thrombin amplifies its own production by the activation of FV, FVIII and FXI. When enough thrombin is generated, it cleaves fibrinogen and FXIII. The generated fibrin is cross-linked by FXIIIa, leading to the fibrin clot.

The serine protease thrombin activates FVIII by cleavage at two sites located in the heavy chain, Arginine (R) 391 and R759, and at one site located in the light chain, R1708 (Figure 1-3, Secreted FVIII)[65,66]. The cleavage leads to the heterotrimeric form of FVIIIa, which consists of A1-a1, A2-a2 and A3-C1-C2[67]. The B domain and the a3 acidic region are lost. In order to stabilize the new heterotrimeric form of FVIII and to alter the protein conformation for maximal activity, hydrogen bonds between A1A2 and A2A3[68–70] are formed and Ca^{2+} or Mn^{2+} is incorporated (Figure 1-3, Activated FVIII)[49,52,71,72].

The structural changes in the tertiary structure mainly alter the interacting partners of FVIIIa, due to loss and exposure of various binding sites[73]. Especially, the loss of a3, an important binding site for vWF, results in the dissociation of vWF from FVIIIa[74]. This allows FVIIIa to bind to phospholipid membranes[75,76], FIXa[73] and FX[77], which leads to the formation of the tenase complex. Although FVIIIa is only a co-factor to FIXa, it increases its activity up to 1.000.000-fold[8,32] by bringing FIXa and FX in close proximity.

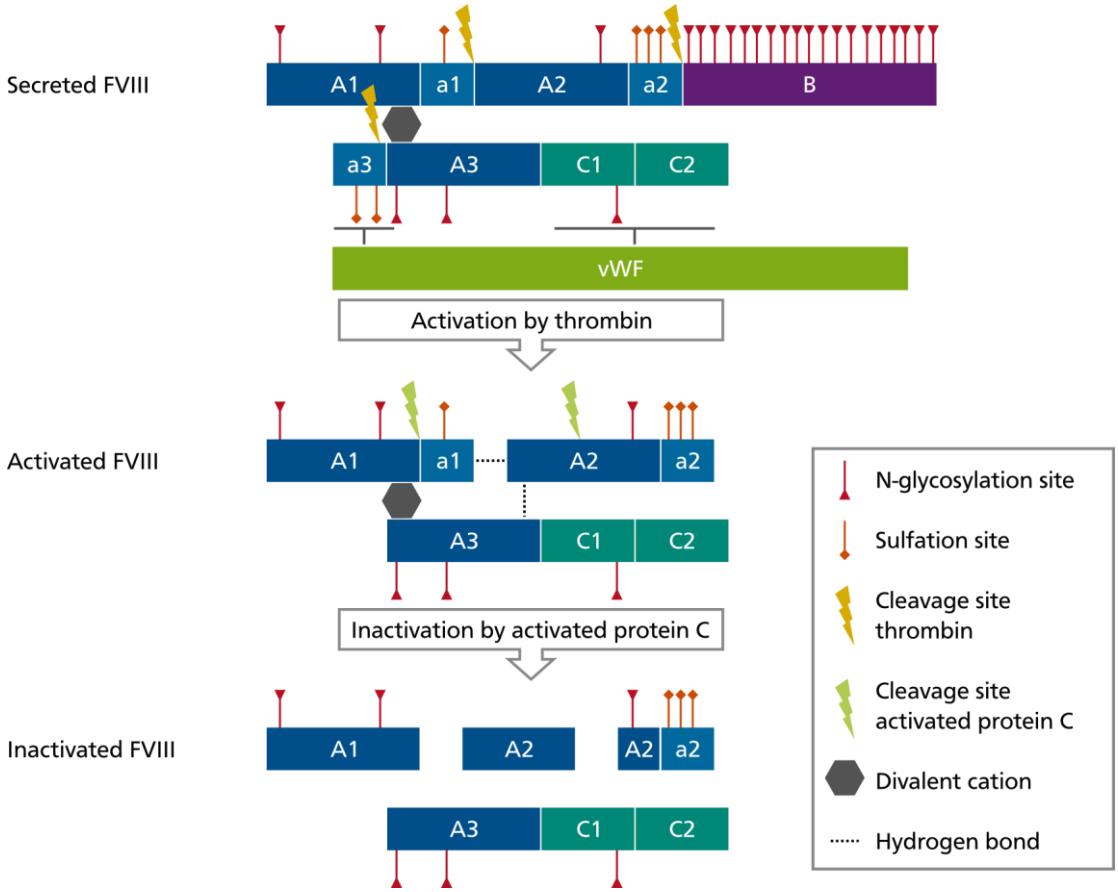

Figure 1-3: Structure of FVIII. The secreted FVIII is activated by thrombin cleavage at three sites, resulting in the heterotrimeric activated form and loss of vWF. FVIIIa is inactivated by the dissociation of the A2 domain and by activated protein C, which cleaves FVIIIa at two sites.

Inactivation of FVIIIa occurs mainly via dissociation of the A2 domain from the tenase complex, which represents the first step of FVIIIa degradation[67]. Apart from that, cleavage by activated protein C can inactivate FVIIIa (Figure 1-3, Inactivated FVIII)[40]. Further degradation occurs via receptor-mediated clearance, mainly depending on receptors of the low-density lipoprotein (LDL) family, especially the LDL receptor-related protein (LRP1)[57]. Furthermore, efficient binding of FVIII to LRP1 is facilitated by heparan-sulfate proteoglycans (HSPG)[78]. In addition to LRP1, the asialoglycoprotein receptor (ASGPR) was identified to take up FVIII via binding to the N-glycosylations of the B domain[79] whereas the macrophage mannose receptor (MMR) clears FVIII via binding the C1 and C2 domain[80].

1.1.3. FVIII products

Therapeutic FVIII products are available since the 1960s[81]. These products contain FVIII purified from plasma of healthy donors. In addition to that, the first rFVIII was launched in 1992[82]. The two main differences between the two kinds of FVIII products are their origin and the amount of additionally contained proteins. All rFVIII products are produced by cell lines, which are transfected with a plasmid coding for the FVIII sequence, and contain only the purified FVIII. In contrast to that, pFVIII products are purified from human plasma and contain additional plasma proteins in varying concentrations. Especially vWF is an important protein in plasma-derived products, as it stabilizes FVIII and is believed to lower the immunogenicity by reducing the uptake of the complex by antigen-presenting cells (APCs)[56,83,84]. However, one major advantage of rFVIII products is the independence from plasma, which can become a limiting resource[13,85].

The rFVIII products evolved since the 1990s (Table 1-1). First-generation products are produced in mammalian cell lines, mostly baby hamster kidney (BHK) cells or Chinese hamster ovary (CHO) cells. These products still contain proteins of human and animal origin, used to enrich the cell culture medium, and human albumin, used to stabilize the final product[13]. During the development of second-generation products albumin was replaced by chemical compounds for stabilization. This decreases the risk of transmission of infectious particles[86,87]. In addition to that, second-generation products contain an additional virus inactivation step and are mostly B domain-deleted (BDD) variants[88]. As the B domain is not essential for the activity of FVIII[89–92] and is lost during activation, the deletion in rFVIII products is not reducing the functionality. Additionally, the B domain deletion reduces the size of the plasmid as well as the size of the whole protein, facilitating the production[89,93]. Third-generation products no longer contain any human or animal derived supplements but are still produced by non-human mammalian cell lines[86,87]. The last step, the development of fourth-generation products, keeps up the standards from the third-generation products regarding supplementation and purification but changes to human production cell lines like human embryonic kidney (HEK) cells[94]. This ensures proper post-translational modification[42,95] similar to endogenous FVIII[86].

Table 1-1: Generations of rFVIII products and their characteristics.

Generation	FVIII length	Production cell line	Origin of medium supplements	Virus inactivation
1st	Full-length	Mammalian, non-human	Animal	No
2nd	Full-length and BDD	Mammalian, non-human	Human	Yes
3rd	Full-length and BDD	Mammalian, non-human	Chemical	Yes
4th	BDD	Human	Chemical	Yes

Until today, it is not finally elucidated whether rFVIII products are more immunogenic than pFVIII products. Studies with different outcomes were published in the recent years. The two observational studies CANAL[96] and RODIN[97] as well as the surveillance project EUHASS[98] revealed no differences in inhibitor development in previously untreated patients (PUPs) treated with either pFVIII or rFVIII[99]. In contrast to that, the only randomized study SIPPET[100] found a 87 % higher incidence for inhibitor development with rFVIII than with pFVIII. Nevertheless, all studies suffer from different drawbacks as group size, ethnicity of the enrolled patients, and considering all generations of rFVIII products as equivalent[85,101]. In addition to that, the ongoing development of rFVIII products makes it difficult to compare all rFVIII products to pFVIII in one single study. Furthermore, patients treated with fourth-generation products, which are potentially less immunogenic, due to production in human cell lines, are not yet included in these studies[85].

Apart from modifications affecting the production of FVIII, the protein itself is modified, mainly to overcome the short half-life of FVIII *in vivo*. Different approaches are followed to extend the half-life. These contain addition of polyethylene glycol (PEG)[102], fusion of antibody-derived Fc-parts[103,104] and single-chain rFVIII constructs[105,106]. However, for these products the half-life of vWF has to be considered as well, due to the fact that rFVIII builds a complex with vWF *in vivo*[107]. The FVIII Fc-fusion probably has the additional effect of being less immunogenic, as the Fc-part contains epitopes, called "Tregitopes", which stimulate regulatory T cells[108,109]. However, the deimmunization of FVIII itself is an important part of ongoing research. Until now, no FVIII product with reduced immunogenicity has been launched.

1.2. Immunogenicity of FVIII

Patients suffering from Hemophilia A are treated either on-demand or in a prophylactic manner with a plasmatic or recombinant FVIII product. The kind of therapy and the dosage depends on different factors like severity, body weight and physical activity of the patients. Most patients apply their intravenous injections at home, offering them a way of life as normal as possible[5].

The major complication during Hemophilia A therapy is the development of inhibitory antibodies against the applied FVIII. These antibodies occur in up to 30 % of the patients suffering from severe Hemophilia A[20] and to a lower extent, up to 13 %, in patients suffering from moderate and mild Hemophilia A[21]. These antibodies reduce the half-life or inhibit the activity of FVIII by blocking interaction sites[52]. Various genetic and environmental risk factors for inhibitor development are known[110,111]. However, not all of these risk factors, like the genetic background, can be influenced.

The main treatment for patients with inhibitors is the ITI therapy. During this therapy the inhibitory antibodies are supposed to be depleted by the application of high amounts of FVIII[22]. This therapy is successful in up to 80 % of patients suffering from Hemophilia A with inhibitors[112].

The mechanism of the immune response against FVIII is based on a T cell dependent activation of B cells. These B cells produce antibodies with a high affinity towards FVIII[113]. However, it is still not known where the immune response is initiated and which danger signals activate the immune system[114]. Discussed interaction sites between FVIII and APCs are either the spleen or the bleeding site itself. Many APCs are present at both sites and the spleen is additionally known to filter blood-borne antigens. The APCs might further on present FVIII peptides to T cells and via that initiate the immune response[115].

1.2.1. Antibodies against FVIII and risk factors for antibody development

Anti-FVIII antibodies are divided into inhibitory and non-inhibitory antibodies. Inhibitory antibodies decrease the activity or the half-life of FVIII, as they bind to essential cleavage and interaction sites. Many antibody-binding regions on FVIII are known, especially in the A2 and C2 domain[19,116,117], but definite epitopes are still part of ongoing research[118,119]. The three-dimensional structure of the B cell epitopes renders the research complicated. In addition to that, not all patients develop antibodies against the same regions of FVIII or the same antibody diversity[120,121]. In contrast to inhibitory antibodies, non-inhibitory antibodies do not influence the activity of FVIII[122]. Interestingly, non-inhibitory antibodies against FVIII can also be detected in healthy people[123,124].

Until today, it is not yet completely understood why patients develop antibodies against therapeutic FVIII and which are the risk factors. Various studies try to link the development of inhibitors to genetic risk factors like the mutation, family history and ethnicity as well as environmental risk factors like the treatment, FVIII product and immune status of the patient[18,110,111,125]. However, it is always a mixture of risk factors, which influence the development of inhibitors[126].

An important reason for antibody production in Hemophilia A patients is the absence of central tolerance to FVIII[127]. Central tolerance is established during the ontogeny of the immune system to prevent the existence of circulating T and B cells, which recognize and react to endogenous proteins. These self-reactive T and B cells are deleted or rendered anergic in the thymus and in the bone

marrow[128]. Patients with severe Hemophilia A produce only fragments or no endogenous FVIII and even patients with moderate and mild Hemophilia A might have endogenous FVIII with large differences in the amino acid sequence compared to normal FVIII. This absence of FVIII or the existence of an altered FVIII leads to the problem that T and B cells are not deleted during ontogeny and central tolerance can not be established[129,130]. In these cases, therapeutically applied FVIII can be recognized as a foreign molecule by B and T cells. This initiates an immune response, which leads to the production of antibodies. Due to this, mutations leading to the total absence of FVIII or to large alterations in the amino acid sequence result in a much higher inhibitor risk compared to other mutations[131].

Nevertheless, not all patients without endogenous FVIII develop antibodies and antibody formation also occurs in patients with endogenous FVIII. Due to that, there is the possibility that not only the discrimination between self and non-self proteins influences antibody production but that also the general immune status and the presence of danger signals might influence the immune system[132]. These danger signals can be infections, vaccinations or probably even a bleeding event itself[114].

Regarding other risk factors, some could be proven to have an influence on inhibitor development, whereas others are still under investigation. An important risk factor is the treatment. Especially the first 20 exposure days to FVIII seem to be crucial for inhibitor development[11,131]. Afterwards, the risk lowers until it is decreased to below 1 % at exposure day 50[133]. Due to this, PUPs have a higher risk to develop inhibitors compared to previously treated patients (PTPs). However, also in the cohort of PTPs with more than 50 exposure days, inhibitors can be detected[134,135]. The genetic background, apart from the FVIII gene, is also important, as some patients also have mutations in some immune-modulating genes, like Interleukin (IL)-10, tumor necrosis factor α (TNF-α) and cytotoxic T-lymphocyte-associated protein 4 (CTLA-4)[136–138]. Additionally, the blood group might be a risk factor, as it was revealed that patients with blood group 0 have a twofold lower risk to develop antibodies compared to non-0 blood group patients. This might be due to different glycosylation patterns of vWF in patients with different blood groups. The glycosylation in the 0 blood group leads to vWF, which is cleared faster from circulation. Consequently, the bound FVIII is also cleared faster and the time of potential contact with immune cells is reduced[139]. Furthermore, ethnicity is discussed as a genetic risk factor, as it was shown that antibody development is more frequent in Africans and Hispanics than in Caucasians[140,141]. The reason for that is not yet fully understood[142].

1.2.2. Treatment of patients with inhibitory antibodies

The ITI therapy for Hemophilia A patients with inhibitors is initiated after the detection of the inhibitor. The first ITI protocol was applied in Bonn in the 1970s[143]. Different protocols are available today, differing in length and dosage. All protocols share the application of a very high FVIII dose, in order to induce tolerance, due to exhaustion of the immune system. This increases the costs for therapy 1.5-3 fold, compared to non-inhibitor treatment[144–146], and lowers the standard of life[24]. The most common ITI protocols range between an application of 50 IU of FVIII per kg body weight three times per week and daily applications of up to 200 IU/kg[147]. Despite the huge differences in the applied FVIII amounts, the rates of ITI success are similar for the distinct protocols[148]. Main differences were observed regarding the bleeding incidences and the time needed to achieve a tolerance induction. Fewer bleedings and a shorter time to achieve ITI were detected when higher amounts of FVIII were applied[147,149]. An ITI therapy is considered to be successful when the inhibitors are no longer detectable (< 0.6 BU/ml), the FVIII recovery is over 66 % and the half-life of FVIII is longer than 6 hours[147].

Different predictors for a successful ITI were investigated, revealing that a low inhibitor titer (<10 BU/ml) before starting an ITI therapy and a historical peak inhibitor below 200 BU/ml were the best indicators for success[150–152]. Due to this, it is recommended for patients with titers above 10 BU/ml to wait until the titer drops[148]. The influence of the age at the beginning of the therapy and the time between the first detection of an inhibitor and start of the ITI therapy are controversial and seen as very unlikely predictors of ITI success[150]. Further evidence is needed regarding the FVIII mutations and the type of FVIII product. Recent studies point to a greater ITI success for patients with a non-null FVIII mutation whereas no significant differences regarding FVIII products were observed until now[150,153].

The molecular mechanisms of the tolerance induction are not yet fully understood. Inactivation or depletion of memory B and T cells, development of anti-idiotypic antibodies and development of regulatory T cells might be possible mechanisms[112,154–156]. The ITI therapy is successful in 60-80 % of the patients with inhibitory antibodies[99]. In the case of an ITI failure a rescue ITI therapy is started. During this therapy, the amount of applied FVIII is further increased up to 200 IU/kg/day and immunosuppressive drugs are additionally applied. Apart from that, a rescue ITI therapy is performed with a pFVIII product containing vWF, in the case that the first ITI therapy was performed with a rFVIII product[157]. When the rescue ITI is not successful, the further therapy depends on bypassing agents like coagulation FVIIa and activated prothrombin complex concentrates (aPCC)[149].

1.2.3. Subclasses of inhibitory antibodies and the involvement of T cells

It was revealed that the inhibitory antibodies produced by the patients' B cells have a high affinity to FVIII and belong to the subclasses of Immunoglobulin G (IgG) 1 and IgG4[158–160]. These subclasses develop after affinity-maturation and class-switching, which only occurs when B cells mature in a T cell-dependent manner, indicating that cluster of differentiation (CD) 4^+ helper T cells are involved in the development of inhibitory antibodies against FVIII[113,114].

Interacting B and T cells have to recognize the same protein but not the same epitope. Whereas B cells recognize their epitope extracellular by surface-bound antibodies, T cells recognize their epitope presented on the surface of APCs[161]. As long as the $CD4^+$ T cells are still naïve and have never been in contact with their epitope, the first important signal for maturation is the recognition of their epitope with their T cell receptor (TCR). Additionally, they are depended on co-stimulation and cytokines provided by the APCs[162]. Naïve $CD4^+$ T cells mainly mature upon contact with Dendritic cells (DCs), a subtype of APCs. These cells take up extracellular proteins[80], process them intracellular and bind them to the major histocompatibility complex (MHC) class II[132]. This peptide-MHC class II complex is then presented on the surface of DCs[130]. A naïve T cell binds with its TCR to this complex, followed by binding to the co-stimulatory DC receptors CD40 and CD80/CD86[163]. Additionally, the T cell takes up the cytokines secreted by the DC (Figure 1-4)[162]. Depending on the cytokines secreted, the naïve T cell differentiates into one of the many T helper cell (Th) subclasses.

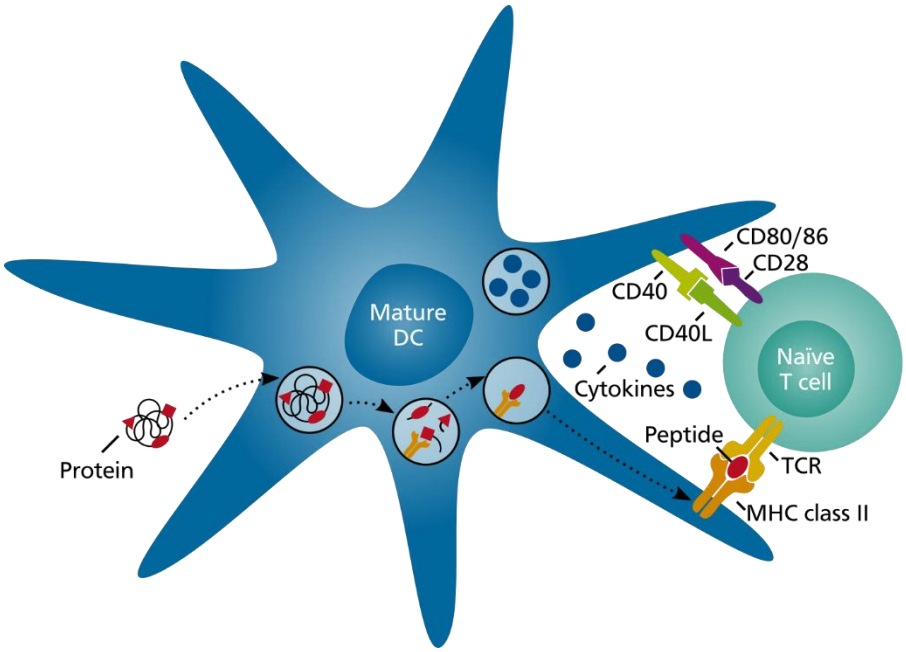

Figure 1-4: Interaction between DC and T cell. The DC takes up extracellular proteins and processes them intracellular. Resulting peptides are bound to the MHC class II and presented on the surface. A naïve T cell can be activated by the DC when the TCR recognizes the peptide-MHC class II complex. Co-stimulation occurs via interaction between CD40-CD40L and CD80/CD86-CD28. Additionally, the T cell takes up the cytokines secreted by the DC.

Most T cells develop into the Th1 or Th2 subclass of T helper cells. Both types are capable of stimulating B cells[130,160]. Th1 cells favor the synthesis of IgG1 and IgG2 and Th2 cells favor the synthesis of IgG4[160]. Nevertheless, B cell stimulation by Th1 or Th2 cells only occurs when the T cells recognize the epitope specific for their TCR on the B cells. Antigen uptake by B cells occurs via binding of the protein by surface-bound immunoglobulins followed by receptor-mediated endocytosis. Afterwards, the protein is processed into peptides, which are bound to the MHC class II and presented on the cell surface. In addition to the interaction via the TCR, T and B cells also interact via CD40L-CD40 binding. The binding of CD40L to CD40 on the B cells and the uptake of cytokines, secreted by the T cells, are the main maturation signals for the B cells. After the interaction with the T cells, B cells differentiate into antibody-secreting plasma B cells and memory B cells (Figure 1-5)[162].

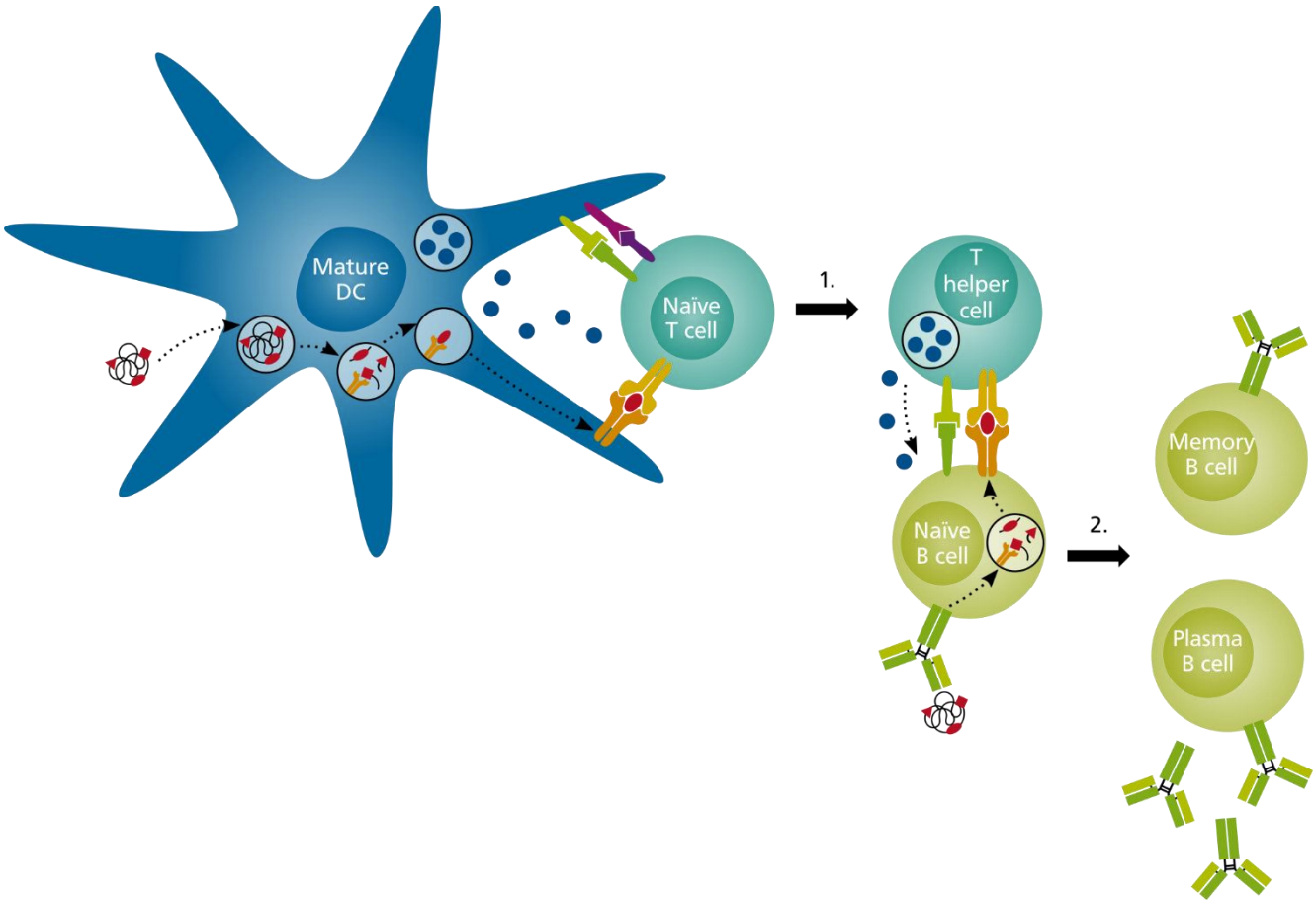

Figure 1-5: T cell-dependent activation of B cells. In the first step, naïve T cells have to differentiate into T helper cells upon detection of their antigen presented by DCs. In the second step, T helper cells detect their antigen presented by naïve B cells. Upon receptor interaction and cytokine secretion by T helper cells, the naïve B cells start to differentiate. The activated B cells differentiate into memory B cells and antibody-secreting plasma B cells.

The MHC class II is the most important complex during the activation of T cells, as it binds and presents the antigen. The extracellular compartment of the complex consists of two alpha helices, building a peptide binding cleft[164]. As the cleft is open at both ends, the length of the bound peptides varies between 10 and 25 amino acids, whereas peptides between 13 and 16 amino acids are most frequent[165–167]. The loading of the peptides occurs intracellularly in the endosomes, where all ingested proteins are digested. In these endosomes reducing conditions and a low pH contribute to the enzymatic degradation of the protein by cathepsins[168]. Not every peptide resulting from enzymatic degradation of the protein can be bound to the MHC class II. Only peptides, which bind with a certain stability to the cleft are presented on the surface[169,170]. On the one hand binding occurs via hydrogen bonds between side-chains of the MHC class II molecule and the peptide backbone, on the other hand amino acid side chains of the peptide bind to defined pockets in the MHC class II binding cleft[164].

The research in the field of MHCs revealed the positions in the MHC class II binding groove (P1, P4, P6 and P9) and the amino acids in the peptides, which are important for the binding of the peptide to the MHC class II. This provides the possibility to predict which peptides of a protein can be bound and presented on the surface of APCs. Nevertheless, this prediction is very extensive, as the genetic diversity of the MHC class II is very high. More than 800 different human leukocyte antigen (HLA)-DR alleles, coding for the MHC class II, are known until today, leading to a vast diversity of MHC class II variants[109]. Fortunately, many of these alleles only differ in minor parts. Over 90 % of the binding clefts can be predicted using eight different HLA-DR supertypes, clustering HLA-DR alleles with similar binding patterns[166,171–173].

In addition to the HLA alleles of a person, also the expression of intracellular enzymes degrading the protein as well as the naïve T cell pool itself influence the development of antibodies. Due to this, two patients with the same HLA alleles do not have to present the same peptides and do not have to possess the same reactive T cells needed to activate the naïve B cells[174].

Until today, it is not known where the applied FVIII is internalized by APCs. In mice accumulation in the liver and the spleen could be proven, although the FVIII levels were only stable in the spleen and the levels in the liver decreased within 30 minutes[175]. In addition, the uptake of FVIII by APCs in the circulation[176] or at the bleeding site[115] is possible. From these sites it might be transported to secondary lymphoid organs, to be presented to $CD4^+$ T cells[177].

1.3. Deimmunization of therapeutic proteins

Antibodies against therapeutic proteins, neutralizing their activity, are widely known and not only limited to FVIII[178]. Due to this, many immunoinformatic tools evolved, in order to predict T and B cell epitopes. Whereas many T cell epitope prediction tools are available, only a few B cell epitope tools were developed. This is due to the fact that B cell epitopes are mostly three-dimensional, compared to the linear T cell epitopes[179], rendering the prediction highly complicated[172]. Apart from that, the development of anti-drug antibodies (ADA) is mostly T cell-dependent, which led to the focus on T cell epitope prediction tools. Whereas some tools only indicate potential immunogenic peptides of a protein by calculating peptide-binding affinities to the MHC, others are also able to indicate amino acid substitutions, in order to deimmunize a protein. Due to this, *in silico* analyses of recombinant proteins became an important method during the development of new therapeutics.

Although the *in silico* tools are constantly improved, the predictions have to be determined *in vitro* and *in vivo*[180]. Regarding *in vitro* analyses, mainly HLA-binding assays as well as T cell stimulation assays are performed. The *in vivo* models focus on HLA-transgenic mice and knockout mice for the protein of interest. However, the analytical methods *in vitro* as well as *in vivo* are constantly improved and refined.

The reduction of the immunogenicity of the FVIII molecule is a major need in FVIII therapy, next to the prolongation of half-life. Due to this, a deimmunized FVIII molecule would be promising, in order to decrease the probability of an antibody response[128,179], and would be an improvement for PUPs as well as PTPs. For PUPs and PTPs without inhibitors, this FVIII would reduce their risk of an initial immune response. For PTPs, who already developed inhibitors, the deimmunized FVIII might be an alternative therapeutic product. Therefore, a FVIII product with a reduced immunogenicity could improve the way of life of the patients and their caregivers as well as reduce the costs for the health system. One approach to deimmunize FVIII is to utilize the available T cell epitope prediction tools, in order to mutate the FVIII amino acid sequence, leading to a reduced binding of FVIII peptides to the MHC class II. Based on this modification, the production of high-affinity antibodies could be prevented at the stage of T cells (Figure 1-6).

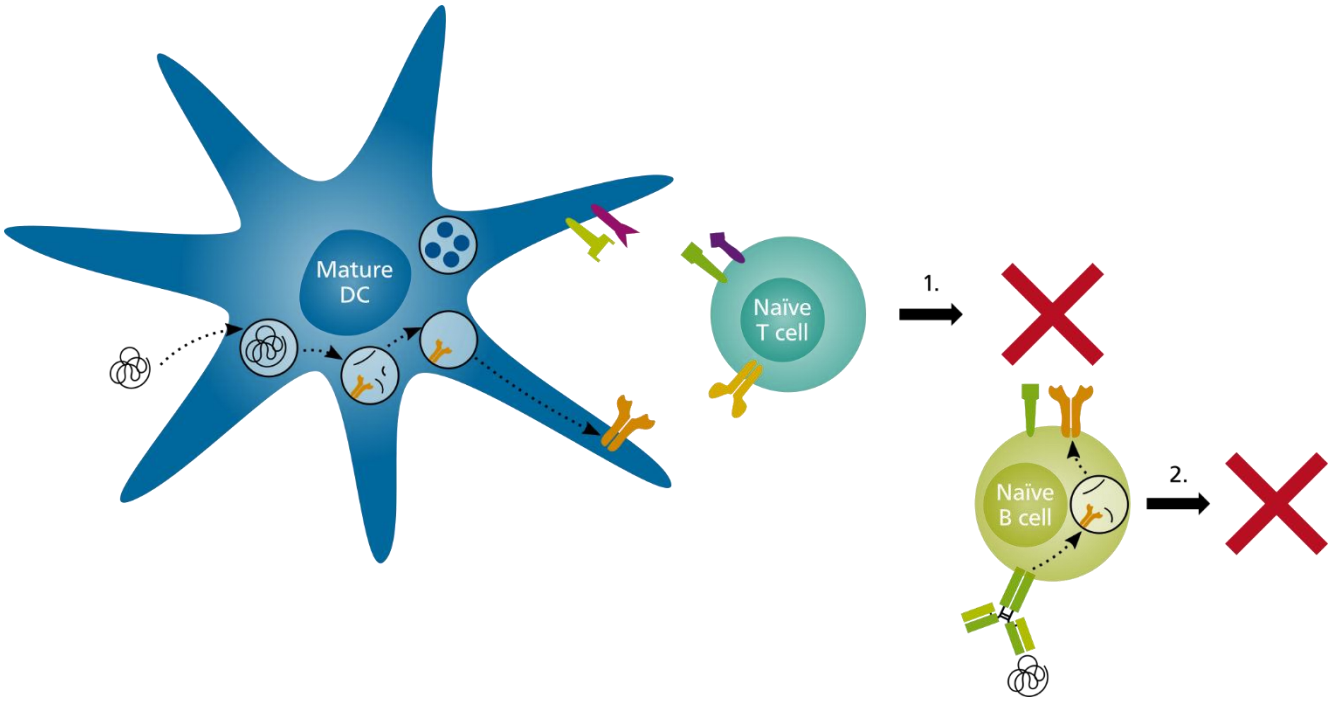

Figure 1-6: Deimmunization prevents B cell activation. Due to deimmunization of the protein, no immunogenic peptides shall be presented on the surface of DCs. This prevents the activation of naïve T cells. As a result of this missing first step, naïve B cells are not activated and cannot differentiate into antibody-secreting plasma and memory B cells.

1.3.1. *In silico* T cell epitope-modelling tools

Using *in silico* modelling tools, a protein can be analyzed regarding the peptides most likely to be presented on the surface of APCs. The first modelling tool was developed in 1995, calculating T cell epitopes for one MHC class II allele[181]. Nowadays, many different tools are available for the calculation of peptide-binding to MHC class I and class II[109]. Many tools calculate the contribution of each amino acid of a peptide to the overall binding affinity. The calculation is matrix-based and utilizes binding data of HLA alleles collected over the years. Further improvement of the prediction tools includes the prediction of binding to HLA alleles without available binding data[182]. Most of the public tools are available from the Immune Epitope Database and Analysis Resource (IEDB)[183]. In addition, commercial T cell epitope-mapping tools are provided. With these tools, the results are further analyzed, epitopes are clustered and even amino acid exchanges for the reduction of peptide-binding are predicted.

In order to deimmunize FVIII, the EpiMatrix tools, commercially provided by EpiVax, were chosen in this thesis. The analysis comprises several steps and tools, starting with the identification of binding peptides, clustering the results, comparing the clusters to other endogenous proteins and finally predicting amino acid exchanges. The provided analysis is optimal, in order to determine which regions of FVIII are most immunogenic regarding MHC class II presentation and provide insight into mutation possibilities and their benefit. The EpiMatrix system was widely proven to deimmunize various proteins[184,185] and even the C2 domain of FVIII has already been analyzed and deimmunized[173].

1.3.2. *In vitro* tools for the determination of a deimmunization

In order to determine whether predicted peptides really bind to the MHC and elicit an immune response, the *in silico* results have to be confirmed *in vitro* and *in vivo*. The analytical *in vitro* methods provide the possibility to compare immunogenic and non-immunogenic peptides or modified and non-modified peptides. Depending on the method, either peptides or whole proteins can be used.

HLA binding assays are performed, in order to determine whether peptides bind to the MHC class II. One possibility is to use MHC class II loaded with fluorescence-labeled peptides and add the peptides of interest. The amount of the released labeled peptides correlate with the bound peptides of interest[109]. Alternatively, the peptides of interest can be added to empty MHC class II. After incubation the amount of bound peptide can be determined via a fluorescence-labeled antibody or the peptide-MHC class II complexes can be purified[186]. When required, the peptides can be removed and analyzed, in order to reveal which peptides of a mixture of peptides were bound by the MHC class II. The strength of binding of a peptide-MHC class II complex can be determined by surface plasmon resonance[109]. However, peptides always have the disadvantage of being artificially designed. In order to circumvent this, the protein of interest can be added to APCs. The MHC class II is isolated afterwards and the bound peptides are analyzed. This ensures a natural processing of the protein. Unfortunately, this method requires a huge amount of protein, which might not be available in every approach.

Another method to test the detected peptides is to perform an *in vitro* T cell assay. Diverse setups and readouts for these assays are possible[109]. Peptides or proteins can be added to either PBMCs or purified T cells and APCs. The cells can be derived from healthy donors or, in the case of testing the deimmunization of a therapeutic protein already used in the clinic, derived from patients[180]. The response of T cells can be detected by flow cytometry, using specific markers or proliferation dyes, or by Enzyme-linked Immunosorbent Assays (ELISA) or Enzyme-linked Immunospot Assays (ELISpot), detecting the secreted cytokines[172]. Due to this, T cell assays are a good tool to evaluate the *in silico* predictions and to test deimmunized proteins in comparison to their wild-type protein.

In order to compare the immunogenicity of a deimmunized and a non-deimmunized FVIII in this thesis, an *in vitro* T cell assay is most promising. Due to the large size of FVIII, the production of overlapping peptides for an HLA assay would be too extensive. However, a huge limitation in the development of an *in vitro* assay for FVIII is the availability of blood samples from Hemophilia A patients. The best approach to prove a deimmunization would be an assay, which reveals a reduced amount of activated T cells derived from PUPs in response to the deimmunized FVIII. Unfortunately, theses patients are babies or toddlers and the amount of available blood is far too low. In addition to that, patient samples are rare, even in the cohort of PTPs, leading to an assay development based on cells from healthy donors. However, the amount of naïve T cells against FVIII in healthy donors is low. Though, restimulation of $CD4^+$ T cells from healthy donors with FVIII is published[124,187]. This is due to the fact that thymic deletion of self-reactive T cells is not complete and self-reactive T cells are known to leave the thymus[188]. These T cells are controlled by natural and induced regulatory T cells in the periphery[115,177,189]. In order to circumvent this suppression of self-reactive T cells by regulatory T cells, the assay is based on regulatory T cell-depleted $CD4^+$ T cells. Using this approach, it was already proven that $CD4^+$ T cells of healthy donors can be restimulated with FVIII[190]. In order to keep the influences of different cell types on each other as predictable as possible, only DCs are chosen as APCs. DCs are able to activate naïve T cells as well as to restimulate mature T cells. This setup makes it feasible to test a deimmunized FVIII in a setup with T cells derived from healthy donors and Hemophilia A patients.

1.3.3. *In vivo* tools for the determination of a deimmunization

Although *in vitro* tools give an impression, regarding the immunogenicity of peptides and proteins, only *in vivo* experiments provide a full immune system with all interacting cells. Nevertheless, mouse models have disadvantages, especially regarding immune response to human proteins. In a normal mouse model a given human protein is differently processed, presented on a murine MHC class II and detected by murine T cells, as a human protein is always foreign to the murine immune system[109]. Additionally, mice mostly express their own endogenous version of the protein of interest and might already have established tolerance towards this protein. Due to that, a normal mouse model cannot be used to draw conclusions regarding the immunogenicity of a protein. In order to circumvent these problems, HLA transgenic mice[191], humanized mice and knockout mouse models were developed.

The T cell response in HLA transgenic mice was proven to correlate with the T cell response in humans[192,193]. However, one mouse strain can only be transgenic for one HLA type. As the *in silico*

analysis covers many HLA types, various HLA transgenic mice strains have to be used, in order to receive a complete analysis. In addition to this, a deimmunization does not result in the total absence of presented peptides. This may influence the results from HLA transgenic mice, as the presented human peptides might be foreign to the murine immune system and due to this might elicit an immune response. A possibility to circumvent this is to use a humanized mouse model. Humanized mice are transplanted with human $CD34^+$ stem cells and develop an immune system with human immune cells. This provides human MHC molecules and human DCs, B and T cells[194,195]. However, as for the HLA transgenic mice, the experiments have to be performed in various mice, transplanted with stem cells from different donors, in order to cover different HLA alleles.

In the case of evaluating the immunogenicity of a deimmunized protein, which is also present in mice, the response might be influenced by central tolerance of the murine immune system to the endogenous protein. Murine T cells, which might react against the human protein, might have been elicited during the ontogeny of the murine immune system. In order to circumvent this possibility, mice with a knockout for the protein of interest were developed[180].

Both types of mice, HLA transgenic or humanized mice as well as knockout mice, provide an important characteristic for the determination of the immunogenicity of a protein and to compare a deimmunized to a non-deimmunized variant. Due to this, a combination of both would be the most promising model.

In order to determine the immunogenicity of a deimmunized FVIII variant *in vivo*, a FVIII-knockout mouse model and a humanized mouse model is applied in this thesis. Unfortunately, a humanized FVIII knockout model was not available. In the E16 FVIII knockout model, the mice will reveal a naïve response to FVIII. Although the deimmunization is predicted based on human HLA alleles, it might also be detectable to a lesser extent in mice, as the MHC class II alleles share several homologies. The humanized mouse model on the other hand provides the largest possible similarity to the human immune system. In the highly developed humanized BRGSF mice the FVIII is processed by human APCs, presented bound to a human MHC class II and detected by human T cells[196]. Due to this, the model provides the possibility to detect *in vivo* whether a deimmunized protein is less frequently presented by APCs and elicits a reduced immune response compared to a wild-type BDD-FVIII molecule.

1.4. Aim of the thesis

The aim of this thesis was the development of a less immunogenic recombinant BDD-FVIII molecule. This deimmunized FVIII shall reduce the risk of inhibitory antibody formation in Hemophilia A patients and via this, improving the life of the patients as well as decreasing the costs for therapy. The modified FVIII should be presented to a much lesser extent on the surface of APCs and therefore have a reduced capacity to activate T cells. Due to this absence of helper T cells, B cells should not be able to differentiate and produce high-affinity inhibitory antibodies against FVIII[113].

In order to deimmunize the FVIII, *in silico* analyses, predicting MHC class II presentation of FVIII peptides, were utilized. Recommended amino acid exchanges were incorporated into the FVIII sequence with the aim to decrease the amount of FVIII peptides displayed on the surface of APCs. However, it was important that the mutated FVIII variant was still produced in the same amount as a non-modified FVIII and remained unchanged regarding its structure, activity in the coagulation cascade and interaction with other proteins. This specific combination of mutations had to be revealed in various rounds of screening, as modelling of the mutated FVIII was not possible[41,52].

The mutated FVIII variants were produced in two human cell lines, in order to reduce the influence of the production cell line on the post-translational modifications and by this on the immunogenicity of FVIII. HEK293-F cells and Cevec's Amniocyte Production (CAP-T) cells were chosen. Both cell lines grew in suspension and the produced FVIII was purified from the cell culture supernatant[197,198]. As both cells were derived from a human origin, a similar post-translational modification of rFVIII compared to pFVIII was highly likely. Consequently, the selected cell lines would circumvent one major drawback of the first to third generation rFVIII products.

In order to determine *in vitro* whether the incorporated mutations led to a less immunogenic FVIII molecule, an assay with human DCs and T cells was developed. This was required, as the deimmunization focused on the presentation of human FVIII peptides on human MHC class II. The artificial approach of an *in vitro* assay containing only DCs and regulatory T cell-depleted $CD4^+$ T cells was chosen, in order to guarantee that enough DCs were present to activate naïve T cells in addition to the recall response induced in already mature T cells. Using this assay, differences in T cell proliferation in response to different FVIII variants and control proteins could be detected.

However, the complex interactions of an immune response to a given protein could only be determined *in vivo*. Due to this, the deimmunized FVIII was also tested in two mouse models. In order to circumvent most of the limitations of a normal mouse model, a humanized mouse model was chosen for this thesis. The mice were transplanted with human stem cells, developing human APCs, B, T and NK cells. This provided the best available pre-clinical *in vivo* model to determine the immunogenicity of the mutated FVIII molecule. In addition to this, a FVIII knockout mouse model was applied, in order to detect a naïve T cell response to the deimmunized FVIII in comparison to a FVIII reference molecule.

2. Material

2.1. Cell culture reagents

Product	Manufacturer	Order number
2-Mercaptoethanol (50 mM)	life technologies	31350-010
Blasticidin	life technologies	R210-01
CAP-CDM medium	Merck Millipore/ Cevec	Customized
CD293 medium	life technologies	11913019
DMSO for cell culture	AppliChem	A3672,0250
EDTA Solution	Sigma-Aldrich	E7889-100ML
GlutaMAX (100 x)	life technologies	35050-30
Heat Inactivated FBS	life technologies	10100-147
HEK293-F cells	life technologies	11625-019
HEPES Buffer Solution (1 M)	life technologies	15630-056
HyClone Cell Boost 5 Supplement	Thermo Scientific	SH30865.01
LONG R3 IGF-I	Sigma-Aldrich	91590C
Lymphoflot	Bio-Rad	824012
MEM NEAA (100 x)	life technologies	11140-035
Plasmids	life technologies	Customized
ProFreeze-CDM NAO (2 x)	Lonza	12-769E
Protein Expression Medium (PEM)	life technologies	12661013
RPMI 1640 Medium	life technologies	11875093
Sodium Pyruvate 100 mM (100 x)	life technologies	11360-039
X-VIVO 15 w/o Gentamicin or Phenol Red	Lonza	04-744Q

2.2. Chemicals and Reagents

Product	Manufacturer	Order number
0.4 % Trypane Blue Solution	Corning	25-900-CI
1 M Tris-HCl pH 7.5	life technologies	15567-027
1 M Tris-HCl pH 8.0	life technologies	15568-025
10 x Deglycosylation Mix Buffer 2	New England BioLabs	B6045S
20 x Modified Dulbecco's PBS Tween 20 Buffer	Thermo Scientific	28346
2-Propanol	Merck Millipore	1.09634.2511
3,3',5,5'-Tetramethylbenzidine	Sigma-Aldrich	T0440-100ML

7-AAD	BioLegend	420404
AccuGENE 10 x PBS	Lonza	51226
Agarose low EEO	AppliChem	A2114,0100
Anhydrous DMSO	life technologies	D12345
Aqua dest.	B. Braun	0082479E
BD CompBeads	BD	552843
Bovine Serum Albumin	Sigma-Aldrich	A7906-100G
$CaCl_2$ Solution	Siemens	ORHO37
Calcium Chloride	AppliChem	A1428,0500
CFSE	BioLegend	422701
CHAPS	Merck Millipore	220201-25MG
Coagulation Factor VIII Deficient Plasma	Siemens	OTXW17
Control Plasma N	Siemens	10484201
CS&T Research Beads	BD	650622
Dade Actin FSL Activated PTT Reagent	Siemens	10284499
DY-680-Ester	Dyomics	680-01
DY-780-Ester	Dyomics	780-01
EndoGrade Ovalbumin	hyglos	321002
Ethylene glycol	Merck Millipore	1.09621.2500
FcR Blocking Reagent, human	Miltenyi Biotec	130-059-901
FcR Blocking Reagent, mouse	Miltenyi Biotec	130-092-575
Human Alpha Thrombin	Enzyme Research	HT 1002a
Human Coagulation Factor VIII Concentrate BRP	Council of Europe	H0920000
Hydrochloric acid	Merck Millipore	1.09057.1000
Imperial Protein Stain	Thermo Scientific	24615
in-tem	TEM	503-02
Iodoacetamide	GE Healthcare	RPN6302
IPG Buffer pH 4-7	GE Healthcare	17-6000-86
L-Histidine	Merck Millipore	1.04351.0100
Methanol	Merck Millipore	1.06009.1011
NaCl 0.9 %	B. Braun	357 0160
N-Glycosidase F	Roche	11365185001
Nonidet P-40 Substitute	amresco	M158-50ML
NuPage Antioxidant	life technologies	NP0005
NuPage LDS Sample Buffer (4 x)	life technologies	NP0008
NuPage MOPS SDS Running Buffer (20 x)	life technologies	NP0001

NuPage Sample Reducing Agent (10 x)	life technologies	NP0009
NuPage Transfer Buffer (20 x)	life technologies	NP0006-1
Odyssey Blocking Buffer	Li-Cor	927-40000
PBS Dulbecco w/o Ca^{2+} w/o Mg^{2+}	Biochrom	L1825
Pierce DTT No-Weigh	Thermo Scientific	20291
PlusOne Bromophenol Blue	GE Healthcare	17-1329-01
PlusOne DryStrip Cover Fluid	GE Healthcare	17-1335-01
PlusOne Urea	GE Healthcare	17-1319-01
Precision Plus Protein All Blue Standards	Bio-Rad	161-0373
SDS 20 % Solution	Ambion	AM9820
Sodium Bicarbonate pH 9.4 (1 M)	Alfa Aesar	J62808
Sodium chloride	Merck Millipore	1.06404.1000
Sodium chloride (5 M)	Applichem	A7006,1000
Sodium hydrogen carbonate	Merck Millipore	1.06329.0500
Sodium hydroxide solution (0.5 N)	Merck Millipore	1.09138.1000
star-tem	Tem	503-10
Sucrose	Merck Millipore	1.07687.0250
Sulfuric acid 98 %	Merck Millipore	1.12080.1000
Technothrombin TGA Calibrator Set	Technoclone	5006345
Technothrombin TGA Reagent C Low	Technoclone	5006213
Technothrombin TGA Substrate	Technoclone	5006230
Thiourea	GE Healthcare	RPN6301
Tris pH 7.5 (1 M)	life technologies	15567-027
Tris-HCl	Serva	39794.01
Tween 20 Solution 10 %	AppliChem	A1284,0100
Tween 80 Solution 10 %	Merck Millipore	655207-50ML
vWF, purified from plasma	Biotest AG	Technical batch
Zombie Aqua	BioLegend	423102
Zombie Violet	BioLegend	423114

2.3. Kits

Product	**Manufacturer**	**Order number**
2-D Clean-Up Kit	GE Healthcare	80-6484-51
Asserachrom VIII:Ag ELISA	Diagnostica Stago	00280
CD14 MicroBeads	Miltenyi Biotec	130-050-201

$CD4^+CD25^+$ Regulatory T Cell Isolation Kit	Miltenyi Biotec	130-091-301
Cell Line Optimization 4D-Nucleofector X Kit	Lonza	V4XC-9064
Coatest SP Factor VIII	Chromogenix	82 4086 63
CyDye DIGE Fluor (minimal dye) labeling kit	GE Healthcare	25-8010-65
Human Th1/Th2/Th17 Antibody Array	abcam	ab169809
SE Cell Line 4D-Nucleofector X Kit L	Lonza	V4XC-1024
SF Cell Line 4D-Nucleofector X Kit L	Lonza	V4XC-2024
SG Cell Line 4D-Nucleofector X Kit L	Lonza	V4XC-3024

2.4. FVIII products

Product	Manufacturer	PZN
Nuwiq 2000 I.E.	Octapharma AG	10538172
ReFacto AF 3000 I.E.	Pfizer Inc.	7773372

2.5. Cytokines

Product	Manufacturer	Order number
GM-CSF	PeproTech	AF-300-03
IL-1β	Miltenyi Biotec	130-093-897
IL-2	PeproTech	AF-200-02
IL-4	PeproTech	AF-200-04
IL-6	Miltenyi Biotec	130-095-352
IL-8	Miltenyi Biotec	130-093-942
TNF-α	Miltenyi Biotec	130-094-014

2.6. Antibodies

Product	Manufacturer	Order number
Anti-HLA-DR FITC	Miltenyi Biotec	130-095-295
Anti-HLA-DR PE	Miltenyi Biotec	130-095-298
Anti-Sulfotyrosine Antibody	Merck Millipore	05-1100
CD14 PerCP	Miltenyi Biotec	130-094-969
CD16 APC-Vio770	Miltenyi Biotec	130-096-655
CD206 APC-Cy7	BioLegend	321120
CD209 PE	Miltenyi Biotec	130-092-869
CD209 VioBlue	Miltenyi Biotec	130-099-985

CD25 APC	Miltenyi Biotec	130-101-435
CD28 PerCP-Cy5.5	BioLegend	302922
CD3 APC-Vio770	Miltenyi Biotec	130-096-610
CD3 PE	Miltenyi Biotec	130-091-374
CD4 FITC	Miltenyi Biotec	130-080-501
CD4 PE-Vio770	Miltenyi Biotec	130-113-255
CD4 VioBlue	Miltenyi Biotec	130-097-333
CD40 BV510	BioLegend	334330
CD45 BV421, mouse	BioLegend	103134
CD45RA PerCP-Vio700	Miltenyi Biotec	130-097-693
CD45RO VioBlue	Miltenyi Biotec	130-099-044
CD71 VioBlue	Miltenyi Biotec	130-101-627
CD8 APC	Miltenyi Biotec	130-091-076
CD80 APC	Miltenyi Biotec	130-097-204
CD86 PerCP-Vio700	Miltenyi Biotec	130-097-918
Donkey anti-mouse IgG IRDye 680RD	Li-Cor	926-68072
Donkey anti-rabbit IgG IRDye 800CW	Li-Cor	926-32213
Donkey anti-sheep IgG CF488A	Biotium	20024-1
Donkey anti-sheep IgG CF680	Biotium	20062
Donkey anti-sheep IgG IRDye 800CW	Abm	SI046
Mouse anti-human Factor VIII Antibody, LC	Merck Millipore	MAB038
Mouse anti-human IgG-Fc-HRPO	Cedarlane	CL6017HP
Mouse anti-human IgM-HRP	abcam	ab99744
Rabbit anti-human Factor VIII Antibody, HC	Sino Biological Inc.	13909-R226
Sheep anti-human Factor VIII:C	Cedarlane	CL20035AP
Streptavidin IRDye 680RD	Li-Cor	926-68079

2.7. Consumables

Product	**Manufacturer**	**Order number**
15 ml Conical Tube	Falcon	352096
5 ml Round-Bottom Tube	Falcon	352052
50 ml Conical Tube	Falcon	352070
50 ml Mini Bioreactor	Corning	421720
Amicon Ultra-15 Centrifugal Filters, 10 kDa	Merck Millipore	UFC901024
Cedex Sample Cups	Roche	05 650 623 001

Cell Scraper	Falcon	353086
Combitips advanced 0.5 ml	Eppendorf	0030 089.421
Combitips advanced 10 ml	Eppendorf	0030 089.464
Combitips advanced 2.5 ml	Eppendorf	0030 089.448
Combitips advanced 5 ml	Eppendorf	0030 089.456
Cryotube vials, 1.8 ml	Thermo Scientific	377267
Cup & Pin pro	Tem	200011
Dualfilter epTIPS, 0.2-5 ml	Eppendorf	0030 077.725
Dualfilter epTIPS, 0.1-10 μl	Eppendorf	0030 077.512
Dualfilter epTIPS, 2-200 μl	Eppendorf	0030 077.555
Dualfilter epTIPS, 50-1000 μl	Eppendorf	0030 077.571
epTIPS, 0.1-20 μl	Eppendorf	0030 073.380
epTIPS, 2-200 μl	Eppendorf	0030 073.428
epTIPS, 50-1000 μl	Eppendorf	0030 073.460
Erlenmeyer Flask, 125 ml	Corning	431143
Erlenmeyer Flask, 250 ml	Corning	431144
Erlenmeyer Flask, 500 ml	Corning	431145
FACSClean	BD	340345
FACSFlow	BD	342003
Immobiline DryStrip pH 4-7, 7 cm	GE Healthcare	17-6001-10
LD columns	Miltenyi Biotec	130-042-901
Leucosep tube, 50 ml	Greiner	227290
LS columns	Miltenyi Biotec	130-042-401
Microplate, 96-well, PS, F-Bottom	Greiner	655001
Microplate, 96-well, PS, F-Bottom, black	Greiner	655906
MS columns	Miltenyi Biotec	130-042-201
NuPage 4-12 % Bis-Tris Gel, 1.0 mm x 10 well	Invitrogen	NP0321BOX
NuPage 4-12 % Bis-Tris Gel, 1.0 mm x 12 well	Invitrogen	NP0322BOX
NuPage 4-12 % Bis-Tris ZOOM Gel, 1.0 mm x IPG well	Invitrogen	NP0330BOX
Odyssey Nitrocellulose Membrane	Li-Cor	926-31090
Sample cups 0.5 ml, safe-lock	Eppendorf	0030 121.708
Sample cups 1.5 ml, safe-lock	Eppendorf	0030 123.328
Sample cups 2.0 ml, safe-lock	Eppendorf	0030 120.094
Serological pipette, 5 ml	VWR	612-1248
Serological pipette, 10 ml	VWR	612-4952
Serological pipette, 25 ml	VWR	612-1245

Serological pipette, 50 ml	VWR	612-4953
Sterling Nitrile-Xtra Gloves	Kimtech	98343
Tissue Culture Testplate, 12-well	TPP	92012
Tissue Culture Testplate, 24-well	TPP	92024
Tissue Culture Testplate, 48-well	TPP	92048
Tissue Culture Testplate, 96-well	TPP	92096
Tissue Culture Testplate, 96-well, U-bottom	TPP	92197
Western Blotting Filter Paper, 7 cm x 8.4 cm	Thermo Scientific	84783

2.8. Equipment and Software

Product	**Manufacturer**
4D-Nucleofector	Lonza
ÄKTA start	GE Healthcare
Amershan Typhoon Imager	GE Healthcare
BCS XP	Siemens
Cedex HiRes	Innovatis
Climo-Shaker ISF1-X	Kuhner
Electrophoresis Power Supply GEPS 200/2000	Elchrom Scientific
Eppendorf Centrifuge 5427 R	Eppendorf
Ettan IPGphor3	GE Healthcare
Ettan IPGphor3 Control Software	GE Healthcare
FACSuite	BD
FACSVerse	BD
FlowJo X	Tree Star
GraphPad Prism	GraphPad Software
HERACell 150i CO_2 Incubator	Thermo Scientific
HERACell 240i CO_2 Incubator	Thermo Scientific
HERASafe KS	Thermo Scientific
ImageStudio	Li-Cor
Integra Vacusafe	Integra
IPG Box	GE Healthcare
MACS magnet	Miltenyi Biotec
MARS	BMG Labtech
Megastar 3.0 R Centrifuge	VWR
Multipette	Eppendorf

Nalgene Freezing Container	Nalgene
Neubauer chamber	Labor Optik
Novex Mini-Cell	life technologies
Odyssey CLx	Li-Cor
Olympus IX53 microscope	Olympus
pHmeter SevenCompact	Mettler Toledo
Pipetus	Hirschmann
PLA 3.0	Stegmann Systems
POLARstar Omega	BMG Labtech
Research pipette, 30-300 μl, 12-channel	Eppendorf
Research plus pipette 0.1-2.5 μl	Eppendorf
Research plus pipette 0.5-10 μl	Eppendorf
Research plus pipette 100-1000 μl	Eppendorf
Research plus pipette 10-100 μl	Eppendorf
Research plus pipette 1-20 μl	Eppendorf
Research plus pipette 20-200 μl	Eppendorf
Research plus pipette 500-5000 μl	Eppendorf
Rocking shaker Rocker 25	Labnet
Shaking Platform	Sea Star
Shaking platform THERMOstar	BMG Labtech
ThermoMixer C	Eppendorf
Unicorn start 1.0	GE Healthcare
VectorNTI Express	life technologies
Water bath	GFL
XCell II Blot Module	life technologies
XCell SureLock	life technologies

2.9. Buffer protocols

FVIII Formulation Buffer pH 7.0
205 mM NaCl
5.3 mM $CaCl_2$
6.7 mM L-Histidine
1.3 % Sucrose
0.013 % Tween 20
In distilled water

Lysis Buffer pH 8.5
30 mM Tris
7 M Urea
2 M Thiourea
4 % CHAPS
In distilled water

MACS Buffer
2 mM EDTA
0.5 % BSA
In PBS

SAEx Elution Buffer pH 6.0
1 M NaCl
20 mM $CaCl_2$
20 mM L-Histidine
0.02 % Tween 80
In distilled water

SAEx Equilibration Buffer pH 7.5
100 mM NaCl
20 mM $CaCl_2$
20 mM L-Histidine
0.02 % Tween 80
In distilled water

Sample Rehydration Buffer
7 M Urea
2 M Thiourea
2 % CHAPS
20 mM DTT
1 % IPG pH 4-7
Bromophenol blue
In distilled water

TBSA Buffer pH 7.4
25 mM Tris
150 mM NaCl
1 % BSA
In distilled water

Thrombin-activation Buffer pH 7.5
20 mM Tris
150 mM NaCl
In distilled water

VIIISelect Elution Buffer pH 6.5
1.5 M NaCl
20 mM $CaCl_2$
20 mM L-Histidine
0.02 % Tween 80
50 % Ethylene glycol
In distilled water

VIIISelect Equilibration Buffer pH 7.0
300 mM NaCl
20 mM $CaCl_2$
10 mM L-Histidine
0.02 % Tween 80
In distilled water

VIIISelect Wash Buffer pH 6.5
1 M NaCl
20 mM $CaCl_2$
20 mM L-Histidine
0.02 % Tween 80
In distilled water

Western Blot Buffer
10 % Methanol
0.1 % Antioxidant
In Transfer Buffer

2.10. Vector

The FVIII vector (Figure 2-1) contained the sequence of the different FVIII variants within the unique restriction sites HindIII and XbaI. An additional unique restriction site, BamHI, occurred naturally in the middle of the FVIII sequence. The unique restriction sites KpnI, XmaI and EcoRI were inserted, in order to be able to exchange smaller parts of the FVIII sequence. The human elongation factor-1 alpha (EF-1α) initiated the transcription of the FVIII gene. Additionally, the vector coded for an ampicillin resistance and a dihydrofolate reductase (dhfr), serving as pro- and eukaryotic selection markers. The simian vacuolating virus 40 (SV40) origin indicates the origin of replication in eukaryotes, whereas the pBR322 origin indicates the origin of replication in prokaryotes.

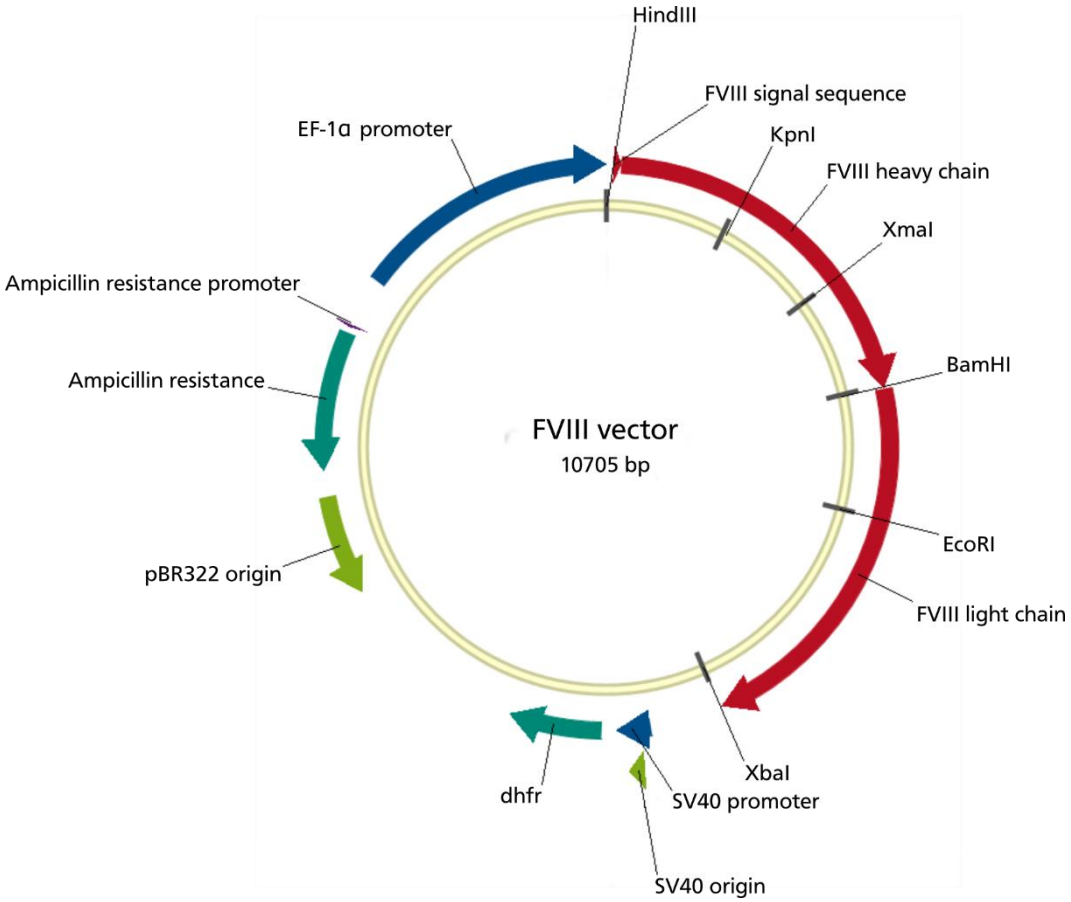

Figure 2-1: FVIII vector card. The arrow indicates the functional orientation of the genes. FVIII signal sequence, FVIII heavy chain and FVIII light chain comprise the coding regions for the whole FVIII molecule. HindIII, KpnI, XmaI, BamHI, EcoRI and XbaI are the unique restriction sites used for cloning. EF-1α is the promotor for the FVIII gene. The ampicillin resistance is the prokaryotic selection marker and dhfr is the eukaryotic selection marker. The SV40 origin provides the origin of replication for eukaryotes and the pBR322 origin provides the origin of replication for prokaryotes.

3. Methods

3.1. *In silico* analyses

The modelling tools used for the *in silico* analyses are commercially available and were performed by EpiVax. The tools analyze protein sequences, in order to detect peptides potentially binding to the MHC class II. These peptides are further analyzed regarding potential amino acid exchanges, in order to reduce the strength of the binding. The functionality of these tools was already proven for FVIII, deimmunizing peptides of the C2 domain[173].

The modelling process, in order to deimmunize a BDD-FVIII, comprised four steps. In the first step, the EpiMatrix tool split the protein into peptides, consisting of nine amino acids, so-called 9-mers. This was due to the fact that the core binding region of the MHC class II comprises nine amino acids[199]. The sequence of a 9-mer and its following 9-mer overlapped by eight amino acids[179]. By building these highly overlapping 9-mers, no potential binding peptides were lost. The binding capacity of all 9-mers was calculated for eight common HLA class II supertype alleles (DRB1*0101, DRB1*0301, DRB1*0401, DRB1*0701, DRB1*0801, DRB1*1101, DRB1*1301, DRB1*1501), covering over 90 % of the human population[172,173]. The potential of each 9-mer to bind a HLA allele was indicated by a "Z score". This score indicated the strength of binding, normalized to the frequency of the given allele in the population[172,200]. A 9-mer with a high Z-score for at least four HLA alleles was regarded as highly immunogenic and a called EpiBar (Figure 3-1)[179].

Frame Start	AA Sequence	Frame Stop	DRB1*0101 Z score	DRB1*0301 Z score	DRB1*0401 Z score	DRB1*0701 Z score	DRB1*0801 Z score	DRB1*1101 Z score	DRB1*1301 Z score	DRB1*1501 Z score	HITS
1	PVSKMRMAT	9					1.91	1.55			1
2	VSKMRMATP	10									
3	SKMRMATPL	11	1.46			1.87				1.90	2
4	KMRMATPLL	12	2.16		1.42			1.45			1
5	MRMATPLLM	13	2.81	2.80	2.54	2.46	1.65	1.62	2.76	2.95	7
6	RMATPLLMQ	14									
7	MATPLLMQA	15								1.44	

Figure 3-1: EpiMatrix results[200]. Example for an analysis of EpiBars in the Class II-associated invariant chain peptide (CLIP) region, a part of the invariant chain, which is bound to the MHC class II groove before peptide loading.

In the following step, overlapping EpiBars were clustered using the program ClustiMer[173]. This analysis led to EpiBar clusters of up to 25 amino acids, binding to class II MHCs derived from multiple HLA alleles[179]. Before the optimization of these clusters, an analysis regarding similarity with other endogenous proteins was performed using the program JanusMatrix. A sequence overlap with at least two other endogenous proteins led to the exclusion of the cluster from further modification. This was because central tolerance has very likely been established to common endogenous peptides. In addition to that, clusters comprising cleavage sites, activation sites or other sites important for the activity of FVIII were set aside and were not altered.

In the last step, amino acid exchanges were calculated using OptiMatrix. This tool evaluated the contribution of each amino acid of a cluster to the MHC class II-binding[173]. Afterwards, OptiMatrix calculated which amino acid substitutions reduced this binding affinity (Figure 3-2)[180]. These optimizations were based on the principles that the amino acid exchanges had to be conservative, preferably occurred in other species and were not registered in the database comprising all known FVIII mutations leading to Hemophilia A[6].

				ORIGINAL SEQUENCE												
Position	254	255	256	257	258	259	260	261	262	263	264	265	266	267	268	269
AA	P	R	G	Y	F	K	I	R	T	G	K	T	T	I	M	R
Score	0	4.72	0	11.92	15.79	15.94	12.99	16.69	3.71	2.98	12.23	3.32	3.32	4.63	1.78	1.72

Figure 3-2: OptiMatrix report[201]. Example for an analysis, which reveals the contribution of each amino acid to binding, indicated by the OptiMatrix score. Color and size of the letters visualize their strength of contribution.

Based on the *in silico* results, the most promising mutations were selected and inserted into the DNA sequence of a BDD-FVIII as single mutations and in combination. The plasmid design was performed using Vector NTI Express. The synthesis of the plasmids was performed by life technologies. HEK293-F and CAP-T cells were transfected with these different plasmids, as described in 3.2.2.3 and 3.2.3.3.

3.2. Cell culture techniques

3.2.1. General techniques

3.2.1.1. Determination of cell numbers

All cells were either counted manually, using a Neubauer chamber, or automatically, using the Cedex HiRes Analyzer. In both cases a trypane blue staining was applied to distinguish viable and dead cells.

The Neubauer chamber comprises nine big squares. The square in the center is used to count platelets and red blood cells, whereas the four squares in the corners are used to count white blood cells and most cell line-derived cells. Each of the four corner squares are subdivided into 4 x 4 small squares and comprise a volume of 0.0001 ml.

In order to determine a cell number, a sample of the cell suspension was diluted at least 1:2 with 0.2 % trypane blue solution. In the case of high cell densities, the sample was pre-diluted in phosphate-buffered saline (PBS) so that each big square contained at least 15 cells and did not exceed 200 cells. 10 μl sample were applied between the chamber and the glass cover. The cells were counted using a microscope. Bright cells were counted as viable cells, whereas dark blue cells, which had taken up the trypane blue solution, were counted as dead cells. Afterwards, the following formulas were applied to calculate the cell concentration of the suspension, the absolute cell number and the viability.

$$\text{Cell concentration (cells/ml)} = \frac{\text{Number of viable cells} \cdot \text{Dilution factor}}{\text{Number of squares} \cdot 0.0001 \text{ ml}}$$

$$\text{Absolute cell number} = \text{Cell concentration} \cdot \text{Total volume}$$

$$\text{Viability (\%)} = \frac{\text{Number of viable cells}}{\text{Number of total cells}} \cdot 100$$

The Cedex HiRes Analyzer stains and counts the cells fully automated. The applied cell suspension is mixed internally with the 0.2 % trypane blue solution and analyzed by a scanner unit. Cell concentrations are calculated by the Cedex HiRes software. 300 μl of the cell suspension were transferred to a Cedex Sample Cup and set into the sample rack of the Analyzer. In the case of high cell densities, the sample was pre-diluted in PBS. The concentration and viability values were taken directly from the software.

3.2.2. HEK293-F cells

The HEK293-F cell line is derived from the original HEK293 cell line[202] and was adapted to suspension growth in serum-free medium[197]. HEK293-F cells are already used in the production of recombinant proteins, even rFVIII[94]. The cells were used for the small-scale production of various mutated FVIII variants.

3.2.2.1. Cryopreservation of HEK293-F cells

HEK293-F cells for cryopreservation were taken from cultures with a low passage number in mid-log phase of growth. The required amount of cells was harvested by centrifugation at 200 x g for 5 minutes. The cells were resuspended in 4 °C chilled cryopreservation medium, consisting of 7.5 % Dimethyl sulfoxide (DMSO) and 92.5 % growth medium, whereas the growth medium consisted of 50 % conditioned and 50 % fresh CD293 medium. The suspension was adjusted to a concentration of $5 \cdot 10^6$ cells/ml in cryopreservation medium. Aliquots of 1 ml were generated and stored in freezing containers at -80 °C, in order to ensure a temperature decrease of 1 °C per minute. The frozen cells were transferred to -150 °C for long-term cryopreservation.

3.2.2.2. Cultivation of HEK293-F cells

HEK293-F cells were cultured in chemically defined CD293 medium supplemented with 4 mM GlutaMAX. In order to thaw the cells, the required amount of frozen vials were transferred to a 37 °C water bath. After thawing, each cryovial was transferred to a 125 ml shake flask, containing 30 ml of warmed, supplemented CD293 medium. The cells were incubated at 37 °C in a humidified incubator with an atmosphere, containing 5 % Carbon dioxide (CO_2). The flasks were set on a shaking platform, rotating at 120 rpm with an orbit of 25 mm.

The cells were subcultured every 3 to 4 days. The fresh cultures were set to $0.3 \cdot 10^6$ cells/ml by transferring the required amount of cell suspension to a new flask and adding supplemented CD293 medium to reach the seeding density of $0.3 \cdot 10^6$ cells/ml. In the case that the transferred cell suspension exceeded 20 % of the total volume, the suspension was centrifuged at 200 x g for 5 minutes and the pellet was resuspended in medium, consisting of 80 % fresh medium and 20 % conditioned medium. The volume of cell suspension per shaking flask was 20 % of the total flask volume.

A minimum of three subcultures were performed after thawing before the first transfection experiments were performed. In addition to that, the cell line was only used until passage 25.

3.2.2.3. Transfection of HEK293-F cells

The HEK293-F cells were transfected using the 4D-Nucleofector. The 4D-Nucleofector is suitable for performing 16 transfections in a 20 μl scale or two transfections in a 100 μl scale in parallel. The Nucleocuvettes are single-use and supplied together with Transfection Buffer SE, SF or SG plus buffer supplements in the respective kits. The 16-well format was used for screening, in order to reveal the appropriate transfection program and buffer for maximal transfection efficacy and viability. The larger transfection format was used for all further experiments. The plasmids were provided in Tris-EDTA (TE)-buffer. The transfected HEK293-F cells were in mid-log growth phase and had a viability above 90 %.

The 16 transfections were performed in Nucleocuvette strips, consisting of 16 separated cuvettes. Each transfection was prepared in a single 15 ml conical tube, containing $0.3 \cdot 10^6$ HEK293-F cells. The cell suspension was centrifuged at 200 x g for 5 minutes. The cells were resuspended in 20 μl of the SE, SF or SG Buffer and 0.4 μg plasmid were added. The cell suspension was transferred to the cuvettes and they were inserted into the 4D-Nucleofector. As each cuvette was pulsed separately, different buffers and transfection programs could be tested within the same strip. For each cuvette, buffer and

transfection program were defined in the software of the 4D-Nucleofector. After the transfection, the strip was taken from the 4D-Nucleofector and 80 µl of warmed RPMI 1640 medium were added to each transfected well. The strip was incubated for 10 minutes at 37 °C. Afterwards, the cell suspensions were transferred to supplemented CD293 medium and incubated as described in 3.2.2.2.

The transfections in the 100 µl Nucleocuvettes were adapted regarding the amount of cells and plasmid, in order to achieve maximal protein production. The transfection of $7 \cdot 10^6$ HEK293-F cells with 7 µg FVIII plasmid was found to be the optimal approach for maximal protein production. This setup was used in all 100 µl transfections. The cells were centrifuged at 200 x g for 5 minutes in 15 ml conical tubes and resuspended in 80 µl of supplemented SG Buffer, taking into account the volume of the pellet and the volume of the plasmid solution. The cell solution was transferred to the Nucleocuvettes. Up to eight Nucleocuvettes were prepared in parallel and transfected successively in pairs of two. The applied transfection program was DU-100. After the transfection, 400 µl of warmed RPMI 1640 were added to each Nucleocuvette and the suspension was incubated for 10 minutes at 37 °C. Afterwards, the cells from one Nucleocuvette were transferred to 50 ml cell culture tubes, containing 2.2 ml supplemented CD293 medium and 0.3 ml HyClone Cell Boost 5. The cells were cultivated for 4 days as described in 3.2.2.2. At day 4 the cells were harvested by centrifugation at 200 x g for 5 minutes. Afterwards, the FVIII activity in the supernatant was determined as described in 3.4.1 and 3.4.2. The pellet and the remaining supernatant were frozen separately at -20 °C for further analyzes.

3.2.3. CAP-T cells

CAP-T cells are derived from amniocytes and optimized for transient transfection. The cell line was developed to produce high amounts of large proteins[198]. As FVIII is a very large and complex protein, the large-scale production of the final deimmunized FVIII molecule was performed in CAP-T cells.

3.2.3.1. Cryopreservation of CAP-T cells

In order to freeze and cryopreserve CAP-T cells, the required amount of cells was harvested by centrifugation at 150 x g for 5 minutes. The pellet was resuspended in chilled CAP-CDM medium to a concentration of $1.7 \cdot 10^7$ cells/ml. This suspension was further diluted 1:2 with chilled ProFreeze-CDM NAO medium, containing 15 % DMSO. Aliquots of 1.8 ml were generated and stored in freezing containers at -80 °C, in order to ensure a temperature decrease of 1 °C per minute. The frozen cells were transferred to -150 °C for long-term cryopreservation.

3.2.3.2. Cultivation of CAP-T cells

CAP-T cells were cultured in CAP-CDM medium supplemented with 50 µg/ml LONG R^3 IGF-I and 6 mM GlutaMAX. In order to thaw the cells, the required amount of frozen vials were transferred to a 37 °C water bath. After thawing, each vial was transferred to 10 ml of chilled, supplemented CAP-CDM medium. The cell suspension was centrifuged at 150 x g for 5 minutes. During this washing step the DMSO was removed. The pellet was resuspended in 15 ml warm, supplemented CAP-CDM medium and transferred to a 125 ml shaker flask. The cells were incubated at 37 °C in a humidified incubator with an atmosphere containing 5 % CO_2. The flasks were set on a shaking platform, rotating at 185 rpm with an orbit of 50 mm.

Subculturing of the cells was performed every 3 to 4 days. The fresh culture was set to $1 \cdot 10^6$ cells/ml by transferring the required amount of cultured cell suspension to a new flask and adding supplemented CAP-CDM medium. In the case that the transferred cell suspension exceeded 20 % of the total volume, the suspension was centrifuged at 150 x g for 5 minutes and the pellet was resuspended in fresh supplemented CAP-CDM medium. The volume of cell suspension per shaking flask was 20 % of the total flask volume.

In order to use CAP-T cells for high yield protein production, the cells were cultivated in PEM medium supplemented with 4 mM GlutaMAX and 5 μg/ml blasticidin. The handling and cultivation conditions remained the same as for the cultivation in CAP-CDM medium.

A minimum of three subcultures were performed after thawing before the first transfection experiments were performed. In addition to that, the cells were only used until passage 25.

3.2.3.3. Transfection of CAP-T cells

The CAP-T cells were transfected using the 4D-Nucleofector as described in 3.2.2.3 for HEK293-F cells. The appropriate transfection program was determined from four possible transfection programs in SE Buffer. In all experiments the CAP-T cells were transfected in the 100 μl Nucleocuvettes. For each transfection $10 \cdot 10^6$ CAP-T cells were centrifuged at 150 x g for 5 minutes in 15 ml conical tubes. The cells were resuspended in 80 μl supplemented SE Buffer, taking into account the volume of the pellet and the volume of the plasmid solution. Afterwards, 5 μg of FVIII-plasmid were added to the cell suspension. The solution was transferred to the Nucleocuvettes. Up to eight Nucleocuvettes were prepared in parallel and transfected successively in pairs of two. The used transfection program was ED-100. After the transfection, the cells from one Nucleocuvette were transferred to 125 ml shaker flasks, containing 12.5 ml supplemented PEM medium. The cells were cultivated for 4 days as described in 3.2.3.2. At day 4 the cells were harvested by centrifugation at 150 x g for 5 minutes. Afterwards, the FVIII activity in the supernatant was determined as described in 3.4.1 and 3.4.2. The pellet and the remaining supernatant were frozen separately at -20 °C for further analyzes.

In order to gain larger amounts of transfected CAP-T cells, multiple transfections were performed and the transfected cells were pooled afterwards. The final culture volume was dependent on the number of transfections, comprising 12.5 ml medium per transfection. As for the small volume transfections, the FVIII activity was determined at day 4 (3.4.1 and 3.4.2). Afterwards, the FVIII was either purified directly from the supernatant as described in 3.5.1 or stored at -20 °C until purification.

3.2.4. Primary cells

3.2.4.1. Purification of PBMCs

Peripheral blood mononuclear cells (PBMCs) are purified from blood via density gradient centrifugation. Particles with a higher density than the separation medium pass through the medium during centrifugation, whereas particles with a lower density stay above. Red blood cells (RBCs), which would not pass the separation medium, due to their low density, aggregate upon contact with the medium. The aggregates have a higher density and can pass the medium. Granulocytes are also able to pass, as they naturally have a higher density than the separation medium. All other cell types stay above the separation medium.

PBMCs were either purified from whole blood or leukapheresis products. In both cases the products were diluted 1:2 with PBS. In the case of a cell suspension derived from a leukapheresis, 25 ml of the suspension were applied to a 50 ml conical tube. Afterwards, 20 ml of the density gradient medium Lymphoflot were slowly pipetted beneath the cell suspension. In the case of whole blood, the 20 ml Lymphoflot were first applied to a 50 ml conical tube and the 25 ml blood were carefully pipetted on top of the Lymphoflot. Both preparations were not allowed to be mingled. The tubes were centrifuged at 1000 x g for 20 minutes, in order to accelerate the separation. The break of the centrifuge was switched off, in order to prevent a mixing of the separated layers at the end of the centrifugation. After the centrifugation, erythrocytes and granulocytes were pelletized at the bottom of the tube. Above that pellet the Lymphoflot was visible, layered by an opaque yellow band of PBMCs. The layer above the PBMCs was the plasma (Figure 3-3). As the minimum purified volume per donor was 400 ml, the sample was split to various tubes. The tubes were filled successively and centrifuged together.

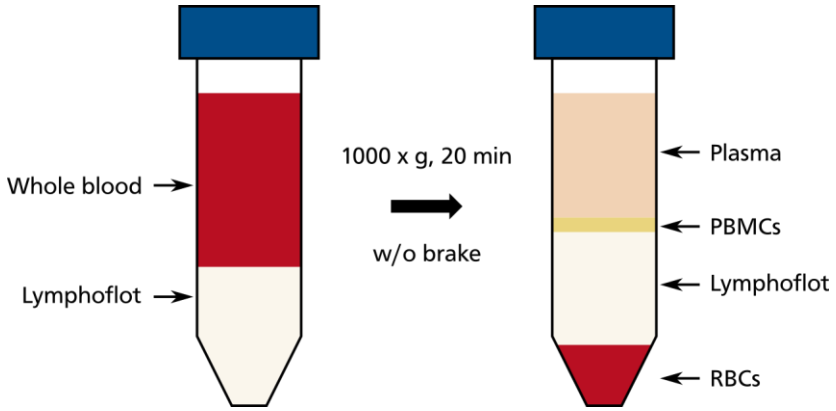

Figure 3-3: Purification of PBMCs. Prior to centrifugation the blood is layered above the Lymphoflot. After centrifugation, four layers were formed. The upper layer is plasma, followed by the PBMC layer. The lower layers are the Lymphoflot and the RBCs.

Using a 10 ml serological pipette, the PBMC layers derived from the same donor were pooled in 50 ml conical tubes. In order to pelletize the cells and to remove the transferred plasma, the cells were centrifuged at 500 x g for 10 minutes. Afterwards, the pellets were resolved in warm X-VIVO 15 medium and pooled in up to ten 50 ml conical tubes, depending on the amount of cells. In an additional washing step, the cells were centrifuged at the same conditions as before. If the cells were pooled in more than one tube, the resolving, pooling and centrifugation was repeated, in order to receive one 50 ml conical tube, containing all PBMCs. The cells were then resuspended in a defined volume of X-VIVO 15 and counted using a Neubauer chamber as described in 3.2.1.1. The PBMCs were cryopreserved as described in 3.2.4.2 and were stored at -150 °C until further purification (3.2.4.3 and 3.2.4.4).

In order to simplify the procedure, Leucosep tubes were used for the purification of whole blood. These 50 ml conical tubes contain a porous barrier, which prevents the mixing of Lymphoflot and blood. 15 ml Lymphoflot were applied to the barrier and the tubes were centrifuged at 1000 x g for 30 seconds, in order to force the Lymphoflot below the barrier. Afterwards, 30 ml of 1:2 diluted blood were applied onto the barrier. The centrifugation was performed at 1000 x g without brake for 10 minutes. After the separation, PBMCs and plasma laid above the barrier and were directly poured to fresh 50 ml conical tubes. The further procedure was performed as described above.

3.2.4.2. Cryopreservation of PBMCs

The PBMCs were cryopreserved immediately after the purification. After the determination of the cell number, the cells were harvested by centrifugation at 300 x g for 10 minutes. The pellet was resuspended in chilled freezing medium, consisting of 90 % fetal bovine serum (FBS) and 10 % DMSO. The final concentration varied between 0.7-6.7·10^7 cells/ml, depending on the required amount per vial. Aliquots of 1.5 ml were generated resulting in 1-10·10^7 cells/vial. The vials were stored in freezing containers at -80 °C, in order to ensure a temperature decrease of 1 °C per minute. The frozen cells were transferred to -150 °C for long-term cryopreservation.

3.2.4.3. Purification of Monocytes

Monocytes were purified from PBMCs with CD14 MicroBeads, using the Magnetic Activated Cell Sorting (MACS) technology. The CD14 MicroBeads consist of monoclonal anti-human CD14 antibodies conjugated to MicroBeads. These antibodies bind to the $CD14^+$ cells and label them. All cells are applied to columns, which are filled with a matrix able to generate a strong magnetic field when attached to a magnet. Due to this magnetic field, the MicroBead-labeled cells are retained inside the column. After the elution of all unbound cells, the column is removed from the magnet and the purified, labeled cells are eluted (Figure 3-4).

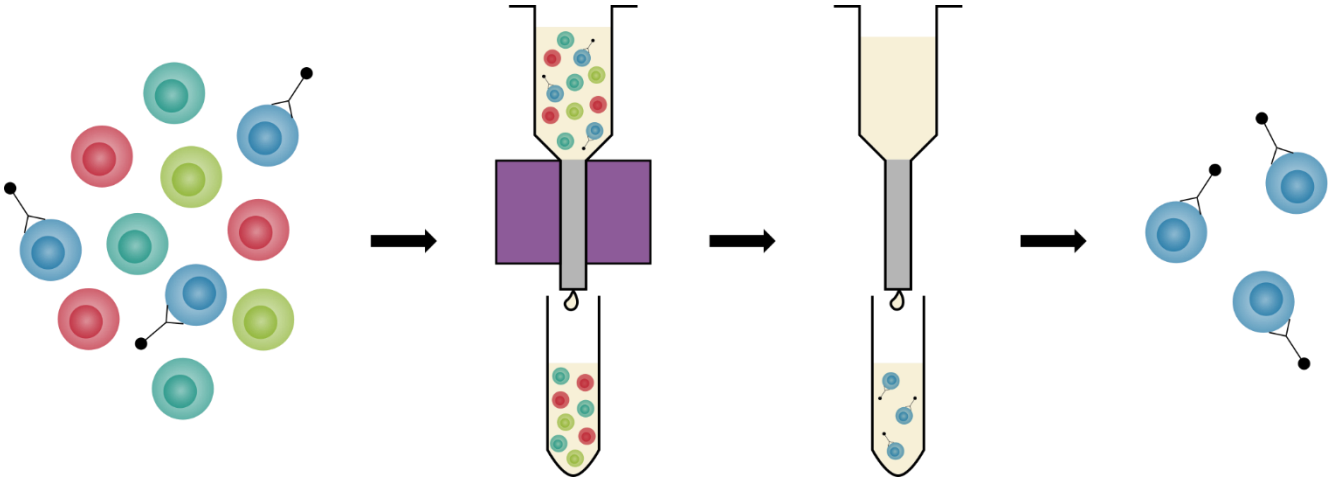

Figure 3-4: Positive selection of CD14$^+$ cells, using MACS. All CD14$^+$ cells in the cell suspension are labeled with MicroBead-coupled anti-CD14 antibodies. The unlabeled cells pass through the column and only labeled cells remain in the column. After removal of the column from the magnetic field, the labeled CD14$^+$ cells can be eluted from the column.

At least one vial of PBMCs was thawed in a 37 °C water bath and transferred to chilled X-VIVO 15. Up to $5 \cdot 10^7$ PBMCs were transferred to 10 ml X-VIVO 15, higher cell numbers were transferred to 40 ml X-VIVO 15. The PBMCs were centrifuged at 300 x g for 10 minutes. The pellet was resuspended in 12 ml X-VIVO 15 for lower cell numbers and 45 ml X-VIVO 15 for higher cell numbers. Afterwards, the total cell number was determined using a Neubauer chamber (3.2.1.1). The cells were again centrifuged using the same settings as before. At first the pellet was resuspended in 80 μl of MACS Buffer per $1 \cdot 10^7$ cells. Afterwards, 20 μl of CD14 MicroBeads per $1 \cdot 10^7$ cells were added. The antibody was incubated for 15 minutes at 4 °C. Afterwards, the tube was filled with MACS Buffer and centrifuged at 300 x g for 10 minutes, in order to remove unbound CD14 MicroBeads. During labeling, MS columns, for up to $2 \cdot 10^8$ total cells, or LS columns, for up to $2 \cdot 10^9$ total cells, were attached to a strong magnet and rinsed with 500 μl or 3 ml of MACS Buffer, respectively. After centrifugation the pellet was resuspended in 500 μl MACS Buffer per $1 \cdot 10^8$ cells and applied to the appropriate column. Three washing steps were performed using 3 x 500 μl MACS Buffer for the MS column or 3 x 3 ml MACS Buffer for the LS column. Afterwards, the column was taken from the magnet and transferred to a 15 ml conical tube. In order to elute the bound cells, 1 ml or 5 ml MACS Buffer were applied to the MS column or LS column. Using a plunger, the cells were flushed out of the column. The suspension contained enriched CD14$^+$ monocytes. The cells were counted using a Neubauer chamber (3.2.1.1) and plated as described in 3.2.4.6.

In order to determine the viability, the composition of the PBMCs and the purity of the monocytes, the cells were analyzed by flow cytometry (3.3.1), using the PBMCs & Monocytes stain (Table 3-1). A sample was taken from the PBMCs prior to purification and from the monocytes after purification.

3.2.4.4. Purification of regulatory T cell-depleted CD4$^+$ T cells

Regulatory T cell-depleted CD4$^+$ T cells were purified from PBMCs, using the MACS technology. In comparison to the monocyte purification (3.2.4.3), during which the cells of interest are labelled with MicroBeads, the CD4$^+$CD25$^+$ Regulatory T Cell Isolation Kit labels all cells except the cells of interest. The kit contains a CD4$^+$ T Cell Biotin-Antibody Cocktail and corresponding Anti-Biotin MicroBeads, as well as CD25 MicroBeads. The CD4$^+$ T Cell Biotin-Antibody Cocktail contains antibodies against CD8, CD14, CD15, CD16, CD19, CD36, CD56, CD123, TCRγ/δ, and CD235a. These antibodies bind to all cell types existing in the PBMCs except CD4$^+$ T cells. The addition of the CD25 MicroBeads specifically labels CD4$^+$CD25$^+$ regulatory T cells. The cells are applied to a column, which is attached to a magnet. All labelled cells remain in the column, whereas the cells of interest pass through the column (Figure 3-5).

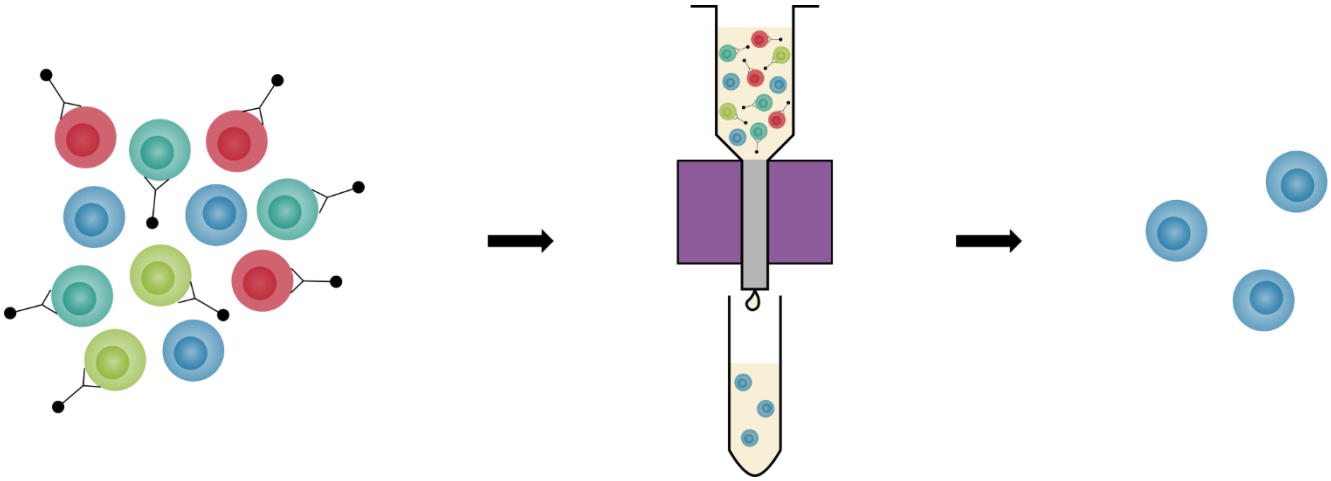

Figure 3-5: Negative selection of $CD25^-$ $CD4^+$ cells, using MACS. All cells in the cell suspension except $CD25^-$ $CD4^+$ cells are labeled with antibodies and MicroBeads. The cells of interest pass through the column and the labeled cells remain in the column.

The PBMCs were thawed, washed and counted, as for the purification of monocytes (3.2.4.3). After the determination of the cell number, the cells were centrifuged at 300 x g for 10 minutes. The pellet was labeled using the $CD4^+CD25^+$ Regulatory T Cell Isolation Kit. The manufacturer's protocol was modified, in order reduce the amount of cell loss, resulting in a combined labeling step and the use of only one column. At first the pellet was resuspended in 80 μl of MACS Buffer per $1 \cdot 10^7$ cells. Afterwards, 10 μl of $CD4^+$ T Cell Biotin-Antibody Cocktail and 10 μl of CD25 MicroBeads per $1 \cdot 10^7$ cells were added. The antibodies were incubated for 5 minutes at 4 °C. Afterwards, 20 μl of Anti-Biotin MicroBeads were added per $1 \cdot 10^7$ cells, in order to magnetically label the biotin-coupled antibodies. The beads were incubated for 10 minutes at 4 °C. During labeling, a LD column, for up to $1 \cdot 10^8$ labeled cells, was attached to a strong magnet and rinsed with 2 ml of MACS Buffer. The labeled cells were applied directly to the column without an additional washing step. Two column washing steps were performed using 2 x 1 ml MACS Buffer. The total effluent was collected containing the regulatory T cell-depleted $CD4^+$ T cells. The column was discarded without elution of the cells. The purified $CD4^+CD25^-$ T cells were labeled with carboxyfluorescein succinimidyl ester (CFSE) directly after purification, as described in 3.2.4.5.

In order to determine the viability and the purity of the regulatory T cell-depleted $CD4^+$ T cells, they were analyzed by flow cytometry (3.3.1), using the T cell stain 1 and 2 (Table 3-3 and Table 3-4). A sample was taken after purification and prior to CFSE-labeling.

3.2.4.5. CFSE labeling of regulatory T cell-depleted $CD4^+$ T cells

Immediately after the purification of the $CD4^+CD25^-$ T cells, the cells were labeled with CFSE, in order to track their proliferation in cell culture. Carboxyfluorescein diacetate succinimidyl ester (CFDA-SE) is able to pass the plasma membrane of cells, due to two acetate groups. Inside the cells, the acetate groups are removed by esterases, leading to the highly fluorescent CFSE, which has a very low membrane permeability and remains inside the cells. Due to the succinimidyl group, CFSE covalently binds to amino groups. These conjugates are able to persist in the cells and are split between daughter cells at each cell division. Due to that, cell proliferation can be tracked via the dilution of the fluorescent CFSE. However, not every CFSE molecule is bound intracellularly. All unbound CFSE molecules are degraded or exit the cell within the first 24 to 48 hours after labeling.

The labeling of the $CD4^+CD25^-$ T cells occurred according to the protocol of Quah *et al.*[203]. The purified T cells were harvested by centrifugation at 300 x g for 10 minutes. Afterwards, the pellet was resuspended in 1 ml warmed PBS, containing 5 % FBS and transferred to a fresh 15 ml conical tube. The tube was laid nearly horizontally and 110 μl PBS were applied to the tube wall, not touching the cell suspension. 1.1 μl of a 5 mM CFSE solution were diluted in the PBS. The tube was capped and the CFSE

solution was mixed with the cell suspension. In order to reduce bleaching, the tube was wrapped in aluminum foil and incubated at room temperature for 5 minutes. Afterwards, the cells were washed by adding ten volumes of warmed PBS, containing 5 % FBS and centrifuged at 300 x g for 10 minutes. The washing step was repeated twice. Afterwards, the cells were cultured for 48 hours as described in 3.2.4.7, in order to cure the cells and to ensure that only steadily bound CFSE remained inside the cells.

The protocol was used for cell numbers between $5 \cdot 10^6$ and $60 \cdot 10^6$ cells. No differences were detected regarding labeling intensity. At cell numbers below $5 \cdot 10^6$ cells the washing steps were decreased from three to two steps, in order to reduce cell loss.

3.2.4.6. Cultivation of monocytes and DCs

Monocytes were cultivated in the chemically defined and serum-free medium X-VIVO 15, in order to keep influences of non-human proteins on the cells as low as possible and to circumvent lot-to-lot variabilities. Monocytes were cultivated in 24-, 48- or 96-well flat-bottom plates, depending on the amount of cells. The concentration of monocytes was $1 \cdot 10^6$ cells/ml and the seeding volume was 0.6 ml/well for 24-well plates, 0.3 ml/well for 48-well plates and 0.1 ml/well for 96-well plates.

Immediately after the purification and determination of the cell number (3.2.4.3), the monocytes were harvested by centrifugation at 300 x g for 10 minutes. Afterwards, the cells were resuspended in the appropriate amount of X-VIVO 15 to reach a final concentration of $1 \cdot 10^6$ cells/ml[204]. This cell suspension was transferred to the wells of a cell culture plate. In order to differentiate the monocytes to immature DCs (iDCs), a final concentration of 4000 U/ml Granulocyte-macrophage colony-stimulating factor (GM-CSF) and 1250 U/ml IL-4 were added to each well. The amount of interleukins was determined in a preceding master thesis[205]. The plates were incubated at 37 °C in a humidified atmosphere, containing 5 % CO_2. After 5 days the monocytes were differentiated to iDCs. In order to obtain mature DCs (mDCs), which present peptides, 0.05 μg/ml Lipopolysaccharide (LPS) or an IL-Mix and an antigen of interest were added to each well. The IL-Mix contained a final concentration of 10 ng/ml IL-1β, 10 ng/ml IL-6 and 10 ng/ml TNF-α and is widely published[206–208]. The antigens of interest were various FVIII products in concentrations of 5 U/ml to 15 U/ml. The control antigen was Ovalbumin (OVA) at a final concentration of 1 mg/ml. The cells were incubated for another 24 hours at the same conditions, in order to maturate. Afterwards, the mDCs were co-cultivated with $CD4^+CD25^-$ T cells as described in 3.2.4.8.

3.2.4.7. Cultivation of regulatory T cell-depleted $CD4^+$ T cells

CFSE-labeled $CD4^+CD25^-$ T cells were cultivated in chemically defined and serum-free X-VIVO 15 medium. The cells were cultivated in 12-, 24-, 48- or 96-well flat-bottom plates, depending on the amount of purified T cells. The concentration of the $CD4^+CD25^-$ T cells was $2 \cdot 10^6$ cells/ml and the seeding volume was 1.3 ml/well for 12-well plates, 0.6 ml/well for 24-well plates, 0.3 ml/well for 48-well plates and 0.1 ml/well for 96-well plates. In order to provide optimal conditions, 20 U/ml IL-2 were added to each well[209,210].

Immediately after the CFSE labeling (3.2.4.5) and the determination of the cell number (3.2.4.4), the T cells were harvested by centrifugation at 300 x g for 10 minutes. Afterwards, the cells were resuspended in the appropriate amount of X-VIVO 15, in order to reach a final concentration of $2 \cdot 10^6$ cells/ml. IL-2 was added to the cell suspension to reach the final concentrations of 20 U/ml. In the last step, the cells were transferred to the wells of the cell culture plate. The plates were incubated at 37 °C in a humidified atmosphere, containing 5 % CO_2 for 48 hours. Afterwards, the cells were co-cultivated with mature DCs as described in 3.2.4.8.

3.2.4.8. Co-cultivation of mature DCs and regulatory T cell-depleted $CD4^+$ T cells

The co-cultivation of DCs and $CD4^+CD25^-$ T cells occurred after the maturation of the DCs and the CFSE-labeling and curing of the T cells. Due to the different cultivation durations, the T cells had to be purified 24 hours prior to the maturation stimulation of the DCs.

After two days of cultivation, the CFSE-labeled T cells were harvested and pooled. Afterwards, the total cell number was determined (3.2.1.1) and a sample was taken, in order to analyze the T cells by flow cytometry (3.3.1), using the T cell proliferation stain (Table 3-5). The cells were co-cultivated at a ratio of at least 1:10 DCs to T cells[210,211]. The T cells were centrifuged at 300 x g for 10 minutes and resuspended in warmed X-VIVO 15 to a final concentration of $2 \cdot 10^6$ cells/ml. The supernatant of the T cell culture was cryopreserved at -20 °C for potential further analyses. The supernatant of the DCs was carefully aspirated, in order not to harm the DCs, which were tightly attached to the bottom of the wells. Immediately after the aspiration, the T cell suspension was added to the wells containing the DCs. Depending on the plates in which the DCs were seeded, the applied T cell suspension was 0.6 ml/well for 24-well plates, 0.3 ml/well for 48-well plates and 0.1 ml/well for 96-well plates. An exact determination of the DC:T cell ratio was not possible, due to the fact that the mDCs were not harvested. However, preceding experiments, counting the mDCs in the wells, revealed that the DC:T cell ratio was at least 1:10. No additional cytokines were applied to the co-cultivation. The plates were incubated at 37 °C for 9 days in a humidified atmosphere, containing 5 % CO_2. After 9 days, the T cells were harvested and centrifuged at 300 x g for 10 minutes. The T cells were further analyzed using a flow cytometer (3.3.1 and Table 3-5), whereas the supernatant was cryopreserved at -20 °C and analyzed later regarding cytokine secretion, using a cytokine array (3.3.2).

3.3. Cellular assays

3.3.1. Flow cytometry

In order to analyze different cell types and their activation status, flow cytometric analyses were performed. Using a flow cytometer, previously fluorescent-labeled cells can be analyzed one by one, due to single-cell dilution inside the instrument. The cells are labeled with fluorochrome-coupled antibodies against various proteins on their cell surface or against intracellular proteins. In addition to that, viability stains and proliferation stains can be applied. Viability stains are based on the permeabilized membrane of dead cells. Due to this, viability dyes can pass the membrane and stain the DNA or amine-groups inside the cell. In contrast to that, proliferation dyes are incorporated into viable cells and are diluted due to cell division. Therefore, highly proliferating cells can be detected by a low signal of the proliferation dye.

Inside the instrument each cell is excited by one or more lasers and the emitted fluorescence is guided via various filters and mirrors inside the instrument until it reaches the specific sensor for the given wavelength. These sensors are photomultiplier tubes (PMTs), which convert the signal of the photon into a voltage pulse, which is depicted as an event in the software. In addition to the detection of the fluorescent dye signal, the forward- and the sideward-scattered light is measured by two detectors. The forward-scattered (FSC) light indicates the size of a cell and the sideward-scattered (SSC) light the granularity (Figure 3-6).

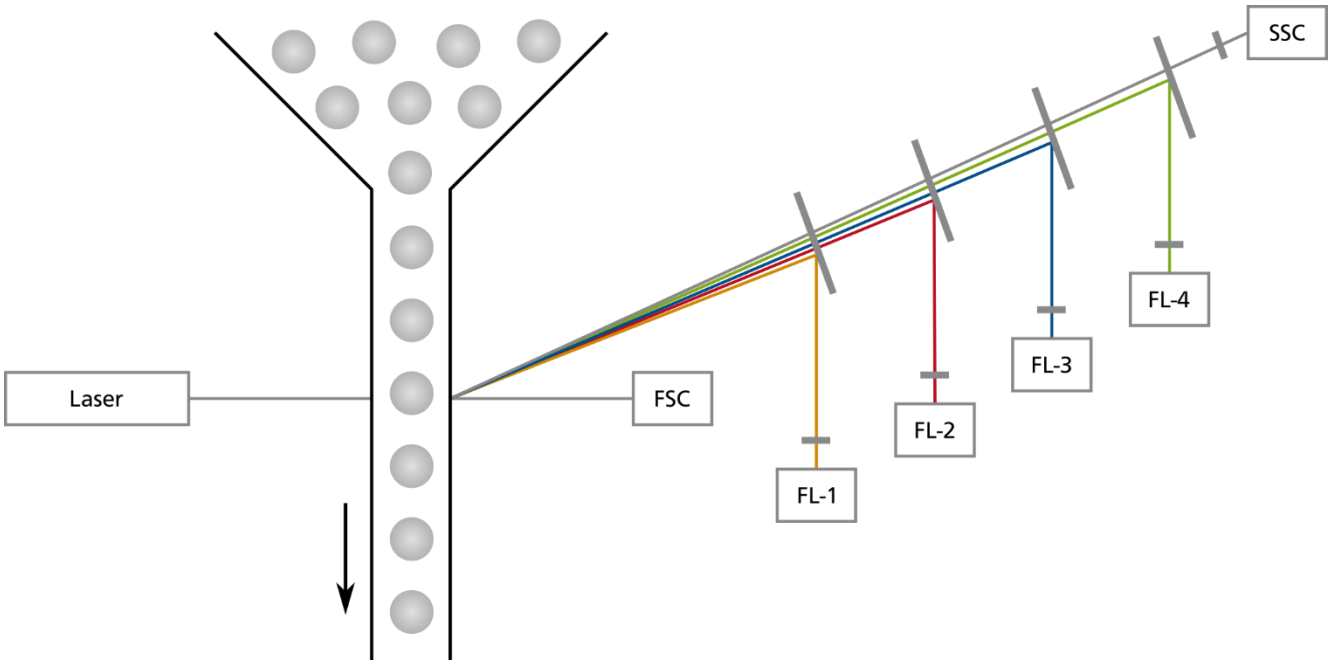

Figure 3-6: Setup of a flow cytometer. Each cell is excited by the laser and the emitted light is detected by the FSC and SSC detectors and the sensors specific for the emitted wavelengths. The different wavelengths are separated by various mirrors and filters.

The applied flow cytometer was a FACSVerse with a blue (488 nm), red (640 nm) and violet (405 nm) laser. Due to the integrated filters, the fluorescent dyes fluorescein isothiocyanate (FITC), phycoerythrin (PE), peridinin-chlorophyll-protein complex (PerCP), PE-cyanine (Cy) 7, allophycocyanin (APC), APC-Cy7, Brilliant Violet V450 and Brilliant Violet V500 could be detected. Apart from these fluorescent dyes, forward and sideward scatter were analyzed. In total, the simultaneous detection of 10 parameters was possible. However, some fluorescent dyes influenced each other and especially the DCs were highly auto-fluorescent. Considering this, the following stains were designed. They were applied, in order to determine the composition of the PBMCs and the purity of the monocytes (Table 3-1), the differentiation and maturation state of the DCs (Table 3-2), the purity of the $CD4^+CD25^-$ T cells before CFSE-labeling (Table 3-3 and Table 3-4) and the proliferation of T cells in the DC-T cell Assay (Table 3-5) or in the humanized mouse cell assay (Table 3-6).

Table 3-1: Antibodies and volumes required for the PBMCs & Monocytes stain.

PBMCs & Monocytes stain			
Excitation laser	*Fluorescence Channel*	*Antibodies*	*Volume per tube*
Blue laser (488 nm)	FITC	CD4 FITC	10 µl
	PE	CD3 PE	10 µl
	PerCP	CD14 PerCP	10 µl
	PE-Cy7	-	-
Red laser (640 nm)	APC	CD8 APC	10 µl
	APC-Cy7	CD16 APC-Vio770	10 µl
Violet laser (405 nm)	BV450	CD209 VioBlue	10 µl
	BV510	Zombie Aqua	0.5 µl

Table 3-2: Antibodies and volumes required for the DC stain.

DC stain			
Excitation laser	*Fluorescence Channel*	*Antibodies*	*Volume per tube*
Blue laser (488 nm)	FITC	HLA-DR FITC	10 μl
	PE	CD209 PE	10 μl
	PerCP	CD86 PerCP-Vio700	10 μl
	PE-Cy7	-	-
Red laser (640 nm)	APC	CD80 APC	10 μl
	APC-Cy7	CD206 APC-Cy7	5 μl
Violet laser (405 nm)	BV450	Zombie Violet	0.5 μl
	BV510	CD40 BV510	5 μl

Table 3-3: Antibodies and volumes required for the T cell stain 1.

T cell stain 1			
Excitation laser	*Fluorescence Channel*	*Antibodies*	*Volume per tube*
Blue laser (488 nm)	FITC	CD4 FITC	10 μl
	PE	CD3 PE	10 μl
	PerCP	CD45RA PerCP-Vio700	10 μl
	PE-Cy7	-	-
Red laser (640 nm)	APC	CD25 APC	10 μl
	APC-Cy7	-	-
Violet laser (405 nm)	BV450	CD45RO VioBlue	10 μl
	BV510	Zombie Aqua	0.5 μl

Table 3-4: Antibodies and volumes required for the T cell stain 2.

T cell stain 2			
Excitation laser	*Fluorescence Channel*	*Antibodies*	*Volume per tube*
Blue laser (488 nm)	FITC	CD4 FITC	10 μl
	PE	CD3 PE	10 μl
	PerCP	CD28 PerCP-Cy7	5 μl
	PE-Cy7	-	-
Red laser (640 nm)	APC	CD25 APC	10 μl
	APC-Cy7	-	-
Violet laser (405 nm)	BV450	CD71 VioBlue	10 μl
	BV510	Zombie Aqua	0.5 μl

Table 3-5: Antibodies and volumes required for the T cell proliferation stain.

T cell proliferation stain			
Excitation laser	*Fluorescence Channel*	*Antibodies*	*Volume per tube*
Blue laser (488 nm)	FITC	CFSE	Pre-stained
	PE	-	-
	PerCP	7-AAD	5 µl
	PE-Cy7	-	-
Red laser (640 nm)	APC	CD25 APC	10 µl
	APC-Cy7	-	-
Violet laser (405 nm)	BV450	CD4 VioBlue	10 µl
	BV510	-	-

Table 3-6: Antibodies and volumes required for the T cell proliferation stain for humanized mouse splenocytes.

Mouse T cell proliferation stain			
Excitation laser	*Fluorescence Channel*	*Antibodies*	*Volume per tube*
Blue laser (488 nm)	FITC	CFSE	Pre-stained
	PE	-	-
	PerCP	7-AAD	5 µl
	PE-Cy7	CD4 PE-Vio770	2 µl
Red laser (640 nm)	APC	CD25 APC	10 µl
	APC-Cy7	CD3 APC-Vio770	10 µl
Violet laser (405 nm)	BV450	Murine CD45 BV421	5 µl
	BV510	-	-

For staining, the cells were harvested in individual 1.5 ml reaction tubes and centrifuged at 300 x g for 5 minutes. The pellets were resuspended in 40 µl MACS Buffer and 5 µl FcR Blocking Reagent per tube. This step blocked all available Fc receptors on the surface of the cells, in order to prevent unspecific binding of the detection antibodies. During the incubation time of 10 minutes at 4 °C, FACS tubes were prepared. Each tube contained the antibodies for the given stain and was filled to 100 µl with PBS. After the incubation of the FcR Blocking reagent, 10 µl – 30 µl of each cell suspension were added to one of the prepared FACS tubes. The cells and antibodies were incubated for 10 minutes at 4 °C. Afterwards, the cells were washed with 1 ml PBS and centrifuged at 300 x g for 5 minutes. The supernatant was aspirated and the pellet was resuspended in 300 µl PBS. The cell suspension was analyzed using the FACSVerse.

The FACSVerse was controlled by the software FACSuite. Using this software, an assay for each stain was designed, which contained the PMT voltages, flow rate and gating strategy. In addition to that, each assay contained the information for the compensation of the given antibodies in one stain. This ensured that the same parameters were applied to each analysis. All stains were automatically compensated by the software, except the T cell proliferation stain, which was not compensated. Automatic compensation was applied every 4 weeks or when a new batch of a tandem dye was used. The final data were evaluated using the software FlowJo X.

3.3.2. Cytokine array

The human Th1/Th2/Th17 Antibody Array allows the simultaneous detection of 34 cytokines from cell culture supernatant. Antibodies against these cytokines are spotted to a membrane in duplicates (Figure 3-7). Upon sample application to the membrane, the cytokines are bound by these antibodies. The detection of the bound cytokines occurs via biotinylated detection antibodies for each cytokine, which are visualized via fluorescence labeled streptavidin. The membrane is analyzed using an Odyssey CLx imager. The imager excites the flurochromes and the emitted light is detected by photodiodes, which convert the light to an electrical signal. Using this system, a detection of secreted cytokines as well as a comparative quantification of the amount of the secreted cytokines is feasible.

	A	B	C	D	E	F	G	H	I	J	K	L
1	Pos	Pos	Neg	Neg	CD30	CD40L	CD40	GCSF	GITR	GM-CSF	IFN-γ	IL-1 sRI
2	Pos	Pos	Neg	Neg	CD30	CD40L	CD40	GCSF	GITR	GM-CSF	IFN-γ	IL-1 sRI
3	IL-1 sRII	IL-10	IL-12 p40	IL-12 p70	IL-13	IL-17	IL-17F	IL-17R	IL-1β	IL-2	IL-21	IL-21R
4	IL-1 sRII	IL-10	IL-12 p40	IL-12 p70	IL-13	IL-17	IL-17F	IL-17R	IL-1β	IL-2	IL-21	IL-21R
5	IL-22	IL-23 p19	IL-28A	IL-4	IL-5	IL-6	IL-6 sR	MIP-3α	sgp 130	TGF-β1	TGF-β3	TNF- α
6	IL-22	IL-23 p19	IL-28A	IL-4	IL-5	IL-6	IL-6 sR	MIP-3α	sgp 130	TGF-β1	TGF-β3	TNF- α
7	TNF-β	TRANCE	Neg	Neg	Neg	Neg	Neg	Neg	Neg	Neg	Neg	Pos
8	TNF-β	TRANCE	Neg	Neg	Neg	Neg	Neg	Neg	Neg	Neg	Neg	Pos

Figure 3-7: Map of the spotted cytokines on the membrane of the human Th1/Th2/Th17 Antibody Array.

The cytokine arrays were performed after all DC-T cell Assays were finished. Due to this a control was generated, in order to be able to compare the cytokine secretion of the T cells derived from different co-cultivations (3.2.4.8). The control was a mixture of all of the analyzed supernatants. This control was applied to every membrane in addition to the sample. Due to this, it was possible to normalize each sample to a given background. In order to be able to separate sample and control, the samples were labeled with streptavidin conjugated to the fluorochrome IRDye 800 whereas the control was labeled with streptavidin conjugated to the fluorochrome IRDye 680.

At first each membrane was prepared by cutting off the edge with the dash mark and transferring the membrane to the provided tray. All membranes were handled with care, not touching the membrane directly, only by using forceps. 2 ml of Odyssey Blocking Buffer, containing 0.05 % Tween 20 were applied to each membrane. The membranes were incubated overnight at 4 °C on a shaking platform at 50 rpm. The next day the biotin-conjugated anti-cytokine antibodies were reconstituted by adding

1460 µl of Odyssey Blocking Buffer, containing 0.05 % Tween 20 to one vial. Per two membranes one vial of anti-cytokine antibodies was reconstituted. Both Streptavidin-IRDye conjugates were diluted 1:200 in Odyssey Blocking Buffer, containing 0.05 % Tween 20. Per two membranes a total of 100 µl of each conjugate was required. All supernatants were thawed at 37 °C. Afterwards, 100 µl of each sample were removed and pooled, in order to build the control. For each membrane 100 µl sample were mixed with 350 µl biotin-conjugated anti-cytokine antibodies and 50 µl streptavidin-IRDye 800. In parallel, 100 µl control were mixed with 350 µl biotin-conjugated anti-cytokine antibodies and 50 µl streptavidin-IRDye 680 for one membrane. As several samples were analyzed at once, the staining of the control occurred in a master mix staining the total volume of control needed in one vial. The staining of the samples occurred for 1 hour at room temperature. After the blocking, the buffer was aspirated from the membranes and 500 µl of the labeled sample and 500 µl of the labeled control were applied per membrane. The membranes were incubated for 45 minutes at room temperature on a shaking platform. Meanwhile the Wash Buffers I and II were diluted 1:20 with distilled water. After the incubation, the samples were decanted and the membranes were washed four times for 5 minutes with 2 ml of 1 x Wash Buffer I and two times for 5 minutes with 2 ml of Wash Buffer II. The membranes stayed in Wash Buffer II until they were scanned using the Odyssey CLx imager. Each scan had a resolution of 84 µm and no focus offset. Afterwards, the membranes were analyzed using the software ImageStudio.

3.4. Coagulation-related assays

3.4.1. Chromogenic FVIII activity assay

The activity of FVIII was determined by a chromogenic assay. In this two-step assay, FIXa and FVIIIa activate FX in the first step. In the second step, the activated FX hydrolyses a chromogenic substrate, resulting in a color change, which can be measured at 405 nm. Due to the fact that calcium and phospholipids are present in optimal amounts and an excess of FIXa and FX is available, the activation rate of FX is only dependent on the amount of active FVIII in the sample.

The reagents for this chromogenic FVIII activity assay were taken from the Coatest SP FVIII Kit. The kit contained phospholipids, calcium chloride ($CaCl_2$), trace amounts of thrombin, the substrate S-2765, a mixture of FIXa and FX and the thrombin inhibitor I-2581. The inhibitor was added, in order to prevent hydrolysis of the substrate by thrombin, which was build during the reaction. All dilutions were performed in distilled water or Tris-BSA (TBSA) Buffer, containing 25 mM Tris, 150 mM sodium chloride (NaCl) and 1 % Bovine serum albumin (BSA), set to pH 7.4. Each sample was diluted at least 1:2 with FVIII-depleted plasma. Further dilutions were performed using the TBSA Buffer.

The assay was performed by the BCS XP, a fully automated hemostasis analyzer. All reagents including water, TBSA Buffer and the samples were inserted into the analyzer. For each sample the analyzer mixed 34 µl calcium chloride, 20 µl TBSA Buffer, 10 µl sample, 40 µl water, 11 µl phospholipids and 56 µl FIXa-FX-mixture. This mixture was incubated for 300 seconds. Afterwards, 50 µl of S-2765 + I-2581 were added to the reaction. Upon addition of the substrate, the absorption at 405 nm was measured for 200 seconds. Each sample was measured in duplicate.

In order to calculate the amount of active FVIII, the software of the analyzer evaluated the slope of the measured kinetic between 30 seconds and 190 seconds after starting the reaction. This result was correlated to a calibration curve, generated with a biological reference preparation (BRP) of FVIII. The activity of the BRP is indicated in IU/ml. However, IU/ml can be assumed equivalent to U/ml. The results were indicated as “% of normal”. These results were converted to U/ml, as 100 % of normal FVIII activity are equivalent to 1 U FVIII activity per ml.

3.4.2. Clotting FVIII activity assay

In addition to the two-stage chromogenic assay (3.4.1), a one-stage clotting assay was performed, in order to determine the amount of active FVIII. During this assay, FVIII-depleted plasma, $CaCl_2$, the activator Actin FSL and the FVIII-containing sample are mixed in one step. The activator leads to the generation of FXIa, which activates FIX. FVIIIa, FIXa and FX built the tenase complex and FX becomes activated. Further activation of prothrombin and fibrinogen finally lead to the formation of a fibrin clot. The time needed to form the clot, the activated partial thromboplastin time (aPTT), is measured. The aPTT varies, depending on the amount of FVIII.

The clotting assay was performed by the BCS XP. TBSA Buffer, FVIII-depleted plasma, Actin FSL, $CaCl_2$ and the sample were inserted into the analyzer. The sample was diluted at least 1:2 with FVIII-depleted plasma. Further dilutions were performed using the TBSA Buffer. For each sample the analyzer mixed 45 μl TBSA Buffer, 5 μl sample, 50 μl FVIII-depleted plasma and 50 μl Actin FSL. The reaction was started by the addition of 50 μl $CaCl_2$. The analyzer measured the time needed for clot formation.

In order to calculate the amount of active FVIII, the software of the analyzer evaluated a baseline extinction at 405 nm at the beginning of the reaction. All of the following extinction values, within a time of 200 seconds, were analyzed regarding their difference to the baseline extinction. The first time point exceeding a defined threshold was determined as the clotting time. This result was correlated to a calibration curve, generated with a BRP of FVIII.

3.4.3. FVIII antigen ELISA

The amount of FVIII antigen was determined using the Asserachrom VIII:Ag ELISA. In this sandwich ELISA, the applied FVIII is bound by mouse monoclonal anti-human FVIII $F(ab')_2$ fragments, which are coated to the plate by the manufacturer. The detection of the bound FVIII occurs via mouse monoclonal anti-human FVIII antibodies, which are coupled to a peroxidase. In the case that FVIII is present, the peroxidase-coupled antibody binds to FVIII and can be detected by the addition of a tetramethylbenzidine (TMB) solution. TMB turns from a clear to a blue-green solution upon reaction with peroxidase. After a short time, this reaction is stopped by the addition of sulfuric acid (H_2SO_4), which turns the solution yellow (Figure 3-8). The amount of bound FVIII correlates with the intensity of the yellow color, which can be measured at 450 nm. The final amounts of FVIII are calculated using a calibration curve generated by the measurement of at least five serial dilutions of a calibrator with a known antigen concentration.

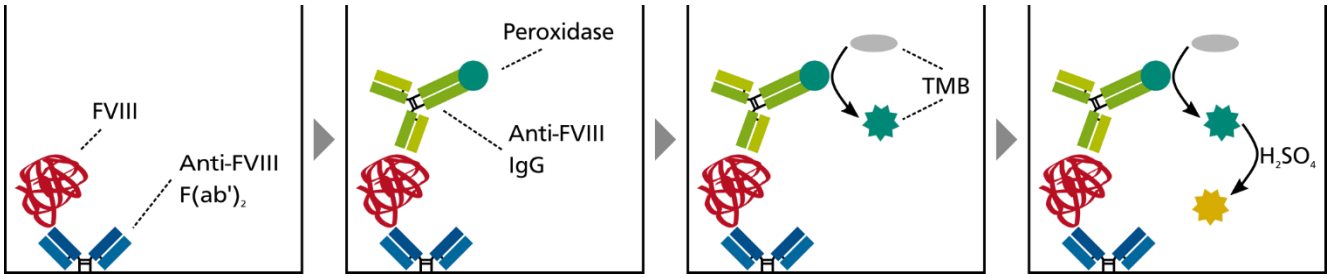

Figure 3-8: FVIII antigen ELISA. The applied FVIII is bound by the coated anti-FVIII $F(ab')_2$ fragments. Bound FVIII is detected by peroxidase-coupled anti-FVIII IgGs. The added TMB solution turns blue-green upon reaction with the peroxidase. The addition of sulfuric acid stops the reaction and turns the solution yellow.

The supplied calibrator and control were reconstituted with 500 μl of distilled water, 30 minutes before starting the ELISA. After this incubation time, the calibrator was diluted 1:10 in the supplied phosphate buffer. This represented the starting concentration. The calibrator was further serially diluted 1:2 up to a dilution of 1:64. As the concentration of the calibrator contained approximately 1 U/ml FVIII, depending on the batch, the starting concentration was equivalent to 0.1 U/ml FVIII whereas the last dilution contained approximately 0.0016 U/ml FVIII. The control was diluted 1:10 and 1:20 with the

phosphate buffer. All samples were diluted with the phosphate buffer, depending on their previously determined activity (3.4.1) with the aim to be in the middle of the calibration curve. After the dilution of FVIII samples, control and calibrator, 200 µl of each solution were applied per well in duplicates. In addition to that, two wells were filled with 200 µl of phosphate buffer as a blank control. The plate was incubated for 2 hours at room temperature covered with a film. During this time, the peroxidase-coupled anti-human FVIII antibodies were reconstituted with 8 ml phosphate buffer and incubated 30 minutes at room temperature. After the antigen immobilization, the wells were washed five times with the supplied washing solution, which was previously diluted 1:20 with distilled water. Immediately after the washing, 200 µl of the peroxidase-coupled anti-human FVIII antibodies were added to each well and incubated for 2 hours at room temperature covered by a film. Afterwards, the plate was washed five times as before. In order to reveal the amount of bound FVIII, 200 µl of TMB solution were added to each well and incubated for exact 5 minutes at room temperature. This reaction was stopped by the addition of 50 µl 1 M H_2SO_4 to each well. After an incubation time of 15 minutes at room temperature, the absorbance of each well was measured at 450 nm using the POLARstar Omega plate reader.

The results of the ELISA were calculated using the MARS software. In a first step, all wells were blank corrected and the mean of the duplicates was calculated. Afterwards, a 4-parameter fit was applied, in order to calculate the concentrations from the calibration curve. According to this calibration curve the amount of FVIII antigen in each well was determined. In the last step, the values were corrected by the dilution factor, resulting in the FVIII antigen amount of each sample.

3.4.4. vWF-binding ELISA

In order to determine the binding of a FVIII sample to vWF, a vWF-FVIII ELISA was performed. In this ELISA, vWF is coated to the wells of a 96-well plate. FVIII samples are added to this plate in serial dilutions. As a control an authorized FVIII product known to bind to vWF is additionally applied. The bound FVIII is detected using the Coatest SP Factor VIII Kit, which is also used for the chromogenic determination of FVIII activity (3.4.1). The absorbance is measured at 405 nm and relative vWF binding is calculated using a Parallel-Line-Assay (PLA) software.

In the first step, the vWF was diluted to a concentration of 0.1 U/ml with a 0.9 % sodium chloride solution. 100 µl were applied to each well of the plate. The plate was incubated at 37 °C and 400 rpm for 2 hours covered by a film. Meanwhile the Wash Buffer was prepared by dilution of the 20 x PBS Tween 20 Buffer to a 1 x solution with distilled water. Additionally, a Dilution Buffer, containing 25 mM Tris and 150 mM NaCl, was prepared in distilled water and adjusted to pH 7.4. The samples and the control ReFacto AF were diluted to 0.25 U/ml with this Dilution Buffer, depending on their previously determined or indicated chromogenic activity (3.4.1). After the coating, the plate was washed three times with 300 µl Wash Buffer per well. Immediately after the washing, the samples were applied to the plate. 200 µl of sample were applied per well and each sample was analyzed in duplicate. The samples were only applied to the first row of the plate. All remaining wells were filled with 100 µl of the Tris-NaCl Buffer. Afterwards, 100 µl of each well of the upper row were transferred to the well below, generating a 1:2 dilution. This serial dilution was continued to the second last row, resulting in seven serial 1:2 dilutions. From the wells of the seventh row 100 µl of sample were discarded, in order to have the same volume in each well. The last row contained only 100 µl of Dilution Buffer. The plate was incubated at 37 °C and 400 rpm for 1 hour covered with a film. During the incubation, the Coatest SP FVIII Kit was reconstituted. 10 ml distilled water were added to the FIXa + FX mixture, whereas 12 ml distilled water were added to the substrate-inhibitor mixture S-2765 + I-2581. The POLARstar Omega plate reader was set to 37 °C. After the incubation, the plate was washed three times as described before. Not until the last washing step, 5 ml of the FIXa + FX solution were mixed with 1 ml of phospholipids. 50 µl of this mixture were applied to each well. The incubation time was 5 minutes at 37 °C and 400 rpm covered by a film. Afterwards, 25 µl $CaCl_2$ were added to each well and the plate was incubated at the same conditions for 5 minutes. In the last step 50 µl of S-2765 + I-2581 were added to each well and the absorbance at 405 nm was measured immediately in the plate reader for a total of 490 seconds.

The analysis of the data was performed using the PLA software. This software performed a 4-parameter fit, resulting in a sigmoidal dose-response correlation curve for each measured FVIII product. The different curves were compared to the curve representing the standard. In order to compare only parallel graphs, the highest and the lowest value for each curve were not taken into the analysis. Based on this, a vWF-binding potency of the FVIII products in relation to the standard was calculated.

3.4.5. Thrombin Generation Assay

The Thrombin Generation Assay (TGA) determines the amount of generated thrombin over time in plasma samples. The clotting cascade in the sample is initiated by the addition of phospholipids, calcium chloride and tissue factor. The generated thrombin finally cleaves an artificial substrate, which emits light at 460 nm upon cleavage. Due to this, the amount of generated thrombin can be correlated to the fluorescence intensity based on a standard curve. As nearly the complete clotting cascade takes place in the TGA, the assay is utilized, in order to determine various coagulation deficiencies and to monitor coagulation-related therapies.

The assay was performed using the Technotrombin TGA reagents comprising the TGA calibrator set, containing buffer and thrombin calibrator, the fluorogenic TGA substrate and the TGA reagent C low. The TGA substrate contained calcium chloride and the fluorogenic substrate, whereas the TGA reagent C low contained low concentrations of phospholipid micelles with TF. In order to generate a calibration curve, the calibrator was diluted 1:2, 1:2.5, 1:3, 1:6, 1:10, 1:20 and 1:200 in the provided buffer. The FVIII samples were diluted to 0.25 U/ml, 0.063 U/ml and 0.016 U/ml in FVIII-deficient plasma, based on their previously determined activity (3.4.1). The samples were pipetted into black 96-well plates with transparent bottom. 40 μl of either the different calibrator dilutions or the FVIII samples were applied per well. The calibrator dilutions were measured in duplicates and the FVIII samples were measured in triplicates. The substrate and the reagent C low were mixed in a ratio of 5:1 immediately prior to starting the reaction. The substrate-reagent-mixture and the plate were placed into the POLARstar Omega plate reader. The reader was set to pipet 60 μl of substrate-reagent mixture to each well. Afterwards the plate was incubated for 5 minutes. Then the generated fluorescence was measured for 75 cycles every 90 seconds at 460 nm.

Due to the known amount of thrombin in the calibrator, a calibration curve was generated with the MARS software after the measurement. A 4-parameter fit was applied, in order to calculate the concentrations from the calibration curve. Based on this the amount of generated thrombin was calculated for each sample. In order to calculate the area under the curve and the time to maximum thrombin generation, the first deviation of the measured curve was calculated using GraphPad Prism.

3.4.6. Thromboelastometry

Thromboelastometry (TEM) is a method for hemostasis testing, revealing various parameters like clotting time, clot formation time and maximum clot firmness. The sample is applied to a cup and a pin is set into the middle of the cup. The sample lies in the space between cup and pin. The pin rotates and its rotation is monitored by a light beam, which is reflected from the pin onto a detector. Upon the onset of coagulation, the generated clot restricts the movement of the pin up to a maximum when the final clot is formed. When performing the experiment over a longer time also lysis parameters can be determined, as the movement of the pin starts to increase again when the clot is lysed. Due to this detected pin movements, the different parameters can be calculated and displayed in a curve.

In order to determine the clotting time for the different FVIII variants, the TEM was performed using the rotation TEM (ROTEM) system. The clotting was initiated using the in-tem and star-tem reagents, which mimic an intrinsic activation. In-tem contained the partial thromboplastin phospholipid whereas the star-tem contained the calcium chloride needed for activation. The FVIII samples were diluted to 1 U/ml, 0.2 U/ml, 0.1 U/ml, 0.05 U/ml and 0.01 U/ml in FVIII-deficient plasma, based on their previously determined chromogenic activity (3.4.1). Each concentration was measured in

duplicate. All reagents and samples were set to 37 °C prior to starting the experiment. The reagents were mixed directly in the cup by pipetting 20 µl star-tem reagent and 20 µl in-tem reagent. Afterwards 300 µl of FVIII sample were added. The regents were mixed by pipetting. The mixture was set into the ROTEM system and the measurement was started immediately. Four reactions were measured in parallel. The analysis was performed for 30 minutes and stopped afterwards, as only clotting parameters were required. The determined clotting times for the different samples and dilutions were directly taken from the ROTEM system.

3.5. Protein analytics

3.5.1. Fast protein liquid chromatography

Fast protein liquid chromatography (FPLC) was used to purify FVIII from cell culture supernatant. Liquid chromatography is based on the principle of a mobile phase passing through a stationary phase. The mobile phase is the buffer and the stationary phase consists of chromatography beads, which build the resin of the chromatography column. Different kinds of chromatography, like ion exchange chromatography (IEX) or affinity chromatography (AC), can be performed. However, all chromatographic methods utilize the different protein properties between required and contaminating proteins for purification.

In order to purify FVIII, a combination of chromatographic methods was applied. The first step was an IEX, using the strong anion exchange columns HiTrap Capto Q. This strong anion exchange chromatography (SAEx) separates proteins due to their surface charge. Negatively charged proteins bind to the positively charged linkers, which are coupled to the agarose matrix of the column (Figure 3-9). Elution of the bound proteins occurs using either a buffer with increased salt concentrations or a change in the pH of the buffer. IEX is suitable for high volumes and leads to a concentration of the sample.

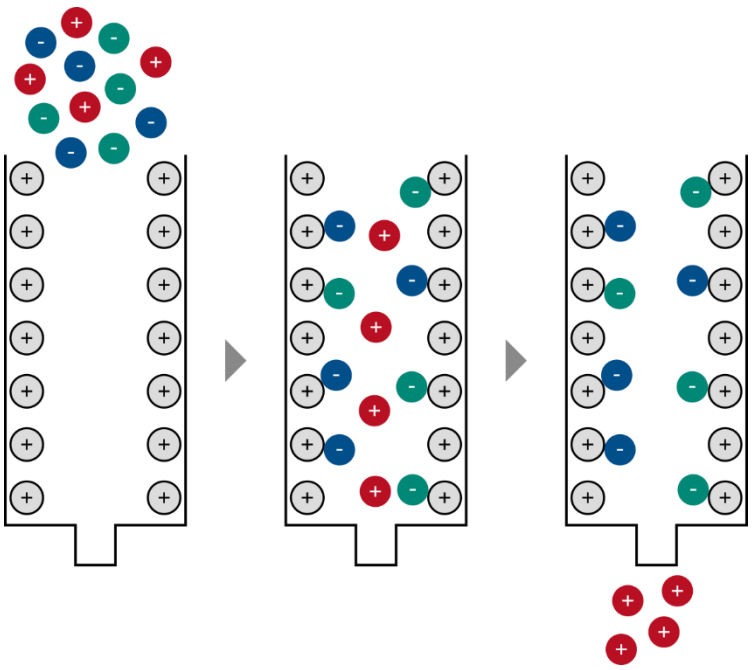

Figure 3-9: Anion exchange chromatography. Negatively charged proteins bind to the positively charged resin. Positively charged proteins flow through.

During FVIII purification, SAEx was used, in order to remove host cell proteins and to concentrate the sample. The cell culture supernatant was adjusted to pH 7.2 prior to purification. By combining five HiTrap Capto Q columns, leading to a total column volume (CV) of 25 ml, up to 375 ml of supernatant were purified, corresponding to 15 x CV. Prior to the application of the supernatant, the column was washed with 5 CV of SAEx Equilibration Buffer, containing 100 mM NaCl, 20 mM $CaCl_2$, 20 mM L-Histidine and 0.02 % Tween 80 at pH 7.5. The supernatant was applied to the column at a flow rate of 5 ml/min. Afterwards, the column was washed with 3 CV SAEx Equilibration Buffer, in order to wash out unbound proteins. The elution of bound proteins occurred by switching to the SAEx Elution Buffer, containing 1 M NaCl, 20 mM $CaCl_2$, 20 mM L-Histidine and 0.02 % Tween 80 at pH 6.0. A total of 6 CV SAEx Elution Buffer were applied to the column at 5 ml/min and the flow through was fractionated in 12.5 ml. Depending on the chromatogram, the fractions containing the eluted proteins were pooled. In the case of starting volumes larger than 375 ml, the columns were equilibrated again and the process was repeated. All elutions were combined and further purified using a second chromatography.

The second step was an AC, using a column packed with VIIISelect resin. During AC, the protein of interest is specifically and reversibly bound to a ligand, which is coupled to the matrix of the column (Figure 3-10). The bound protein is eluted using a buffer, which either contains a competitive ligand or which leads to conditions that impair binding, like variations in the pH.

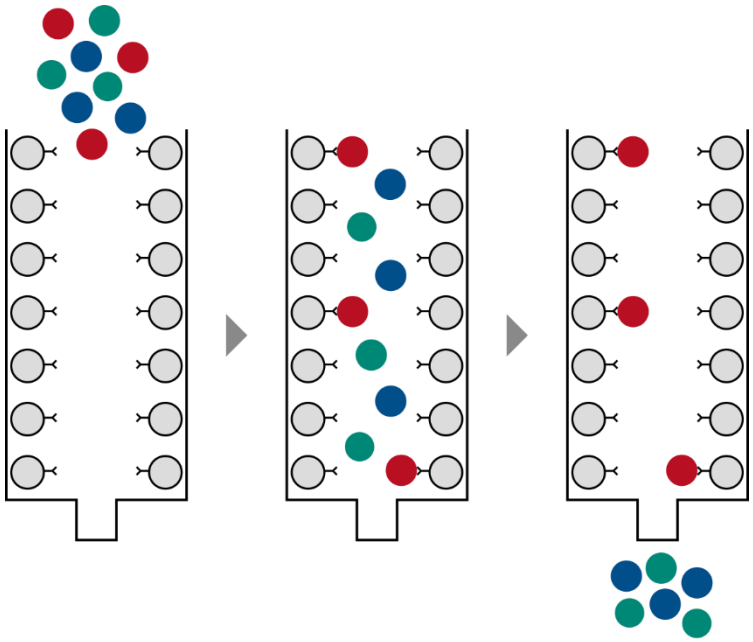

Figure 3-10: Affinity chromatography. The protein of interest is specifically bound by antibodies coupled to the resin. Proteins not bound by the antibody flow through.

During the AC, FVIII was specifically bound by Camelidae-derived, single domain antibody fragments, which were coupled to an agarose matrix. This AC was applied, in order to specifically purify FVIII and to further concentrate the protein. The VIIISelect column comprised 0.94 ml of column volume and was run with a maximum flow rate of 2.5 ml/min. The column was equilibrated with 5 CV of VIIISelect Equilibration Buffer, containing 300 mM NaCl, 20 mM $CaCl_2$, 10 mM L-Histidine and 0.02 % Tween 80 at pH 7.0. The eluted sample from the SAEx chromatography was diluted 1:2 with VIIISelect Equilibration Buffer and adjusted to pH 7.0. The sample was loaded to the column at a flow rate of 2.5 ml/min. In order to remove unbound proteins, the column was washed after the sample application with 5 CV VIIISelect Wash Buffer, containing 1 M NaCl, 20 mM $CaCl_2$, 20 mM L-Histidine and 0.02 % Tween 80 at pH 6.5. The bound FVIII was eluted from the column by 17.5 CV of VIIISelect Elution Buffer, containing 1.5 M NaCl, 20 mM $CaCl_2$, 20 mM L-Histidine, 50 % ethylene glycol and 0.02 % Tween 80 at pH 6.5. The eluted protein was collected in fractions of 5 ml. As for the SAEx chromatography, the

fractions revealing a protein elution in the chromatogram were pooled. This sample, containing purified FVIII, was either directly applied to the last column or stored at -80 °C until further processing.

The last step during FVIII purification was a buffer exchange by size exclusion chromatography (SEC), using the HiTrap Desalting columns. During SEC no binding of the applied proteins occurs. The chromatography is based on the different sizes of the applied substances. Whereas large proteins can migrate alongside the dextran beads of the matrix, small molecules, like salts, enter the beads, leading to a longer retention time in the column (Figure 3-11). In the case of a buffer exchange, the column is equilibrated with the new buffer and the old buffer with the protein is applied to the column. Due to their large size, proteins pass the column quickly and are eluted together with the new buffer, whereas the components of the old buffer reside in the column.

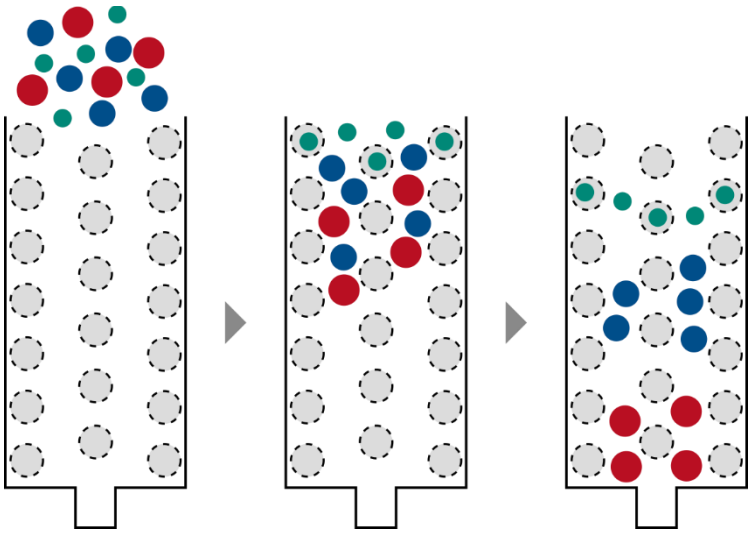

Figure 3-11: Size exclusion chromatography. Larger proteins pass alongside the particles of the resin and elute earlier compared to smaller molecules, which enter the particles, leading to a longer retention time in the column.

This step was applied during FVIII purification, in order to transfer the FVIII from the AC Elution Buffer into the FVIII Formulation Buffer, containing 205 mM NaCl, 5.3 mM $CaCl_2$, 6.7 mM L-Histidine, 1.3 % Sucrose and 0.013 % Tween 20 at pH 7.0. Four HiTrap Desalting columns were combined resulting in a total column volume of 20 ml, in order to exchange the buffer of 6 ml purified FVIII. The column was equilibrated with 5 CV FVIII Formulation Buffer at a flow rate of 5 ml/min. Afterwards, 6 ml of the FVIII sample were applied to the column. The elution occurred with 0.5 CV FVIII Formulation Buffer. The flow through of the column was fractionated in 2 ml fractions. The fractions revealing a high ultraviolet (UV) peak and a stable conductivity peak in the chromatogram were pooled. In the case of more than 6 ml initial volume, the column was equilibrated again with FVIII Formulation Buffer and the process was repeated until the whole FVIII sample was transferred to FVIII Formulation Buffer.

In the case of a low FVIII concentration after the buffer exchange, the sample was concentrated using Amicon Centrifugal Filters with a molecular weight cut-off of 10 kDa. These filters are placed into a 50 ml conical tube and, due to centrifugation, all molecules smaller than 10 kDa pass the membrane. Depending on the length of centrifugation, the sample can be concentrated up to 80-fold. In order to concentrate the purified FVIII sample, 15 ml were applied to one column and centrifuged at 4000 x g for 20 minutes. In the case of sample volumes larger than 15 ml, the column was refilled with sample solution after the first centrifugation and the process was repeated. When the preferred FVIII concentration was reached, the sample was transferred from the filter to cryovials and stored at -80 °C.

In order to monitor the purification process, samples were taken from every step, including wash and flow through of each column. The amount of active FVIII was determined for every sample in parallel to the purification (3.4.1). After the purification, all samples were also applied to a sodium dodecyl sulfate polyacrylamide gel electrophoresis (SDS-PAGE) and a Western Blot (3.5.2 and 3.5.3), in order to visualize the increasing grade of purity and possible changes in the structure of the protein.

3.5.2. SDS-PAGE

Proteins can be separated depending on their size in a SDS-PAGE. During sample preparation, the proteins are mixed with dithiothreitol (DTT) and sodium dodecyl sulfate (SDS). DTT reduces disulfide bonds and destroys the tertiary structure of the protein, whereas SDS binds to the proteins. Due to the negative charge of SDS, the binding results in negatively charged, denatured proteins. The prepared proteins are applied to a Bis-Tris polyacrylamide gel, consisting of a stacking gel and a separating gel. Upon voltage application, the negatively charged proteins move towards the anode. In the stacking gel the proteins travel between chloride (Cl^-) leading ions from the gel buffer and 3-(N-morpholino) propane sulfonic acid (MOPS) trailing ions from the running buffer. This step concentrates all proteins to a small region until they reach the separating gel. In this separating gel the former leading and trailing ions quickly move to the anode, due to their small size, and the proteins are separated depending on their size. Smaller proteins can move faster than larger proteins, resulting in various bands, each representing proteins of a specific size. After the SDS-PAGE, the proteins are either visualized by staining with Coomassie solution or blotted to a membrane and specifically labeled with antibodies (3.5.3).

All SDS-PAGE were performed using the NuPage system with pre-cast 4-12 % Bis-Tris gels. Each sample was diluted 1:2 with 2 x Loading Buffer, consisting of lithium dodecyl sulfate (LDS) Sample Buffer, Reducing Agent, containing DTT, and distilled water. In the case of further dilution of the sample, this was performed using 1 x Loading Buffer. The samples were incubated at 70 °C for 10 minutes. The pre-cast gels were set into the XCell SureLock Mini-Cell electrophoresis chamber. The upper and lower buffer chambers were filled with 1 x MOPS SDS Running Buffer. Additionally, 500 μl Antioxidant were added to the upper chamber. The samples were applied to the wells of the gel, 10 μl per well. In addition to the samples, 4 μl of Precision Plus Protein All Blue Standard was applied to at least one well. The standard was diluted 1:10 with 1 x Loading Buffer. The chamber containing the gel was connected to the power supply and run at 200 V for 50 minutes. Afterwards, the gel was taken from its plastic cover and either stained with Coomassie or transferred to a membrane (3.5.3).

In the case of Coomassie staining, the gel was rinsed in water and transferred to Imperial Protein Stain Solution, containing Coomassie Brilliant Blue R-250. The gel was incubated overnight at room temperature on a shaking platform. Coomassie Brilliant Blue R-250 bound to the basic amino acids of the proteins in the gel. Excessive Coomassie was washed away by incubation of the gel in distilled water for 1 hour on a shaking platform. The washing step was performed twice. In the last step, the stained gel was scanned using the Odyssey CLx imager at a resolution of 86 μm and a focus offset of 0.5 mm.

3.5.2.1. Thrombin-activation of FVIII for SDS-PAGE

In order to determine whether the FVIII variants can be activated, the samples were incubated with thrombin prior to a SDS-PAGE. The FVIII samples were diluted to 20 U/ml in Thrombin-activation Buffer, containing 20 mM Tris and 150 mM NaCl at pH 7.5. The thrombin solution was diluted from 1000 U/ml to 10 U/ml in the same buffer and warmed to 37 °C. Afterwards, 50 μl of FVIII were transferred to 1.5 ml tubes, placed in a 37 °C ThermoMixer. 50 μl thrombin solution were added to each tube and incubated for 8 minutes at 37 °C. In order to stop the reaction, 100 μl 2x Loading Buffer were added to each reaction and incubated for 10 minutes at 70 °C, as described for sample preparation in 3.5.2. The non-activated control samples were treated in the same way, except that no thrombin was added. The samples were further processed as described in 3.5.2.

3.5.2.2. Deglycosylation of FVIII for SDS-PAGE

In order to determine whether the produced FVIII was glycosylated, a SDS-PAGE was performed containing every sample in its original form and in a deglycosylated form. For deglycosylation 40 μl of a 20 U/ml FVIII sample were incubated with 5 μl of Deglycosylation Mix Buffer 2 and incubated for 10 minutes at 75 °C. After the reaction was cooled to room temperature, 0.1 μl Nonidet P-40 and 5 μl N-

Glycosidase F were added. N-Glycosidase F removes all asparagine-bound glycosylations. The reaction was at first incubated at room temperature for 25 minutes and afterwards for 1 hour at 37 °C. In the last step 30 μl 20 % SDS were added. The original samples were treated in the same way, except that no N-Glycosidase F was added. The samples were further processed as described in 3.5.2.

3.5.3. Western Blot

During Western Blotting, proteins separated by SDS-PAGE (3.5.2) are transferred to a nitrocellulose membrane, in order to detect them with specific antibodies. The proteins are transferred from the gel to the membrane by an electric field. As in the PAGE, the negatively charged proteins migrate towards the anode. The membrane is a barrier for further migration and the proteins bind to the membrane. After blotting, the membrane is blocked to prevent unspecific binding of the detection antibodies. These antibodies are applied, in order to bind to the blotted proteins. The primary antibody specifically binds the protein of interest, whereas the secondary antibody is coupled to a fluorochrome and binds to the primary antibody. The bound antibodies can be detected by an imager.

Western Blots were performed using the XCell II Blot Module. A nitrocellulose membrane was activated by incubation in distilled water followed by incubation in 1 x Western Blot Buffer, consisting of the commercially available Transfer Buffer, 10 % methanol, 0.1 % Antioxidant and distilled water. Filter papers and sponges were also soaked in Western Blot Buffer. The gel from the SDS-PAGE (3.5.2) was transferred to a filter paper. The membrane was applied to the other side of the gel and covered with a filter paper. This was placed between soaked sponges and into the Blot Module. Western Blot Buffer was applied to the upper chamber and water for cooling to the lower chamber. The Blot Module was connected to the power supply and run at 30 V for 1 hour. Afterwards, the membrane was rinsed in distilled water and transferred to Blocking Buffer. Blocking was performed overnight at 4 °C. The next day the Blocking Buffer was decanted and 15 ml Blocking Buffer, containing 0.05 % Tween 20 and the primary antibody, were added to the membrane (Table 3-7). The primary antibody was incubated for 1 hour on an orbital shaking platform at room temperature.

Table 3-7: Primary and corresponding secondary antibodies used for Western Blot.

Primary antibody		**Secondary antibody**	
Antibody	*Dilution*	*Antibody*	*Dilution*
Sheep anti-human Factor VIII:C Antibody	1:5000	Donkey anti-sheep IgG IRDye 800CW or Donkey anti-sheep IgG CF680	1:15 000 1:15 000
Rabbit anti-human Factor VIII Antibody, heavy chain	1:1000	Donkey anti-rabbit IgG IRDye 800CW	1:15 000
Mouse anti-human Factor VIII Antibody, light chain	1:2500	Donkey anti-mouse IgG IRDye 680RD	1:15 000
Mouse anti-human Sulfotyrosine Antibody	1:1000	Donkey anti-mouse IgG IRDye 800CW	1:15 000

Afterwards, the membrane was washed four times 5 minutes with PBS, containing 0.1 % Tween 20, on a shaking platform. The secondary antibody was also applied diluted in 15 ml Blocking Buffer, containing 0.05 % Tween 20, and incubated for 1 hour on an orbital shaking platform (Table 3-7). The four washing steps were performed as before. Afterwards, two additional washing steps with PBS were performed for 5 minutes each. In the last step, the membrane was washed in distilled water and afterwards dried between filter paper. The dried membrane was scanned with the Odyssey CLx imager at a resolution of 86 μm and a focus offset of 0.02 mm.

3.5.4. 2D-DIGE

In order to gain a more detailed insight into the differences of distinct rFVIII proteins, a two-dimensional difference gel electrophoresis (2D-DIGE) was performed. The 2D gel electrophoresis (2D-GE) separates proteins not only by their molecular weight but also by their isoelectric point (pI). The first dimension of separation is the isoelectric focusing (IEF) along an immobilized pH gradient. The second dimension is a SDS-PAGE as described in 3.5.2. In addition to that, for a 2D-DIGE the proteins were previously labeled with different fluorescent CyDye DIGE Fluor minimal dyes. This allows multiplexing of up to three proteins on one gel. Using this method, similarities and differences in diverse FVIII products can be directly detected by overlapping and not overlapping fluorescence signals.

The proteins used for 2D-DIGE were precipitated in the first step, using the 2-D Clean-Up Kit, in order to concentrate the proteins and to remove detergents, salts and other impurities. For one 2D-DIGE 5-10 μg of each FVIII product were precipitated. The different FVIII products were kept separate during precipitation. In the case that the required volume of a FVIII product exceeded 100 μl, the sample was split into 100 μl aliquots in sterile 1.5 ml reaction tubes. In the first step 300 μl of precipitant solution were added to each tube, vortexed and incubated on ice for 15 minutes. Afterwards, 300 μl of a co-precipitant solution were added to each tube, mixed and centrifuged at 30 000 x g for 5 minutes at 4 °C. The supernatant was carefully removed and the tubes were centrifuged again briefly to bring down the remaining supernatant. When the whole supernatant was removed, 40 μl of co-precipitant solution were added to each pellet without disturbing the pellet and incubated on ice for 5 minutes. Subsequently the tubes were centrifuged at 30 000 x g for 5 minutes at 4 °C. The supernatant was carefully removed and 25 μl of distilled water were added to each pellet. The tubes were vortexed for at least 10 seconds and afterwards 1 ml of chilled Wash Buffer plus 5 μl of wash additive were added to each tube. The tubes were incubated at -80 °C overnight and vortexed after 30 minutes and 2 hours of incubation. After the precipitation, the tubes were centrifuged at 30 000 x g for 5 minutes. The supernatant was removed and the pellets were dried.

The precipitated proteins were immediately labeled, using the CyDye DIGE Fluor Minimal Labeling Kit when combining three proteins per DIGE or DY-680-Ester and DY-780-Ester when combining two proteins per DIGE. The flurochromes covalently bind to the amino group of lysine. Due to the limiting amount of dye only 1-2 % of all lysines are labeled. This ensures that only one lysine per protein is labeled and the molecular weight of the protein is only altered by 500 Da, which does not alter the protein pattern in the SDS-PAGE. Additionally, each dye carries a +1 charge, in order to replace the +1 charge of the bound lysine. This ensures no alteration in the pI of the protein. The pellets were resuspended in Lysis Buffer, containing 30 mM Tris, 7 M Urea, 2 M Thiourea and 4 % CHAPS at pH 8.5. Each FVIII was resuspended in a final volume of 25 μl Lysis Buffer when combining two proteins per DIGE or 17 μl Lysis Buffer when combining three proteins per DIGE. If one FVIII product was precipitated in more than one tube, the resuspended FVIII was pooled by transferring the Lysis Buffer from one tube to the next. In order to label the proteins, the dye stock solutions were diluted to a final concentration of 400 pM, by adding 1 volume of dye stock solution to 1.5 volumes anhydrous DMSO. The amount of added dye was calculated for each protein, as 1 μl of 400 pM dye solution was added to 50 μg of protein. After the addition of the dyes, the FVIII samples were incubated on ice for 30 minutes. In order to stop the labeling reaction, an equal amount of lysine was added and the samples were incubated on ice for 20 minutes. The differently labeled FVIII samples were pooled afterwards, leading to a total volume of 75 μl.

In order to prepare the sample for isoelectric focusing, 75 μl of Sample Rehydration Buffer were added. This buffer contained 7 M Urea, 2 M Thiourea, 2 % CHAPS, bromophenol blue and freshly added 20 mM DTT and 1 % IPG Buffer pH 4-7. Afterwards, the sample was applied to one lane in the IPGbox and an Immobiline DryStrip pH 4-7, was laid on top, with the gel side facing towards the sample. The DryStrip was rehydrated overnight. The next day the rehydrated strip was transferred to the Ettan IPGphor 3 system and isoelectric focusing was started. The program began with a holding step at 50 V for 15 hours, in order to perform the IEF overnight. In the second step, the voltage was set to 300 V and kept for 50 minutes. This was followed by the first gradual increase of voltage from 300 V to 1000 V in

50 minutes. The second gradual increase was from 1000 V to 5000 V in 2 hours and 20 minutes. In the last step the 5000 V were kept for 5200 Vh. Afterwards, the program was automatically stopped.

After the first dimension of IEF, the strip was prepared for the transfer to a NuPage 4-12 % Bis-Tris ZOOM Gel. The strip was taken from the IPGphor and transferred to a 15 ml conical tube. 5 ml of reducing SDS-PAGE Sample Buffer were added, consisting of 1 x LDS Sample Buffer, 1 x reducing agent and distilled water. After 15 minutes of incubation on a rocking platform, the SDS-PAGE Sample Buffer was removed and 5 ml of 125 mM iodoacetamide in 1 x LDS Sample Buffer were added to the strip and incubated for 15 minutes on a rocking platform. Prior to the transfer of the IEF strip to the gel, the strip was carefully washed in distilled water to remove remaining buffer. The strip was transferred to the gel and fixed by the addition of a 0.5 % agarose solution. Afterwards, the SDS-PAGE was performed as described in 3.5.2, using MOPS Buffer. The gels were scanned after the SDS-PAGE, using the Typhoon Imager.

In the case that only two samples were applied to the 2D-DIGE and only two colors were used for labeling, the gel was blotted after scanning, as described in 3.5.3. The blotted proteins were stained afterwards, using a polyclonal anti-FVIII primary antibody and a secondary antibody coupled to the fluorochrome CF488 A (Table 3-8). The Blot was scanned using the Typhoon imager.

Table 3-8: Primary and corresponding secondary antibody used for Western Blot of a 2D-GE.

Primary antibody		**Secondary antibody**	
Antibody	*Dilution*	*Antibody*	*Dilution*
Sheep anti-human Factor VIII:C Antibody	1:5000	Donkey anti-sheep IgG CF488A	1:15 000

3.6. Mouse studies

3.6.1. *In vivo* experiments

3.6.1.1. Immunization of humanized mice

The generation of human immune system (HIS) mice and the immunization of the mice with FVIII was performed by Axenis. The utilized mice were BRGSF-A2 (BALB/c Rag2$^{-/-}$ IL-2R$\gamma_C^{-/-}$ SIRPα^{NOD} Flk2$^{-/-}$ TgHLA-A2) mice. Due to genetic modifications this mouse strain is transgenic for HLA-A2[212] and supports the development of a human immune system. Knockouts of the recombination activating gene 2 (*Rag2*) and the IL-2 receptor gamma chain (*IL-2Rγ_c*) gene prevent the generation of murine T, B and natural killer (NK) cells[213]. An additional knockout of the fetal liver kinase-2 (*Flk2*) gene (also fms like tyrosine kinase 3 (*Flt3*)) reduces the amount of murine DCs[196,214]. The introduction of the signal regulatory protein α (*SIRPα*) gene from non-obese diabetic (NOD) mice (*SIRPα^{NOD}*) results in murine macrophages tolerating human hematopoietic cells. This is due to a proper interaction between SIRPα on the murine macrophages and CD47 on human T and NK cells, inhibiting phagocytosis[215].

The newborn mice were sublethally irradiated and 24 hours after the irradiation intra-hepatically transplanted with $1{\cdot}10^5$ human hematopoietic progenitor cells (Figure 3-12). The transplanted progenitor cells were purified $CD34^+$ cells derived from human umbilical cord blood[196]. Three different donors were used for the study. After the stem cell transplantation, the mice were treated with Flt3-Ligand and plasmids coding for IL-4 and GM-CSF were delivered hydrodynamically to promote the generation of human monocytes, macrophages and DCs[196,216]. All the genetic variations, the treatment and the stem cell transplantation led to mice, which express human APCs, T, B and NK cells. After the

last treatment with Flt3-Ligand, the immunization with FVIII was started. FVIII was applied intravenously at 200 U/kg per mouse. The FVIII amounts were based on the chromogenic activity values of each variant. Four injections were administered within an interval of one week. On day 36, a final application of 400 U/kg FVIII was injected per mouse. Three days after the last FVIII injection the mice were euthanized and plasma and spleen were harvested and cryopreserved at -150 °C (Figure 3-12). The plasma was further analyzed in an ELISA detecting antibodies against the FVIII, as described in 3.6.2.3. The splenocytes were isolated and restimulated with FVIII, in order to detect whether $CD4^+$ T cells against FVIII evolved during the immunization (3.6.2.1 and 3.6.2.2).

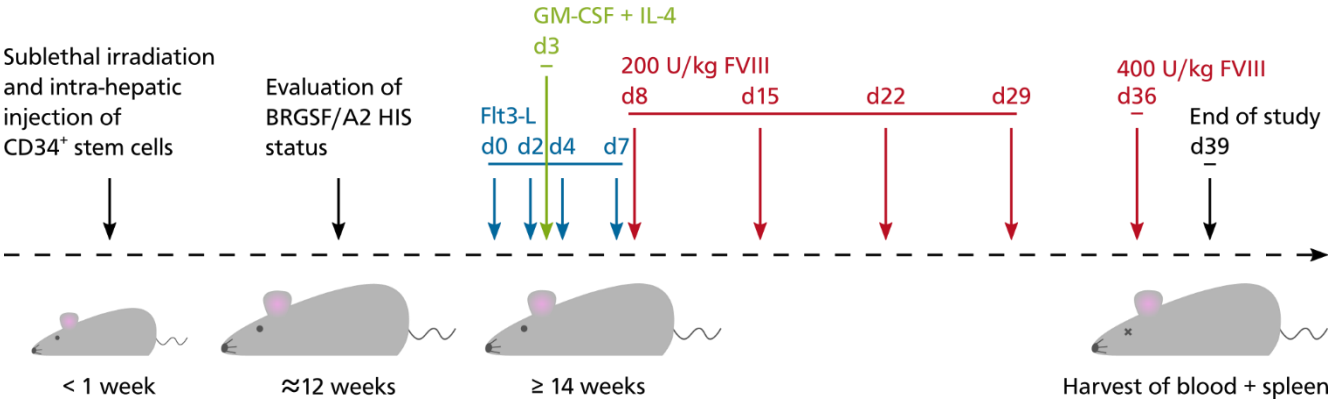

Figure 3-12: Immunization scheme of humanized mice. The newborn mice were sublethally irradiated and intra-hepatically injected with $CD34^+$ stem cells. The HIS mice were further treated with Flt3-L and plasmids coding for GM-CSF and IL-4. On day 8, 15, 22 and 29 after the first Flt3-L treatment, 200 U/kg FVIII were injected. On day 36 400 U/kg FVIII were injected. The study ended at day 39.

3.6.1.2. Immunization of FVIII-deficient mice

The immunization and analysis of FVIII-deficient mice was performed by EpiVax. The mice were Exon 16 (E16) FVIII knockout (KO) mice. This mouse model is based on a C57BL/6 mice background. Blastocysts of these mice were injected with embryonic stem cells of 129S4/SvJae mice, containing the E16 disruption, leading to a knockout of the FVIII gene. Immunization occurred four times every 7 days with 4 U FVIII per mouse or FVIII Formulation Buffer via intravenous injection. The last FVIII injection was 8 U FVIII per mouse or FVIII Formulation Buffer. The amount of FVIII was calculated based on the FVIII antigen values. After five applications of FVIII Formulation Buffer or FVIII, the mice where euthanized at day 32. Blood and spleen of the mice were harvested (Figure 3-13). The plasma of the mice was analyzed in an ELISA, as described in 3.6.2.3, in order to detect an antibody response to the applied FVIII in the immunized mice. The splenocytes were purified from the spleen and cultured as described in 3.6.2.2., in order to determine whether T cells detecting the FVIII had evolved.

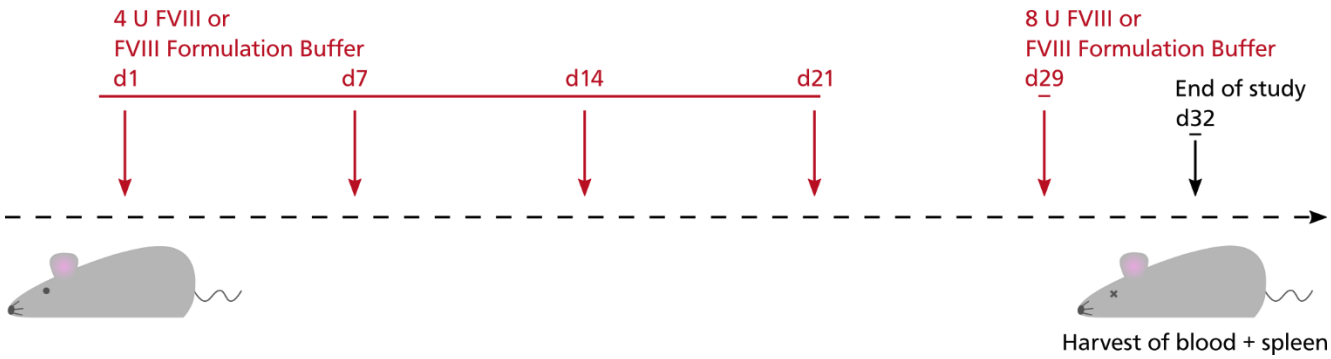

Figure 3-13: Immunization scheme of FVIII-deficient mice. The mice were injected with 4 U FVIII or FVIII Formulation Buffer at day 1, 7, 14 and 21. At day 29 the mice were injected with FVIII Formulation Buffer or 8 U FVIII. The study ended at day 32.

3.6.2. *In vitro* experiments

3.6.2.1. Thawing of mouse splenocytes

The spleens derived from the humanized BRGSF mice immunized with FVIII (3.6.1.1) were further analyzed *in vitro*. The splenocytes were provided by Axenis, where the *in vivo* experiments were conducted. The spleens were extracted after the end of the experiment. The splenocytes were isolated and red blood cells were lysed. The cells were frozen in FBS containing 10 % DMSO and shipped on ice.

The splenocytes were thawed in a 37 °C water bath and transferred to chilled complete RPMI 1640 medium (cRPMI), containing 10 % FBS, 50 μM 2-Mercaptoethanol, 25 mM HEPES, 1 x Sodium Pyruvate and 1 x MEM Non-Essential Amino Acids Solution. The splenocytes were centrifuged at 500 x g for 10 minutes. The pellet was resuspended in warm cRPMI and centrifuged as before. Afterwards, the cells were labeled with CFSE (3.2.4.5). After the last washing step, the cells were resuspended in 1 ml cRPMI and counted (3.2.1.1). The cells were immediately plated as described in 3.6.2.2.

3.6.2.2. Cultivation and restimulation of mouse splenocytes

The isolated splenocytes of the immunized mice (3.6.1.1 and 3.6.1.2) were cultivated, in order to determine whether a restimulation of the $CD4^+$ T cells with FVIII was possible. In the case of a successful immunization of the mice with the applied FVIII product, $CD4^+$ T cell would have evolved, recognizing different FVIII epitopes. A restimulation of these cells *in vitro* would lead to a detectable proliferation and activation of these cells.

The cells were plated in 96-well U-bottom plates at a concentration of $1.5 \cdot 10^6$ cells/ml and 200 μl per well. Splenocytes were plated either in cRPMI or in cRPMI, containing 10 U/ml FVIII for restimulation. The FVIII product used for restimulation was the same as used for the immunization. The plates were incubated at 37 °C in a humidified atmosphere, containing 5 % CO_2. On day 3, 100 μl of cell suspension were removed from every well and replaced by 100 μl fresh cRPMI with or without 10 U/ml FVIII, depending on the initial stimulation. On day 4 the cells were harvested and analyzed by flow cytometry (3.3.1), using the T cell proliferation stain for humanized mouse splenocytes (Table 3-6).

3.6.2.3. Determination of anti-FVIII antibodies in mouse plasma

In order to determine whether anti-FVIII-antibodies were generated during the immunization, an ELISA was performed. In this ELISA, FVIII is coated to the wells and the plasma samples are added in serial dilutions. The bound anti-FVIII antibodies are detected by a peroxidase-coupled secondary anti-IgG or anti-Immunoglobulin M (IgM) antibody. The peroxidase cleaves the added TMB substrate and the absorbance is measured at 450 nm after stopping the reaction with sulfuric acid (Figure 3-14).

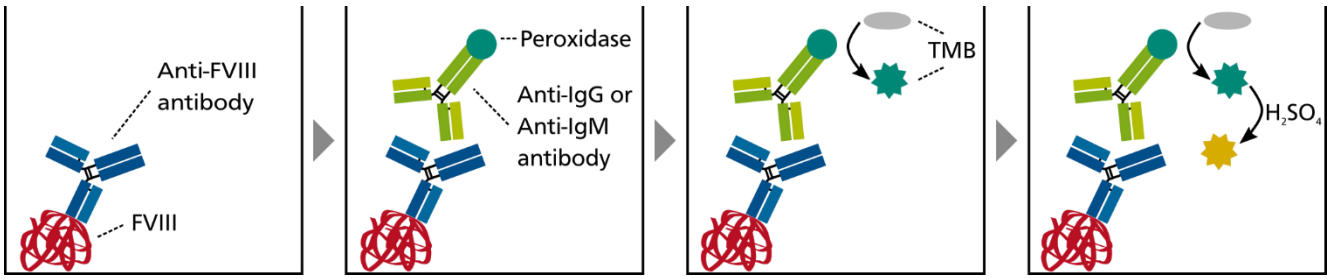

Figure 3-14: Anti-FVIII antibody ELISA. FVIII is coated to the bottom of each well. Plasma samples are added and the anti-FVIII-specific antibodies bind to the coated FVIII. Bound antibodies are detected by peroxidase-coupled anti-IgG or anti-IgM antibodies. The added TMB solution turns blue-green upon reaction with the peroxidase. The addition of sulfuric acid stops the reaction and turns the solution yellow.

A 96-well plate was coated with FVIII, either ReFacto AF, FVIII-19M or FVIII-6rs, depending on the product used for immunization. Each well was coated with 50 µl of a 10 U/ml FVIII solution. The dilutions were performed in 50 mM Sodium Bicarbonate Buffer pH 9.6 and the units FVIII referred to the antigen values, in order to receive comparable amounts of FVIII protein in each well for each product. In the case that mice were immunized with FVIII Formulation Buffer, the wells were coated with ReFacto AF. Coating was performed overnight at 4 °C. The next day the FVIII solution was removed and the wells were washed twice with 100 µl Blocking Buffer per well, consisting of 0.5 % FBS in PBS with 0.05 % Tween 20. Afterwards 100 µl Blocking Buffer were added to each well and incubated for 1 hour at 4 °C. After blocking, the plate was washed twice with 100 µl Washing Buffer per well, consisting of PBS with 0.05 % Tween 20. The plasma of each E16 FVIII KO mouse was diluted 1:10 in Washing Buffer and 75 µl of each dilution were added to one well in the first row of the plate. Plasma of BRGSF mice was added undiluted to the first row of the plate. Commercially available human FVIII inhibitor plasma was used as a positive control for the ELISA with the anti-human detection antibodies. The plasma of the mice from both models were serially diluted 1:3 in each column. Therefore, 50 µl of Washing Buffer were applied to each well except for the wells in the first row. 25 µl of the plasma from the first row were then transferred to the well below and mixed. Again, 25 µl of this well were transferred to the well below. This was continued until seven serial dilutions were performed. From the well containing the last dilution, 25 µl were discarded. The plate was incubated at 4 °C for 2 hours. Afterwards the plate was washed thrice with 100 µl of Washing Buffer per well. Then 100 µl of secondary antibody were added per well. In the case of the E16 FVIII KO mice the secondary antibody was a goat anti-mouse IgG-Peroxidase diluted 1:5000 in Washing Buffer. In the case of the BRGSF mice, a mouse anti-human IgG-Horseradish Peroxidase (HRP) and a mouse anti-human IgM-HRP were used. The anti-IgG antibody was diluted 1:9000 in Washing Buffer, whereas the anti-IgM antibody was diluted 1:6000 in Washing Buffer. The secondary antibodies were incubated for 1 hour at 4 °C. The plate was then washed thrice with 100 µl Washing Buffer per well. Afterwards 50 µl TMB were added to each well. After 5 minutes the reaction was stopped by adding 50 µl of 1 M sulfuric acid. After stopping the reaction, the absorbance at 450 nm was measured, using the POLARStar Omega plate reader.

In order to determine the antibody titer, the measured absorbance values were plotted against the corresponding dilutions. The first dilution leading to an absorbance value above 0.2 was considered to be the antibody titer.

3.7. Statistical analyses

All statistical analyses were performed using the software GraphPad Prism. Due to the low amount of replicates in the different assays, variabilities and outliners, all results were considered to be non-parametric[217,218] and the analyses were based on the median instead of the mean. The Wilcoxon test or the Mann-Whitney test were used in order to compare two groups, depending on whether the results were analyzed in pairs or groups. The Friedman test was applied when more than two groups were analyzed but the results were paired. In the case that the results were not paired, the Kruskal-Wallis test was applied. The results are indicated as not significant (ns) or marked with asterisks, depending on the significance. One asterisk corresponds to P value ≤ 0.05 and two asterisk correspond to a P value ≤ 0.01. P values > 0.05 were considered not significant.

4. Results

4.1. *In silico* analysis of the BDD-FVIII variant

The first step in the deimmunization of a BDD-FVIII was the *in silico* analysis performed by EpiVax. The EpiMatrix tools were used to identify which peptides of the FVIII sequence were most likely bound by the MHC class II. For the identified clusters, amino acid exchanges were suggested, in order to reduce the binding (3.1). The analysis was run for a FVIII sequence, comprising 1514 amino acids, excluding the 19 amino acids of the signal sequence and 818 amino acids of the B domain. The excluded amino acids of the B domain did not interfere with either the furin or the thrombin cleavage sites.

The *in silico* tools revealed a total of 52 immunogenic peptide clusters, with cluster scores ranging between 4 and 34, indicating a very high binding affinity at high values and a lower affinity at low values. The clusters comprised between 14 and 22 amino acids and some clusters were overlapping by a few amino acids. For 12 of the 52 clusters no amino acid mutations were recommended, either due to interference with regions important for activity, binding or stability or due to the lack of possible exchanges. In order to deimmunize the remaining 40 clusters, 74 mutations were recommended. The exchanged amino acids were preferably based on natural occurring changes in other species. If no natural changes were available, amino acid exchanges were selected from point accepted mutation (PAM) matrices[219], which contain mutations that occurred by natural selection (Table 4-1).

Table 4-1: Accepted amino acid substitutions used for the deimmunization of FVIII.

Original amino acid	Potential amino acids for exchange
Arginine	Glutamine, Histidine (H), Serine
Asparagine (N)	Aspartic Acid (D), Histidine, Serine
Glutamine (Q)	Arginine, Aspartic Acid, Glutamic Acid (E), Histidine, Lysine
Isoleucine (I)	Threonine (T)
Leucine (L)	Asparagine, Glutamine
Lysine (K)	Asparagine, Aspartic Acid, Glutamic Acid, Glutamine, Serine, Threonine
Methionine (M)	Arginine, Glutamine, Lysine, Threonine
Phenylalanine (F)	Histidine, Serine
Serine (S)	Alanine (A), Asparagine, Glycine (G), Threonine
Tryptophan (W)	Arginine, Histidine, Serine
Tyrosine (Y)	Asparagine, Histidine
Valine (V)	Alanine, Threonine

For some clusters up to three mutations were indicated, all leading to a strong reduction in the cluster score. In these cases, all mutations were selected for the incorporation. In the case that an additional mutation only led to a low reduction in the score, this mutation was set aside. Additionally, mutations in five clusters were completely set aside, as the total score of the cluster was already low and the predicted improvement by the mutations was marginal. These exclusion criteria led to the reduction from 74 to 57 mutations for the incorporation into the BDD-FVIII.

4.2. Incorporation of the mutations into the BDD-FVIII variant

The incorporation of the mutations was performed in three rounds. Whereas in the first round only single mutations were incorporated, the second and third round comprised the combination of the successfully incorporated single mutations from the first round. For each round, the most important readout was the activity of the mutated FVIII variants in comparison to the non-mutated control FVIII.

The DNA sequence for all FVIII variants was synthesized by life technologies and cloned into a provided vector backbone (2.10). In order to reduce the size of the synthesized fragments, three additional restriction sites were integrated into the FVIII sequence by silent mutations. The sequence already had a restriction site at the beginning (HindIII) and at the end (XbaI) of the FVIII sequence, for cloning into the backbone. One additional restriction site (BamHI) occurred naturally after the removal of the B domain sequence. This led, in combination with the additionally incorporated three restriction sites (KpnI, XmaI and EcoRI), to a FVIII molecule with six unique restriction sites, as shown in Figure 4-1. As a result, not only the sequences to be synthesized were shortened but a modular system emerged which made the combination of mutations easier. The FVIII molecule, derived from the sequence with the six restriction sites, was the reference molecule for all the experiments and was called FVIII-6rs.

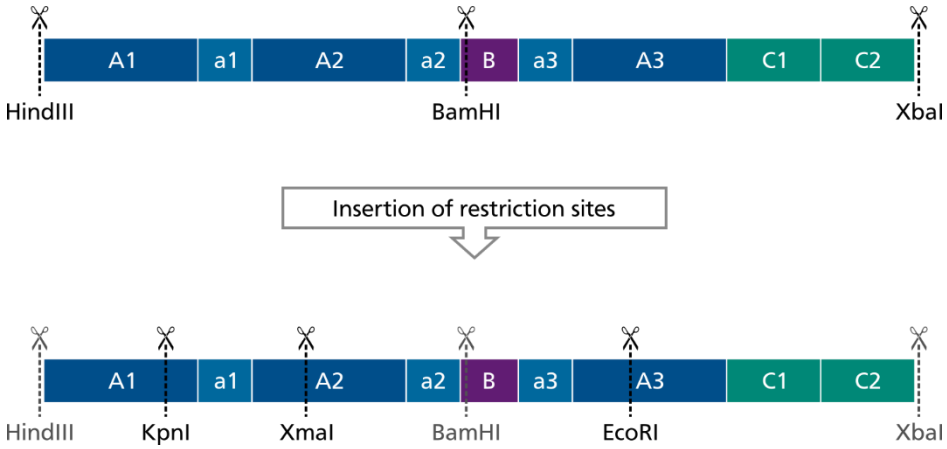

Figure 4-1: Restriction sites in the BDD-FVIII sequence. The original insert contained three restriction sites (HindIII, BamHI and XbaI) located at the ends and in the middle of the FVIII sequence. Three additional sites (KpnI, XmaI and EcoRI) were inserted by silent mutations. This led to a FVIII sequence with six restriction sites.

4.2.1. First screening round

In the first round of screening, the 57 single mutations were inserted into the FVIII sequence. A scheme of the positions of the mutations in the FVIII molecule is shown in Figure 4-2. The selection of base triplets for the new amino acids was based on a human codon usage table[220]. The most frequently used base triplet for an amino acid was chosen.

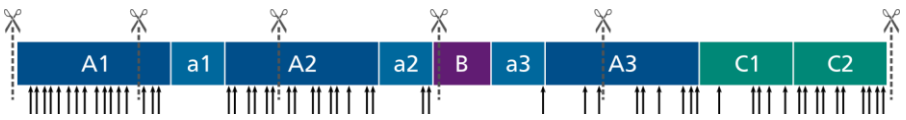

Figure 4-2: Mutations in the FVIII sequence. 57 single mutations were inserted into the FVIII sequence. The arrows indicate the positions of the mutations.

The FVIII variants containing the single mutations were produced in small-scale HEK293-F culture. The HEK293-F cells were transfected in duplicates for each FVIII construct in the Nucleocuvettes, as described in 3.2.2.3. The transfected cells were cultured for 4 days (3.2.2.2). After the cultivation, the supernatant, containing the FVIII, was harvested by centrifugation. The FVIII activity in the supernatant

was analyzed with the chromogenic method in duplicates (3.4.1). The remaining supernatant was frozen until the FVIII antigen ELISA was performed (3.4.3). Per day HEK293-F cells were transfected with five different FVIII constructs in duplicate. In order to compare the activity results for different constructs from different transfection days, HEK293-F cells were additionally transfected with the reference vector, coding for the FVIII-6rs. The FVIII activity for each variant was therefore not indicated in U/ml but the relative activity was calculated, indicating the activity of the variant in relation to the FVIII-6rs of the same transfection day.

In Figure 4-3 the relative activities of the single mutation variants are displayed, allocated to the domains of FVIII. The analyses revealed that only eight mutations led to a total loss of FVIII activity in the cell culture supernatant, whereof L1963Q was a control mutation, known to lead to severe Hemophilia A. Eleven mutations led to a FVIII activity in the supernatant, which was below 50 % of the activity of the control. Thus, in total 19 mutations were excluded from further experiments, due to low or absent FVIII activity. Nevertheless, although the 19 excluded mutations were spread over 16 immunogenic clusters, only ten immunogenic clusters had to be excluded, as further mutations were successfully incorporated in the other six clusters. The remaining 38 mutations led to FVIII variants with activities, which were at least equivalent to half of the activity of the FVIII-6rs.

In addition to the activity, the antigen values of the FVIII variants and the resulting specific activities were determined (Figure 4-4). As the specific activity is the relation of FVIII activity to FVIII antigen, 100 % indicated that the amount of FVIII activity was equivalent to the amount of FVIII antigen. However, most values were above 100 %. Values up to 150 % were assumed to be in the normal range and derived from inaccuracies in the measurement. Even higher values might indicate an improvement of the activity of the variants. Of the 38 active FVIII variants, 35 had specific activities of at least 100 %. The three remaining variants had specific activities below 100 % but above 70 %, indicating that a fraction of the produced FVIII was inactive. Five of the excluded FVIII variants revealed specific activities below 70 %, whereof three had values even below 25 %, indicating that most of the secreted FVIII was inactive. In contrast to that, six of the excluded variants had high specific activities above 100 %, hinting towards active FVIII but a reduced secretion. All eight variants with no FVIII activity, which led to a specific activity of 0 %, also revealed no FVIII antigen. This indicated that the incorporated mutations led either to no production or to no secretion of the FVIII variants.

Although all of the 38 successfully incorporated single mutations had the characteristics to be transferred to the second round, only one mutation for each immunogenic cluster was chosen, in order to keep the combination of the single mutations feasible. Hence, the mutation resulting in a lower FVIII activity was excluded. Additionally, mutation S2030A was found not to be part of the cluster comprising S2037G and N2038D but of a preceding cluster. As the calculated score of this cluster was already very low without the mutation, S2030A was also excluded. This led to 25 mutations, which were transferred to the second round of screening.

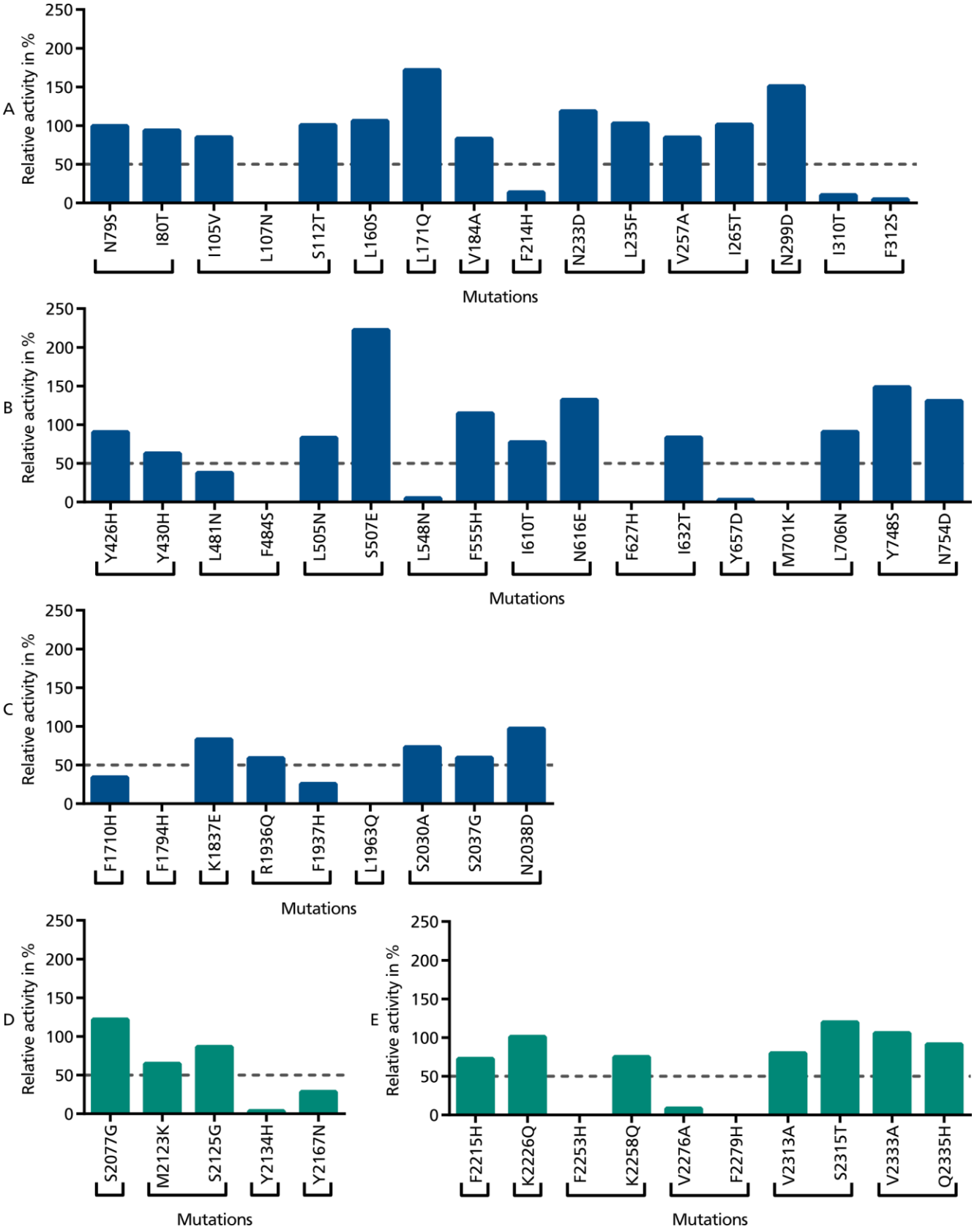

Figure 4-3: Relative activities of FVIII variants with single mutations. The FVIII activity of each single-mutation variant was calculated in relation to the FVIII activity of the control FVIII-6rs. The brackets indicate mutations, which belong to one cluster. (A) FVIII variants with mutations in the A1 domain. (B) FVIII variants with mutations in the A2 domain. (C) FVIII variants with mutations in the A3 domain. (D) FVIII variants with mutations in the C1 domain. (E) FVIII variants with mutations in the C2 domain.

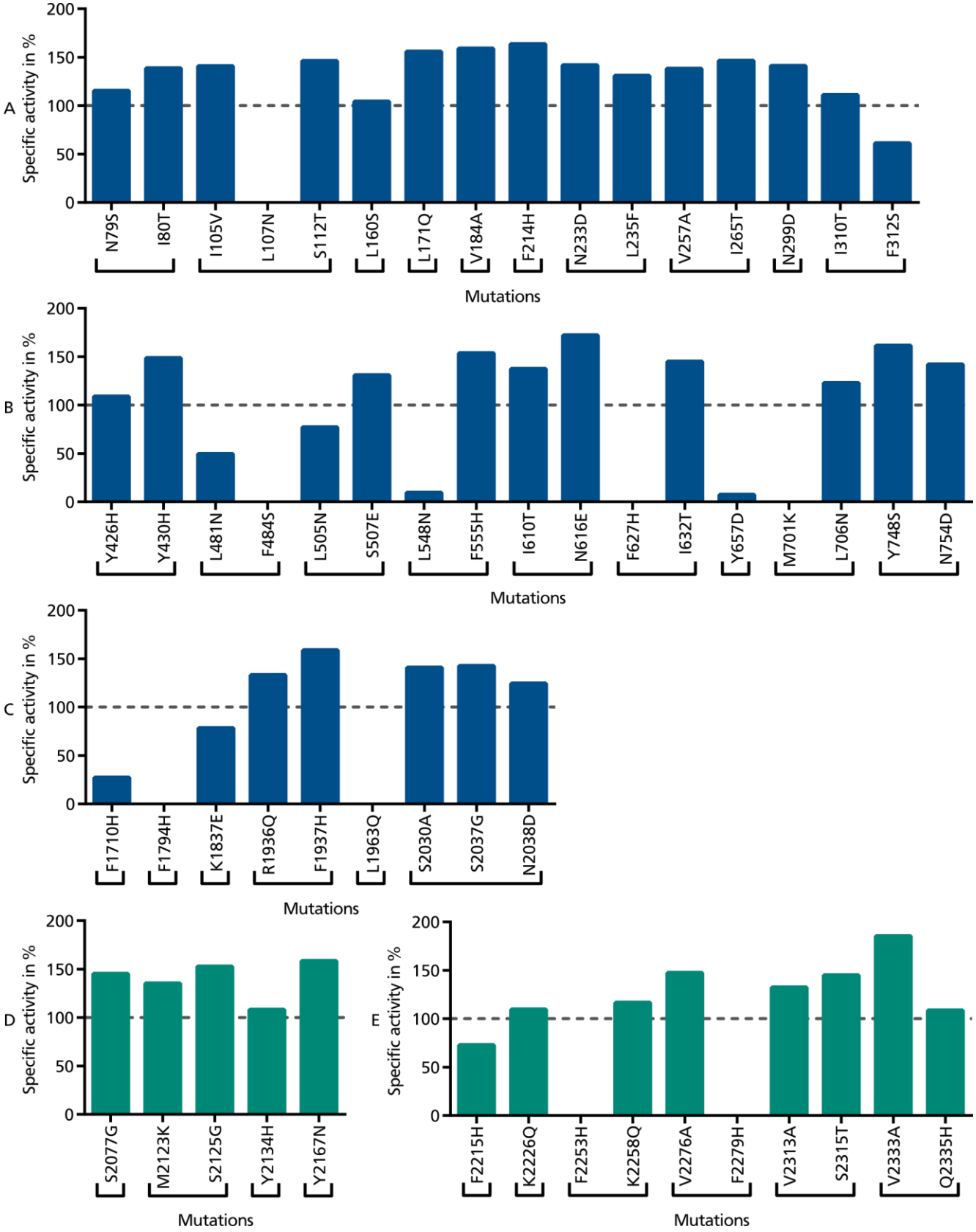

Figure 4-4: Specific activities of FVIII variants with single mutations. The relation of FVIII activity to FVIII antigen was calculated for each single-mutation variant. The brackets indicate mutations, which belong to one cluster. (A) FVIII variants with mutations in the A1 domain. (B) FVIII variants with mutations in the A2 domain. (C) FVIII variants with mutations in the A3 domain. (D) FVIII variants with mutations in the C1 domain. (E) FVIII variants with mutations in the C2 domain.

Prior to starting the combination of the mutations, five additional single mutations were tested. These mutations were proposed for four of the immunogenic clusters, which had to be excluded in the first screening round, due to non-functional mutated variants. These five mutations were originally not tested, as they had a lower calculated influence on the reduction of immunogenicity. However, analyses of the variants revealed only low or no FVIII activity in the supernatant, although the specific activities were around 100 % for three of the variants (Figure 4-5). Nevertheless, the mutations were not transferred to the second round of screening, as the activities were quite low, only exceeding the 50 % limit by about 10 % for I658T and N2137H.

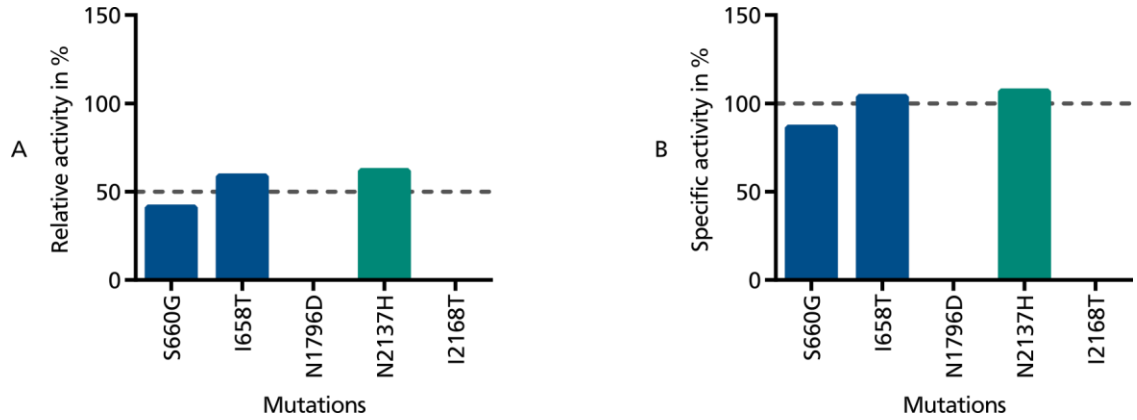

Figure 4-5: Results of the additionally tested single-mutation variants. (A) Relative activities of the FVIII variants. The FVIII activity of each single-mutation variant was calculated in relation to the FVIII activity of the control FVIII-6rs. (B) Specific activities of the FVIII variants. The relation of FVIII activity to FVIII antigen was calculated for each single-mutation variant.

Altogether, the first screening round led to a reduction from 57 mutations to 25 mutations (Figure 4-6). Exclusions were mainly based on the activity results, setting aside the mutations, which led to a reduction in FVIII activity. Additionally, only one mutation per immunogenic cluster was transferred to the second round of screening, further reducing the amount of mutations.

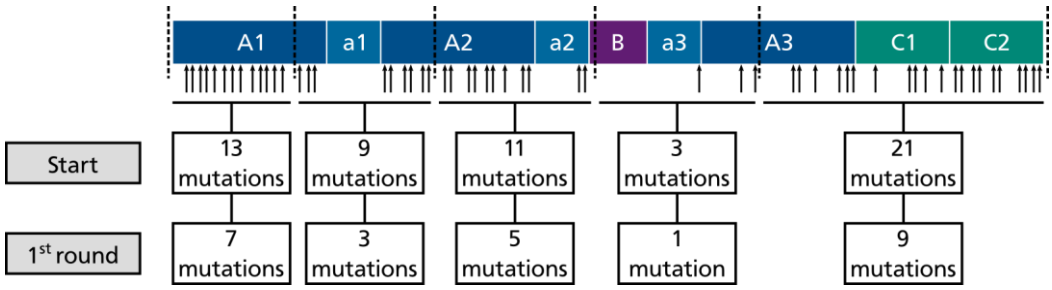

Figure 4-6: Summary of the first screening round. 57 single mutations were initially tested. 19 mutations were excluded due to low activities of the single-mutation variants and 13 mutations were excluded due to the decision that only one mutation per immunogenic cluster was transferred to the second round.

4.2.2. Second screening round

In the second screening round, the 25 mutations, leading to active FVIII variants in the first round, were combined. As no modelling of the FVIII variants was possible, the combination occurred in sections. This kept the identification of mutations, which led to an inactive FVIII, feasible. The sections were defined by the restriction sites, leading to section A1, A1A2, A2 and A3C1C2. The names indicated the comprised FVIII domains. The section BA3, comprising the remaining parts of the B domain and parts of the A3 domain, was missing, as only one mutation in this section was left after the first screening round. For every section one vector was designed containing all mutations, which led to FVIII variants with relative activities above 50 %. Additionally, one vector was designed containing only the mutations, which led to relative activities above 80 % and reduced the immunogenicity score for the cluster by at least 15 points. For section A1A2 and A2 only one vector was constructed, as all mutations had relative activities above 80 % and reduced the score by more than 15 points. Based on this, the vectors shown in Table 4-2 were designed.

Table 4-2: Mutations combined in the indicated sections of FVIII for the second screening round.

Section	Number of mutations	Relative activities of the single mutations	Incorporated mutations
A1	4	> 80 %	N79S, S112T, N233D, I265T
A1	7	> 50 %	N79S, S112T, L160S, L171Q, V184A, N233D, I265T
A1A2	3	> 80 %	N299D, Y426H, S507E
A2	5	> 80 %	F555H, N616E, I632T, L706N, Y748S
A3C1C2	6	> 80 %	N2038D, S2077G, S2125G, K2258Q, S2315T, V2333A
A3C1C2	9	> 50 %	R1936Q, N2038D, S2077G, S2125G, F2215H, K2226Q, K2258Q, S2315T, V2333A

The production of the FVIII variants occurred as described for the first round. After four days of production, the FVIII activity in the cell culture supernatant was determined. Activities comparable to or even better than the control FVIII-6rs were achieved in the sections A1 and A1A2 (Figure 4-7 A, bar one to three). Especially the combination of the three mutations in section A1A2 seemed to have a positive effect on either production or secretion of the FVIII variant, leading to more than twice the amount of FVIII-6rs. Due to the good activities, the seven mutations in A1 and the three mutations in A1A2 were taken to the third round. In section A2 the activity of the FVIII variant was below 80 % (Figure 4-7 A, bar four) and the two variants of the A3C1C2 section revealed activities below 40 % (Figure 4-7 A, bar five and six). Due to these results, the mutations combined in A2 and A3C1C2 had to be further analyzed. The specific activities for all combinations were above 100 %, indicating that the produced FVIII variants were functional, except for the variant with nine mutations in the A3C1C2 section (Figure 4-7 B). The low specific activity of this variant indicated that mainly inactive FVIII was secreted.

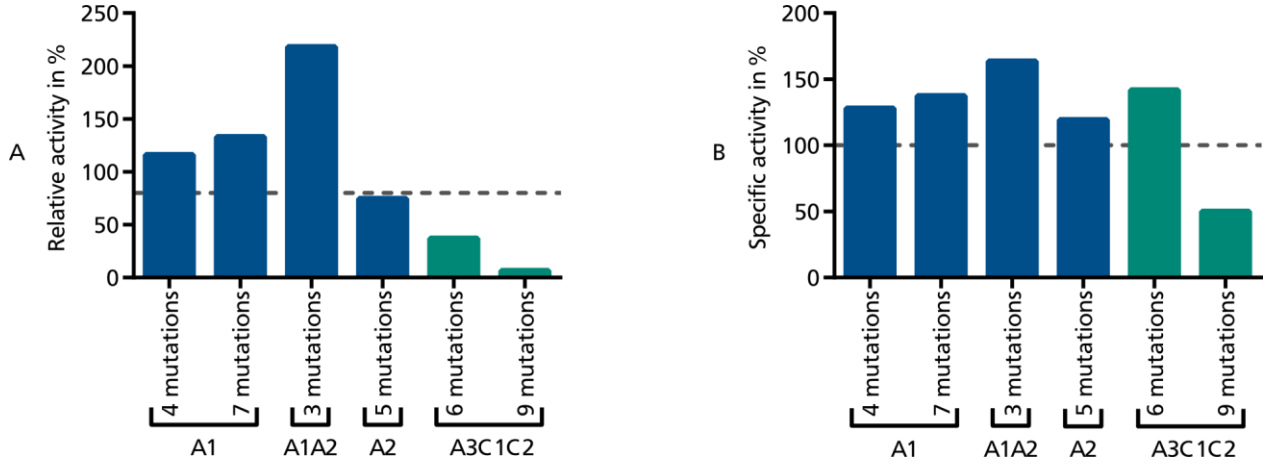

Figure 4-7: Results for the FVIII variants with combined mutations in section A1, A1A2, A2 and A3C1C2. (A) Relative activities of the FVIII variants. The FVIII activity of each variant was calculated in relation to the FVIII activity of the control FVIII-6rs. (B) Specific activities of the FVIII variants. The relation of FVIII activity to FVIII antigen was calculated for each variant.

In order to detect the mutations in the A2 and A3C1C2 section, which interfered with the activity of the FVIII variant, two design-of-experiment (DOE) matrices were generated. However, as full factorial designs, comprising every possible combination of the mutations, would have resulted in too many vectors, the five mutations in the A2 section were modelled in a half factorial design, whereas the six mutations in the A3C1C2 section were analyzed in an 8^{th} fraction fractional design. Setting aside the variants which were already tested (single-mutant, full-mutant and naïve variant), ten additional vectors were designed for the A2 section and 14 additional vectors were designed for the A3C1C2 section. As before, the variants were produced in HEK293-F cells and the FVIII activity in the supernatant was determined. The analysis revealed that mutation I632T in the A2 section probably was responsible for the reduced activity, as it was incorporated in all variants with activities below 100 % (Figure 4-8 A). In the A3C1C2 section three mutations, N2038D, S2125G and K2258Q, seemed to decrease the FVIII activity (Figure 4-8 B). However, an obvious influence on a decreased activity was only detectable for mutation S2125G. For N2038D and K2258Q it was not clearly identifiable whether their influence on the activity only occurred in combination with each other or S2125G.

The specific activities of all variants in the A2 and the A3C1C2 section were at least around 100 % (Figure 4-9). This revealed that the reduced FVIII activities compared to FVIII-6rs were probably due to production or secretion problems and not due to inactive FVIII. Based on the specific activity results no further mutations had to be excluded.

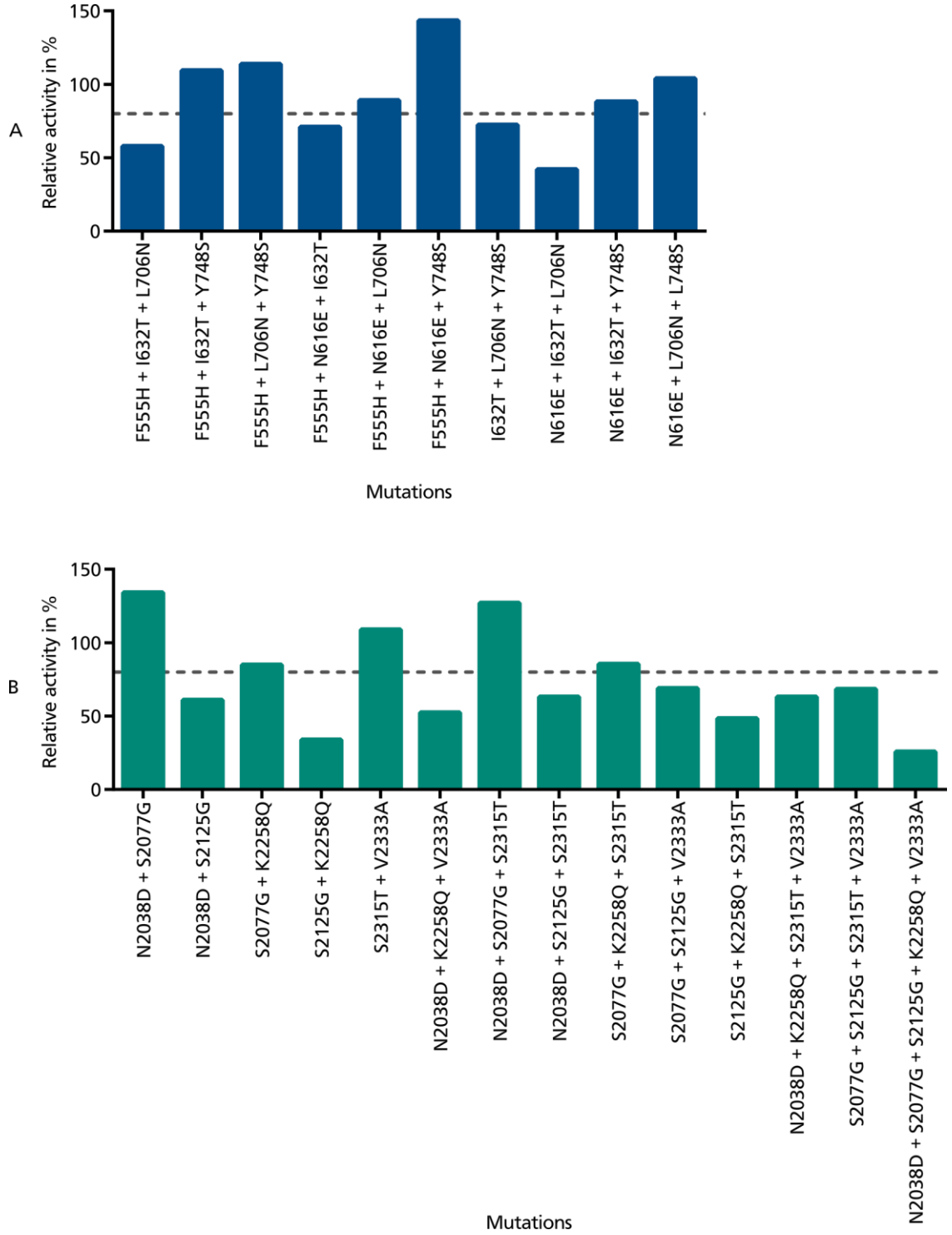

Figure 4-8: Relative activities of FVIII variants comprising different mutations based on DOE matrices. The FVIII activity of each variant was calculated in relation to the FVIII activity of the control FVIII-6rs. (A) Results for the FVIII variants with mutations in the A2 domain. (B) Results for the FVIII variants with mutations in the A3C1C2 domain.

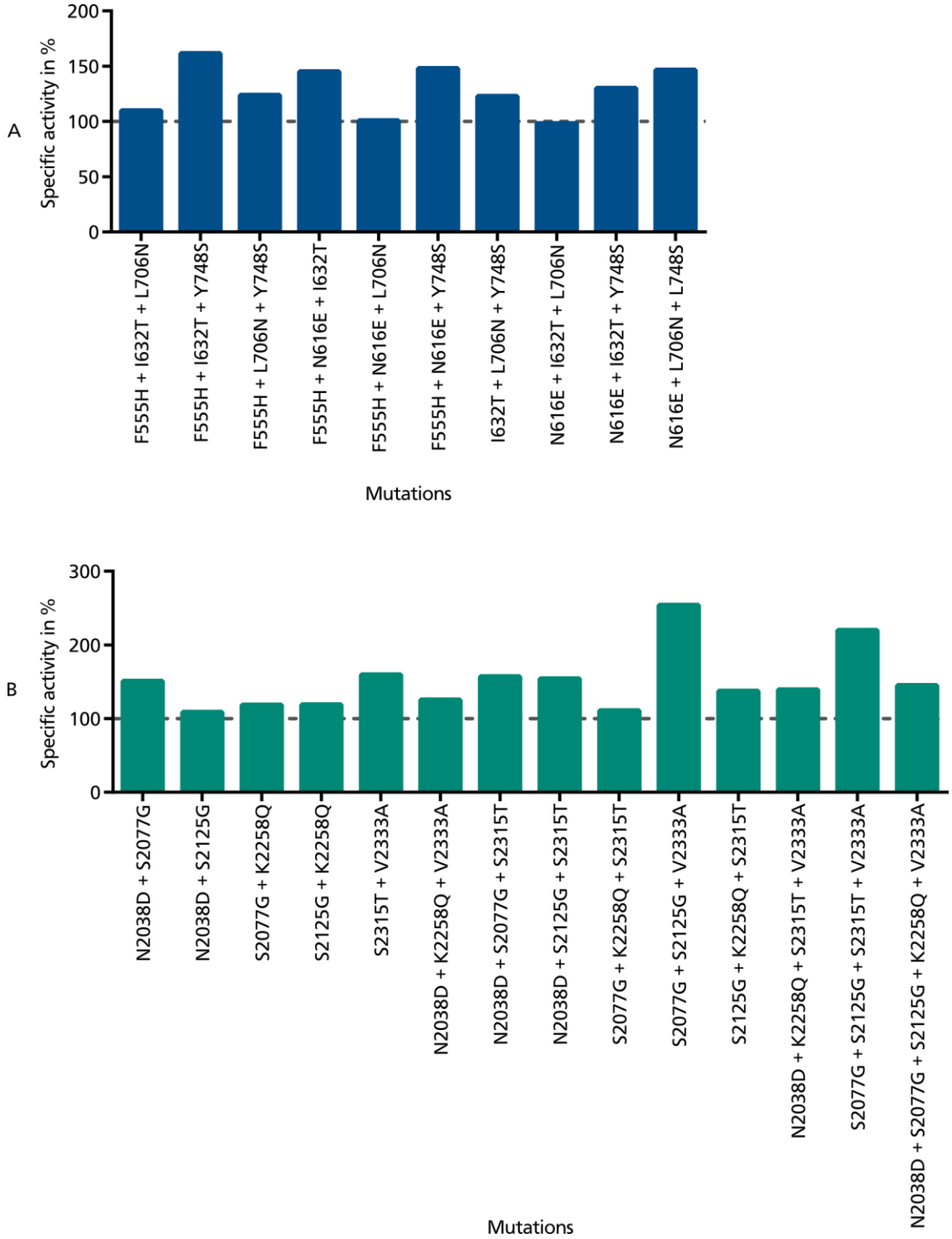

Figure 4-9: Specific activities of FVIII variants comprising different mutations based on DOE matrices. The relation of FVIII activity to FVIII antigen was calculated for each variant. (A) Results for the FVIII variants with mutations in the A2 domain. (B) Results for the FVIII variants with mutations in the A3C1C2 domain.

Based on the results from the DOE matrices, one vector for the A2 section and four vectors for the A3C1C2 section were designed. The four A3C1C2 vectors omitted either only mutation S2125G, or mutation S2125G in combination with K2258Q or N2038D, or all three mutations. The incorporated mutations in the five vectors are indicated in Table 4-3.

Table 4-3: Mutations combined in the sections A2 and A3C1C2 after testing different FVIII variants based on two DOE matrices.

Section	Number of mutations	Incorporated mutations
A2	4	F555H, N616E, L706N, Y748S
A3C1C2	3	S2077G, S2315T, V2333A
A3C1C2	4	N2038D, S2077G, S2315T, V2333A
A3C1C2	4	S2077G, K2258Q, S2315T, V2333A
A3C1C2	5	N2038D, S2077G, K2258Q, S2315T, V2333A

The measurement of the FVIII activity in the supernatant of the HEK293-F cells, transfected with the different vectors, revealed that the activity of the variant with four mutations in the A2 section was comparable to the activity of FVIII-6rs (Figure 4-10 A, first bar). In contrast to that, although all four A3C1C2 variants were active, the activity of the variants comprising five mutations and four mutations without mutation N2038D revealed a reduced activity compared to FVIII-6rs (Figure 4-10 A, bar two to five). This indicated that the exclusion of mutation N2038D alone had no influence on the production or secretion of FVIII, as the relative activity remained low. In contrast to that, the exclusion of K2258Q led to an increase in FVIII activity. However, although not effective as a single deletion, removal of N2038D in combination with K2258Q had an additive effect and further improved the FVIII activity of the variant. Nevertheless, the combination of four mutations, still containing the N2038D, was transferred to the third round. This was due to the aim to incorporate as many mutations as possible. Additionally, the relative activity of this variant was around 100 % and similar to the results for combinations in other sections. The specific activities for all variants were at least 100 %, indicating that only active FVIII was present (Figure 4-10 B).

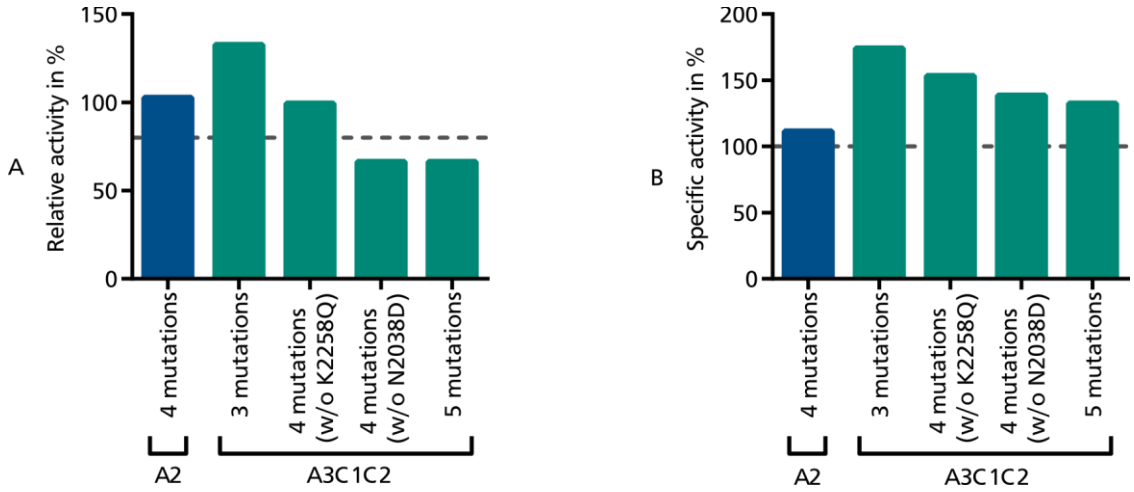

Figure 4-10: Results for the FVIII variants with combined mutations in the sections A2 and A3C1C2 after the DOE matrices. (A) Relative activities of the FVIII variants. The FVIII activity of each variant was calculated in relation to the FVIII activity of the control FVIII-6rs. (B) Specific activities of the FVIII variants. The relation of FVIII activity to FVIII antigen was calculated for each variant.

Finally, the second screening round revealed 19 mutations, which could be combined in five sections (Figure 4-11). For section A1 and A1A2, the combination of all mutations from the first round was feasible. This was not possible for the sections A2 and A3C1C2. Based on DOE matrices one mutation had to be excluded in the A2 section and five mutations had to be excluded in the A3C1C2 section.

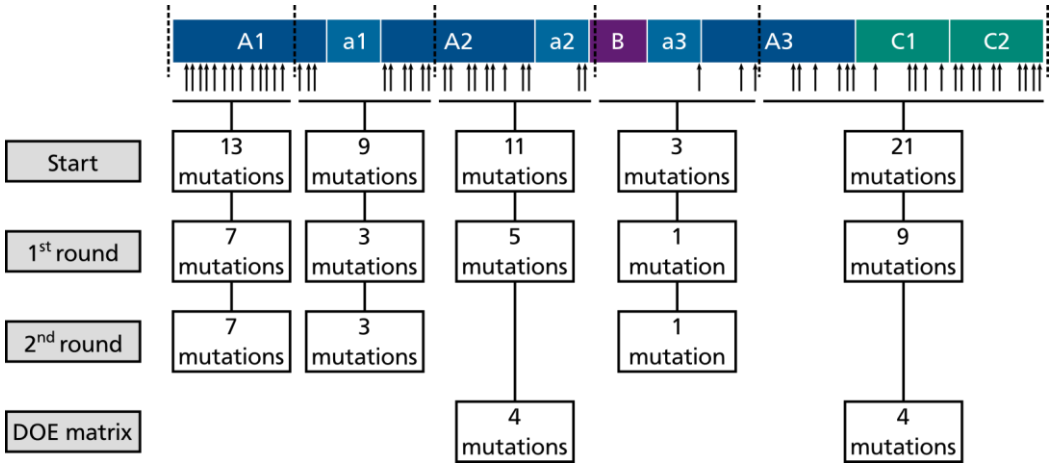

Figure 4-11: Summary of the first a second screening round. Of the 25 mutations from the first round, 6 mutations had to be excluded in the second round, as they led to a reduction of the FVIII activity, when combined with other mutations.

4.2.3. Third screening round

In the third round all combined mutations, leading to functional FVIII variants in the second round, were incorporated into one vector. However, as the A3C1C2 section revealed to be mostly influenced by the incorporation of mutations, an additional vector was designed with no mutations in section A3C1C2, in order to compare the activities. This led to two vectors comprising in total 15 and 19 mutations. The analysis of the FVIII activity in the supernatant revealed activities, for both vectors, at least comparable to FVIII-6rs, whereas the variant with the 15 mutations revealed a higher concentration of active FVIII compared to the one with the 19 mutations (Figure 4-12 A). The specific activities were nearly 100 % for the FVIII-15M and above 100 % for FVIII-19M (Figure 4-12 B).

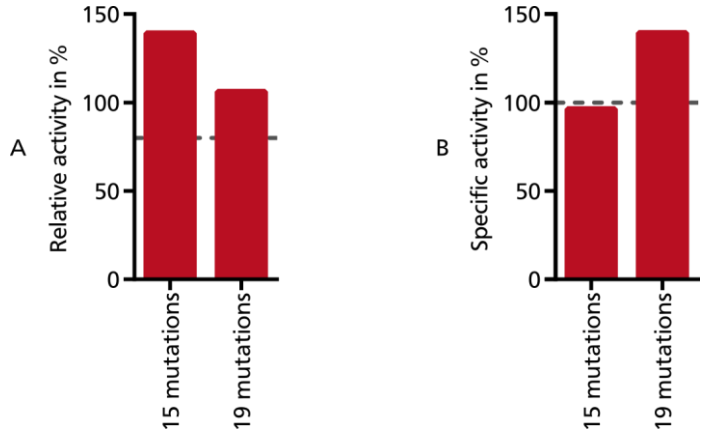

Figure 4-12: Results from the third screening round of the FVIII variants comprising 15 or 19 mutations in the whole molecule. (A) Relative activities of the FVIII variants. The FVIII activity of each variant was calculated in relation to the FVIII activity of the control FVIII-6rs. (B) Specific activities of the FVIII variants. The relation of FVIII activity to FVIII antigen was calculated for each variant.

Of the initially tested 57 mutations 19 mutations were finally incorporated into the FVIII sequence, leading to the new variant FVIII-19M. The FVIII-19M was preferred over the FVIII-15M, as the aim was to incorporate as many mutations as possible, in order to gain a maximal reduction in the immunogenicity score while conserving FVIII activity. Additionally, the activity of FVIII-19M was comparable to the control FVIII-6rs. The three screening rounds are summarized in Figure 4-13.

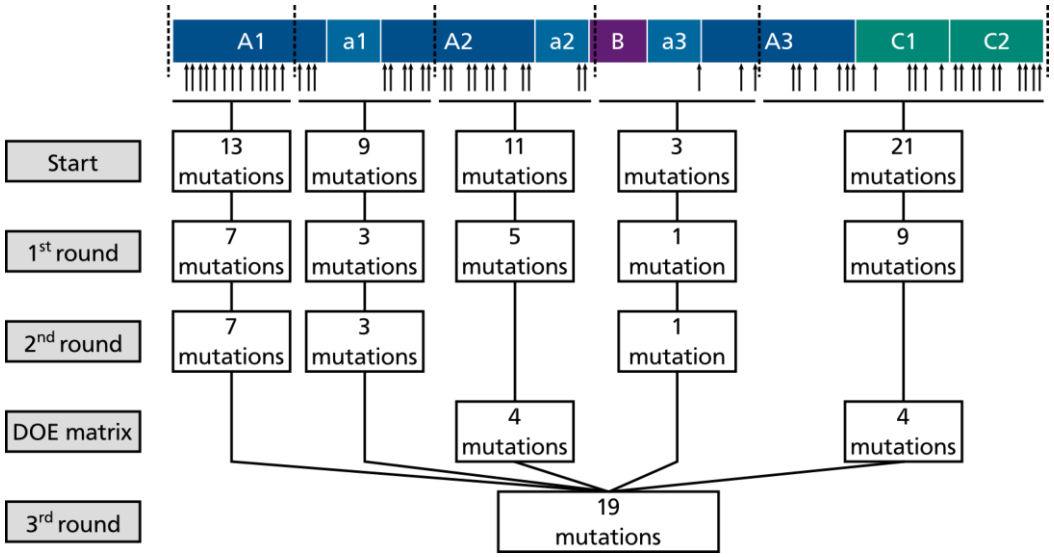

Figure 4-13: Summary of all three screening rounds. In the third round, all mutations from the second round were combined in one FVIII molecule.

Due to the incorporation of the 19 mutations into the FVIII sequence, the initial immunogenicity score of the FVIII-6rs of 7.01 was reduced to -10.55 for the FVIII-19M. The immunogenicity score indicates the immunogenicity of the protein of interest in relation to a protein with a random sequence. The immunogenicity score of the random protein is set to 0. In order to be able to compare the scores for different proteins of different length, the score was given per 1000 of the 9-mers, to which a protein is split for *in silico* analysis (3.1). The scores for FVIII-6rs and FVIII-19M and scores of other proteins are illustrated in Figure 4-14.

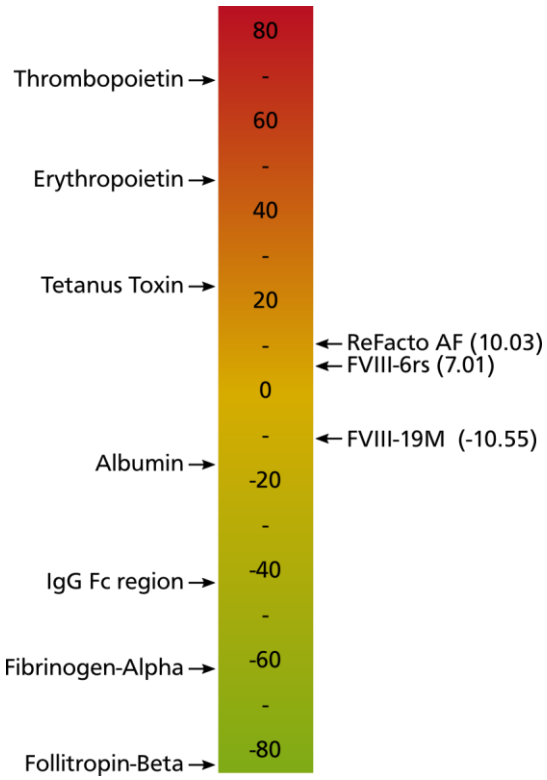

Figure 4-14: Immunogenicity scale. The score indicates the immunogenicity of a protein. For comparability, the immunogenicity score of a protein is indicated in relation to a protein with a randomized sequence. The immunogenicity score of the randomized protein is 0. The immunogenicity score for each protein is given per 1000 9-mers, in order to be able to compare proteins of different lengths.

4.3. Production and purification of FVIII-19M and FVIII-6rs

The FVIII-19M and the reference molecule FVIII-6rs were produced and purified for further analyses. This production of higher amounts, compared to the screening rounds, occurred in CAP-T cells. Per 12.5 ml cell culture, $10 \cdot 10^6$ CAP-T cells were transfected with 5 μg of plasmid (3.2.3.3). The first production of FVIII-19M occurred in a total volume of 800 ml. Further productions were performed by Cevec under the same conditions, leading to a 400 ml FVIII-19M production and a 400 ml and a 800 ml FVIII-6rs production. The FVIII of all four productions was purified by FPLC. The purification began with a SAEx, followed by an AC and in the final step a SEC (3.5.1). In order to keep the required FVIII volumes for cell culture experiments as low as possible, the FVIII products were concentrated after purification (3.5.1). Each purification was performed during one day, except the last purification of FVIII-6rs. In this case, the elution from the AC was frozen at -80 °C and thawed the following day, proceeding with the SEC. An exemplarily chromatogram for each chromatography is depicted in Figure 4-15 (SAEx), Figure 4-16 (AC) and Figure 4-17 (SEC). The fractions, containing FVIII, were taken according to the chromatogram and are indicated by green, dashed boxes. In every chromatogram, an UV peak was clearly detectable. This was the main indicator for fractions containing protein. The pooled fractions 9-12 from the SAEx were diluted 1:2 in AC Equilibration Buffer and transferred to the AC column. The eluted fractions 21 and 22 from the AC, containing the purified FVIII, were pooled and the buffer was exchanged to FVIII Formulation Buffer by SEC. For the selection of the fractions from the SEC, a stable conductivity peak was important in addition to a high UV peak. Based on this, the fractions 6-9 were pooled, and finally concentrated.

Figure 4-15: Chromatogram of the SAEx. The chromatography was performed according to the protocol. The UV peak indicated that fractions 9 to 12 contained the eluted proteins (green, dashed box). The fractions were pooled and taken to the AC.

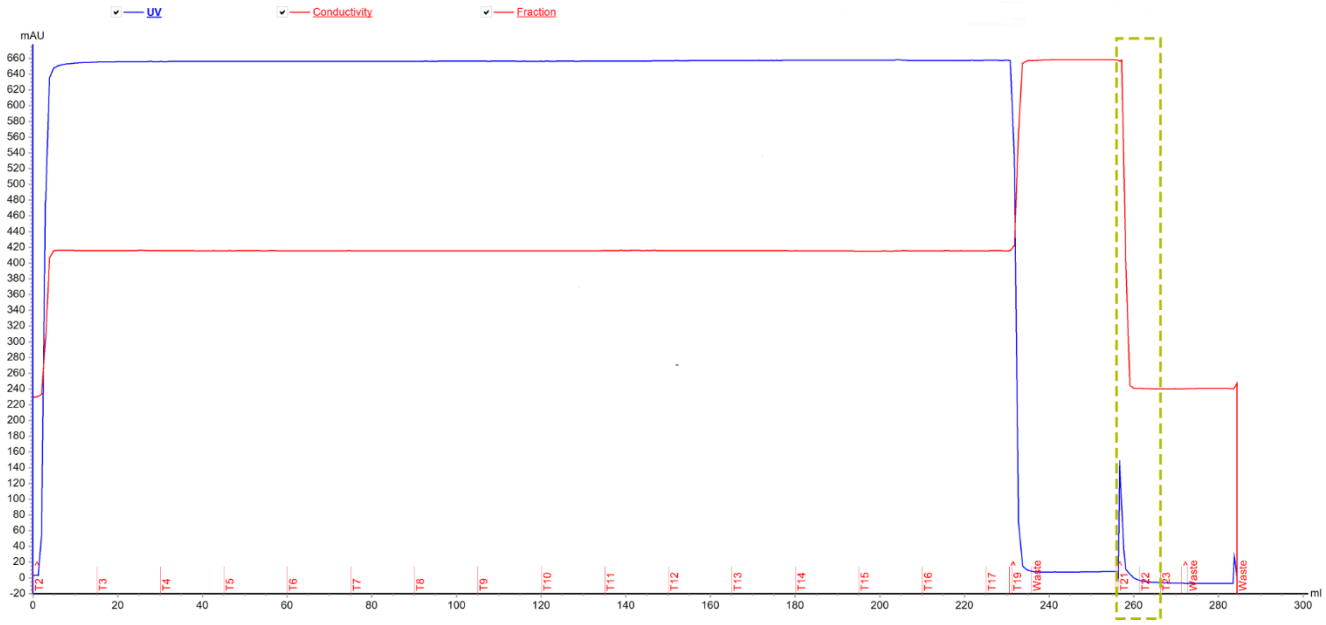

Figure 4-16: Chromatogram of the FVIII AC. The chromatography was performed according to the protocol. The UV peak indicated that fractions 21 and 22 contained the eluted FVIII (green, dashed box). The fractions were pooled and taken to the SEC.

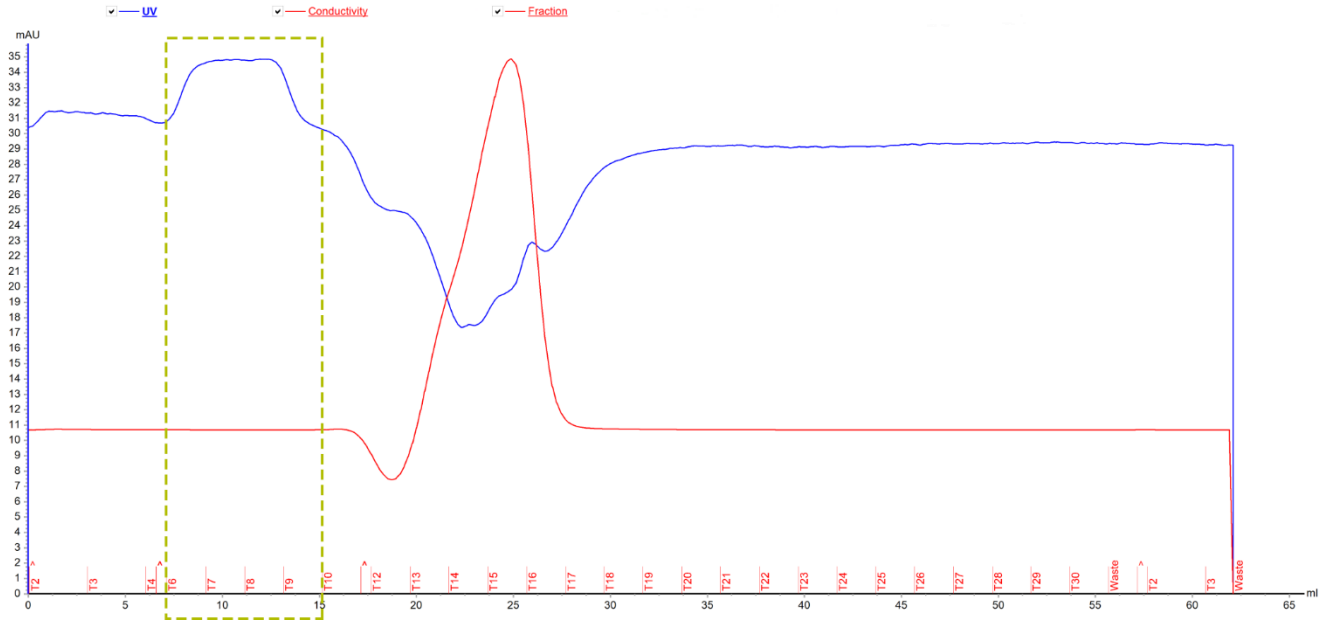

Figure 4-17: Chromatogram of the FVIII buffer exchange by SEC. The chromatography was performed according to the protocol. The high UV peak and the stable conductivity indicated that fractions 6 to 9 contained the buffer-exchanged FVIII (green, dashed box). The fractions were pooled and concentrated.

During all purification steps samples were taken, including wash and flow through samples, in order to determine the FVIII activity and antigen of each step. The activity was determined in parallel to the purification (3.4.1), whereas the antigen was determined afterwards from frozen samples (3.4.3). Figure 4-18 illustrates the FVIII activities and the specific activities for all purification steps of the two FVIII-19M and the two FVIII-6rs purifications. In the case of purification from 800 ml supernatant, the volume was split and the SAEx was performed twice. The indicated values are the mean of the results derived from both runs. The activity values illustrate the constant increase of the FVIII concentration in the eluates of the different chromatographic columns. The highest increase in concentration was

achieved in the last step by concentration. The decrease in active FVIII concentrations from the elution of the SAEx to the source of the AC was due to the 1:2 dilution of the elution volume with AC Equilibration Buffer. In addition to that, the decrease in FVIII concentration from the elution of the AC to the elution of the SEC was also due to an increase in total volume during the buffer exchange. The very low specific activities in the flow through and wash fraction of the AC column indicate that mainly inactive FVIII was lost during this step. All elution fractions and the concentrated, purified FVIII revealed specific activities of about 100 % and above, indicating that only active FVIII was present.

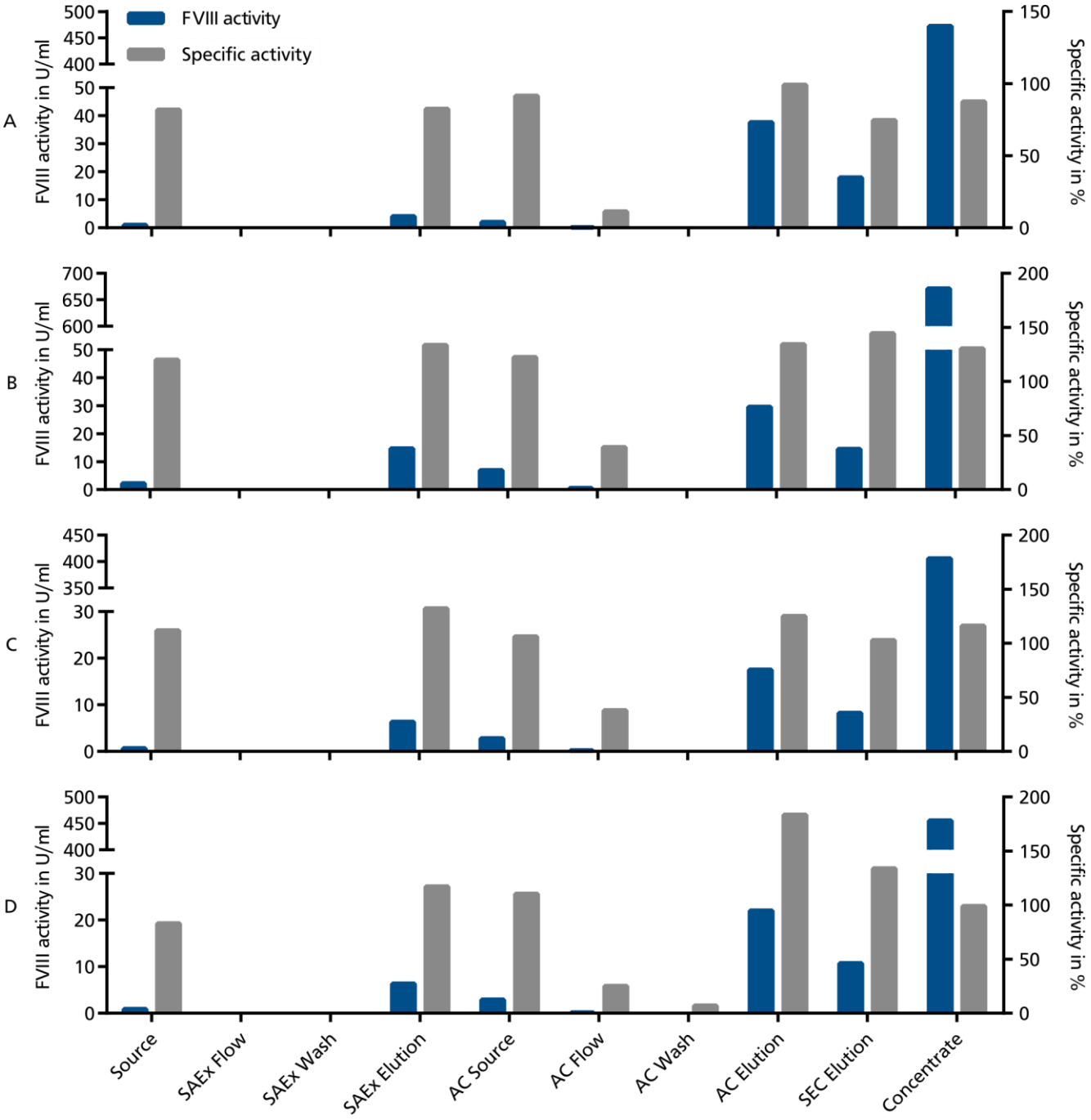

Figure 4-18: Activities and specific activities of FVIII-19M and FVIII-6rs in different purification steps. The concentrations of active FVIII (left y-axis) and the specific activities (right y-axis) are indicated for every purification step. In the case that two SAEx were performed, the indicated values are the mean values of the two performed runs. (A) First purification of FVIII-19M from an 800 ml batch. (B) Second purification of FVIII-19M from a 400 ml batch. (C) First purification of FVIII-6rs from a 400 ml batch. (D) Second purification of FVIII-6rs from an 800 ml batch.

The yield of the steps, compared to the total amount of FVIII activity in the source, is displayed in Figure 4-19 for every purification. The data revealed that the concentrating step was one of the steps, which led to the highest loss of FVIII. However, the loss seemed to be associated with manufacturing differences of the filters, as all samples were handled in the same way but different batches of filters were used. Another step associated with loss of FVIII was the SAEx, especially when FVIII-19M was purified. It was not clear why FVIII-19M was lost during SAEx, as the mutations even led to the introduction of five negatively charged amino acids. One reason might have been that the buffers for the different chromatographic methods were not especially adapted to FVIII-19M. In total, the yield of FVIII was between 40 % and 70 % after the FPLC and reduced to 40 % to 50 % after concentration.

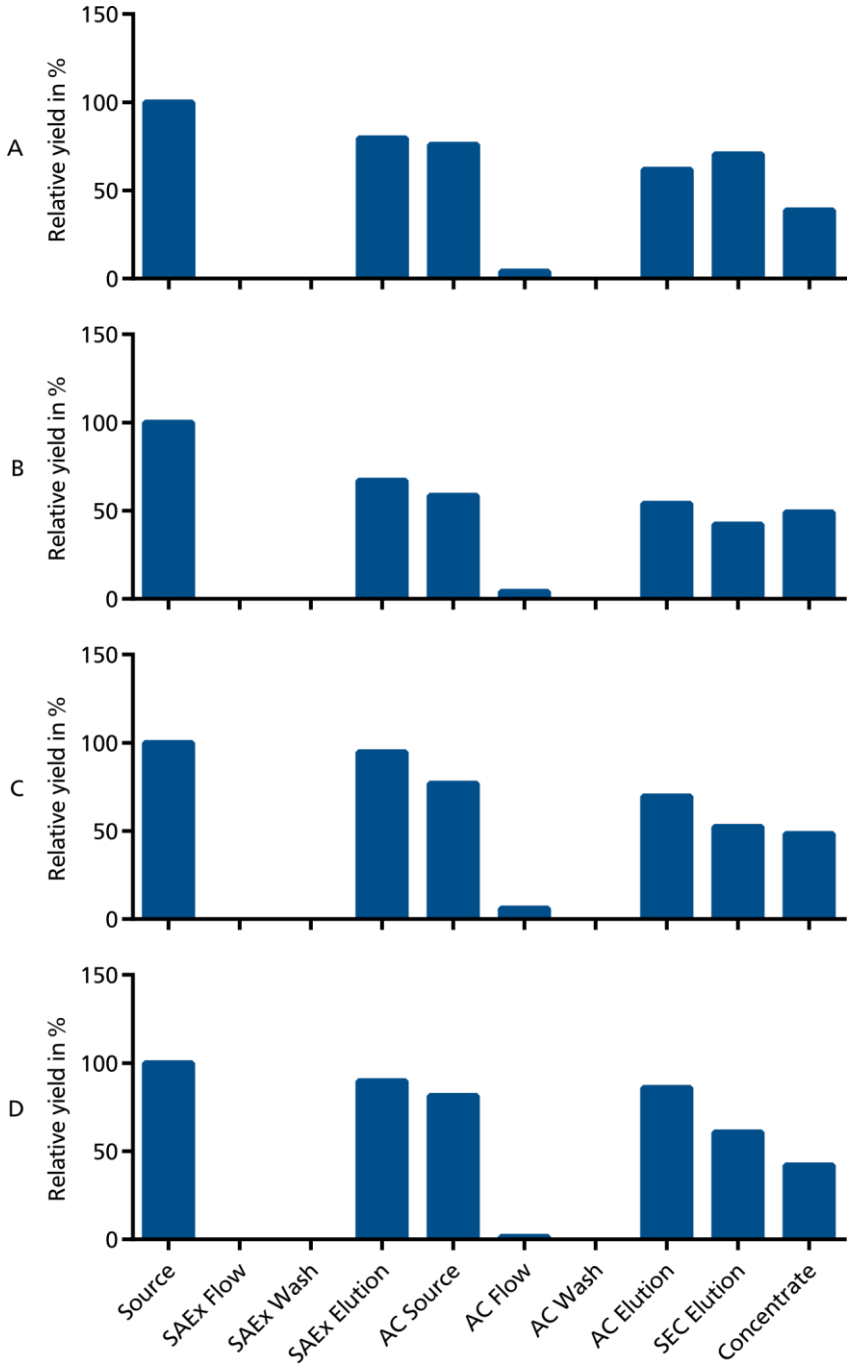

Figure 4-19: Yield of FVIII-19M and FVIII-6rs during the purification steps. The yield of each step was calculated in reference to the total amount of active FVIII in the source. (A) First purification of FVIII-19M from an 800 ml batch. (B) Second purification of FVIII-19M from a 400 ml batch. (C) First purification of FVIII-6rs from a 400 ml batch. (D) Second purification of FVIII-6rs from an 800 ml batch.

The purification steps were additionally monitored via SDS-PAGE (3.5.2) and Western Blot (3.5.3), in order to detect contaminations and degraded FVIII. For each purification a SDS-PAGE with a total protein stain and a Western Blot, specifically detecting FVIII, was performed. Figure 4-20 displays the SDS-PAGE of the first purification of FVIII-19M and FVIII-6rs. The SDS-PAGE of the other purifications can be found in the Appendix (Figure A-1 and Figure A-2). The total protein stain of the SDS-PAGE revealed that the SAEx mainly led to concentration of the proteins, as only low amounts of protein were lost during flow and wash. The purification of FVIII from other proteins occurred during the AC, as most of the contaminating proteins were detectable in this flow through. The lower intensity of these bands compared to the bands of the SAEx elution was due to the 1:2 dilution of the SAEx elution sample prior to the application onto the AC column. No proteins were visible in the SEC elution, as contaminating proteins were lost during AC and the FVIII concentrations were too low to be visualized.

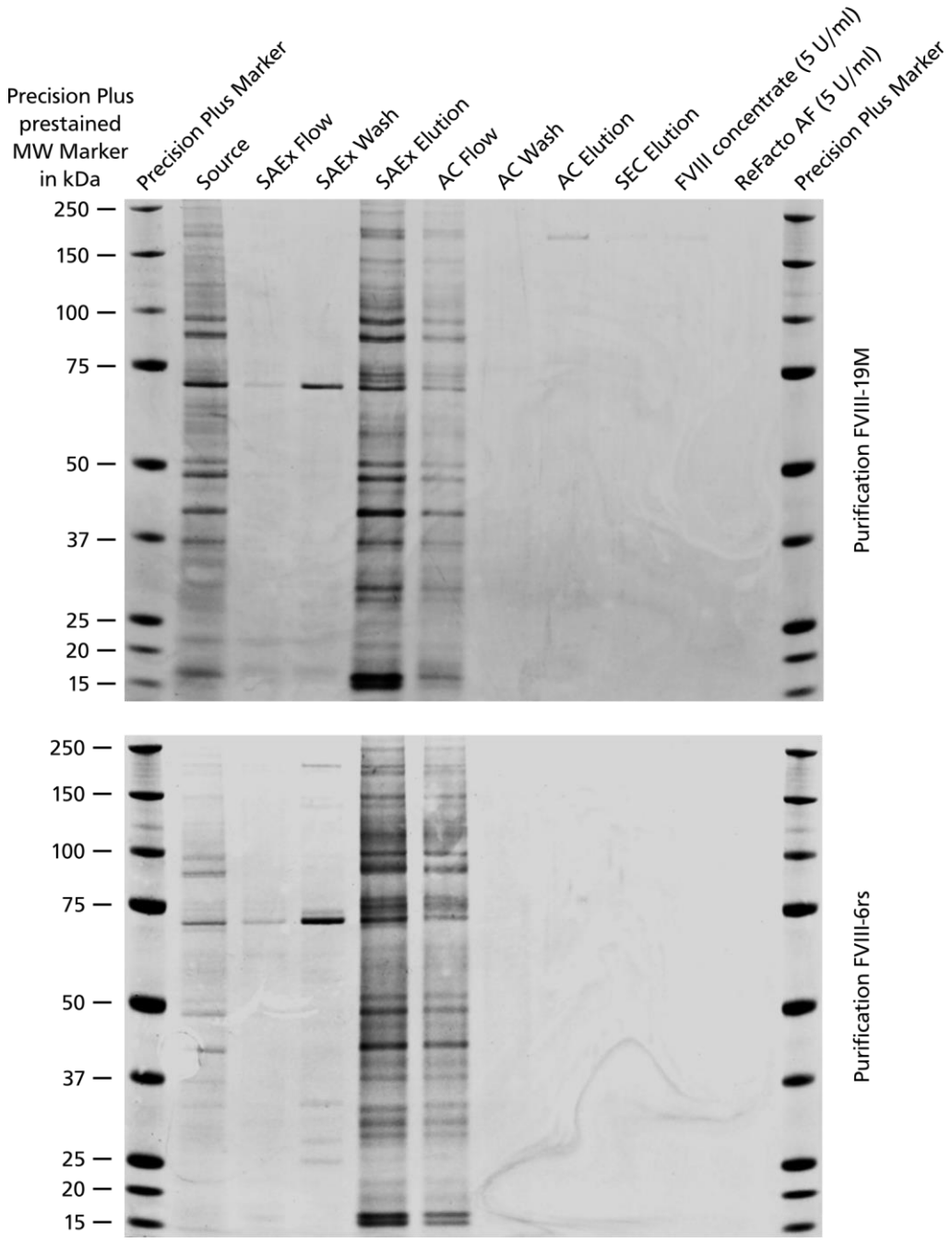

Figure 4-20: SDS-PAGE of the first FVIII-19M and FVIII-6rs purification developed with Imperial Protein Stain. The samples from the purification were not pre-diluted, except for the FVIII concentrates and the reference ReFacto AF, which were set to 5 U/ml FVIII.

As the FVIII amounts were too low to be visualized on the SDS-PAGE, due to the high amounts of contaminating proteins, Western Blots were performed (Figure 4-21, Figure A-3 and Figure A-4). FVIII was specifically detected with a polyclonal anti-FVIII antibody and revealed to be present in all source and elution fractions. As already detected in the chromogenic FVIII assay, some FVIII was also present in the flow through and wash fractions of the AC. Although the FVIII in these fractions was not degraded, specific activity values revealed that this FVIII was mainly inactive (Figure 4-18). Some degraded FVIII was visible in the elution of the SAEx but was removed during AC. However, concentrating FVIII seemed to have led to the degradation of a small amount of FVIII.

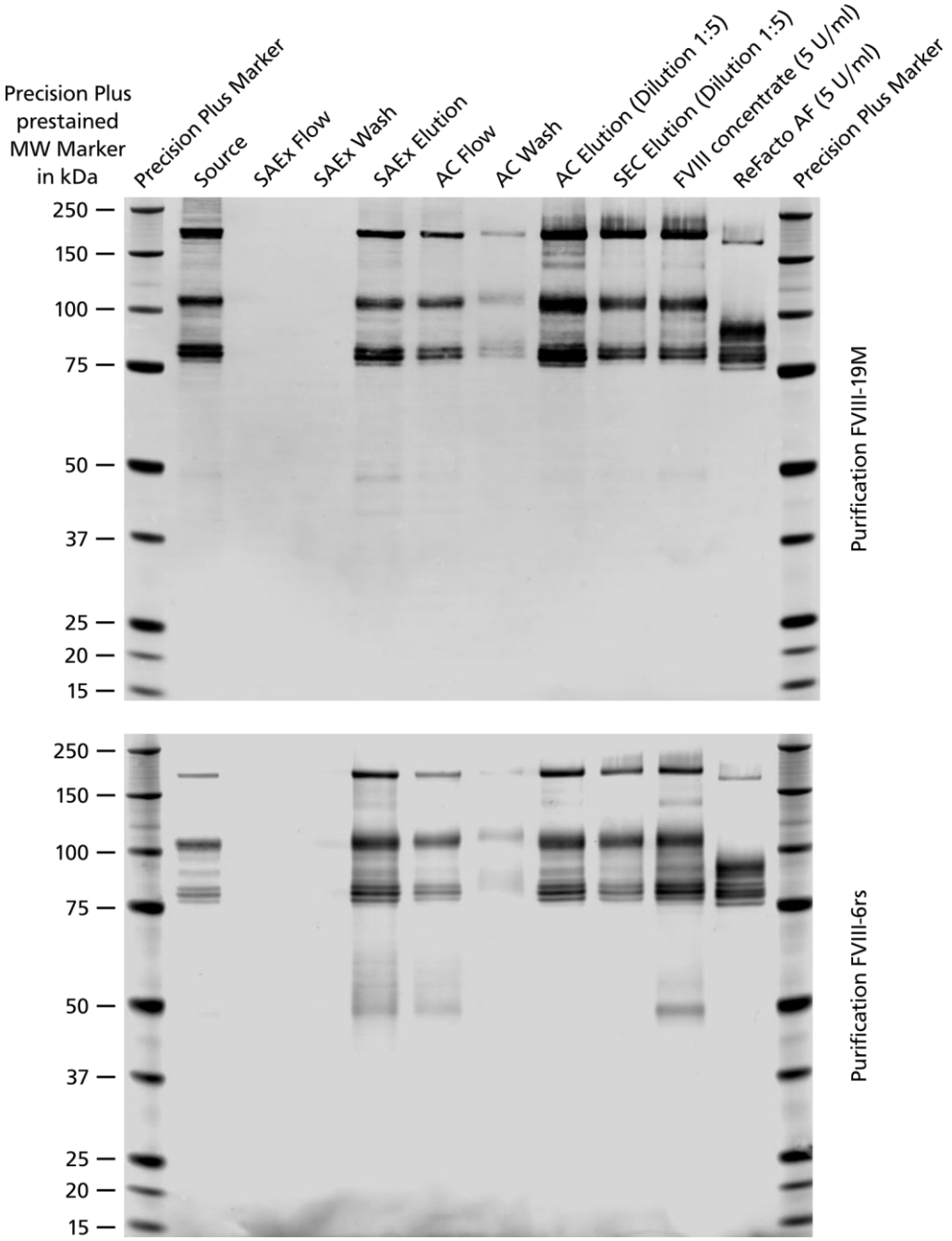

Figure 4-21: Western Blot of the first FVIII-19M and FVIII-6rs purification. The samples were not pre-diluted, except for the elutions from the AC and the SEC, which were pre-diluted 1:5. The FVIII concentrates and the reference ReFacto AF were set to 5 U/ml FVIII. The upper band (≈ 200 kDa) represents single-chain FVIII, not processed by furin. The second band (≈ 110 kDa) represents the heavy chain and the following set of bands (≈ 80-90 kDa) are differently glycosylated forms of the light chain. The bands around 50 kDa represent degraded FVIII. FVIII was detected with the primary polyclonal sheep anti-human Factor VIII antibody and the secondary donkey anti-sheep IgG IRDye 800CW.

Due to the fact that high amounts of FVIII-19M and FVIII-6rs were needed for the analysis of the proteins themselves as well as for the DC-T cell Assay and the *in vivo* studies, more protein had to be produced. These productions and purifications were performed by Cevec, the provider of the CAP-T cell line. The cultivation, transfection and production protocols were similar to the ones described in 3.2.3. Differences only occurred during purification. Although the main purification step, the AC with the VIIISelect medium, was the same, Cevec performed a tangential flow filtration (TFF) prior to the AC instead of a SAEx. The TFF led to a concentration of the cell culture supernatant and the buffer was exchanged to the AC Equilibration Buffer. After the AC, the buffer exchange to FVIII Formulation Buffer occurred also via SEC. A Western Blot of the differently purified FVIII molecules revealed that no variations were detectable between the four previously described purifications and the purifications performed by Cevec (Figure 4-22).

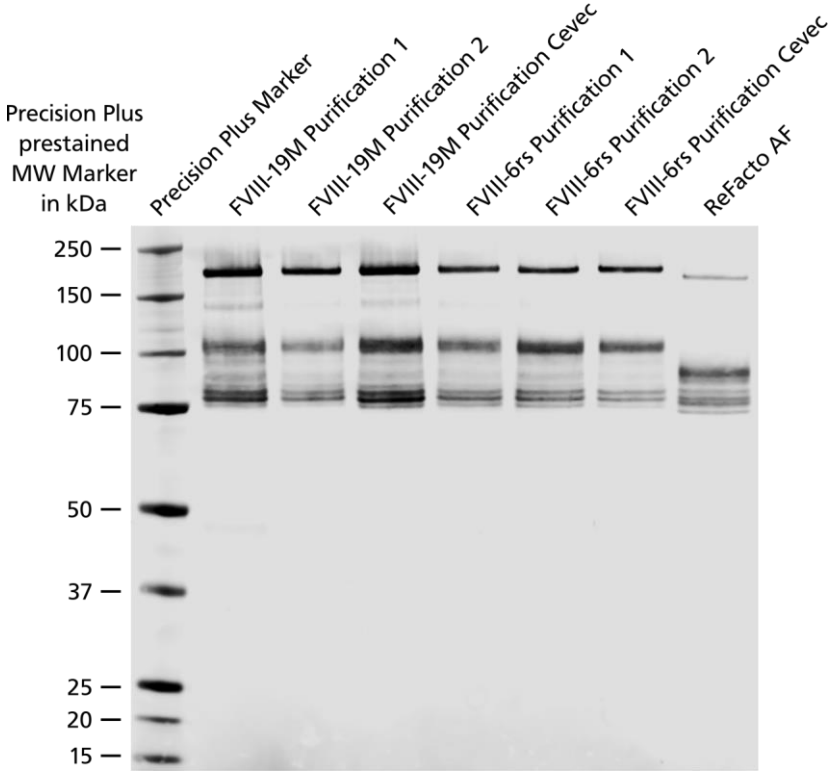

Figure 4-22: Western Blot of the different FVIII purifications. All samples were diluted to 5 U/ml FVIII. The FVIII-19M and FVIII-6rs purifications show similar band patterns for the single chain (≈ 200 kDa), heavy chain (≈ 110 kDa) and light chain (≈ 80-90 kDa). FVIII was detected with the primary polyclonal sheep anti-human Factor VIII antibody and the secondary donkey anti-sheep IgG IRDye 800CW.

The SDS-PAGE and Western Blots revealed that the productions and purifications of FVIII-19M and FVIII-6rs were successful. The purification yield was similar for both products, although the total amount of active FVIII-6rs was lower, due to lower initial concentrations in the cell culture supernatant. Additionally, the purified products derived from the different productions did not reveal differences on a Western Blot.

4.4. Analyses of FVIII-19M and FVIII-6rs

The produced FVIII-19M and FVIII-6rs were at first analyzed regarding their chromogenic and clotting activity in comparison to the determined antigen values. In further analyses, post-translational modifications and functionality of FVIII-19M were compared to FVIII-6rs and the two clinically used rFVIII products ReFacto AF and Nuwiq. Both commercial products are also B-domain deleted. ReFacto AF is produced in CHO cells, whereas Nuwiq is produced in HEK cells. The analyses comprised Western Blots detecting FVIII heavy and light chain, thrombin cleavage, glycosylation and sulfation, 2D-DIGE and the functional assays ROTEM, TGA and a vWF-FVIII ELISA.

4.4.1. Activities and specific activities

The first analysis was the comparison of the activity and antigen values of the FVIII-19M and FVIII-6rs from the different productions, in order to ensure similarity for the following experiments. For each production the relation of the amount of active FVIII to the amount of FVIII antigen, the specific activity, was calculated. The FVIII activity was either determined with the chromogenic or the clotting method (3.4.1 and 3.4.2), whereas the antigen value was measured via ELISA (3.4.3). This led to two different specific activities, one based on the chromogenic activity and the other based on the clotting activity. The results are illustrated in Figure 4-23. The specific activities based on the chromogenic activities (Figure 4-23 A), revealed similar results when comparing each of the four productions of the FVIII-6rs and FVIII-19M. Additionally, the median of the four productions was not significantly different between FVIII-6rs and FVIII-19M (Figure 4-23 A and Table A-1). The specific activities based on the clotting activities were lower compared to the specific activities based on the chromogenic activities (Figure 4-23 B). Generally, this is a known phenomenon for rFVIII products in the clotting assay. The reason for this is not yet elucidated[221]. However, this did not explain the reduced specific activity of FVIII-19M compared to FVIII-6rs. Although the difference was not significant (Table A-2), the result hinted towards a slight impairment of the clotting cascade with FVIII-19M, which was not detectable with the chromogenic activity test. Nevertheless, when comparing the specific activities for the four productions of each product, the results were similar. Based on this, all productions were used for further experiments. However, the different productions were not mixed within one block of experiments. The protein analyses were performed with the FVIII-6rs and FVIII-19M from the first Cevec purification, the *in vitro* assays were performed with the material from the two purifications shown in chapter 4.3 and the *in vivo* studies were performed with the material of the second production and purification by Cevec.

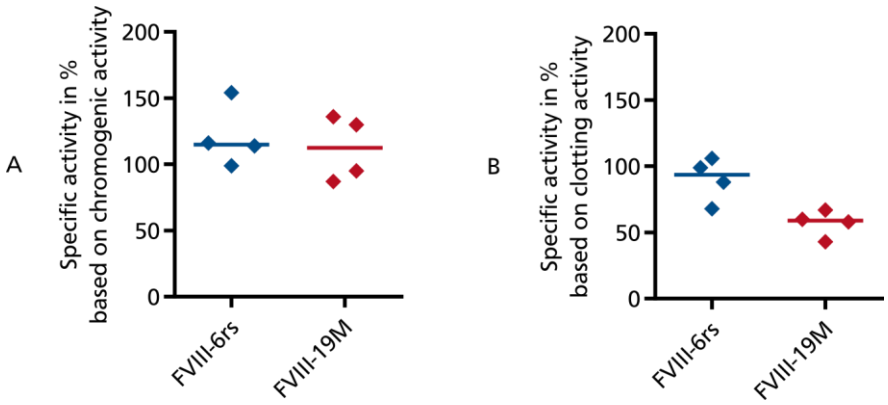

Figure 4-23: Specific activities of the four independent productions of FVIII-6rs and FVIII-19M. (A) Specific activities based on the chromogenic FVIII activity measurement. The line indicates the median of the four measurements. (B) Specific activities based on the clotting FVIII activity measurement. The line indicates the median of the four measurements.

4.4.2. Western Blots and 2D-DIGE

The Western Blot (3.5.3), detecting light chain and heavy chain of FVIII, revealed that the constructs FVIII-19M and FVIII-6rs were secreted nearly in equal parts as double-chain FVIII, comprising heavy (red band) and light chain (green bands), and as single-chain FVIII (yellow band) (Figure 4-24). In contrast to that, the commercially available FVIII products ReFacto AF and Nuwiq were mainly present in the double-chain form. The different molecular weights of the heavy chains of the four FVIII products were due to the deletion of a larger B domain fraction in ReFacto AF and Nuwiq, compared to FVIII-19M and FVIII-6rs, leading to a lower molecular weight. The slight differences in the molecular weight of the light chain were probably due to differences in processing and post-translational modification. The detected variations in the ratios of double-chain to single-chain FVIII as well as the differences in post-translational modification were probably due to the different cell lines (CHO, HEK and CAP-T) used for the production of the FVIII variants.

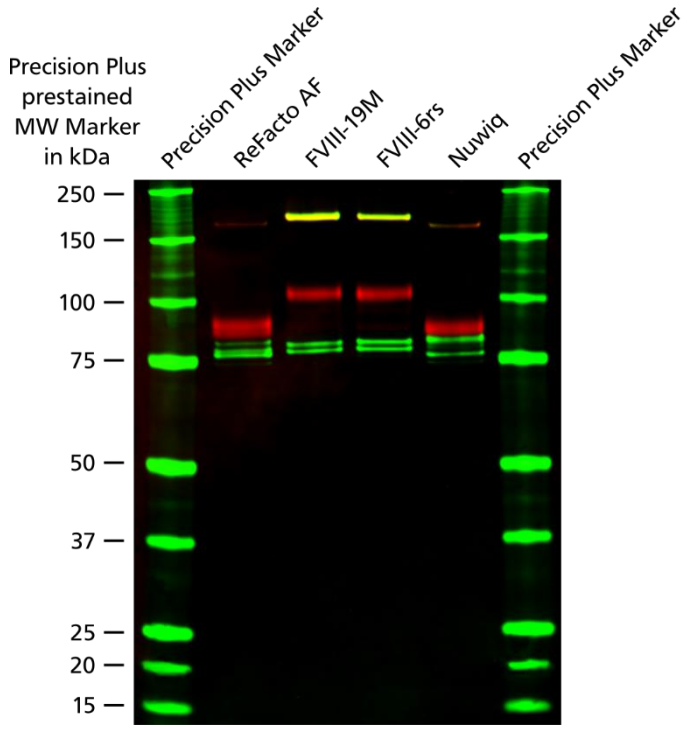

Figure 4-24: Western Blot specifically detecting the FVIII heavy and light chain. The different FVIII products were applied at a concentration of 5 U/ml. The heavy chains (≈ 95-110 kDa) are indicated in red and the light chains (≈ 80-90 kDa) are indicated in green. Single-chain FVIII (≈ 200 kDa), consisting of heavy and light chain, is indicated in yellow, due to the overlay of green and red. The heavy chains were detected with the primary rabbit anti-human Factor VIII antibody and the secondary donkey anti-rabbit IgG IRDye 800CW. The light chains were detected with the primary mouse anti-human Factor VIII antibody and the secondary donkey anti-mouse IgG IRDye 680RD.

In order to detect whether the FVIII variants 19M and 6rs were glycosylated, another Western Blot was performed (3.5.3). Each sample was applied in its original form and in a deglycosylated form to a SDS-PAGE (3.5.2). Deglycosylation was performed with N-Glycosidase F, which specifically removed N-linked glycosylations (3.5.2.2). O-glycosylations were not expected to be present, as these glycosylation sites lay in the B domain regions which were deleted in all four products. The original samples were treated as the deglycosylated ones, except that no N-Glycosidase F was added. In the Western Blot the FVIII was detected with a polyclonal anti-FVIII antibody. As shown in Figure 4-25, the deglycosylation of FVIII-19M and FVIII-6rs as well as of the controls ReFacto AF and Nuwiq led to a band shift, due to the removal of the glycosylations. The shift appeared to be very similar for all variants. Unfortunately, various light chains were still detectable indicating that the deglycosylation was incomplete. In addition to that, it was not possible to determine whether all four N-glycosylation sites, which were still present

in the B-domain deleted variants, were originally glycosylated. In order to obtain detailed information on the glycosylation, mass spectrometric analyses would have been necessary. Using this method, a defined determination of the sugar types would be possible. However, the amounts of available FVIII-19M and FVIII-6rs were too low for a detailed analysis of the glycosylation pattern.

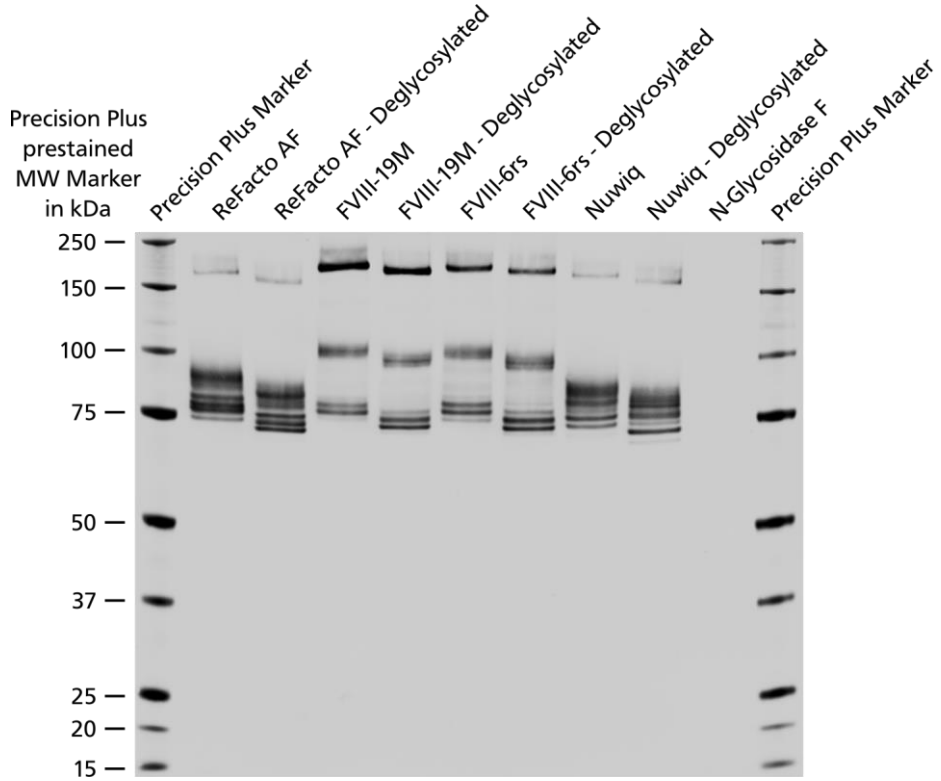

Figure 4-25: Western Blot with glycosylated and deglycosylated FVIII variants. Glycosylated and deglycosylated FVIII products were applied at a concentration of 5 U/ml. FVIII was detected with the primary polyclonal sheep anti-human Factor VIII antibody and the secondary donkey anti-sheep IgG IRDye 800CW.

The sulfation of FVIII-19M and FVIII-6rs was also analyzed with a Western Blot (3.5.3). FVIII was specifically detected by a polyclonal FVIII antibody, revealing heavy, light and single chain of FVIII. A second antibody specifically detected sulfotyrosines. Sulfation was expected at four sites in the heavy chain (Y365, Y737, Y738 and Y742) and at two sites in the light chain (Y1683 and Y1699). In the Western Blot the sulfation was detectable as a yellow band, resulting from the overlay of the green signal, representing the FVIII, and the red signal, representing the sulfotyrosine (Figure 4-26 A). The commercially available product Nuwiq revealed a positive sulfation signal especially in the heavy chain, whereas ReFacto AF showed nearly no sulfation. The two variants FVIII-6rs and FVIII-19M revealed sulfation mainly in their single-chain form and nearly no sulfation was detectable in the heavy and light chain. In order to show the sulfotyrosine signal in more detail, Figure 4-26 B presents only the signal from the secondary antibody donkey anti-mouse IgG IRDye 800CW, which bound to the mouse anti-human sulfotyrosine antibody. This figure revealed that at least a small amount of ReFacto AF was sulfated and that the light chains of Nuwiq, and the light and heavy chain of FVIII-19M and FVIII-6rs were also sulfated. This indicated that sulfation was not generally defective in the double-chain form of FVIII-19M and FVIII-6rs. In general, the Western Blot revealed the expected results with the highest sulfation signal for the single chain, containing all six sulfation sites, less signal for the heavy chain and the lowest signal for the light chain, containing only two sulfation sites. The variations between the products might have occurred, due to the different cell lines used for the production.

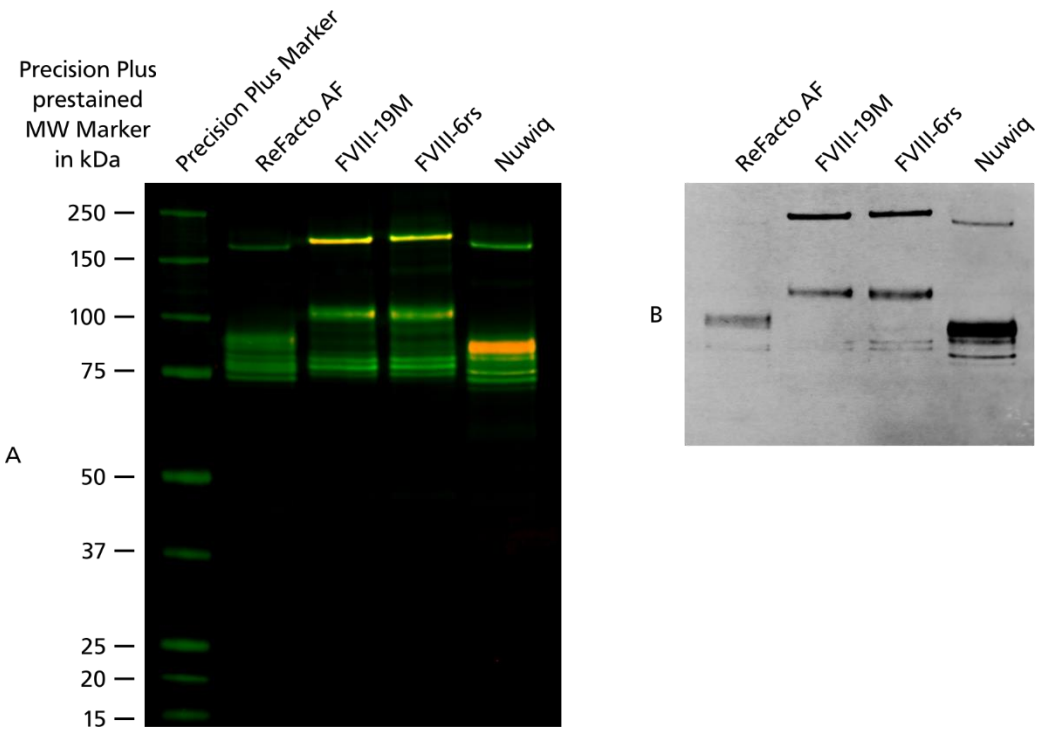

Figure 4-26: Western Blot detecting FVIII and sulfotyrosines. The FVIII products were applied at a concentration of 10 U/ml. FVIII was detected with the primary polyclonal sheep anti-human Factor VIII antibody and the secondary donkey anti-sheep IgG CF680. Sulfotyrosines were detected with the primary mouse anti-human sulfotyrosine antibody and the secondary donkey anti-mouse IgG IRDye 800CW (A) FVIII is indicated in green and sulfotyrosines in red. The overlay of red and green results in a yellow signal. (B) Only the signal of the sulfotyrosine antibody is displayed.

In order to compare the FVIII variants 19M and 6rs in more detail, 2D-DIGE was performed (3.5.4). Two DIGEs were specifically detecting FVIII, whereof one DIGE contained FVIII-19M and FVIII-6rs and the other contained ReFacto AF and Nuwiq. For these electrophoreses the proteins were labelled with different fluorochromes. As these fluorochromes labelled all proteins in the solution, also contaminating proteins were labelled. In order to distinguish FVIII from contaminating proteins, the gel was blotted and the polyclonal anti-FVIII antibody was applied to the Blot, followed by a secondary antibody labelled with a third fluorochrome. The overlay of the different fluorochromes revealed which protein spots were FVIII. In a third DIGE, FVIII-19M, FVIII-6rs and ReFacto AF were labelled with three different fluorochromes and compared on one gel, which was not blotted but scanned after the electrophresis, taking into consideration which spots were representing FVIII.

Figure 4-27 shows the Western Blot of the 2D-DIGE with ReFacto AF and Nuwiq. In all three pictures only two of the three colours were overlayed. Unfortunately, the light chain was not completely focussed as the IEF strips were focussing from pH 4 to pH 7 and the light chain needed pH 8 for optimal focusing. Also the single chain was not optimally focussed, probably due to its size. Figure 4-27 A and B show the FVIII products (ReFacto AF in green, Nuwiq in red) together with the polyclonal anti-FVIII antibody (yellow). For both products, all spots were overlayed with the signal of the FVIII antibody, indicating that no contaminating proteins were detectable. However, more yellow FVIII bands than green or red bands were visible. This was due to the fact, that the anti-FVIII antibody, together with the secondary antibody, was more sensitive than the labeling of the proteins. The spots indicate that FVIII was present in these areas but it was not identifiable which product was bound by the antibody, as the green and red signals were too low. In both products, regarding the first dimension representing the IEF, more than one spot was detectable for the single chain (1), the heavy chain (2) and the light chain (3 and 4). This was probably due to differences in the post-translational modification, as glycosylation and sulfation influence the pI. Regarding the light chain, ReFacto AF and Nuwiq showed more than one band in the second dimension, the separation by molecular weight. This was expected as more than one band was already detected by 1D-SDS-PAGE (Figure 4-24). These differences were probably also due to

different glycosylation patterns as well as slight differences in processing of the light chain. Additionally, ReFacto AF revealed two heavy chain bands in the second dimension. These two bands were also detectable in the Western Blot detecting the FVIII heavy and light chain (Figure 4-24) but not as clear as on this Blot of the 2D-DIGE. These two chains might have been derived from different processing of the heavy chain. A second heavy chain was also detectable for Nuwiq. However, the intensity of this band was much lower compared to ReFacto AF and not yet identified in the Western Blots before. Figure 4-27 C displays the overlay of ReFacto AF and Nuwiq. This picture shows that the original colours of ReFacto AF and Nuwiq were turquoise and pink, only resulting in green and red, when overlayed with the yellow signal. In the areas where ReFacto AF and Nuwiq overlayed, the color changed to blue. This was especially the case for the major part of the light chain (3), whereas the minor parts of the light chain (4) were slightly different. The major parts of the heavy chain (2) were also similar, except for the upper bands. The overlay confirms that the amount of the upper heavy chain is higher for ReFacto AF. Additionally, the upper heavy chains of ReFacto AF and Nuwiq slightly differ in the first dimension, indicating different pIs. Altogether the Western Blot of the 2D-DIGE revealed that ReFacto AF and Nuwiq were very similar regarding heavy and light chain. The singlchain FVIII was only detectable by the anti-FVIII antibody, as the amounts were very low. None of the products revealed contamininations with other proteins.

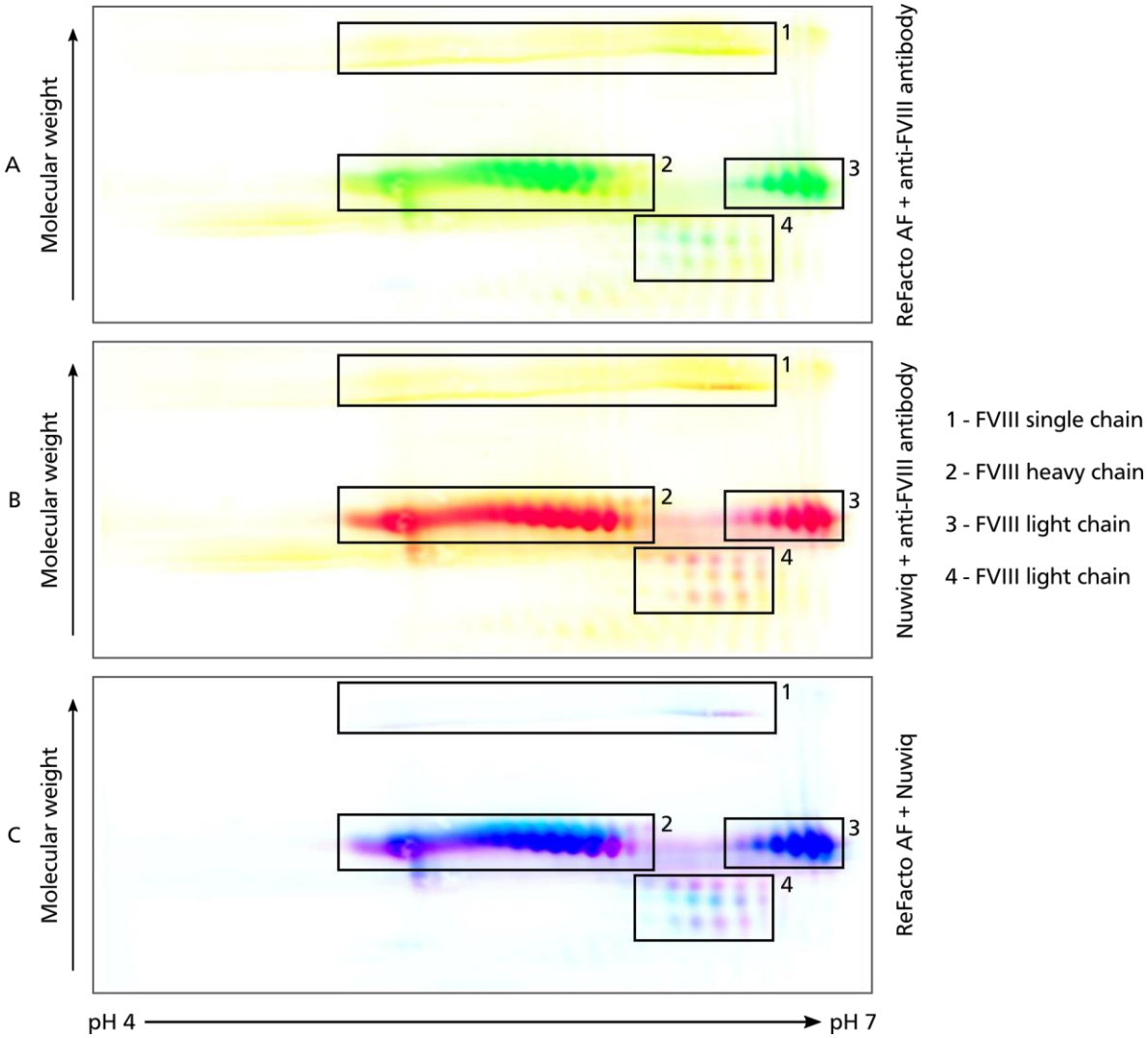

Figure 4-27: Western Blot of a 2D-DIGE. ReFacto AF was labelled with DY-680 and Nuwiq was labelled with DY-780. FVIII was detected with the primary polyclonal sheep anti-human Factor VIII antibody and the secondary donkey anti-sheep IgG CF488A. (A) Overlay of the ReFacto AF signal (green) and the polyclonal anti-FVIII signal (yellow). (B) Overlay of the Nuwiq signal (red) and the polyclonal anti-FVIII signal (yellow). (C) Overlay of the ReFacto AF signal (turquoise) and the Nuwiq signal (pink). The overlaying regions are colored in blue.

In Figure 4-28 the Western Blot of the 2D-DIGE with labelled FVIII-19M and FVIII-6rs is displayed. As for ReFacto AF and Nuwiq, FVIII was specifically detected on the Blot with the polyclonal anti-FVIII antibody. In contrast to the commercially available products Nuwiq and ReFacto AF, the Blot revealed that FVIII-19M and FVIII-6rs still contained contaminating proteins. In Figure 4-28 A and B pink or turquoise spots were detectable, which were not overlaid with the yellow signal of the anti-FVIII antibody. In addition to the spots for the single chain (1), the heavy chain (2) and the variants of the light chain (4 and 5), spots were detectable below the main spots of the heavy chain (3). These spots probably represented heavy chain with differently processed B domain, leading to a lower molecular weight. Compared to the Blot of ReFacto AF and Nuwiq, the amount of single chain was higher, which made it possible to detect an overlay of the FVIII antibody signal and the signal of the labelled proteins. This was expected, as a high amount of single chain was already visible on the Blots of the 1D-SDS-PAGE (Figure 4-24). Figure 4-28 C shows the overlay of the FVIII-19M and the FVIII-6rs. As expected, the spots were very similar and overlapping, leading to the blue color. Slight shifts were seen in the first dimension which might have been due to the slightly reduced pI of the FVIII-19M, because of the incorporation of the 19 mutations.

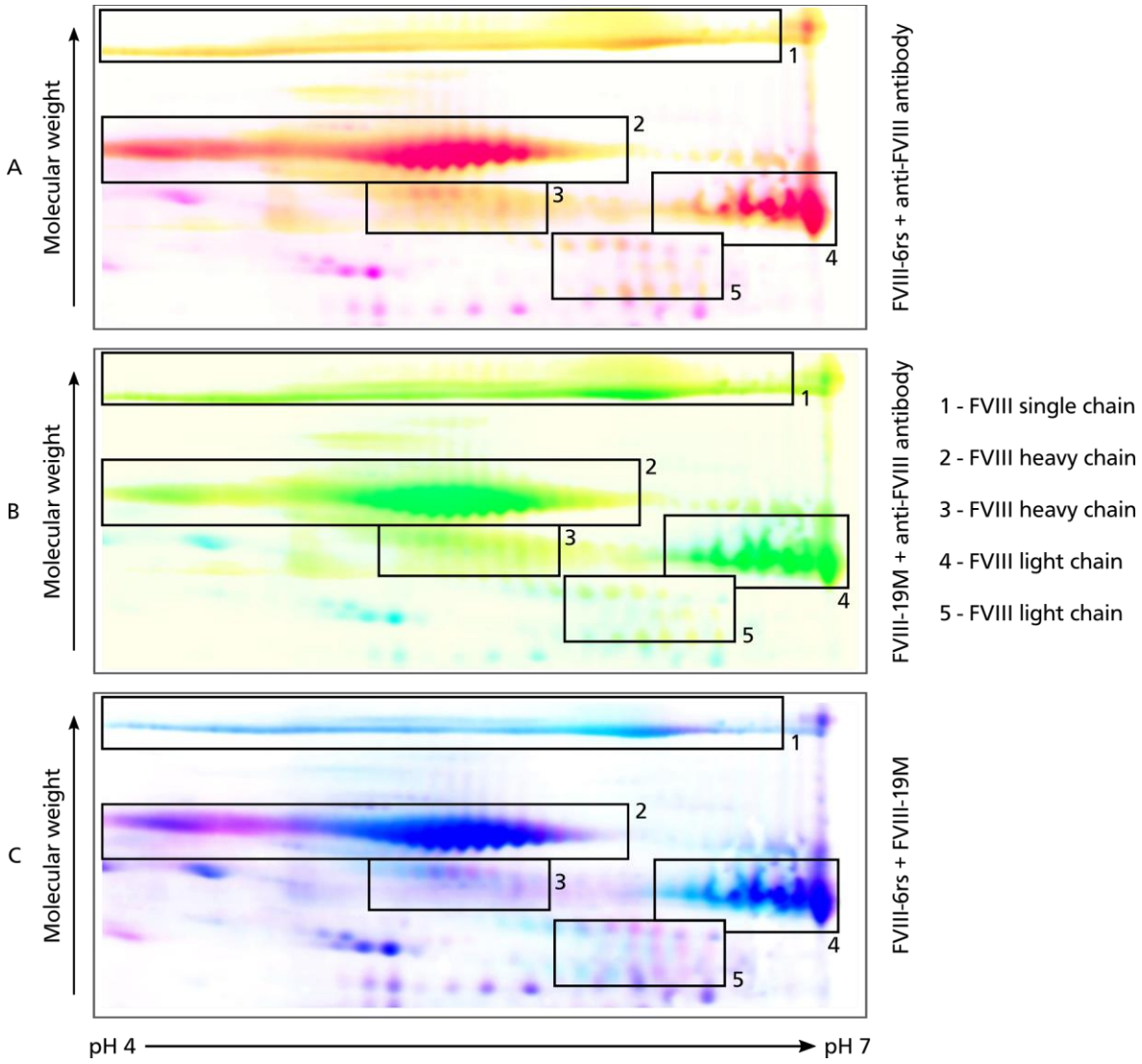

Figure 4-28: Western Blot of a 2D-DIGE with labelled FVIII-6rs and FVIII-19M. FVIII-19M was labelled with DY-680 and FVIII-6rs was labelled with DY-780. FVIII was detected with the primary polyclonal sheep anti-human Factor VIII antibody and the secondary donkey anti-sheep IgG CF488A. (A) Overlay of the FVIII-6rs signal (red) and the polyclonal anti-FVIII signal (yellow). (B) Overlay of the FVIII-19M signal (green) and the polyclonal anti-FVIII signal (yellow). (C) Overlay of the FVIII-19M signal (turquoise) and the FVIII-6rs signal (pink). The overlaying regions are colored in blue.

Figure 4-29 represents the overlay of ReFacto AF, FVIII-19M and FVIII-6rs. All three FVIII products were labeled with different flurochromes before the IEF. Due to this, the gel was not blotted after the SDS-PAGE but directly scanned, leading to the detection of the three proteins. As seen before, no single-chain form of ReFacto AF (yellow) was visible, whereas FVIII-19M (turquoise) and FVIII-6rs (pink) single chain was detectable (1). The main spots for the light chain mainly overlapped, although the resolution was impaired due to an air bubble (3). The lighter spots of the light chain were very diverse and mostly overlapping for FVIII-19M and FVIII-6rs, resulting in the blue color (4). The main differences were detectable for the heavy chain (2). The ReFacto AF heavy chain was in the second dimension clearly separated from the heavy chain of FVIII-6rs and FVIII-19M, because ReFacto AF lacked a larger part of the B domain.

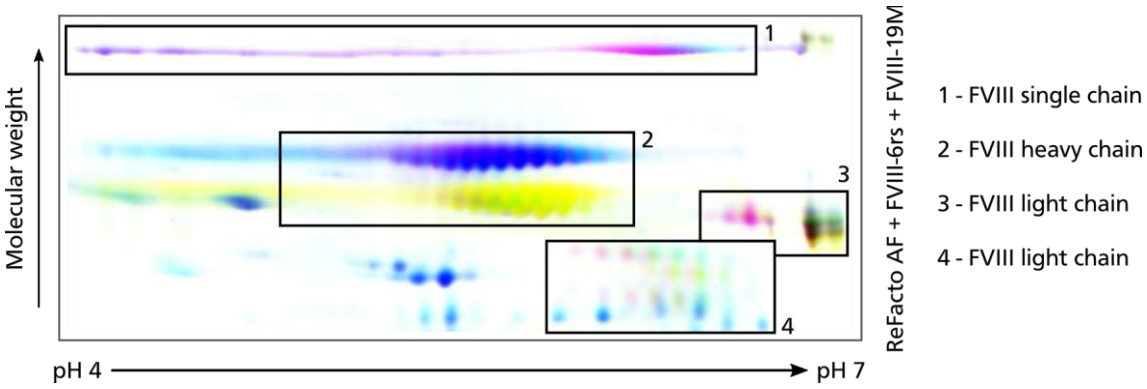

Figure 4-29: 2D-DIGE with labelled FVIII-6rs, FVIII-19M and ReFacto AF. The picture represents the overlay of the FVIII-6rs signal (pink), the FVIII-19M signal (turquoise) and the ReFacto AF signal (yellow). The blue regions represent an overlap of signal from FVIII-6rs and FVIII-19M. The red regions represent an overlap of signal from FVIII-6rs and ReFacto AF. The green regions represent an overlap of signal from FVIII-19M and ReFacto AF. ReFacto AF was labelled with Cy-2, FVIII-19M was labelled with Cy-3 and FVIII-6rs was labelled with Cy-5.

In total, the 2D-DIGE made it possible to detect similarities and differences between the FVIII variants 19M and 6rs, between ReFacto AF and Nuwiq and between ReFacto AF, FVIII-19M and FVIII-6rs. The method confirmed results, which were already seen in different Western Blots and gave insights regarding the pI of the different products. In addition, it revealed that impurities were still present in the purified FVIII-19M and FVIII-6rs products.

4.4.3. Functional analyses

Several analyses were performed, in order to compare FVIII-19M and FVIII-6rs to ReFacto AF and Nuwiq, regarding their functionality. At first, all products were analyzed on a Western Blot before and after the activation with thrombin (3.5.3). The thrombin activation occurred as described in 3.5.2.1. The treatment of the samples was the same for activated and non-activated samples, except that no thrombin was added to the non-activated samples. After blotting, the FVIII fragments were detected with the polyclonal anti-FVIII antibody. All four products were spliced by thrombin and characteristic fragments were detectable (Figure 4-30). The thrombin cleavage of the heavy chain, at R391 and R759, led to the fragments of A1 and A2, which were visible between 40 and 50 kDa. More than one band was visualized for each domain, which was probably due to different glycosylation and processing and was consistent with the two bands seen in the non-activated heavy chain of ReFacto AF and Nuwiq especially on the Blot of the 2D-DIGE (Figure 4-27). The remaining part of the B domain, resulting from the cleavage at R759, was too small to be detected. The cleavage of the light chain at R1708 led to the large fragment, comprising the A3, C1 and C2 domain, at around 70 kDa. The a3 domain, also resulting from this cleavage, was too small to be detected. Two fragments were additionally detected in the FVIII-19M and FVIII-6rs variants. The fragment consisting of the remaining B domain and a3, detected around 20 kDa, was probably derived from the single-chain variant. The single chain was cleaved at all three thrombin

cleavage sites but due to missing furin cleavage, the combination of B domain and a3, too small to be detectable individually, was still visible on the Blot. These fragment might also have been existent for ReFacto AF and Nuwiq but the amount of single chain was too low, compared to FVIII-19M and FVIII-6rs, so that the visualization was not possible. The fragment of about 90 kDa probably consisted of A1 and A2 domain and was derived either from incomplete activation of the heavy chain or from the single chain, missing the cleavage at R391. In general, all products were activated by thrombin and revealed the expected band patterns.

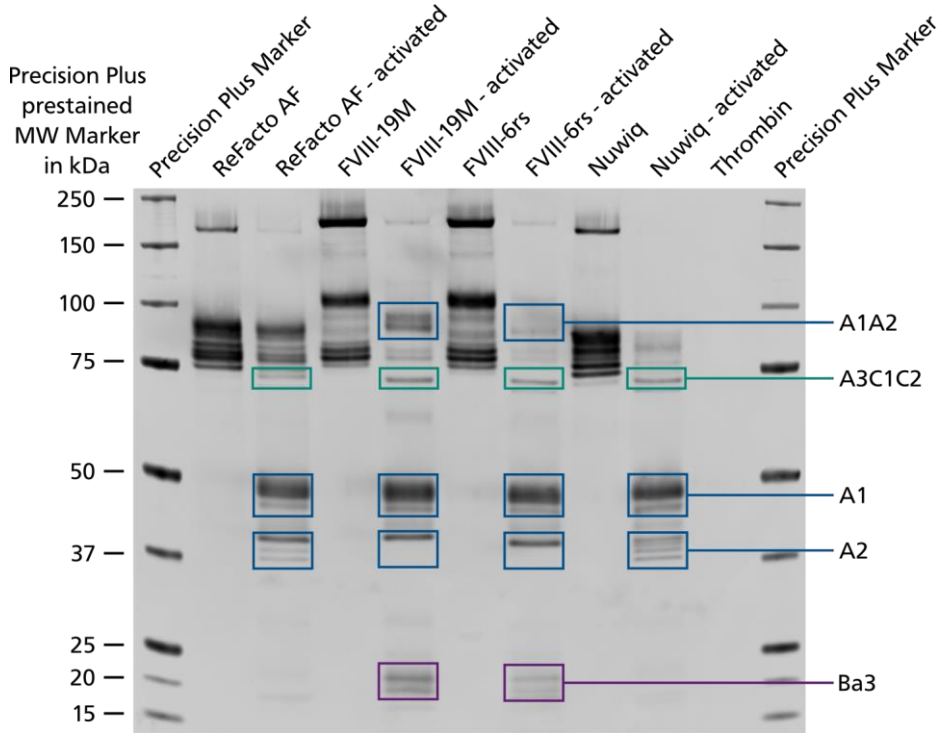

Figure 4-30: FVIII products activated by thrombin. Each product was applied in its non-activated and activated form. In the non-activated form, the typical bands for the single chain (≈ 200 kDa), heavy chain (≈ 95-110 kDa) and light chain (≈ 80-90 kDa) were detectable. After thrombin cleavage additional bands for A1A2 (≈ 90 kDa), A3C1C2 (≈ 70 kDa), A1 (≈ 50 kDa), A2 (≈ 40 kDa) and Ba3 (≈ 20 kDa) were detectable. FVIII was detected with the primary polyclonal sheep anti-human Factor VIII antibody and the secondary donkey anti-sheep IgG IRDye 800CW.

The clotting time for the different FVIII products was determined using the ROTEM method (3.4.6). During this analysis, the clotting time of plasma is analyzed depending on the amount and the functionality of the applied FVIII. The FVIII products were added to FVIII-deficient plasma and the clotting was initiated via the intrinsic pathway. The time until a clot was starting to form was measured. By adding different concentrations of FVIII, an increase of the clotting time was detected in correlation to decreasing concentrations of FVIII. When comparing the different products, ReFacto AF and Nuwiq revealed very similar clotting times, whereas the clotting times were slightly prolonged for FVIII-6rs and even more for FVIII-19M (Figure 4-31). However, all clotting times only varied between 120 seconds and 160 seconds at 1 U/ml FVIII, which was still in the normal clotting time range of 100-240 seconds in healthy people[222].

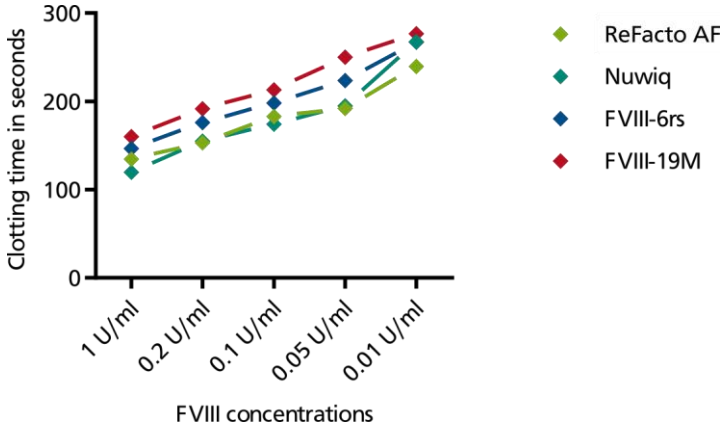

Figure 4-31: Clotting time for different FVIII products. The clotting time for FVIII-19M and FVIII-6rs was measured in comparison to the clotting times for ReFacto AF and Nuwiq. Different FVIII concentrations were analyzed. The measurements were performed in duplicates and the mean values are displayed.

In addition to the determination of the clotting time, a TGA was performed. This assay measures the amount of generated thrombin. As it is performed in FVIII-deficient plasma, the amount of generated thrombin depends on the amount and functionality of the added FVIII products. In contrast to the initiation via the intrinsic pathway in the ROTEM measurement, the clotting cascade in the TGA is started with tissue factor, pursuing the extrinsic pathway. All FVIII products were diluted to 0.25 U/ml, 0.063 U/ml and 0.016 U/ml FVIII, depending on their chromogenic activity. Due to the high sensitivity of the assay, it was performed four times and the median was calculated for each product and concentration (3.4.5). Three different values were calculated: the amount of generated peak thrombin, the area under the curve and the time to peak thrombin generation. For the calculations the first deviation of the original curve was used (Figure 4-32). The amount of generated peak thrombin was calculated based on a thrombin standard. The area under the curve and the time to peak thrombin generation made it possible to detect differences not only in the amount of generated peak thrombin but also in the velocity and the whole clotting process, including inactivation. The area under the curve is equivalent to the total amount of generated thrombin. The results are presented in Figure 4-33 (detailed statistical results Table A-3 to Table A-5). Comparable to the analysis of the clotting times, ReFacto AF and Nuwiq revealed similar results regarding peak thrombin generation, area under the curve and time to peak thrombin generation. FVIII-6rs resembled ReFacto AF and Nuwiq regarding the amount of generated peak thrombin and the time to peak thrombin generation but showed a slightly reduced area under the curve. Unfortunately, FVIII-19M revealed significantly lower results for generated peak thrombin, area under the curve and time needed to reach peak thrombin generation, especially compared to ReFacto AF and Nuwiq. However, these results were comparable with the ROTEM results (Figure 4-31), revealing a prolonged clotting time for FVIII-19M. Concentrations above 0.25 U/ml FVIII were not analyzed, as it is published that from 0.5 U/ml on FVIII is no longer rate limiting[223]. Unfortunately, as the assay is so variable, no standardized value for the amount of generated peak thrombin was available. Due to this, only the comparison between the different FVIII products was possible and these were consistent with the results of the clotting times, revealing slightly reduced activity of the FVIII-19M compared to its reference FVIII-6rs.

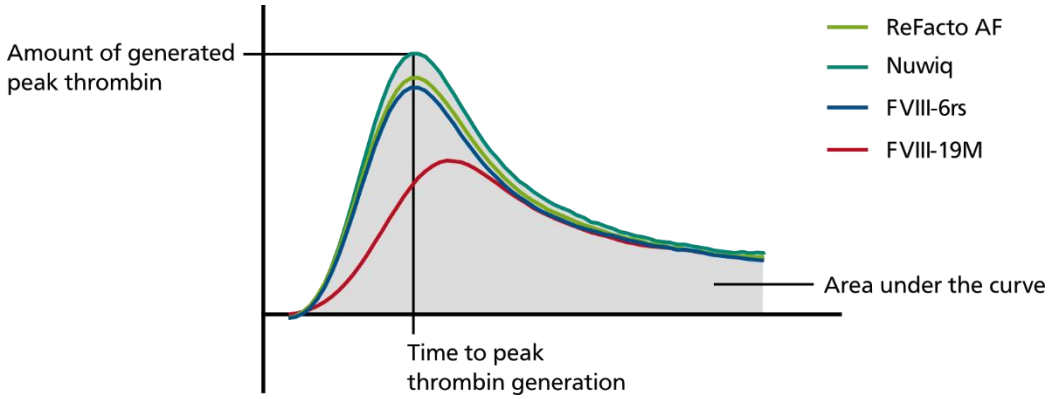

Figure 4-32: Exemplary TGA curve for ReFacto AF, Nuwiq, FVIII-6rs and FVIII-19M. The graph indicates the amount of generated peak thrombin, the area under the curve and the time to peak thrombin generation.

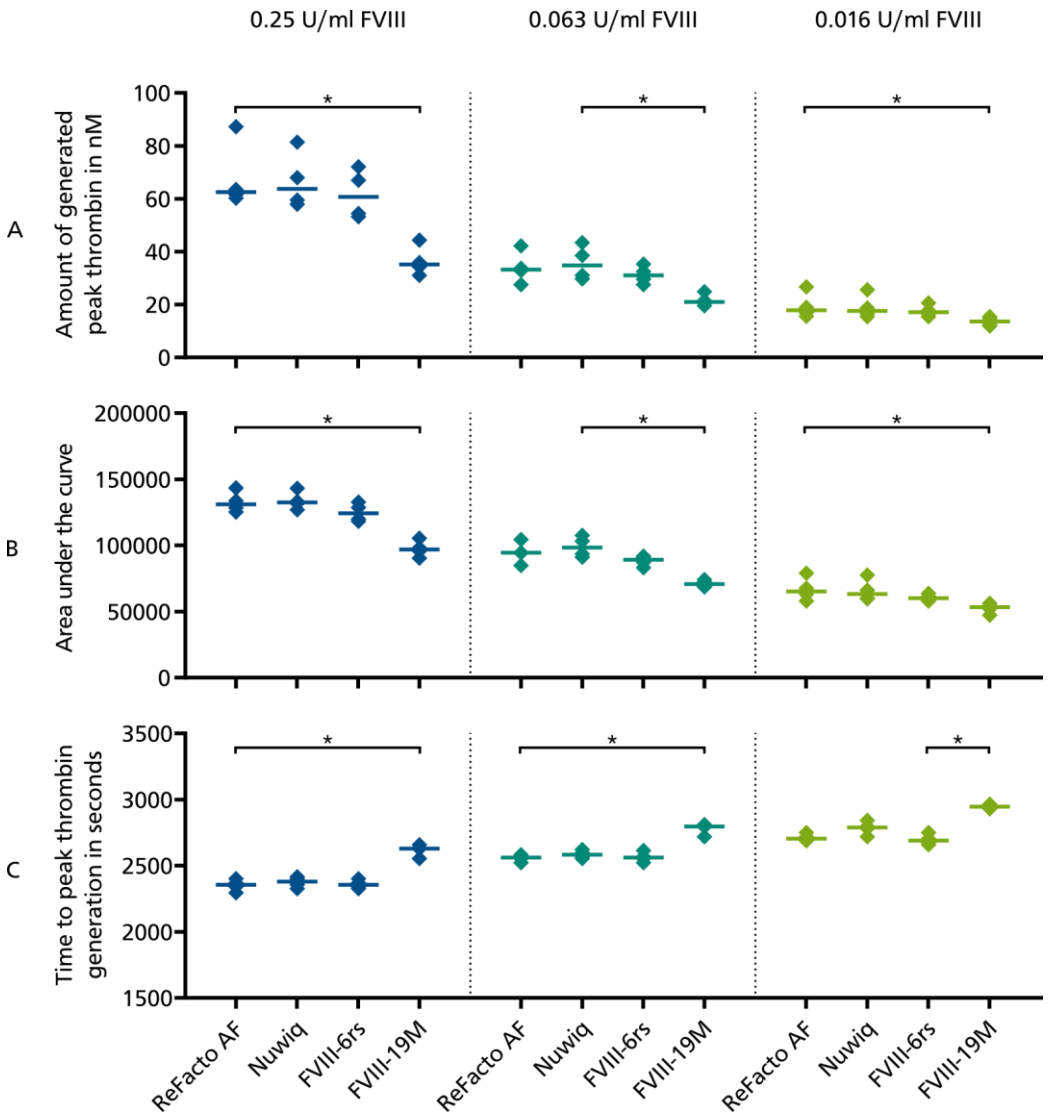

Figure 4-33: Results of the TGA for ReFacto AF, Nuwiq, FVIII-19M and FVIII-6rs. All products were diluted to 0.25 U/ml, 0.063 U/ml and 0.016 U/ml FVIII activity. Each point indicates the results from one TGA. The line indicates the median of the four performed assays. Statistical analysis was performed using the Friedman test. (A) Amount of generated peak thrombin for each product at the given concentration based on a thrombin standard. (B) Area under the curve for each product at the given concentration. (C) Time to peak thrombin generation for each product at the given concentration.

As the interaction with vWF is important for FVIII, the binding potency of FVIII-19M and FVIII-6rs to vWF was determined in an ELISA-based approach (3.4.4). ReFacto AF was used as a reference and the potency of the binding of ReFacto AF to vWF was set to 1. All other potencies were calculated in relation to ReFacto AF. The data revealed that the vWF binding was similar for ReFacto AF and Nuwiq but impaired for FVIII-6rs and FVIII-19M (Figure 4-34). However, the only significant difference could be detected between Nuwiq and FVIII-19M (Table A-6). The reduced binding, also of FVIII-6rs, might have been due to different post-translational modifications made by the CAP-T cells. This could be correlated with the reduced sulfation detected in the in the Western Blot (Figure 4-26). Missing sulfation might have influenced the vWF binding, as especially the sulfation at Y1699 is important for the binding of vWF. However, decreased sulfation could not have been the only reason for the reduced vWF-binding, as ReFacto AF revealed nearly no sulfation on the Western Blot but good vWF-binding. The reduction in the potency of FVIII-19M in comparison to FVIII-6rs might have been due to additional structural changes, derived from the incorporated mutations, influencing the vWF binding.

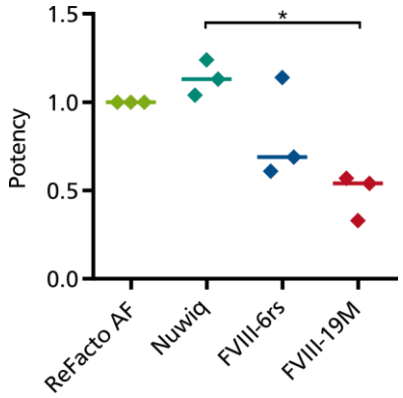

Figure 4-34: Potency of the vWF binding of the different FVIII products. The potency of ReFacto AF binding to vWF was set to 1 and was the reference for the other products. Each point indicates the results from one ELISA. The line indicates the median of the three performed assays. Statistical analysis was performed using the Friedman test.

In total, the analyses revealed similar band patterns for FVIII-19M and FVIII-6rs, regarding heavy, light and single chain amounts, as well as after deglycosylation and thrombin activation. In comparison to that, the amount of single chain was lower for Nuwiq and ReFacto AF. The shift of the heavy chain bands of ReFacto AF and Nuwiq compared to FVIIII-19M and FVIII-6rs were expected, as a larger part of the B domain was deleted in these constructs. The deglycosylation revealed a band shift for all four FVIII products, indicating that glycosylation took place during production of all FVIII variants. The band patterns after thrombin activation were also similar for all products, except for the two additional bands derived from the cleavage of the single chain forms of FVIII-19M and FVIII-6rs. The main differences between the controls and FVIII-19M and FVIII-6rs were detectable regarding sulfation. The Western Blot revealed nearly no sulfation in the heavy and light chain of FVIII-19M and FVIII-6rs, only slight sulfation in ReFacto AF and high sulfation in Nuwiq. The reduced sulfation in the heavy and light chain of FVIII-19M and FVIII-6rs might explain the detected reduced potency to bind vWF. Nevertheless, this cannot be the only explanation as the slightly sulfated ReFacto AF revealed good vWF-binding. Regarding clotting time, all four products were similar, although a slight prolongation was detected for FVIII-6rs and FVIII-19M. Nevertheless, these prolonged clotting times were still in the regular range. The TGA results were similar to the clotting times, revealing a slightly lower amount of generated thrombin with FVIII-19M compared to ReFacto AF, Nuwiq and FVIII-6rs. These results indicated, together with the reduced clotting activity, that the generated FVIII variant containing 19 amino acid mutations had a slightly reduced activity compared to the other products. However, FVIII-19M proved to be functional in all performed assays.

4.5. *In vitro* immunogenicity assay

In order to determine whether less $CD4^+$ T cells become activated, due to a reduced presentation of FVIII-19M peptides on the surface of DCs, an *in vitro* DC-T cell Assay was established. The assay consisted of DCs, derived from monocytes, and $CD4^+CD25^-$ T cells. The $CD4^+CD25^+$ T cells were depleted prior to co-cultivation, as this subpopulation comprised mainly regulatory T cells. This was important, due to the fact that the cells for the assay were derived from healthy donors and expected to contain regulatory T cells, suppressing the FVIII-specific $CD4^+$ T cells which were not depleted during ontogeny[190]. Consequently, as the aim of the assay was to stimulate these FVIII-specific T cells, the regulatory T cells had to be depleted. The approach to use only DCs as APCs, was chosen due to two reasons. On the one hand, the focus was on the activation of $CD4^+$ T cells based on the interaction with the presented FVIII epitopes. Influences due to interaction with other immune cells might have distorted the results. On the other hand, the assay was planned to be performed also with cells derived from Hemophilia A patients. These patients might still have naïve T cells and the activation of naïve T cells primarily occurs by DCs. In the case of choosing a general PBMCs assay, the amount of DCs would probably have been too low to activate the naïve $CD4^+$ T cells.

The assay was developed in several steps. In the beginning the cells were co-cultured in 24-well plates. Using this approach, it was possible to harvest and analyze the adherent DCs and determine whether differentiation to mDCs occurred. In order to reduce the amount of cells, the assay was then set to a 48-well format. In this setup the DCs were no longer harvested and the $CD4^+CD25^-$ T cells were directly added to the mDCs. The cells for each experiment were purified from PBMCs. These PBMCs, derived from either whole blood donations or leukapheresis, were frozen after purification (3.2.4.2). As the generation of mature DCs took 6 days whereas the $CD4^+CD25^-$ T cells were only cultured for 2 days prior to co-cultivation, purification of the two cell types occurred at different days. A scheme of the assay structure is illustrated in Figure 4-35. The monocytes were purified from PBMCs as described in 3.2.4.3 and further on differentiated to iDCs, using IL-4 and GM-CSF, and finally stimulated for 24 hours, in order to obtain mDCs (3.2.4.6). In parallel, the $CD4^+CD25^-$ T cells were purified from PBMCs two days prior to the co-cultivation with the mDCs (3.2.4.4). After the purification, the $CD4^+CD25^-$ T cells were labelled with CFSE (3.2.4.5) and cultured for 2 days, in order to recover from the purification and labeling process (3.2.4.7). Co-cultivation finally occurred as described in 3.2.4.8. After 9 days of co-cultivation, the cells were analyzed by flow cytometry (3.3.1) and the remaining supernatant was frozen for cytokine arrays (3.3.2).

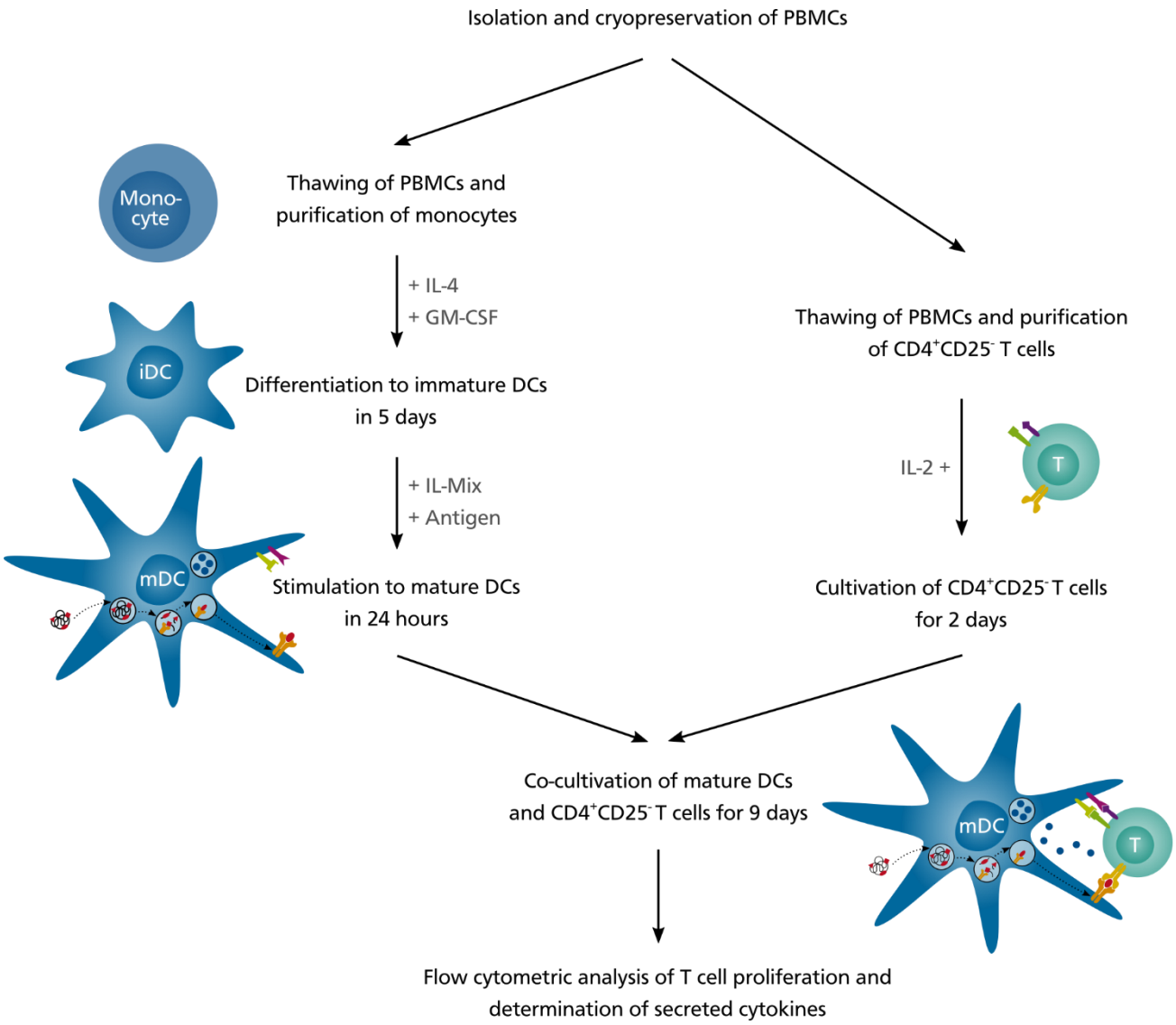

Figure 4-35: Scheme of the DC-T cell Assay. DCs and T cells were processed in parallel. Monocytes were purified from PBMCs, differentiated to iDCs and finally stimulated to become mDCs. $CD4^+CD25^-$ T cells were also purified from PBMCs and cultivated prior to co-cultivation, in order to regenerate. The co-culture occurred for 9 days and afterwards the cells were analyzed by flow cytometry and the remaining supernatant was applied to a cytokine array.

In order to determine the appropriate stimulus for the maturation of the monocyte-derived iDCs, different approaches were tested. These approaches comprised stimulation with 0.05 μg/ml LPS, an IL-Mix consisting of IL-1β, IL-6, IL-8 and TNF-α and an IL-Mix consisting only of IL-1β, IL-6 and TNF-α. All interleukins were applied to a final concentration of 10 ng/ml, except for IL-6, which was applied to a final concentration of 20 ng/ml. All stimuli were also tested in combination with either 1 mg/ml OVA or 5 U/ml ReFacto AF. The cells were harvested after 24 hours of stimulation and the expression of the surface receptors HLA-DR, CD40, CD80 and CD86 was analyzed by flow cytometry (3.3.1), using the DC stain (Table 3-2). As a reference, unstimulated iDCs were also analyzed. The gating strategies for the DCs after 24 hours of stimulation is depicted in Figure 4-36.

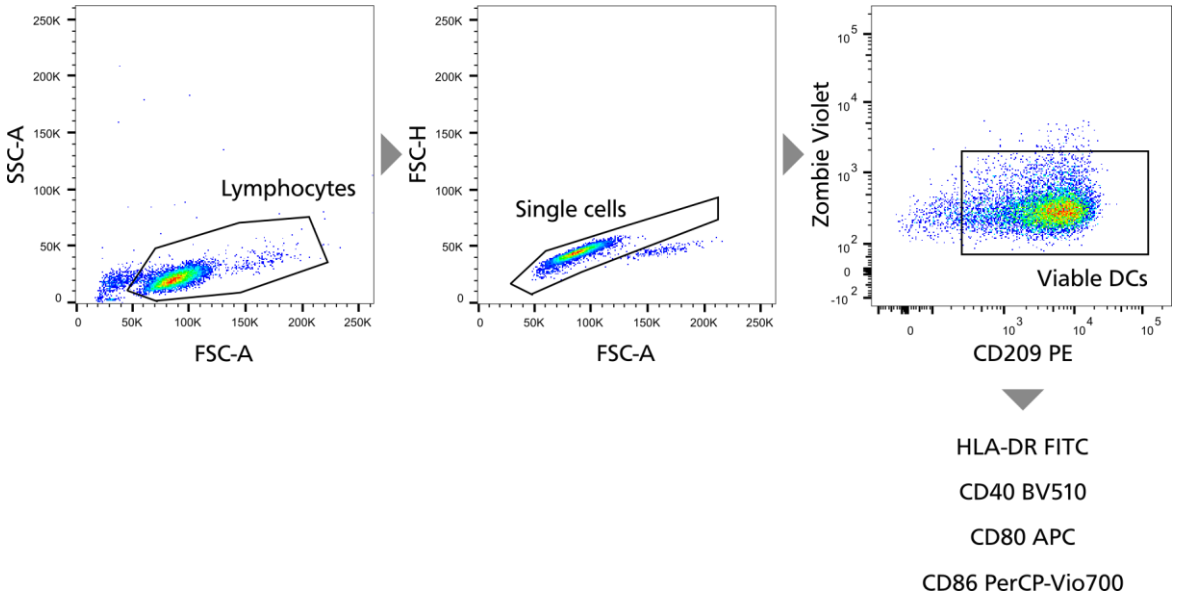

Figure 4-36: Gating strategy for DCs. In the first step, the lymphocyte population was determined via sideward and forward scatter. In the next step, only single cells were selected. Further on, viable DCs were detected by the expression of CD209 and a low signal for the viability dye Zombie Violet. This population was used for the determination of the expression of HLA-DR, CD40, CD80 and CD86.

The results of the mean fluorescence intensities (MFI), for the fluorochrome-coupled antibodies detecting the different receptors on the DCs, are summarized in Figure 4-37 (median of MFIs see Table A-7). Only the MFIs of viable CD209$^+$ DCs were used based on the gating presented in Figure 4-36. The floating bars represent the results of three to five healthy donors. The bars range from the lowest to the highest value and the middle line indicates the median of the results. For all receptors, except for CD86, the MFI results were widely spread, which was due to the natural diversity of the different donors. In general, all receptors were upregulated upon the addition of the maturation stimuli. This indicates that the iDCs differentiated to mDCs and were able to present peptides via HLA-DR as well as to provide co-stimulatory signals via CD40 and CD80/CD86. However, no significant differences were detectable between LPS and the two IL-Mixes (Table A-8). Upon the addition of the proteins OVA and ReFacto AF a slight but not significant decrease in the expression of CD80 and CD86 were detectable, especially when the DCs were stimulated with LPS. The reason for this was not further investigated. Without the addition of an IL-Mix or LPS the antigens OVA and ReFacto AF led to nearly no increase of the co-stimulatory receptors. Only a slight increase in HLA-DR was detectable indicating that antigen presentation might have occurred without additional stimuli. However, as the co-stimulatory signals were required, LPS or an IL-Mix had to be added to the iDCs. Depending on the results, all three stimuli would have been appropriate for the maturation of iDCs, as all revealed a clear although not significant difference in the MFIs, compared to the unstimulated iDCs.

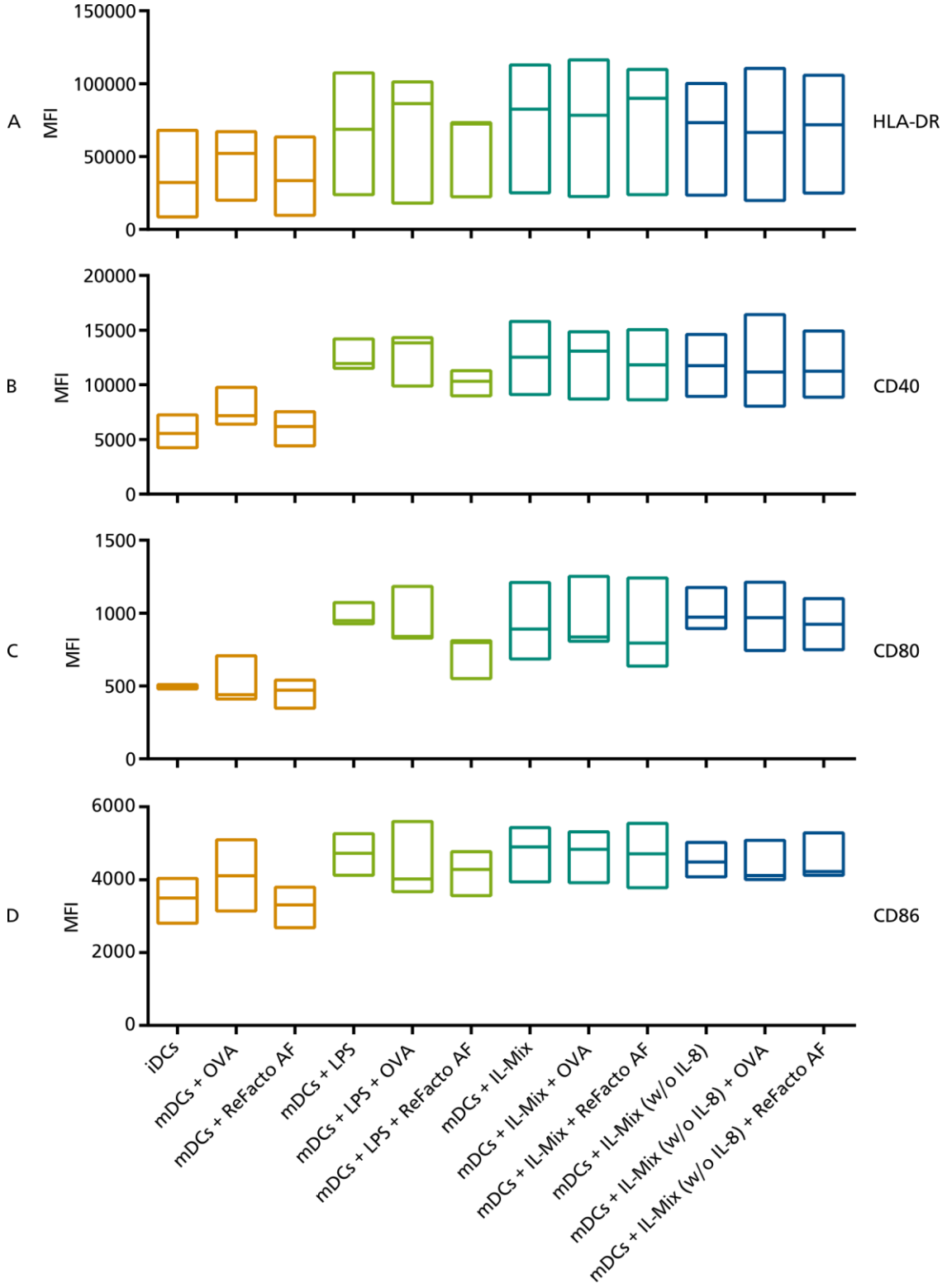

Figure 4-37: MFI of fluorochrome-coupled antibodies against the indicated surface receptors. The floating bars represent the MFI values of three to five healthy donors, indicating the minimum, maximum and median value. Only the MFI of viable, single-cell CD209^{+} DCs were used for the analysis. (A) Expression of HLA-DR detected with the antibody anti-HLA-DR FITC. (B) Expression of CD40 detected with the antibody anti-CD40 APC-H7. (C) Expression of CD80 detected with the antibody anti-CD80 APC. (D) Expression of CD86 detected with the antibody anti-CD86 PerCP-Vio700.

The viability of the DCs after 24 hours of stimulation was also determined using the DC stain. The results are displayed in Figure 4-38 and Table 4-4. The viabilities ranged between 78 % and 92 %. Reduced viabilities were mainly detected for the stimulated DCs, however the differences were not significant (Table A-9) and the values were still appropriated for cells cultured for 6 days and also for further co-cultivation with T cells. The addition of OVA led to the largest reduction of viability in all setups. This was not expected, however it might have been due to the preparation of the OVA, although an endotoxin-free preparation was used. Nevertheless, this preparation might still have contained additional substances, influencing the viability of the cells.

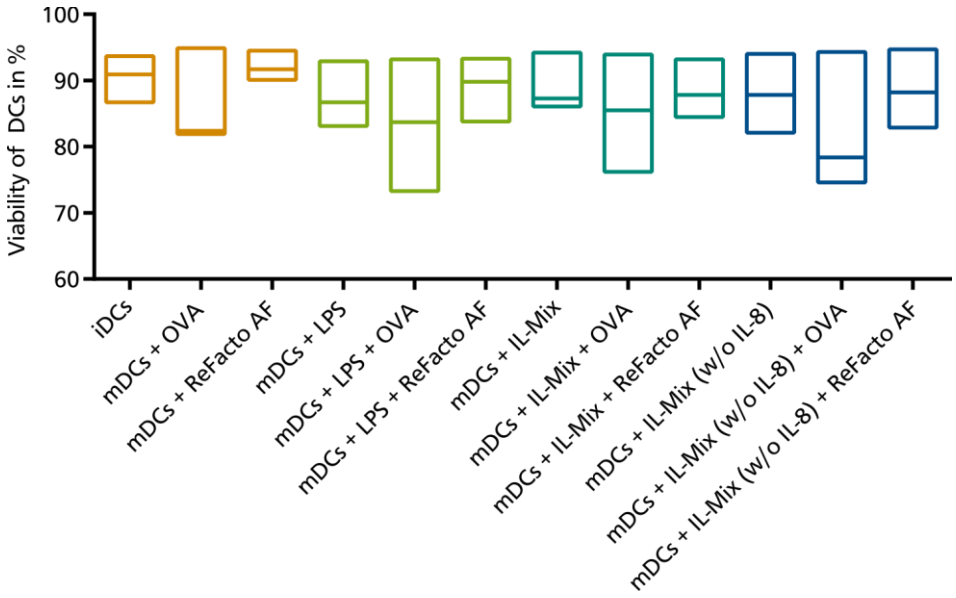

Figure 4-38: Viability of the DCs after 24 hours of stimulation. The floating bars represent the viability of three to five healthy donors, indicating the minimum, maximum and median value. The viability was detected using the viability dye Zombie Violet. The viability was calculated on all single lymphocytes.

Table 4-4: Median viability of the differently stimulated DCs. The median was calculated from the viability of three to five healthy donors per DC stimulation condition.

DC stimulus	Added protein	Median viability of DCs
No stimulus	No protein	90.9 %
	OVA	82.4 %
	ReFacto AF	91.7 %
LPS	No protein	86.7 %
	OVA	83.7 %
	ReFacto AF	89.8 %
IL-Mix	No protein	87.3 %
	OVA	85.5 %
	ReFacto AF	87.8 %
IL-Mix (w/o IL-8)	No protein	87.8 %
	OVA	78.4 %
	ReFacto AF	88.2 %

The stimulated DCs were further on co-cultivated with $CD4^+CD25^-$ T cells. As the co-cultivation occurred in fresh medium, no proteins or interleukins from the DC stimulation were present that could have influenced the T cell proliferation. Due to low amounts of available $CD4^+CD25^-$ T cells, not all differently stimulated DCs could be tested in combination with $CD4^+CD25^-$ T cells for every donor. However, three to six co-cultures, with cells from different donors, were performed for every stimulation approach. After 9 days of co-cultivation the $CD4^+$ T cells were harvested and analyzed by flow cytometry (3.3.1), using the T cell proliferation stain (Table 3-5). The DCs remained in the plates, attached to the surface. The proliferation of the T cells was determined by the fluorescence reduction of the incorporated dye CFSE, as the amount of CFSE was equally split during cell division. Additionally, the expression of CD25 indicated activated T cells. The gating strategy is illustrated in Figure 4-39.

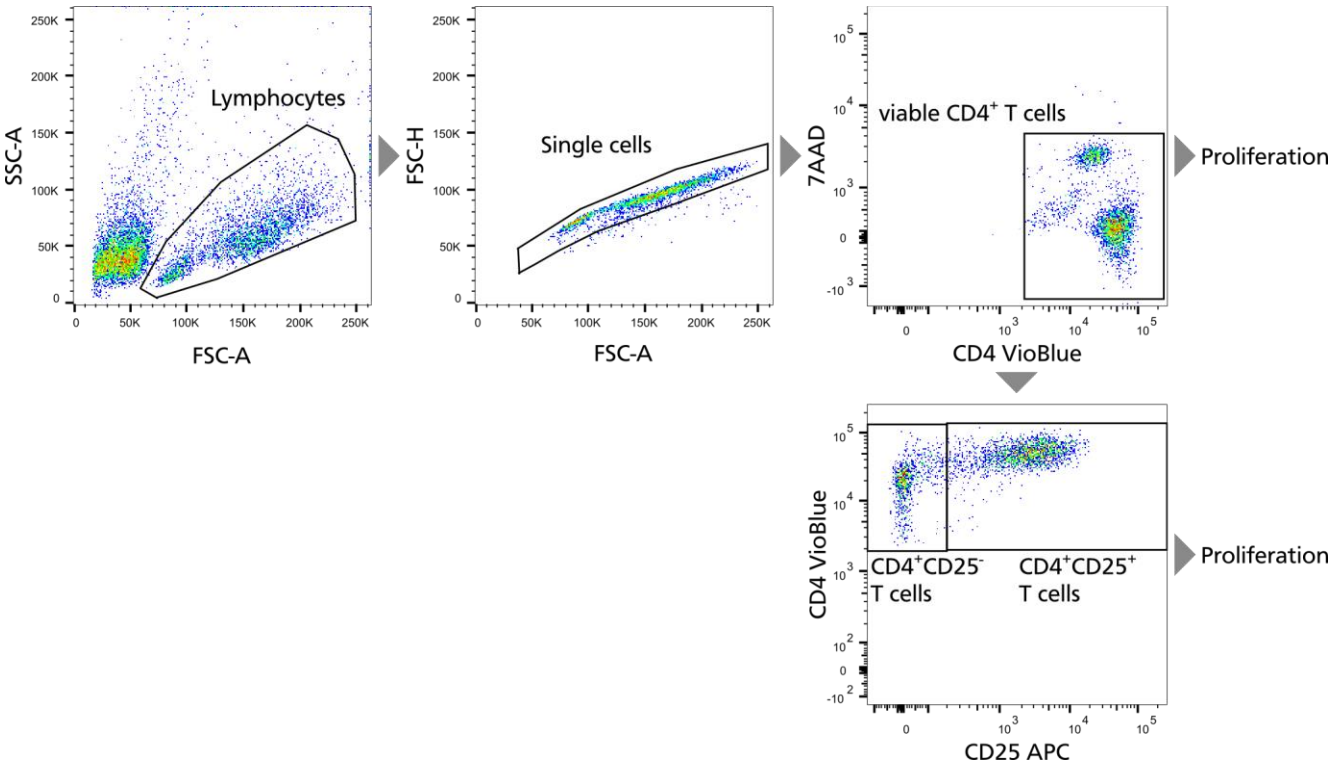

Figure 4-39: Gating strategy for T cells. In the first step, the lymphocyte population was determined via sideward and forward scatter. In the next step, only single cells were selected. Further on viable $CD4^+$ T cells were detected by the expression of CD4 and a low signal for the viability dye 7-AAD. This population was used for the determination of the expression of CD25. Proliferation was determined for the populations of $CD4^+$ T cells, $CD4^+CD25^-$ T cells and $CD4^+CD25^+$ T cells via CFSE intensity.

The analyses of the T cells after 9 days of co-cultivation revealed that the proliferation of all $CD4^+$ T cells was increased when the DCs were previously stimulated with one of the IL-Mixes (Figure 4-40 A and Table 4-5). When stimulated with LPS an increase in proliferation was detectable, however the response did not reach the results generated with IL-Mix-stimulated DCs. When comparing the influence of the added proteins, OVA led to an increase in T cell proliferation in combination with all stimuli compared to the addition of ReFacto AF or no protein. Interestingly, the addition of ReFacto AF led to a reduction of T cell proliferation in the group with LPS stimulation and in the group without any further stimulation compared to the stimulation containing no additional protein. In the groups stimulated with the two IL-Mixes, the addition of ReFacto AF however led to an increase in T cell proliferation compared to the stimulation containing no additional protein. When investigating the T cell response in more detail, the data revealed that most of the proliferating $CD4^+$ T cells were also $CD25^+$, indicating T cell activation, whereas the $CD25^-$ T cells revealed nearly no proliferation (Figure 4-40 B and C and Table 4-5). In line with the results of low receptor expression on DCs that were not stimulated with LPS or an IL-Mix (Figure 4-37), $CD4^+$ T cell proliferation was also very low in these co-cultivations. In general, no DC stimulation condition led to significantly increased $CD4^+$ T cell proliferation (Table A-10).

Nevertheless, LPS could be excluded as stimulus, due to the lower proliferation results. The differences in proliferation in response to the IL-Mixes with and without IL-8 were only small. Due to this, the IL-Mix without IL-8 was further on used for DC stimulation, as it was comparable to the published DC stimulation protocols. In order to be in line with the published concentrations of the given interleukins, the added concentration of IL-6 was reduced to 10 ng/ml[207,210]. This stimulus was further on called IL-Mix. The published Prostaglandin E_2 (PGE_2) was not added to the IL-Mix, as PGE_2 was mainly added to induce homing of the generated DCs to secondary lymphoid organs and this was not necessary in the DC-T cell Assay[208,224].

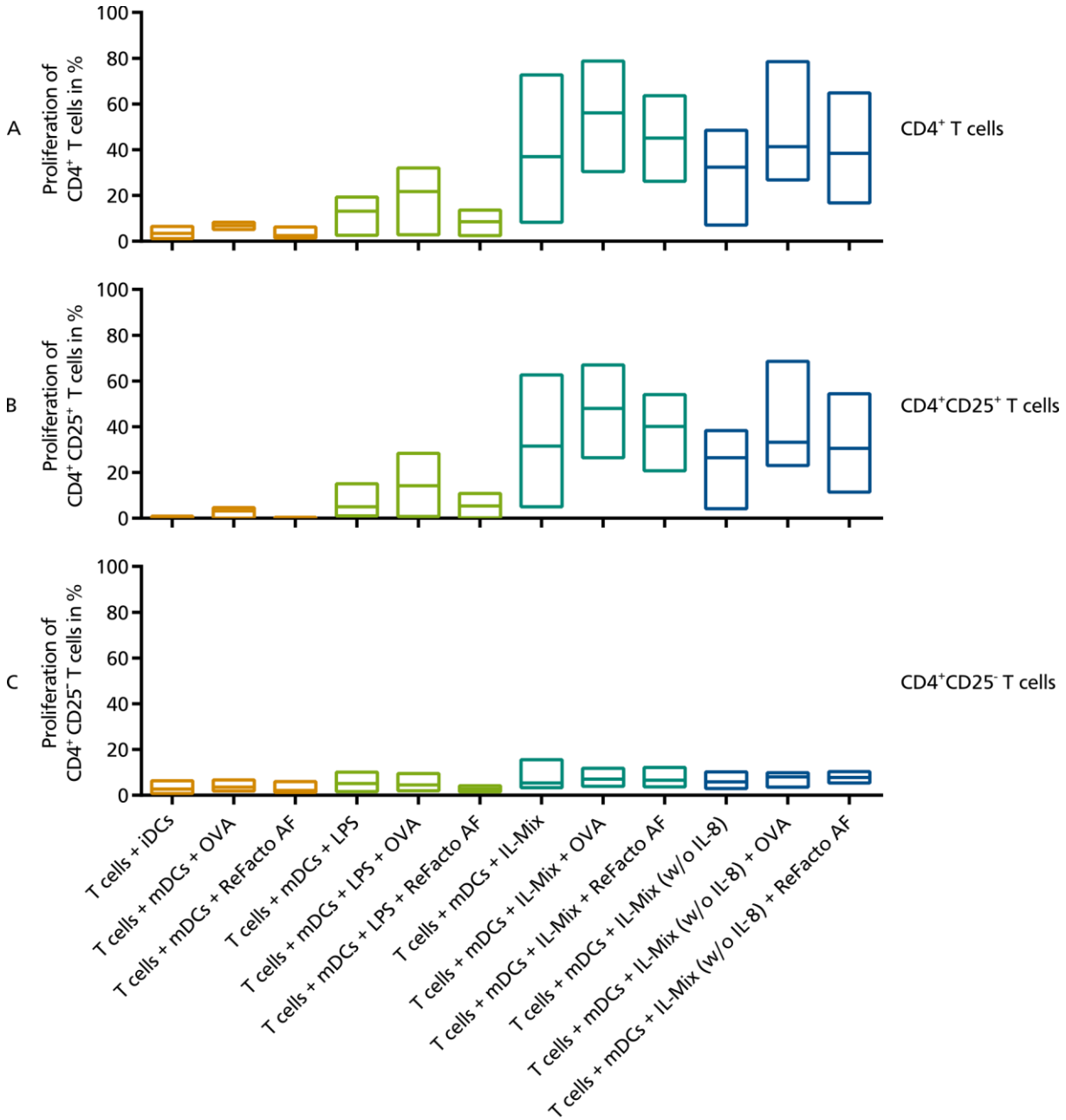

Figure 4-40: Floating bars representing the proliferation of $CD4^+$ T cells. The floating bars represent the proliferation of the $CD4^+$ T cells of three to six healthy donors, indicating the minimum, maximum and median value. The proliferation was calculated on all viable $CD4^+$ T cells. (A) Proliferation of all $CD4^+$ T cells. (B) Proliferation of $CD4^+CD25^+$ T cells. (C) Proliferation of $CD4^+CD25^-$ T cells.

Table 4-5: Median of proliferation of the different T cell populations in response to the differently stimulated DCs. The median was calculated from the response of three to six healthy donors per DC stimulation condition.

DC stimulus	Added protein	Median proliferation of $CD4^+$ T cells	Median proliferation of $CD4^+CD25^+$ T cells	Median proliferation of $CD4^+CD25^-$ T cells
No stimulus	No protein	3.5 %	0.2 %	2.7 %
	OVA	6.8 %	3.2 %	3.6 %
	ReFacto AF	2.5 %	0.3 %	2.1 %
LPS	No protein	13.2 %	5.0 %	5.2 %
	OVA	21.7 %	14.2 %	4.5 %
	ReFacto AF	8.5 %	5.3 %	2.7 %
IL-Mix	No protein	37.0 %	31.6 %	5.4 %
	OVA	56.1 %	48.0 %	7.1 %
	ReFacto AF	45.2 %	40.1 %	6.6 %
IL-Mix (w/o IL-8)	No protein	32.4 %	26.5 %	5.9 %
	OVA	41.4 %	33.2 %	8.1 %
	ReFacto AF	38.4 %	30.6 %	7.8 %

The next step in the development of the assay was the reduction of the culture volume from 600 μl in a 24-well plate to 300 μl in a 48-well plate, in order to reduce the amount of cells. A reduction to 100 μl in a 96-well plate was not possible, because this volume would have been too small to perform cytokine arrays after the co-cultivation. As the 48-wells were too small to harvest the DCs using a cell scraper, the $CD4^+CD25^-$ T cells were directly added to the adherent DCs after removal of the cell culture supernatant. In order to ensure a DC:T cell ratio of at least 1:10, the amount of DCs of five healthy donors after differentiation and stimulation was determined by counting the adherent cells. Prior to counting, the supernatant was removed and fresh X-VIVO 15 was added, in order to remove dead cells. Initially $3{\cdot}10^5$ monocytes were seeded in each well. The results of the cell count after 5 days of differentiation and 24 hours of stimulation is shown in Figure 4-41. The cells were counted in an area of 1.4 mm^2. The chosen area comprised neither the middle of the well nor the borders, in order not to distort the results. The final cell number was calculated for the full area of 87.5 mm^2. The cell numbers varied between $1{\cdot}10^4$ DCs and $7{\cdot}10^4$ DCs with medians of $3{\cdot}10^4$ DCs and $4{\cdot}10^4$ DCs, depending on donor and stimulus. Excluding the highest and the lowest value, which only occurred once, the amount of added $CD4^+CD25^-$ T cells per well was set to $6{\cdot}10^5$ cells for all further experiments. This ensured a DC:T cell ratio of at least 1:10, assuming a maximum of $6{\cdot}10^4$ DCs.

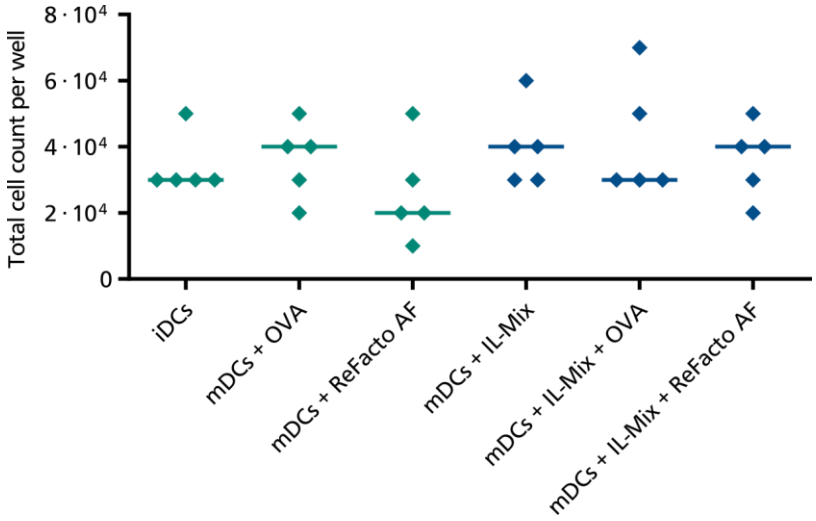

Figure 4-41: Cell number of mDCs per well of a 48-well plate. A defined area of each well was counted and the total cell number was calculated for the whole area. The cell number was calculated for different maturation stimuli and for five different healthy donors. The lines indicate the median cell number for each maturation stimulus.

After the determination of the assay conditions, the DC-T cell Assay was performed with FVIII-19M and FVIII-6rs. The cells were purified from PBMCs of healthy donors (3.2.4.3 and 3.2.4.4). The DCs were stimulated after differentiation either with the previously determined IL-Mix alone or with the IL-Mix and additional proteins. The additional proteins were ReFacto AF as a positive control for FVIII-specific $CD4^+$ T cell proliferation and FVIII-6rs and FVIII-19M as the proteins of interest. Based on published data, the concentration of the FVIII products was increased to 15 U/ml[190]. The co-cultivation occurred in 48-well plates, as described in 3.2.4.8 leading to a DC:T cell ratio of at least 1:10. All cells were analyzed by flow cytometry (3.3.1) after their purification (Table 3-2 to Table 3-4), in order to ensure purity, prior to co-cultivation, in order to exclude pre-activation, and after 9 days of co-cultivation (Table 3-5).

The results from the flow cytometric analyses of the T cells after 9 days of co-cultivation were further analyzed. The proliferation of all $CD4^+$ T cells was determined for every approach. In total 23 different healthy donors were analyzed. Donors, which revealed a higher $CD4^+$ T cell response to DCs only treated with the IL-Mix than with the IL-Mix and ReFacto AF or FVIII-6rs, were excluded form the final analysis. These healthy donors were assumed not to react to FVIII, which was expected, as not all healthy donors possess $CD4^+$ T cells against FVIII. Based on this selection, the results of 17 healthy donors were taken to the final statistical analysis (detailed proliferation results Table A-11). Additionally, when comparing the viabilities of the differently stimulated T cells after 9 days of co-cultivation, seven donors revealed a difference in the amount of viable T cells stimulated with either IL-Mix plus FVIII-19M or IL-Mix plus FVIII-6rs larger than 50 % (detailed viability results Table A-12). This was not detectable for the other donors and the reason could not be identified.

Figure 4-42 displays the difference between the $CD4^+$ T cell proliferation to DCs stimulated with IL-Mix plus FVIII-19M and the $CD4^+$ T cell proliferation to DCs stimulated with IL-Mix plus FVIII-6rs. Results below 0 indicate a reduced $CD4^+$ T cell response to FVIII-19M compared to FVIII-6rs. The turquoise bars indicate the seven donors with the high difference in the amount of viable T cells. A reduced response to FVIII-19M was detected in most donors. However, results above 0 were detected in five donors. Even though, the differences in proliferation were below 10 % for these donors, whereas even higher differences were detected in the group of donors, showing a reduced response to FVIII-19M. Altogether the amount of donors revealing a reduced response to FVIII-19M was larger, leading to a significant reduction in $CD4^+$ T cell proliferation to DCs stimulated with IL-Mix and FVIII-19M when comparing all 17 donors (Table A-13). However, even after the exclusion of the seven indicated donors the result was still significant, only leading to a slight increase of the P value (Table A-13).

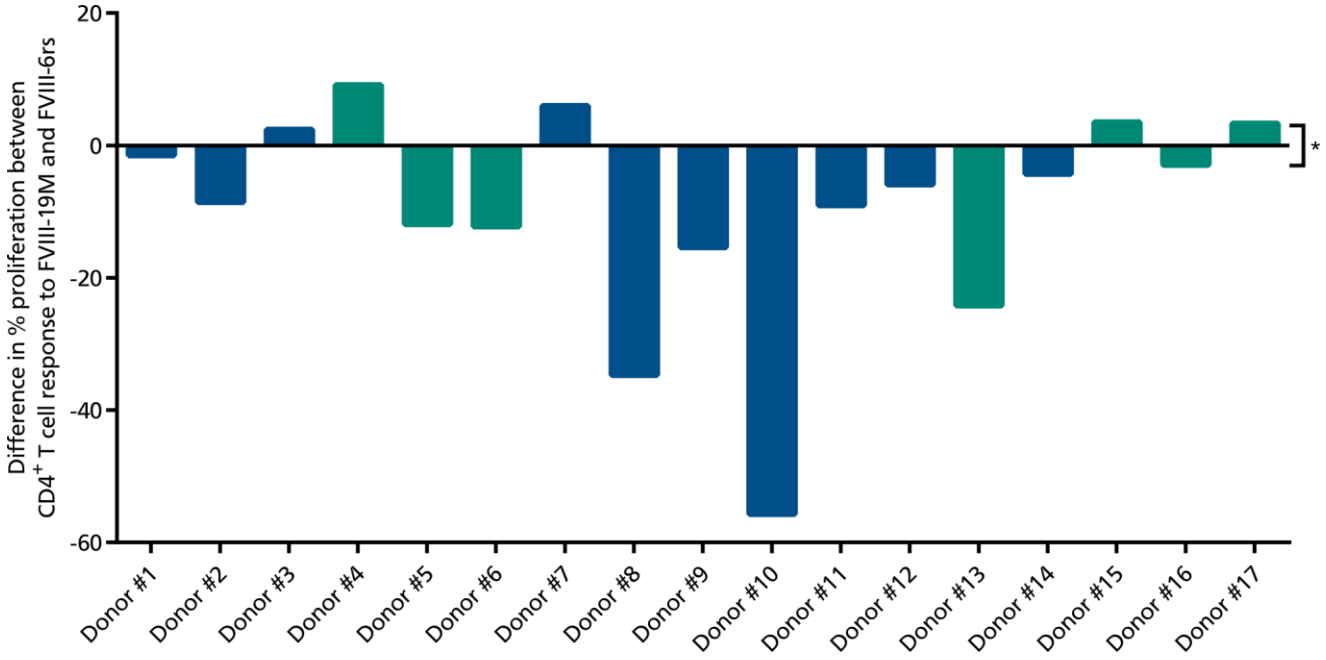

Figure 4-42: Difference between the $CD4^+$ T cell proliferation against DCs stimulated with IL-Mix plus FVIII-19M and DCs stimulated with IL-Mix plus FVIII-6rs. The bars below 0 indicate a reduced $CD4^+$ T cell response to FVIII-19M. The green bars indicate donors with a huge difference in the viability of the differently stimulated T cells. The lower $CD4^+$ T cell response to FVIII-19M compared to FVIII-6rs is significant using the Wilcoxon test.

The supernatants of the co-cultivations were further analyzed in a cytokine array (3.3.2). The cytokine profiles for the co-cultivations stimulated with IL-Mix plus FVIII-19M and IL-Mix plus FVIII-6rs were determined. In total, the cytokines were analyzed for 14 of the 17 donors, missing Donor #4, #13 and #14. Due to the small volume of available supernatant and the preparation of a control, only 100 μl of supernatant were applied to a membrane. For a better comparability of the results, the signals for the different cytokines were normalized to the signal of the control. Unfortunately, no meaningful conclusion could be drawn from the array (Figure A-5). For nearly all cytokines, relative signals between 30-40 % were detected (Table A-14). This was independent of the FVIII variant present in the co-cultivation. The signals for cytokines expressed by macrophages, monocytes and all different T helper cell lines were similar. As this was also true for the five cytokines with significant differences in the signal between co-cultivations containing FVIII-6rs and FVIII-19M, these results were not considered meaningful. In general, the similar results for all cytokines might have been a consequence of the artificial assay setup or the small volume applied, which was only 10 % of the recommended volume. *In vivo* a larger amount of different cytokines and cells would interact, probably leading to a more meaningful cytokine profile.

For five of the donors included in the final proliferation analysis, the HLA genotype was available. This was used to calculate the Individual T cell Epitope Measure (iTEM) scores. The iTEM scores were calculated using the same tools as described in 3.1. However, whereas the previous analyses were performed for HLA class II supertype alleles, the iTEM score indicates the immunogenicity of a protein for the specific genotype of one person. This was performed for the FVIII-19M and FVIII-6rs for Donors #1, #2, #3, #6, #8 and #10. The difference in the iTEM scores between FVIII-19M and FVIII-6rs for each donor was plotted against the corresponding difference in $CD4^+$ T cell proliferation (Figure 4-43). This revealed that with an increasing difference in iTEM score, corresponding to a higher influence of the deimmunization on the given genotype, the difference in proliferation increased too. This was the case for Donor #2, #8 and #10. Donor #1 and #6 revealed a lower influence of the deimmunization on the proliferation than expected based on iTEM score. This shows that immunogenicity is not only dependent on the sequence of the peptides. Donor #3, who showed an increase in $CD4^+$ T cell proliferation to FVIII-19M, was however the one with the lowest difference in iTEM scores, indicating the lowest influence of the incorporation of the 19 mutations on the immunogenicity. These data revealed that the *in silico* analyses could be confirmed with the developed *in vitro* DC-T cell Assay.

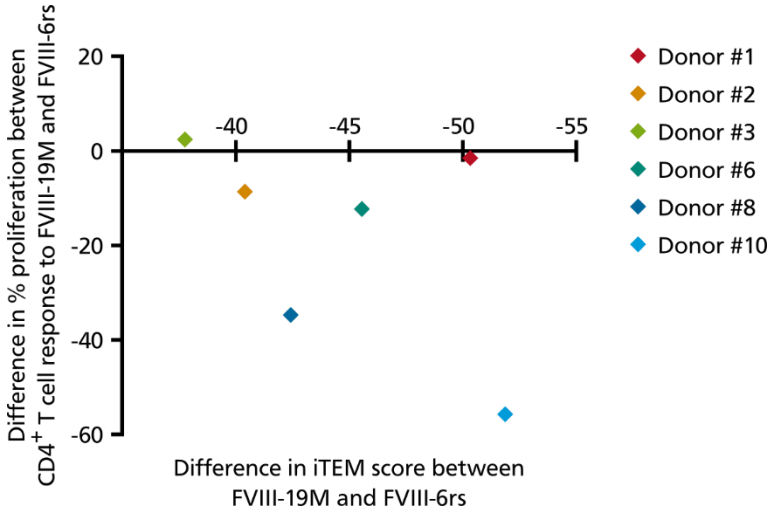

Figure 4-43: Relation between the differences in iTEM scores and proliferation. The iTEM scores for FVIII-19M and FVIII-6rs were calculated for donor #1, #2, #3, #6, #8 and #10, based on their HLA genotype. The differences of the iTEM scores were plotted against the differences in $CD4^+$ T cell proliferation, determined in the DC-T cell Assay.

Altogether, the results from the *in vitro* DC-T cell Assay revealed a reduced $CD4^+$ T cell proliferation in response to the deimmunized FVIII variant containing the 19 amino acid mutations. However, some donors showed an increase in $CD4^+$ T cell proliferation to FVIII-19M. Unfortunately, the HLA genotype of only one of these donors was available. Nevertheless, the iTEM analysis for this donor revealed that the incorporation of the 19 mutations only led to a slight reduction in immunogenicity with the given HLA genotype. This might have been one reason why no reduction in $CD4^+$ T cell proliferation was detectable. Nevertheless, not only the HLA genotype had an influence on the presented peptides but also other factors, like the expression of intracellular proteases and the available $CD4^+$ T cell pool, which differ between persons. This is the reason why even patients with the same HLA genotype do not present the same peptides of a protein[174]. Even though, the assay demonstrated to be a useful tool to determine immunogenicity of a protein *in vitro* and indicated a correlation to the *in silico* modelled immunogenicity.

Unfortunately, it was not possible to determine the proliferation of $CD4^+$ T cell derived from Hemophilia A patients. This was because the amount of available blood was even smaller than expected and the amount of available PBMCs was not sufficient to perform the established DC-T cell Assay.

4.6. *In vivo* mouse models

For the first *in vivo* experiments, the E16 FVIII KO model was used. All experiments were performed by EpiVax. Prior to the study an *in silico* analysis was performed, in order to determine how many epitopes were present in the FVIII-19M, FVIII-6rs and ReFacto AF, taking into account the murine HLA background. The results are presented in Table 4-6. The analysis revealed that the deimmunized FVIII-19M contained 86 immunogenic epitopes compared to 94 epitopes in the FVIII-6rs. Due to this, a reduction in immunogenicity might be detectable in these mice, however no large differences were expected. ReFacto AF was found to have one epitope less compared to FVIII-6rs, which was due to the differences in the B domain deletion. However, the total immunogenicity score of FVIII-6rs was lower than the immunogenicity score of ReFacto AF. This was also due to the larger B domain deletion in ReFacto AF compared to FVIII-6rs and FVIII-19M, as the immunogenicity score was calculated in relation to the size of the protein.

Table 4-6: *In silico* analysis of the different FVIII products based on the HLA background of the E16 FVIII KO mice. The total amount of epitopes and the immunogenicity score was calculated for FVIII-19M, FVIII-6rs and ReFacto AF.

Amount of epitopes			**Immunogenicity score**		
FVIII-19M	FVIII-6rs	ReFacto AF	FVIII-19M	FVIII-6rs	ReFacto AF
86	94	93	4.89	16.89	22.58

The mice were immunized with FVIII-19M, FVIII-6rs, ReFacto AF or FVIII Formulation Buffer, as described in 3.6.1.2. Each product was applied to ten mice. After four injections of 4 U FVIII product or FVIII Formulation Buffer and a fifth injection of 8 U FVIII or FVIII Formulation Buffer per mouse, the mice were euthanized. The plasma was isolated for the determination of the generation of anti-FVIII antibodies and the splenocytes were purified and restimulated in an *in vitro* assay, in order to determine whether FVIII-specific $CD4^+$ T cells had evolved.

The anti-FVIII antibody ELISA was performed as described in 3.6.2.3, using the goat anti-mouse IgG-Peroxidase as secondary detection antibody. The results are presented in Figure 4-44. The ELISA revealed anti-FVIII antibodies in at least four of ten mice, regardless whether they were immunized with ReFacto AF, FVIII-19M or FVIII-6rs. Only the mice injected with FVIII Formulation Buffer developed no antibodies, showing that the response was FVIII-specific. Although the antibody titers were slightly higher for ReFacto AF and FVIII-6rs compared to FVIII-19M no significant difference was detectable (Table A-15).

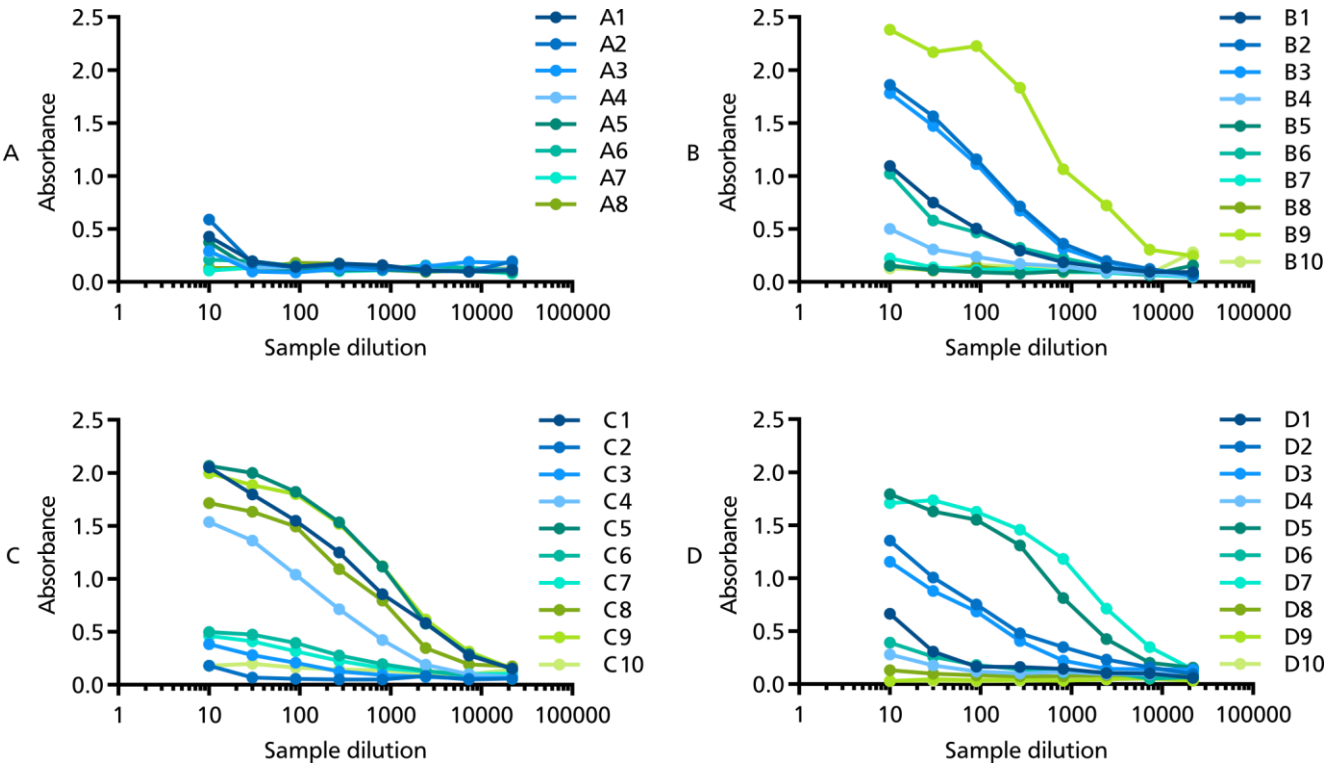

Figure 4-44: Anti-FVIII antibody ELISA for the immunized E16 FVIII KO mice. Plasma samples were applied in 1:3 serial dilutions. The detection of the bound antibodies occurred via a goat anti-mouse IgG-Peroxidase secondary antibody. (A) Results for mice injected with FVIII Formulation Buffer. ReFacto AF was coated to the plate. Two mice died during the experiment. (B) Results for mice injected with ReFacto AF. (C) Results for mice injected with FVIII-6rs. (D) Results for mice injected with FVIII-19M.

The isolated splenocytes of the mice were cultivated as described in 3.6.2.2. This *in vitro* assay was performed directly after the isolation of the cells, avoiding freezing and thawing of the cells. The splenocytes of each mouse were stimulated with either PBS or the FVIII product used for immunization. The control mice, which were immunized with FVIII Formulation Buffer, were stimulated with ReFacto AF. After 4 days of cultivation, the cells were harvested and analyzed by flow cytometry. The proliferation of the $CD4^+$ T cells is displayed in Figure 4-45. A restimulation of the $CD4^+$ T cells with FVIII was possible when the mice were initially immunized with FVIII. When PBS was used for restimulation no proliferation was detectable, indicating that the proliferation was FVIII-specific. When comparing the median of $CD4^+$ T cell proliferation for PBS- and FVIII-restimulation for each FVIII product, ReFacto AF and FVIII-6rs led to a significant increase in proliferation (Table A-16). In contrast to that, only a slight but not significant increase in $CD4^+$ T cell proliferation was detectable when FVIII-19M was used for restimulation compared to PBS. The restimulation of $CD4^+$ T cells derived from the control mice with ReFacto AF also revealed no significant proliferation compared to PBS restimulation. These results matched the antibody titers determined in the ELISA and hint towards a reduced immunogenicity of the FVIII-19M.

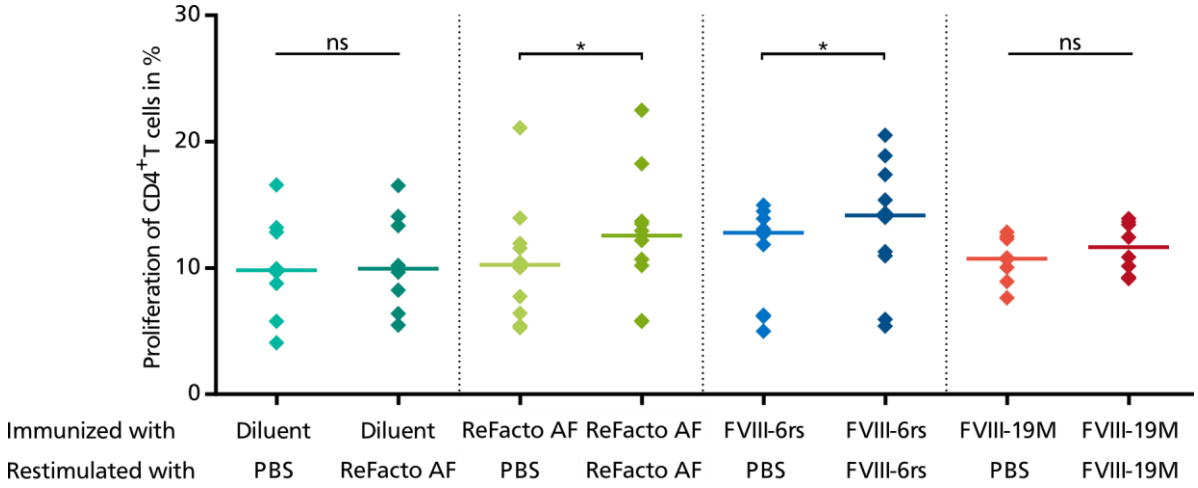

Figure 4-45: Proliferation of $CD4^+$ T cells derived from splenocytes of E16 FVIII KO mice. The amount of proliferating $CD4^+$ T cells is indicated for every mouse restimulated with either PBS or FVIII, depending on their initial immunization. The line indicates the median for each group. Statistical analysis was performed using the Wilcoxon test.

Based on the results of the anti-FVIII antibody ELISA and the $CD4^+$ T cell restimulation assay a slightly reduced immunogenicity of the FVIII-19M in the E16 FVIII KO model was detected. However, a higher reaction of the murine immune system to the applied FVIII products was expected, as E16 FVIII KO mice do not produce functional FVIII. Generating a higher response might have led to a greater range in which differences in response to the FVIII products would have been easier to detect. However, it is known that non-functional parts of the murine FVIII heavy chain are present in these mice[225]. Probably these peptides induced tolerance, leading to the low response to the applied FVIII products. When repeating the study, nearly no response to the positive control ReFacto AF was detectable. This may have been due to the fact that the final boost of the murine immune system with 8 U FVIII was replaced by an application of 4 U FVIII per mouse.

In the second *in vivo* experiment, BRGSF mice were immunized with ReFacto AF, FVIII-6rs and FVIII-19M. These mouse experiments were performed by Axenis. Compared to the E16 FVIII KO mice, the BGRSF mice had a human immune system and due to this, human MHC class II. Therefore, the originally calculated immunogenicity scores (Figure 4-14) were applicable to this mouse model. Unfortunately, the BRGSF mice were not FVIII-deficient and were expected to be able to develop tolerance to the murine FVIII. Three different stem cell donors were used for the generation of the BRGSF mice. Five mice were immunized per FVIII product as described in 3.6.1.1. For each group, mice with two to three different HLA backgrounds were used. After four injections of 200 U FVIII product per kg body weight and a final injection of 400 U/kg FVIII the mice were euthanized. The plasma was isolated

and the splenocytes were purified. Plasma and splenocytes were frozen for shipment and stored at -150 °C for the anti-FVIII antibody ELISA and the *in vitro* $CD4^+$ T cell restimulation assay.

The anti-FVIII antibody ELISA was performed similar to the ELISA with the plasma of the E16 FVIII KO mice, except that the plasma samples were initially applied undiluted (3.6.2.3). Additionally, mouse anti-human IgM-HRP and mouse anti-human IgG-HRP were used as secondary detection antibodies, as humanized mice were expected to produce IgM as well as IgG. The detection of anti-FVIII IgG and IgM was performed in parallel for each mouse. The results for the study are presented in Figure 4-46. Unfortunately, no anti-FVIII-IgG were detectable in any of the three groups of mice. A detection of very low amounts of anti-FVIII-IgM was possible, however as a mouse was considered to be antibody-negative when the absorbance was below 0.2, only one mouse at all, immunized with FVIII-19M, revealed anti-FVIII-IgM. Even for this mouse the absorbance was below 0.4 at a sample dilution of 1:30, indicating only a very low amount of anti-FVIII antibodies.

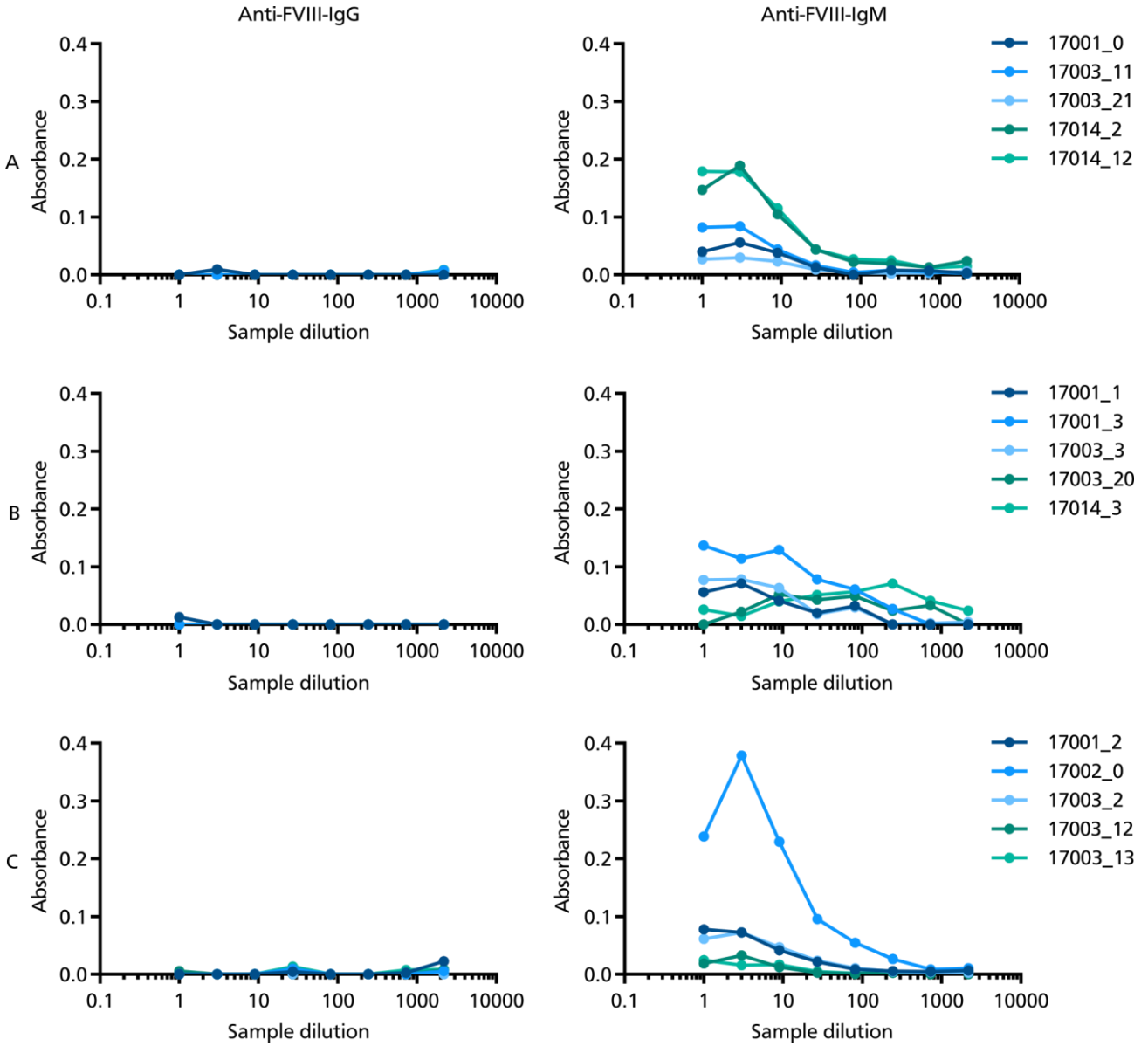

Figure 4-46: Anti-FVIII antibody ELISA for the immunization experiment with BRGSF mice. Plasma samples were applied in 1:3 serial dilutions. The detection of the bound antibodies occurred via a mouse anti-human IgG-HRP or a mouse anti-human IgM-HRP secondary antibody. 17001, 17002, 17003 and 17014 indicate the three different human stem cell donations used for the transplantation, whereof 17001 and 17002 are based on the same donor. The numbers 0-21 indicate a specific mouse in a group with identical stem cell background. (A) Results for mice injected with ReFacto AF. (B) Results for mice injected with FVIII-6rs. (C) Results for mice injected with FVIII-19M.

The isolated splenocytes were thawed and cultivated as described in 3.6.2.1 and 3.6.2.2. The splenocytes of each mouse were restimulated with either cell culture medium or the FVIII product used for immunization. Due to the freezing and thawing, a loss of cells was inevitable, which made it impossible to perform both stimulations for some splenocyte preparations. In these cases, the restimulation with the FVIII product was preferred. After 4 days of cultivation, the cells were harvested and analyzed by flow cytometry (3.3.1), using the T cell proliferation stain for humanized mouse splenocytes (Table 3-6). The proliferation of the $CD4^+$ T cells is illustrated in Figure 4-47. Unfortunately, nearly no proliferation of $CD4^+$ T cells was detectable. Due to this no significant differences could be detected (Table A-17). Only $CD4^+$ T cells of 1 out of 15 mice revealed proliferation comparable to the results with the E16 FVIII KO mice.

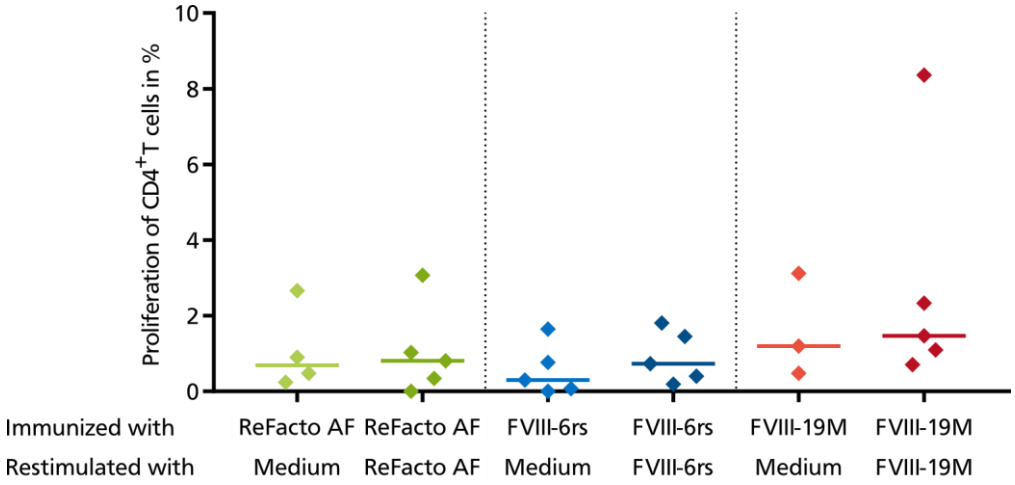

Figure 4-47: Proliferation of $CD4^+$ T cells derived from splenocytes of BRGSF mice. The amount of proliferating $CD4^+$ T cells is indicated for every mouse restimulated with either medium or FVIII depending on their initial immunization. The line indicates the median for each group.

The anti-FVIII antibody and the $CD4^+$ T cell restimulation results from the BRGSF mice indicate that this mouse model is not appropriate for the detection of an immune response to FVIII. Only one mouse revealed a low amount of anti-FVIII antibodies and one mouse showed a slight proliferation in response to FVIII. Although both mice were of the FVIII-19M-immunized group, the mouse producing antibodies and the mouse revealing $CD4^+$ T cell proliferation were not the same. The absence of an immune response indicates that the BRGSF mice developed tolerance to the murine FVIII, which seemed to suppress an immune response to human FVIII.

In total, the humanized immune system of the BRGSF mice is preferred over the murine immune system of the E16 FVIII KO mice. Due to the human MHC class II, this model is the only possibility to prove the influence of the incorporated mutations on the presentation of peptides on the surface of antigen-presenting cells. However, the results of both mouse models also revealed the importance of the total absence of FVIII in these mice. In both mouse models, tolerance to FVIII seemed to be present, which suppressed the immune response to FVIII, especially in the BRGSF mice. Based on these results a humanized mouse model with a total knockout of the FVIII gene is required, in order to be able to determine an influence of a deimmunized FVIII variant on the immune response.

5. Discussion

One of the major drawbacks in FVIII therapy is the development of inhibitors against the therapeutic FVIII product. Although the rFVIII product by Bioverativ, Eloctate, might be less immunogenic, due to immune regulatory sequences in the attached Fc-part[108], no deimmunized FVIII was yet developed. It was the aim of this thesis to develop such a FVIII molecule, in order to improve the FVIII therapy and by this the life of the patients.

The *in silico* analyses were performed with the EpiMatrix tools provided by EpiVax. This system was chosen, as it not only provides the detection of immunogenic peptides but also additional tools leading to a recommendation of mutations for deimmunization. Additionally, the system was already successfully used to deimmunize other proteins[184,185]. For deimmunization, the sequence of a B domain-deleted FVIII was chosen. B domain deletion is implemented since second generation rFVIII products, as it reduces the size of the protein without impairing its functionality[89,226,227]. In addition to that, potential immunogenic peptides in the B domain were already removed without the need to insert mutations.

The EpiMatrix tool revealed many immunogenic clusters throughout the whole molecule (4.1). This was expected, as the antibody repertoire of the patients is known to be very diverse[121]. Of the 52 detected immunogenic clusters 36 overlapped with already published, experimentally determined peptides[84,174,228,229]. In these publications, peptides were eluted from the MHC class II, derived from different Hemophilia A donors with different HLA types, and subsequently sequenced. Taking into consideration that the immunogenic clusters are larger than the eluted peptides, 28 peptides overlapped completely with the *in silico* determined clusters and eight overlapped by two to eight amino acids. Thirteen of the clusters deimmunized in the FVIII-19M were still overlapping with the experimentally defined peptides. Nine peptides overlapped completely and four overlapped partly with the mutated clusters in the FVIII-19M. In addition to the exact determination of presented peptides, restimulation experiments of $CD4^+$ T cells with FVIII peptides were published[127,230–232]. Peptides from the A2, A3, C1 and C2 domain were used for the restimulation of T cells either only derived from Hemophilia A patients with inhibitors or from Hemophilia A patients with and without inhibitors, acquired Hemophilia A patients and healthy donors. Although differences were detectable among the different groups, dominant peptides, leading to a high $CD4^+$ T cell response in several groups, could be detected. Only two of the 14 published dominant peptides were not detected during the *in silico* calculations. Finally, three of the 19 mutations in FVIII-19M laid within these peptide sequences. Another study already indicated that the incorporation of amino acid mutations into FVIII leads to a reduced binding to MHC class II *in vitro* and to a reduced immunogenicity *in vivo*[173]. The experiments were performed with the C2 domain of FVIII. The *in silico* analyses were conducted with the previously describes tools (3.1) and up to three mutations were incorporated into different C2 peptides. The *in vitro* binding assays revealed reduced binding for most of the mutated peptides and a reduced immunogenicity was detectable for some peptides in different mouse models. *In vitro* as well as *in vivo* the peptides containing more mutations led to a greater reduction in binding and immunogenicity. Although the experimental setup was artificial, due to the addition of peptides and not a full protein, the results indicated that the *in silico* calculated mutations influenced the binding to the MHC class II and by that the immunogenicity. Three of these mutated amino acids were part of the initially tested 57 mutations, which were recommended for the FVIII deimmunization, although different amino acids were selected for substitution. Unfortunately, none of the three mutations from the publication was incorporated into the final FVIII-19M. This was mainly because in the publication only peptides were investigated, not taking into consideration whether the mutations disrupt the FVIII activity. Additionally, the publication only focused on the C2 domain. In general, deimmunizations based on *in silico* analyses were already successfully performed for other proteins like erythropoietin[178] and the bispecific, FVIII-mimicking antibody Emicizumab[184]. Altogether these published results hint towards a clinical relevance of the identified immunogenic clusters and indicate that the used *in silico* method was appropriate for the analysis of immunogenic FVIII peptides and the deimmunization of FVIII.

Nevertheless, the results also revealed that some clusters could not be altered, neither *in silico* nor experimentally (4.2). *In silico* alterations failed in cases where immunogenic clusters comprised cleavage or binding sites or where possible mutations were known to lead to Hemophilia A. Only one alteration

near a cleavage site was tested. As expected the incorporation of mutation F1710H near the thrombin cleavage site at R1708 led to a strong reduction in activity, probably due to impaired thrombin cleavage (Figure 4-3 C). Although in this case an aromatic amino acid was replaced by another aromatic amino acid, a histidine is naturally not very common in this position[233]. For some clusters, the insertion of up to three different mutations was tested. However, in some cases none of the single mutations could be incorporated into the FVIII sequence (Figure 4-3). Although none of these mutations were associated with Hemophilia A or in close proximity to sites of post-translational modification, cleavage or binding, the incorporations led to reduced activities or the total absence of the FVIII variants. The reasons for this remain to be elucidated but most likely the mutations had a negative influence on the structure of FVIII, impairing proper folding and due to this functionality. This indicates how important further investigations on the secondary and tertiary structure of FVIII are. A high-resolution model of FVIII would provide the possibility to model the incorporation of mutations *in silico*, revealing mutations that might impair the structure.

When comparing the amount of immunogenic clusters per domain, taking into account the size of the domain, no large differences were detectable between the domains. Only the C2 domain revealed a slightly higher amount of immunogenic clusters. However, after identifying the mutations that could be incorporated into the FVIII molecule, it became obvious that most of the 19 mutations were located in the A1 and A2 domain. These results might be due to the importance of the A3, C1 and C2 domain for the functionality of FVIII. Especially in the tenase complex these domains are essential for interactions. The FVIII antigen results also support this theory, as the variants with more mutations in the A3C1C2 domain were mostly expressed but revealed reduced activity (Figure 4-8 to Figure 4-10). This indicated that production and secretion of these FVIII molecules was not impaired by the mutations.

Whether the incorporated 19 amino acid mutations also disrupt B cell epitopes was not further investigated. It is known that T and B cell epitopes can cluster within a short sequence[127,234]. Based on the known B cell epitopes for FVIII, the mutations S507E, F555H and K1837E are also part of B cell epitopes[235–237]. Additionally, the mutations S2315T and V2333A are in close proximity to B cell epitopes[238,239]. However, apart from disrupting B cell epitopes, the incorporation of amino acid mutations can also generate new ones. However, further work is needed, in order to determine whether the mutations have an influence on B cell epitopes.

In general, the introduction of the mutations into the FVIII sequence was feasible and the chosen strategy to perform several rounds was very successful (Figure 4-13). The decision to transfer only one mutation per immunogenic cluster to the second screening round was made, in order to reduce the probability of an inactive FVIII, and was based on the calculations indicating that the introduction of both mutations would not further reduce the immunogenicity score. The DOE matrices proved to be a good tool, in order to detect the mutations that interfered with the activity of the FVIII molecule (Figure 4-8). Finally, a combination of mutations could be found for the A2 and A3C1C2 domain, using this tool (Figure 4-10). Further variants with alternative mutations were not generated, as for most of the excluded mutations no alternatives were available. Nevertheless, it would be interesting to determine, whether the incorporation of more than one mutation per cluster would still lead to a functional FVIII molecule and whether this would result in a further reduction of the immunogenicity of the molecule, although *in silico* calculations indicate that the influence is marginal. However, based on the findings from the three rounds, adding more mutations would be associated with the need to produce many variants, in order to find a combination of mutations not interfering with the activity of FVIII.

The final FVIII-19M was calculated to have an immunogenicity score of -10.55 compared to an initial score of 7.01 for the FVIII-6rs, revealing a reduction by 17.56 points (Figure 4-14). Taking into consideration that this reduction was achieved by changing only 1.25 % of the FVIII amino acid sequence, the process was very efficient. Additionally, a negative immunogenicity score corresponds to a lower amount of immunogenic epitopes compared to a protein with a random sequence. This and the proximity to the immunogenicity score of albumin, a well tolerated endogenous protein, supports the assumption that FVIII-19M would be better tolerated by the immune system.

For the production of FVIII-19M and FVIII-6rs the cell line was switched from HEK 293-F to CAP-T. This cell line was shown to be superior in the production of high amounts of large and complex proteins[198,240,241]. This was confirmed, as up to 2 U/ml FVIII were produced by CAP-T cells whereas only

about 1 U/ml were reached using HEK 293-F cells. The applied production and purification methods were appropriate for this stage of development (4.3). Due to the high amounts of FVIII produced by the CAP-T cells after transient transfection, the yield of about 50 % after purification was still enough for further experiments. However, these techniques have to be improved for large-scale productions. On the one hand, a stable transfection of CAP cells and the selection of single cell clones, highly expressing the FVIII molecule, will increase the amount of produced FVIII-19M. On the other hand, adaptions during chromatography and concentration of the purified product will increase the yield. Adaptions in the chromatography buffers and the replacement of spin columns for concentration by tangential flow filtration might already lead to an improvement, as seen with other FVIII molecules.

The different structural and functional analyses of the FVIII-19M and FVIII-6rs proved to be useful for the characterization of the two molecules (4.4). The comparison to the already approved products ReFacto AF and Nuwiq provided encouraging results. However, the analyses also revealed where further investigations are needed.

The detection of the different FVIII products on a Western Blot, with antibodies specifically detecting the heavy and the light chain of FVIII, revealed the first similarities and differences between the products (Figure 4-24). In general, heavy chain, light chain and single chain of FVIII was present in all four products, however the ratios were different. Whereas Nuwiq and ReFacto AF consisted mainly of double-chain FVIII, detected as heavy and light chain, nearly no single-chain FVIII was present. In contrast to that, the FVIII-19M and FVIII-6rs samples revealed about 50 % single chain. As neither the B domain deletion nor the incorporated mutations interfered with the furin cleavage site responsible for the generation of the double-chain variant, it is unlikely that the high amount of single chain was due to variations in the amino acid sequence. The strongest influence, on whether single- or double-chain FVIII was secreted, might have had the cell line in which the FVIII was produced. Different expression levels of furin or other intracellular proteases in the different cell lines HEK, CHO and CAP-T, might have led to different cleavage patterns of FVIII. Another reason for the low amounts of single chain in ReFacto AF and Nuwiq might have been due to a depletion of single-chain FVIII during the purification process, as this is more extensive than for FVIII-19M and FVIII-6rs. However, this issue was not further followed, as the activation by thrombin was not impaired in the single-chain variant compared to the double-chain variant. In addition to this, the rFVIII product Afstyla, by CSL Behring, which is especially designed to be secreted as a single chain, is already approved as a therapeutic FVIII product[103,106]. This indicates that the presence of FVIII as a single-chain variant is not a negative result. The development of future FVIII products might even concentrate on single-chain variants, as it facilitates production and purification of the FVIII product, due to the fact that the molecule is more stable than the double-chain variant, which is mainly held together by a divalent cation.

In addition to the different amounts of single and double chain, the blot revealed the different molecular weights of the heavy chains between the four products (Figure 4-24). The FVIII-19M and FVIII-6rs heavy chains revealed a higher molecular weight compared to the heavy chains of ReFacto AF and Nuwiq. This was expected as more amino acids of the B domain were deleted in ReFacto AF and Nuwiq. Additionally, two slightly distinct heavy chains were detected for ReFacto AF, due to proteolytic variations at the C-terminus[227]. These differences were not detectable for any of the other products and might have been due to the different production cell lines. In contrast to that, more than one light chain band was detectable for every product. Differences in the molecular weight of the light chain were probably based on slight differences at the N-terminus and on post-translational modifications[227]. These modifications were most likely different glycosylations[242,243] as the difference between a Tyrosine and a Sulfotyrosine is only 80 Da and due to that not detectable on the presented Western Blot. In total, four different bands for the light chain were identified, considering that the light chains with a higher molecular weight contained a higher amount of glycosylation. FVIII-19M and FVIII-6rs revealed to posses light chains with high molecular weights whereas Nuwiq and ReFacto AF possessed mainly one high and one lower molecular weight light chain. The lower molecular weight light chain was more dominant in ReFacto AF whereas the high molecular weight light chain was more dominant in Nuwiq. The amount of the two light chain forms in FVIII-19M and FVIII-6rs were similar. The light chain with the lowest molecular weight could only be detected for Nuwiq and ReFacto AF. The results were consistent with the published characteristics for ReFacto AF and Nuwiq[227,243]. In general, these were the first results

hinting towards differences in the glycosylation of FVIII-19M, FVIII-6rs and Nuwiq compared to ReFacto AF. All three products were produced in human cell lines whereas ReFacto AF was produced in a non-human mammalian cell line. Still, the Western Blot did not reveal whether this was due to different glycosylation patterns or due to more glycosylated sites in general. In order to determine this, a detailed mass spectrometric analysis of the glycosylations is required.

The Western Blot presenting the FVIII products in their glycosylated and deglycosylated form supported the assumptions made from the Western Blot detecting the heavy and light chain of FVIII. A clear band shift was detectable after deglycosylation for each band of every FVIII product, indicating that glycosylation occurred in every cell line (Figure 4-25). Unfortunately, the deglycosylation of the products was not complete, as even after the deglycosylation, light chains with different molecular weights were still detectable. In the case of a complete deglycosylation a maximum of two bands for the light chain were expected based on published results for ReFacto[227]. As before, no conclusion could be drawn regarding the amount and kind of glycosylations. Different glycosylation patterns are expected for the different cell lines and were already proven for ReFacto AF and Nuwiq[42,227]. These analyses also revealed that only four of the available six N-glycosylations sites were occupied, similar to pFVIII. Additionally, different glycosylation patterns for the same glycosylation site occurred within one cell line. Detailed glycosylation analyses for FVIII-19M and FVIII-6rs are outstanding and new production and purification of the two variants is required for this, as high amounts of protein are needed for glycosylation analyses. Still, these analyses are expected to reveal diverse glycosylation patterns, as the production is not yet restricted to a single cell clone.

Most of the findings from the Western Blot detecting heavy and light chain of FVIII were also shown in the 2D-DIGE results (Figure 4-27 to Figure 4-29). This method provided an even more detailed analysis of the different products, as a direct overlay was possible. Regarding ReFacto AF and Nuwiq, the 2D-DIGE confirmed the existence of two heavy chains in ReFacto AF and also revealed a second heavy chain for Nuwiq, though in an even lower amount compared to ReFacto AF. In addition to the differences in molecular weight, the FVIII was also separated based on the pI. Unfortunately, the IEF was not very clear but it revealed that different pIs were present in the heavy and light chains probably due to different post-translational modifications. Additionally it might indicate the slightly reduced pI of the FVIII-19M compared to FVIII-6rs, as some spots, especially of the light chain, differed in this first dimension (Figure 4-28 C). In order to be able to draw more conclusions from the IEF, the method has to be improved for FVIII. The main differences detected on the 2D-DIGE were impurities. Whereas ReFacto AF and Nuwiq revealed no contaminating proteins, the purifications of FVIII-19M and FVIII-6rs still contained proteins other than FVIII (Figure 4-28 A and B). This was expected, as the purification method was not adapted to the clinical standard of the commercially available products. Due to this, it is highly likely that these contaminating proteins were host cell proteins, which were not removed during purification. Mass spectrometric analysis could be used, in order to identify these spots.

The last analysis of the FVIII proteins confirmed the presence of sulfotyrosines in all tested FVIII products (Figure 4-26). However, the Western Blot did not indicate how many tyrosines were sulfated. In general, the lowest signal was detected in the light chains, containing only two of the six sulfation sites. The highest signal was detected for the single chain, as this form contains all six sulfation sites. Compared to the other products, the detected amount of sulfotyrosines appeared to be lower in ReFacto AF. This was in line with published data, investigating the sulfation of the most important site Y1699. The mass spectrometric data revealed that non-sulfated Y1699 is present in ReFacto but not in Nuwiq[42]. In order to confirm the Western Blot results, the detection of the sulfotyrosines has to be improved and repeated. For more detailed analyses of FVIII-19M and FVIII-6rs, mass spectrometric analyses are required.

As the FVIII-19M demonstrated to be functional after production and purification, no differences in structure and post-translational modifications were expected compared to the other FVIII products. This was confirmed by the different SDS-PAGE and Western Blots. The main difference was the amount of single chain present in the FVIII-19M and FVIII-6rs, however this is not expected to have an influence on the functionality of these variants. Sulfation and glycosylation was similar for the different products, confirming post-translational modification of the FVIII products produced in the CAP-T cells. Whether these modifications match the ones on pFVIII in structure and amount has to be confirmed. In general,

these modifications are very important *in vivo*. Although glycosylation patterns of rFVIII products are no longer considered to be the main reason for the immunogenicity, glycosylation is important for the proper function of FVIII[244,245]. However, it cannot be excluded that potentially immunogenic glycosylation patterns derive from non-human mammalian cell lines like BHK and CHO. In contrast to that, correct sulfation, especially at Y1699, is important for vWF-binding and due to this for a reduced immunogenicity. The shielding of FVIII from uptake by APCs is one of the many advantages of the FVIII-vWF interaction. As only FVIII taken up and presented by APCs can elicit an immune response, vWF-binding can reduce the amount of FVIII presented to the immune system and based on this the immune response[56,244]. Additionally, a study revealed that the binding to vWF not only reduces the uptake of FVIII but also alters the presented peptides[84]. The profile of presented peptides of cells pulsed with FVIII-vWF revealed missing but also additional peptides in comparison to cells only pulsed with FVIII. The study also revealed that the amount of peptides, which are no longer presented, increased with increasing vWF concentrations. Further analyses with FVIII-19M and FVIII-6rs will reveal the detailed glycosylation and sulfation patterns and indicate whether they are more similar to Nuwiq than ReFacto AF, due to the production in a human cell line.

The first analysis regarding functionality of the FVIII-19M was the determination of the thrombin-cleavage pattern (Figure 4-30). Cleavage by thrombin was expected, as the FVIII-19M was active. However, the detailed cleavage pattern was unknown. In general, the fragments of FVIII after thrombin cleavage were similar for all four FVIII products and comprised all expected fragments[227]. In contrast to ReFacto AF and Nuwiq, FVIII-19M and FVIII-6rs showed two additional bands on the Western Blot which probably resulted from the cleavage of the single chain. As for the deglycosylation, the thrombin activation was not complete, revealing a low amount of bands not cleaved by thrombin. Even though, the thrombin activation showed the expected pattern of FVIII fragments, confirming that the insertion of the mutations did not influence the thrombin cleavage.

First indications for influences of the 19 mutations on the functionality of FVIII were received from the ROTEM and TGA analyses. Whereas the ROTEM indicated a prolonged clotting time for FVIII-19M in contrast to FVIII-6rs and especially to ReFacto AF and Nuwiq, the TGA confirmed significantly lower amounts of generated peak thrombin, area under the curve and a longer time to peak thrombin generation with FVIII-19M compared to ReFacto AF and Nuwiq (Figure 4-31, Figure 4-33 and Table A-3 to Table A-5). For both assays, the differences were less pronounced with FVIII concentrations around 0.01 U/ml. This was probably due to the highly reduced clotting capacity at this concentration, resembling severe Hemophilia A, which made differences less obvious. The reason for the differences in thrombin generation and clotting time with FVIII-19M compared to the other products is not clear. Either the mutations really influenced the functionality of the FVIII-19M or the determined chromogenic activity values for FVIII-19M were overestimated. When comparing the specific activities based on the chromogenic activities between FVIII-19M and FVIII-6rs the results were similar (Figure 4-23) and in line with published specific activities for Nuwiq and ReFacto[243]. When the specific activities were based on the clotting activities, the results were generally reduced compared to the specific activities based on the chromogenic activity. Additionally, a discrepancy between the specific activities of FVIII-19M and FVIII-6rs became obvious (Figure 4-23). That the chromogenic assay leads to higher activity results for rFVIII products compared to the clotting assay is known[31,221], nevertheless the chromogenic assay is preferred over the clotting assay and commonly used. Clotting activity:chromogenic activity ratios of 0.88 for Nuwiq and 0.75 for ReFacto are published[243] and in line with the ratio of 0.78 for FVIII-6rs. The reduction of the ratio to 0.51 for FVIII-19M was not expected. These results hint towards an overestimation of the FVIII-19M activity with the chromogenic assay. As the activities for all analyses were based on these chromogenic activities, less active FVIII-19M might have been present in the ROTEM and TGA analyses compared to the other FVIII products. Considering the clotting activities, in these experiments only 50-70 % active FVIII-19M, depending on the used production and purification, were present compared to FVIII-6rs. This might be one explanation for the potentially impaired functionality of the FVIII-19M. However, it is not clear why the two activity assays lead to different results. Further work is needed, in order to determine the reason for the different results. Additionally, TGA and ROTEM should be replicated with FVIII activities based on the clotting method.

Comparable to the ROTEM and TGA results, also the FVIII-binding to vWF was impaired for FVIII-19M (Figure 4-34 and Table A-6). This was not expected as the primary structure and the post-translational modifications, especially the sulfation, were proven to be present in the FVIII-19M and comparable to FVIII-6rs. The overestimation of the FVIII-19M activity is unlikely to be a reason for this result, as the same reagents were used for the chromogenic assay and the development of the vWF-FVIII ELISA. Due to this, the overestimation would be expected in both assays. The only difference was the dilution of FVIII in FVIII-deficient plasma for the chromogenic assay and in Tris-NaCl Buffer for the ELISA. As all required clotting factors, except FVIII, were present in sufficient amounts in the Coatest SP FVIII Kit, the FVIII-deficient plasma might only have had an influence on the stability of FVIII. This influence could not be ruled out as a reason for reduced vWF binding, as all other assays were always performed with FVIII diluted in this plasma. Nevertheless, this would indicate that FVIII-19M is more instable than the other FVIII products. Another reason for reduced vWF-binding could be a slightly different folding of the protein, which has an influence on the binding to vWF. This would not have been detected with the Western Blot analyses. Due to the important impact of vWF-binding on FVIII, further work is needed, in order to determine the kinetics and affinity of the binding between FVIII-19M and vWF. Using the surface plasmon resonance method, these parameters were already published for Nuwiq and ReFacto, revealing no significant difference between these two products[243].

In general, these analyses prove that the FVIII-19M is functional and structural intact, possessing all expected post-translational modifications. These are the first results for a FVIII molecule containing deliberately incorporated mutations in the whole molecule, which is still functional. However further investigations are needed. On the one hand, mass spectrometric analyses have to be performed, in order to reveal glycosylation and sulfation in detail. On the other hand, the presumably reduced activity of FVIII-19M has to be further evaluated and the functional assays should be repeated based on the clotting activities. Nevertheless, these results prove that the incorporation of mutations into FVIII for deimmunization is feasible without disrupting the structure and functionality of the molecule.

The *in vitro* DC-T cell Assay was developed, in order to determine whether the incorporation of the 19 amino acid mutations led to a reduction in $CD4^+$ T cell response (4.5). Originally, the assay was designed to consist of naïve $CD4^+$ T cells and DCs, in order to monitor the initial response to FVIII. The development of this assay was feasible with cells derived from healthy donors, using Ovalbumin as the antigenic protein. However, for the final analysis PBMCs derived from PUPs would have been required. Unfortunately, it proved to be impossible to receive sufficient amounts of blood from these patients, as they are mainly babies and toddlers, leading to blood donation samples of about 3 ml. Combining different samples of one patient, collected at different time points, was not possible as the patients were mostly treated after the detection of the disease. Combination of blood donations from different patients was also impossible, as this would have led to a mixture of different HLA types, leading to invalid results. However, it was published that anti-FVIII antibodies[123,159] as well as FVIII-reactive $CD4^+$ T cells[124,187] can be detected in healthy people. A response to FVIII by $CD4^+$ T cells derived from healthy donors was even shown to be enhanced when regulatory T cells were depleted[190]. Probably, these self-reactive $CD4^+$ T cells were not depleted during ontogeny and regulatory mechanisms evolved, in order to protect the immune system from an autoimmune response. Based on this, the T cell population of the assay was switched from a naïve $CD4^+$ T cell population to a regulatory T cell-depleted $CD4^+$ T cell population. Due to this modification, the use of cells derived from healthy donors became possible. However, not all healthy donors were expected to have $CD4^+$ T cells reacting to FVIII. In addition to the cells derived from healthy donors, also cells from PTPs could be tested with this assay setup. As these patients' immune system has already been in contact with FVIII, PTPs without inhibitors are expected to be tolerant to the therapeutic FVIII. These patients either developed tolerance during ontogeny in the case that they are expressing endogenous FVIII or developed regulatory T cells, in order to suppress an immune response to therapeutic FVIII. The group of PTPs with inhibitors is expected to have $CD4^+$ T cells reacting to FVIII, as they are required for the development of the high-affinity antibodies. Unfortunately, it is not yet understood which mechanisms lead to a successful ITI. Different theories are published, considering the development of anti-idiotypic antibodies and regulatory B and T cells as well as the death of the reacting B and T cells[112,155,156,246]. Except for the case that the $CD4^+$ T cells were deleted during ITI, also cells from inhibitor patients could be tested in the DC-T cell Assay after the depletion of the regulatory T cells.

All experiments during the development of the assay revealed good results. Differentiation and maturation of the DCs was successful and the widely published IL-Mix[207,210] proved to lead to a good expression of HLA-DR and co-stimulating receptors (Figure 4-37), resulting in the published phenotype of mature monocyte-derived DCs[210,247]. These mDCs were further on able to stimulate the proliferation of $CD4^+CD25^-$ T cells (Figure 4-40). The T cells revealed to be pure and viable after purification and prior to the co-cultivation. Neither $CD4^+CD25^+$ T cells nor unspecific proliferation was detected after two days of cultivation. In order to reduce the amount of required cells, the DCs were not harvested for the final assays. This was possible as the cells tightly attached to the surface of the cell culture plate. However, due to this no exact DC:T cell ratios were available for the experiments. Nevertheless, based on the pre-experiments, a minimum of ten $CD4^+$ T cells per DC was ensured (Figure 4-41). This was appropriate, as one DC was considered to be sufficient for the activation of up to 20 $CD4^+$ T cells[248].

The results of the DC-T cell Assay with the healthy donors revealed a reaction to FVIII in more than 70 % of the patients, which was in line with the literature[124]. However, as expected, $CD4^+$ T cells derived from some donors did not show any reaction to FVIII. The final analysis of proliferating cells was based on all $CD4^+$ T cells. Statistical analyses were performed on the one hand for all 17 healthy donors, which responded to FVIII, and on the other hand, for a smaller group containing only 10 healthy donors, excluding donors, which revealed large differences in the amount of viable $CD4^+$ T cells. A reason for the differences in viability could not be found, as none of the used materials was changed and no contaminations were detectable. Nonetheless, the statistical analysis revealed a significantly reduced proliferative response of $CD4^+$ T cells to FVIII-19M compared to FVIII-6rs for both groups (Figure 4-42 and Table A-13). However, a reaction to FVIII-19M was not completely absent. Even though, this was expected, as some regions of FVIII could not be altered and were still immunogenic. Unfortunately, the assay could not be performed with cells from PTPs, as the volume of received blood was less than expected and for most donors the amount of available cells was too low to perform the assay. Additionally, a replication of the results with cells derived from the same healthy donors was not possible, due to the limited numbers of available cells. Therefore, the DC-T cell Assay should be repeated either with fresh cells from the same donors or with cells from additional donors, in order to rule out assay variabilities and to further validate the determined significant difference in immunogenicity of FVIII-19M and FVIII-6rs.

The performed cytokine arrays with the supernatants derived from the co-cultivations did not lead to meaningful results. Similar signals were detected for nearly all cytokines, even for cytokines not expected to be present like IL-28A, which is naturally expressed upon viral infection[249,250]. One reason for this might have been deviations from the manufacturer's protocol. On the one hand, the amount of cell culture supernatant applied to the membrane was only 10 % of the recommended volume, as the amount of available supernatant was low. On the other hand, the samples were labeled with the fluorescent dyes prior to application to the membrane, in order to enable the detection of the differently labeled sample and control on one blot. Another reason might have been the artificial setup of the assay. *In vivo* $CD4^+$ T cells also interact with other immune cells especially by secretion and uptake of different cytokines. As no cytokines derived from cells other than DCs were present, this might have led to the highly variable results.

The iTEM scores calculated for the five donors with the known HLA genotype supported the results of the DC-T cell Assay (Figure 4-43). For all donors a reduced iTEM score for FVIII-19M compared to FVIII-6rs was calculated. Donor #3 showed the lowest difference in the iTEM scores. Consistent with this result, this was a donor revealing a slightly higher proliferation to FVIII-19M than to FVIII-6rs. For Donors #2, #8 and #10 the *in silico* calculated deimmunization of FVIII-19M was clearly confirmed in the *in vitro* assay. Higher differences in the iTEM scores corresponded with higher differences in proliferation. However, Donors #1 and #6 proved that *in silico* analyses are limited. Although a high difference between the iTEM scores were calculated, only low differences in the proliferation to FVIII-19M and FVIII-6rs were detectable. This was expected, as the available $CD4^+$ T cell pool of a donor and the expression of proteases cleaving the protein also influence the *in vitro* results[174]. Nevertheless, a repetition of the DC-T cell Assay with cells from these donors would be beneficial. The correlation might become significant when assay variabilities can be ruled out due to sufficient replicates.

Taking into consideration the results from the functional analysis, indicating that the FVIII-19M activity might has been overestimated with the chromogenic assay, this might also have influenced the DC-T cell Assay. The added amounts of FVIII-19M and FVIII-6rs were based on the chromogenic activity results, whereas the amount of ReFacto AF was based on the activity indicated on the package insert. The activity values and not the antigen values were used for the assay, as this is analogous to the clinical treatment, where FVIII is applied according to the activity. In the case that the chromogenic activity values for FVIII-19M were actually overestimated, less FVIII-19M would have been added to the cells compared to FVIII-6rs. However, when comparing the antigen values, the added amounts of FVIII-19M and FVIII-6rs were nearly similar. Due to this, possibly incorrect FVIII-19M activity values might not have had an influence on the assay, as the FVIII did not have to be active in the DC-T cell Assay.

Altogether the DC-T cell Assay confirmed a reduced immunogenicity of the FVIII-19M compared to FVIII-6rs in healthy donors. This *in vitro* analysis supported the *in silico* calculations. Based on this, the established DC-T cell Assay proved to be a useful tool in the determination of FVIII immunogenicity *in vitro*. The possibility to be able to perform this assay with cells derived from healthy donors and Hemophilia A patients, PTPs as well as PUPs, is a huge advantage. Although PBMCs are not the optimal cell population for this assay, cells derived from spleen or lymph nodes are not available, neither from healthy donors nor from patients. Nevertheless, the results revealed a restimulation of $CD4^+$ T cells, which was high enough to lead to reliable results. The only drawback of the assay is the high amount of cells, which is needed to perform this assay. This is mainly due to the need to split monocyte and $CD4^+CD25^-$ T cell purification and the loss of cells during purification and CFSE labeling. Further development might solve this problem. If possible, the cells could be sorted by FACS and the proliferation dye could be changed. Another possibility would be the shift from DCs and T cells to an assay containing all PBMCs. A purification of monocytes would no longer be required, as DCs and especially B cells, acting as APCs, would be already present. This would reduce the amount of cells and the total time needed to perform the assay. However, in this setup a depletion of regulatory T cells as well as a labeling with a proliferation dye would still be needed.

Whether the results from the DC-T cell Assay can be used to predict the response to the different FVIII variants *in vivo* needs to be elucidated. Although the assay is very artificial compared to the complex interactions *in vivo*, the most important cell types were present. In order to gain further proof of the concept and to support the *in vitro* results, a detailed analysis of the presented peptides would be very beneficial. However, as this is dependent on the purification of the MHC class II from the cells, elution of the bound peptides and mass spectrometric analyses, high amounts of FVIII are needed. Nevertheless, this is a very effective method, in order to prove that the peptides containing the mutations are no longer presented. In the case that this mass spectrometric analysis corresponds to the *in vitro* DC-T cell Assay results, a success *in vivo* with a deimmunized FVIII-19M would be likely.

The confirmation of the *in vitro* results *in vivo* was limited, due to the lack of an appropriate mouse model (4.6). Although the results from the E16 FVIII KO model hinted towards a reduced immunogenicity of FVIII-19M, no explicit results could be detected in any of the two mouse models. In the E16 FVIII KO model, a reaction to ReFacto AF and FVIII-6rs as well as to FVIII-19M was expected based on *in silico* calculations, taking into consideration the murine HLA background. Nevertheless, the *in silico* tools still calculated a slightly reduced immunogenicity for FVIII-19M compared to FVIII-6rs and ReFacto AF (Table 4-6). The study revealed slightly lower but not significantly different anti-FVIII antibody titers in FVIII-19M immunized mice compared to ReFacto AF or FVIII-6rs immunized mice (Figure 4-44 and Table A-15). However, a significant lower amount of proliferating $CD4^+$ T cells was detected upon restimulation with FVIII-19M (Figure 4-45 and Table A-16). Unfortunately, these results could not be confirmed in a second study, as the positive control ReFacto AF did not lead to an immune reaction in these mice. This might have been due to a change in the immunization protocol, injecting 4 U FVIII instead of 8 U FVIII at the last time point. As pre-experiments with ReFacto AF and the protocol containing the 8 U FVIII injection revealed antibodies to FVIII in all mice, which is in line with published data[251], this change in protocol might have led to the lack of an immune response. In general, only about 50 % of the mice revealed an immune response at all. Especially for ReFacto AF and FVIII-6rs, a clear immune response was expected in most of the mice, based on the *in silico* immunogenicity calculations in which the murine HLA background was taken into consideration. One reason for this weak immune

response might have been the endogenous expression of parts of the FVIII heavy chain[225], which might have induced tolerance to parts of FVIII. Based on this, these mice are not the appropriate model, in order to determine differences in immune response to deimmunized and non-deimmunized human FVIII variants. Nevertheless, the study should be repeated, in order to confirm the results from the first study.

The results from the BRGSF mice did not correspond to the *in vitro* results, although the mice were humanized and three different HLA backgrounds were available. Whereas only a low response to FVIII-19M was expected, the absent response to FVIII-6rs and ReFacto AF did not match the immunogenicity scores (Figure 4-14). However, as these mice produce endogenous murine FVIII, which has a homology to human FVIII of about 74 %[245], tolerance can be expected. This corresponds to the results, revealing no anti-FVIII antibodies and no $CD4^+$ T cell proliferation upon restimulation with FVIII in 14 of 15 mice (Figure 4-46 and Figure 4-47). A low titer antibody and a slight proliferative response were detected once each. However, these two results occurred in different mice. Although this might be possible, as the $CD4^+$ T cells in the one mouse might not yet have let to a stimulation of B cells and antibody production whereas the generation of the anti-FVIII antibody in the other mouse might have been T cell-independent, it is more likely that these results were artefacts. The detected antibody titer and the amount of $CD4^+$ T cell proliferation were even lower than most of the results gained with the E16 FVIII KO mice. Nevertheless, the experiment has to be replicated, in order to confirm this assumption.

In general, these two mouse models prove how important a total absence of FVIII is, in order to detect an evaluable response. A mouse model with total absence of FVIII ($F8^{TKO}$)[252], as well as HLA transgenic E16 FVIII KO mouse models[173] are already available. Although HLA transgenic versions of the $F8^{TKO}$ model might also lead to evaluable results, different models would have to be generated, as one model is only transgenic for one HLA-type. This can be avoided by using the BRGSF mice, transplanted with cells from different donors. Additionally, BRGSF mice are the best available model of humanized mice, additionally providing human DCs, T, B and NK cells. Due to this, a BRGSF $F8^{TKO}$ model would be optimal, in order to determine differences in immune response to different human FVIII variants. These mice would not have established any tolerance to FVIII and would provide a humanized immune system. Based on this it would be possible to directly confirm the *in silico* calculations without having to take a murine HLA background into consideration. The current absence of such a mouse model underlines the importance of a reliable *in vitro* assay with human cells for the determination of FVIII immunogenicity.

Taking together all results, the data revealed that *in silico* calculated amino acid mutations can be incorporated into FVIII, still leading to a functional molecule. The FVIII-19M can be produced and purified similar to the reference FVIII and different methods comparing the protein structure and functionality revealed only minor differences to FVIII-6rs and commercially available products. In an *in vitro* DC-T cell Assay the incorporation of 19 mutations, changing only 1.25 % of the whole FVIII sequence, were confirmed to lead to a significant reduction in $CD4^+$ T cell proliferation compared to the reference FVIII molecule without mutations. Due to this, FVIII-19M is the first FVIII molecule, which was deimmunized throughout the whole sequence, revealing reduced immunogenicity while retaining its functionality.

Finally, if these results can be confirmed *in vitro* with cells derived from Hemophilia A patients as well as in an appropriate *in vivo* mouse model, this FVIII variant is capable of improving the FVIII therapy. The FVIII-19M will be a safer FVIII product for PUPs by reducing their risk of developing antibodies at all. Due to the lowered immunogenicity, a switch to FVIII-19M would also be expedient for PTPs without inhibitors, as it is known that inhibitors can still arise after years of treatment[253]. In the case of patients with inhibitors the FVIII-19M could be used after an ITI therapy or in case that an ITI therapy with a conventional FVIII failed. Although the mechanism underlying a successful ITI therapy is not yet clearly identified[156,246], a deimmunized FVIII would support the aim to downregulate an immune response by reducing the amount of activated T helper cells and thereby the amount of newly emerging B cells. Patients with acquired Hemophilia A, although a very rare and diverse population[3], might also benefit from this reduced T helper cell activation upon treatment with FVIII-19M. It could provide a possible therapy after the elimination of the inhibitor. Due to this the FVIII-19M will be a huge improvement of which nearly all Hemophilia A patients can benefit. In the long-term, this deimmunized variant can reduce the number of patients with inhibitors and the need for ITI therapy. By this, the FVIII-19M will not only improve the life of the patients but also reduce the costs for therapy.

References

1. Oldenburg, J., Ananyeva, N. M. & Saenko, E. L. Molecular basis of haemophilia A. *Haemophilia* 10 Suppl 4, 133–139 (2004).
2. Sharma, V., Khalid, A. & Cohen, A. J. Management of Pregnancy in a Patient with Severe Hemophilia Type A. *AJP reports* 3, 29–32 (2013).
3. Mo, L. & Bao, G. C. Acquired factor VIII deficiency: two case reports and a review of literature. *Experimental hematology & oncology* 6, 1–7 (2017).
4. Cugno, M., Gualtierotti, R., Tedeschi, A. & Meroni, P. L. Autoantibodies to coagulation factors: from pathophysiology to diagnosis and therapy. *Autoimmunity Reviews* 13, 40–48 (2014).
5. Plug, I. *et al.* Thirty years of hemophilia treatment in the Netherlands, 1972-2001. *Blood* 104, 3494–3500 (2004).
6. Kemball-Cook, G., Tuddenham, Edward G. D. & Wacey, A. I. The Factor VIII Structure and Mutation Resource Site: HAMSTeRS Version 4. *Nucleic Acids Research* 26, 216–219 (1998).
7. Hoyer Leon W. Hemophilia A. *The New England Journal of Medicine* 330, 38-47 (1994).
8. Mann, K. G. Biochemistry and Physiology of Blood Coagulation. *Thrombosis and Haemostasis* 82, 165–174 (1999).
9. White II, G. C. *et al.* Definitions in Hemophilia. Recommendation of the Scientific Subcommittee on Factor VIII and Factor IX of the Scientific and Standardization Committee of the International Society on Thrombosis and Haemostasis. *Thromb Haemost* 85, 560 (2001).
10. Fischer, K. *et al.* Changes in treatment strategies for severe haemophilia over the last 3 decades: effects on clotting factor consumption and arthropathy. *Haemophilia* 7, 446–452 (2001).
11. Peyvandi, F., Garagiola, I. & Young, G. The past and future of haemophilia. Diagnosis, treatments, and its complications. *The Lancet* 388, 187–197 (2016).
12. Chen, S.-L. Economic Costs of Hemophilia and the Impact of Prophylactic Treatment on Patient Management. *American Journal of Managed Care* 22, S126-S133 (2016).
13. Key, N. S. & Negrier, C. Coagulation factor concentrates. Past, present, and future. *The Lancet* 370, 439–448 (2007).
14. Tiede, A. Half-life extended factor VIII for the treatment of hemophilia A. *Journal of thrombosis and haemostasis : JTH* 13 Suppl 1, 176-179 (2015).
15. Björkman, S., Folkesson, A. & Jönsson, S. Pharmacokinetics and dose requirements of factor VIII over the age range 3-74 years: a population analysis based on 50 patients with long-term prophylactic treatment for haemophilia A. *European journal of clinical pharmacology* 65, 989–998 (2009).
16. Berntorp, E. & Shapiro, A. D. Modern haemophilia care. *The Lancet* 379, 1447–1456 (2012).
17. Gringeri, A., Wolfsegger, M., Steinitz, K. N. & Reininger, A. J. Recombinant full-length factor VIII (FVIII) and extended half-life FVIII products in prophylaxis - new insight provided by pharmacokinetic modelling. *Haemophilia* 21, 300–306 (2015).
18. Gouw, S. C. *et al.* F8 gene mutation type and inhibitor development in patients with severe hemophilia A: systematic review and meta-analysis. *Blood* 119, 2922–2934 (2012).
19. Scandella, D. Human Anti-Factor VIII Antibodies: Epitope Localization and Inhibitory Function. *Vox Sanguinis* 70, 9–14 (1996).
20. van den Berg, H. Marijke. Different impact of factor VIII products on inhibitor development? *Thrombosis J* 14, 55-58 (2016).

21. Hay, C. R. Factor VIII inhibitors in mild and moderate-severity haemophilia A. *Haemophilia* 4, 558–563 (1998).

22. DiMichele, D. M., Hoots, W. K., Pipe, S. W., Rivard, G. E. & Santagostino, E. International workshop on immune tolerance induction: consensus recommendations. *Haemophilia* 13 Suppl 1, 1–22 (2007).

23. Dekoven, M. *et al.* Health-related quality of life in haemophilia patients with inhibitors and their caregivers. *Haemophilia* 19, 287–293 (2013).

24. Lindvall, K. *et al.* Increased burden on caregivers of having a child with haemophilia complicated by inhibitors. *Pediatric blood & cancer* 61, 706–711 (2014).

25. Hollestelle, M. J. *et al.* Tissue Distribution of Factor VIII Gene Expression *In Vivo* - A Closer Look. *Thromb Haemost* 86, 855–861 (2001).

26. Shahani, T. *et al.* Human liver sinusoidal endothelial cells but not hepatocytes contain factor VIII. *J Thromb Haemost* 12, 36–42 (2014).

27. Wood, W. I. *et al.* Expression of active human factor VIII from recombinant DNA clones. *Nature* 312, 330-337 (1984).

28. Koedam, J. A., Hamer, R. J., Beeser-Visser, N. H., Bouma, B. N. & Sixma, J. J. The effect of von Willebrand factor on activation of factor VIII by factor Xa. *Eur J Biochem* 189, 229–234 (1990).

29. Schaub, R. G. Recent advances in the development of coagulation factors and procoagulants for the treatment of hemophilia. *Biochemical Pharmacology* 82, 91–98 (2011).

30. Oldenburg, J. & El-Maarri, O. New Insight into the Molecular Basis of Hemophilia A. *International Journal of Hematology* 83, 96–102 (2006).

31. Orfeo, T., Elsman, R., Gissel, M., Mann, K. G. & Butenas, S. Activation, activity and inactivation of factor VIII in factor VIII products. *Haemophilia* 22, 462–473 (2016).

32. Thompson, A. R. Structure and Function of the Factor VIII Gene and Protein. *Semin Thromb Hemost* 29, 11–22 (2003).

33. Gitschier, J. *et al.* Characterization of the human factor VIII gene. *Nature* 312, 326-330 (1984).

34. Toole, J. J. *et al.* Molecular cloning of a cDNA encoding human antihaemophilic factor. *Nature* 312, 342–347 (1984).

35. Vehar, G. A. *et al.* Structure of human factor VIII. *Nature* 312, 337–342 (1984).

36. Bontempo, F. A. *et al.* Liver Transplantation in Hemophilia A. *Blood* 69, 1721–1724 (1987).

37. Wion, K. L., Kelly, D., Summerfield, J. A., Tuddenham, Edward G. D. & Lawn, R. M. Distribution of factor VIII mRNA and antigen in human liver and other tissues. *Nature* 317, 726-729 (1985).

38. Everett, L. A., Cleuren, A. C. A., Khoriaty, R. N. & Ginsburg, D. Murine coagulation factor VIII is synthesized in endothelial cells. *Blood* 123, 3697–3705 (2014).

39. Fahs, S. A., Hille, M. T., Shi, Q., Weiler, H. & Montgomery, R. R. A conditional knockout mouse model reveals endothelial cells as the principal and possibly exclusive source of plasma factor VIII. *Blood* 123, 3706–3713 (2014).

40. Fay, P. Factor VIII Structure and Function. *International Journal of Hematology* 83, 103–108 (2006).

41. Ngo, Jacky Chi Ki, Huang, M., Roth, D. A., Furie, B. C. & Furie, B. Crystal Structure of Human Factor VIII: Implications for the Formation of the Factor IXa-Factor VIIIa Complex. *Structure* 16, 597–606 (2008).

42. Kannicht, C. *et al.* Characterisation of the post-translational modifications of a novel, human cell line-derived recombinant human factor VIII. *Thrombosis Research* 131, 78–88 (2013).

43. Pipe, S. W. Differential Interaction of Coagulation Factor VIII and Factor V with Protein Chaperones Calnexin and Calreticulin. *Journal of Biological Chemistry* 273, 8537–8544 (1998).

44. Dorner, A. J., Bole, D. G. & Kaufman, R. J. The Relationship of N-linked Glycosylation and Heavy Chain-binding Protein Association with the Secretion of Glycoproteins. *The Journal of Cell Biology* 105, 2265–2674 (1987).

45. Michnick, D. A., Pittman, D. D., Wise, R. J. & Kaufman, R. J. Identification of Individual Tyrosine Sulfation Sites within Factor VIII Required for Optimal Activity and Efficient Thrombin Cleavage. *Journal of Biological Chemistry* 269, 20095–20102 (1994).

46. Pittman, D. D., Wang, J. H. & Kaufman, R. J. Identification and Functional Importance of Tyrosine Sulfate Residues within Recombinant Factor VIII. *Biochemistry* 31, 3315–3325 (1992).

47. Leyte, A. *et al.* Sulfation of Tyr1680 of Human Blood Coagulation Factor VIII Is Essential for the Interaction of Factor VIII with von Willebrand Factor. *Journal of Biological Chemistry* 266, 740–746 (1991).

48. Siner, J. I. *et al.* Circumventing furin enhances factor VIII biological activity and ameliorates bleeding phenotypes in hemophilia models. *JCI Insight* 1, 1–17 (2016).

49. Wakabayashi, H., Koszelak, M. E., Mastri, M. & Fay, P. J. Metal Ion-independent Association of Factor VIII Subunits and the Roles of Calcium and Copper Ions for Cofactor Activity and Inter-Subunit Affinity. *Biochemistry* 40, 10293–10300 (2001).

50. Bihoreau, N., Pin, S., Kersabiec, A.-M., Vidot, F. & Fontaine-Aupart, M.-P. Copper-atom identification in the active and inactive forms of plasma-derived FVIII and recombinant FVIII-ΔII. *Eur J Biochem* 222, 41–48 (1994).

51. Tagliavacca, L., Moon, N., Dunham, W. R. & Kaufman, R. J. Identification and Functional Requirement of Cu(I) and Its Ligands within Coagulation Factor VIII. *Journal of Biological Chemistry* 272, 27428–27434 (1997).

52. Shen, B. W. *et al.* The tertiary structure and domain organization of coagulation factor VIII. *Blood* 111, 1240–1247 (2007).

53. Saenko, E. L. & Scandella, D. The Acidic Region of the Factor VIII Light Chain and the C2 Domain Together Form the High Affinity Binding Site for von Willebrand Factor. *Journal of Biological Chemistry* 272, 18007–18014 (1997).

54. Jacquemin, M. *et al.* A human antibody directed to the factor VIII C1 domain inhibits factor VIII cofactor activity and binding to von Willebrand factor. *Blood* 95, 156-163 (2000).

55. Koedam, J. A., Meijers, J. C., Sixma, J. J. & Bouma, B. N. Inactivation of human factor VIII by activated protein C. Cofactor activity of protein S and protective effect of von Willebrand factor. *The Journal of clinical investigation* 82, 1236–1243 (1988).

56. Dasgupta, S. *et al.* VWF protects FVIII from endocytosis by dendritic cells and subsequent presentation to immune effectors. *Blood* 109, 610–612 (2007).

57. Lenting, P. J. *et al.* The Light Chain of Factor VIII Comprises a Binding Site for Low Density Lipoprotein Receptor-related Protein. *Journal of Biological Chemistry* 274, 23734–23739 (1999).

58. Over, J. *et al.* Survival of ^{125}iodine-labeled Factor VIII in normals and patients with classic hemophilia. Observations on the heterogeneity of human Factor VIII. *The Journal of clinical investigation* 62, 223–234 (1978).

59. Nesheim, M. *et al.* The Effect of Plasma von Willebrand Factor on the Binding of Human Factor VIII to Thrombin-activated Human Platelets. *Journal of Biological Chemistry* 266, 17815–17820 (1991).

60. Saenko, E. L. & Scandella, D. A Mechanism for Inhibition of Factor VIII Binding to Phospholipid by von Willebrand Factor. *Journal of Biological Chemistry* 270, 13826–13833 (1996).

61. Lenting, P. J., Donath, Marie-José S. H., van Mourik, Jan A. & Mertens, K. Identification of a Binding Site for Blood Coagulation Factor IXa on the Light Chain of Human Factor VIII. *Journal of Biological Chemistry* 269, 7150–7155 (1994).

62. Butenas, S. & Mann, K. G. Blood Coagulation. *Biochemistry* 67, 3–12 (2002).

63. Bombeli, T. & Spahn, D. R. Updates in perioperative coagulation: physiology and management of thromboembolism and haemorrhage. *British journal of anaesthesia* 93, 275–287 (2004).

64. Gailani, D. & Renné, T. Intrinsic pathway of coagulation and arterial thrombosis. *Arteriosclerosis, Thrombosis, and Vascular Biology* 27, 2507–2513 (2007).

65. Pieters, J., Lindhout, T. & Hemker, H. C. In Situ-Generated Thrombin Is the Only Enzyme That Effectively Activates Factor VIII and Factor V in Thromboplastin-Activated Plasma. *Blood* 74, 1021–1024 (1989).

66. Eaton, D., Rodriguez, H. & Vehar, G. A. Proteolytic processing of human factor VIII. Correlation of specific cleavages by thrombin, factor Xa, and activated protein C with activation and inactivation of factor VIII coagulant activity. *Biochemistry* 25, 505–512 (1986).

67. Fay, P. J. & Smudzin, T. M. Characterization of the Interaction between the A2 Subunit and A1/A3-C1-C2 Dimer in Human Factor VIIIa. *Journal of Biological Chemistry* 267, 13246–13250 (1992).

68. Monaghan, M., Wakabayashi, H., Griffiths, A. E. & Fay, P. J. Stabilizing interactions between D666-S1787 and T657-Y1792 at the A2-A3 interface support factor VIIIa stability in the blood clotting pathway. *Journal of Thrombosis and Haemostasis* 14, 1021–1030 (2016).

69. Wakabayashi, H., Monaghan, M. & Fay, P. J. Cofactor Activity in Factor VIIIa of the Blood Clotting Pathway Is Stabilized by an Interdomain Bond between His281 and Ser524 Formed in Factor VIII. *Journal of Biological Chemistry* 289, 14020–14029 (2014).

70. Bloem, E., Meems, H., van den Biggelaar, Maartje, Mertens, K. & Meijer, A. B. A3 domain region 1803-1818 contributes to the stability of activated factor VIII and includes a binding site for activated factor IX. *The Journal of biological chemistry* 288, 26105–26111 (2013).

71. Wakabayashi, H., Schmidt, K. M. & Fay, P. J. Ca^{2+} Binding to Both the Heavy and Light Chains of Factor VIII Is Required for Cofactor Activity. *Biochemistry* 41, 8485–8492 (2002).

72. Wakabayashi, H., Zhen, Z., Schmidt, K. M. & Fay, P. J. Mn^{2+} binding to factor VIII subunits and its effect on cofactor activity. *Biochemistry* 42, 145–153 (2003).

73. Fay, P. J., Mastri, M., Koszelak, M. E. & Wakabayashi, H. Cleavage of Factor VIII Heavy Chain is Required for the Functional Interaction of A2 Subunit with Factor IXa. *The Journal of biological chemistry* 276, 12434–12439 (2001).

74. Lollar, P., Hill-Eubanks, D. C. & Parker, C. G. Association of the Factor VIII Light Chain with von Willebrand Factor. *Journal of Biological Chemistry* 263, 10451-10455 (1988).

75. Andersson, L. O. & Brown, J. E. Interaction of factor VIII-von Willebrand Factor with phospholipid vesicles. *Biochem. J.* 200, 161–167 (1981).

76. Nogami, K. A novel mechanism of factor VIII protection by von Willebrand factor from activated protein C-catalyzed inactivation. *Blood* 99, 3993–3998 (2002).

77. Lapan, K. A. & Fay, P. J. Localization of a Factor X Interactive Site in the A1 Subunit of Factor VIIIa. *Journal of Biological Chemistry* 272, 2082–2088 (1997).

78. Lenting, P. J., van Schooten, C. J. & Denis, C. V. Clearance mechanisms of von Willebrand factor and factor VIII. *J Thromb Haemost* 5, 1353–1360 (2007).

79. Bovenschen, N., Rijken, D. C., Havekes, L. M., van Vlijmen, B. J. M. & Mertens, K. The B domain of coagulation factor VIII interacts with the asialoglycoprotein receptor. *Journal of Thrombosis and Haemostasis* 3, 1257–1265 (2005).

80. Gangadharan, B. *et al.* The C1 and C2 domains of blood coagulation factor VIII mediate its endocytosis by dendritic cells. *Haematologica* 102, 271–281 (2017).

81. Pool, J. G., Hershgold, E. J. & Pappenhagen, A. R. High-potency Antihaemophilic Factor Concentrate prepared from Cryoglobulin Precipitate. *Nature* 203, 312 (1964).

82. Kingdon, H. S. & Lundblad, R. L. An adventure in biotechnology: the development of haemophilia A therapeutics -- from whole-blood transfusion to recombinant DNA to gene therapy. *Biotechnology and applied biochemistry* 35, 141–148 (2002).

83. Ettingshausen, C. E. & Kreuz, W. Recombinant vs. plasma-derived products, especially those with intact VWF, regarding inhibitor development. *Haemophilia* 12 Suppl 6, 102–106 (2006).

84. Sorvillo, N. *et al.* von Willebrand factor binds to the surface of dendritic cells and modulates peptide presentation of factor VIII. *Haematologica* 101, 309–318 (2016).

85. van den Berg, H. M., Pipe, S. & Ljung, R. Plasma products do not solve the inhibitor problem. *Haemophilia* 23, 346–347 (2017).

86. Mazurkiewicz-Pisarek, A., Plucienniczak, G., Ciach, T. & Plucienniczak, A. The factor VIII protein and its function. *Acta biochimica Polonica* 63, 11–16 (2016).

87. United Kingdom Haemophilia Centre Doctors' Organisation. Guidelines on the selection and use of therapeutic products to treat haemophilia and other hereditary bleeding disorders. *Haemophilia* 9, 1–23 (2003).

88. Recht, M. *et al.* Clinical evaluation of moroctocog alfa (AF-CC), a new generation of B-domain deleted recombinant factor VIII (BDDrFVIII) for treatment of haemophilia A: demonstration of safety, efficacy, and pharmacokinetic equivalence to full-length recombinant factor VIII. *Haemophilia* 15, 869–880 (2009).

89. Pittman, D. D. *et al.* Biochemical, Immunological, and In Vivo Functional Characterization of B-Domain-Deleted Factor VIII. *Blood* 81, 2925–2935 (1993).

90. Toole, J. J. *et al.* A large region (=95 kDa) of human factor VIII is dispensable for in vitro procoagulant activity. *Proceedings of the National Academy of Sciences* 83, 5939–5942 (1986).

91. Eaton, D. L. *et al.* Construction and Characterization of an Active Factor VIII Variant Lacking the Central One-Third of the Molecule. *Biochemistry* 25, 8343-8347 (1986).

92. Bihoreau, N. *et al.* Structural and functional characterization of Factor VIII-ΔII, a new recombinant Factor VIII lacking most of the B-domain. *Biochem. J.* 277, 23–31 (1991).

93. Miao, H. Z. Bioengineering of coagulation factor VIII for improved secretion. *Blood* 103, 3412–3419 (2004).

94. Casademunt, E. *et al.* The first recombinant human coagulation factor VIII of human origin: human cell line and manufacturing characteristics. *Eur J Haematol* 89, 165–176 (2012).

95. Nielsen, P. F., Bak, S. & Vandahl, B. Characterization of tyrosine sulphation in rFVIII (turoctocog alfa) expressed in CHO and HEK-293 cells. *Haemophilia* 18, e397-8 (2012).

96. Gouw, S. C. *et al.* Recombinant versus plasma-derived factor VIII products and the development of inhibitors in previously untreated patients with severe hemophilia A: the CANAL cohort study. *Blood* 109, 4693–4697 (2007).

97. Gouw, S. C. *et al.* Factor VIII Products and Inhibitor Development in Severe Hemophilia A. *N Engl J Med* 368, 231–239 (2013).

98. Fischer, K. *et al.* Inhibitor development in haemophilia according to concentrate. Four-year results from the European HAemophilia Safety Surveillance (EUHASS) project. *Thrombosis and Haemostasis* 113, 968–975 (2015).

99. Peyvandi, F. *et al.* New findings on inhibitor development: from registries to clinical studies. *Haemophilia* 23 Suppl 1, 4–13 (2017).

100. Peyvandi, F. *et al.* A Randomized Trial of Factor VIII and Neutralizing Antibodies in Hemophilia A. *The New England Journal of Medicine* 374, 2054–2064 (2016).

101. Goudemand, J., Peyvandi, F. & Lacroix-Desmazes, S. Key insights to understand the immunogenicity of FVIII products. *Thrombosis and Haemostasis* 116 Suppl 1, S2-9 (2016).

102. Giangrande, P. *et al.* Clinical evaluation of glycoPEGylated recombinant FVIII: Efficacy and safety in severe haemophilia A. *Thrombosis and Haemostasis* 117, 252–261 (2017).

103. Mahlangu, J. *et al.* Efficacy and safety of rVIII-SingleChain: results of a phase 1/3 multicenter clinical trial in severe hemophilia A. *Blood* 128, 630–637 (2016).

104. Powell, J. S. *et al.* Safety and prolonged activity of recombinant factor VIII Fc fusion protein in hemophilia A patients. *Blood* 119, 3031–3037 (2012).

105. Zollner, S. *et al.* Non-clinical pharmacokinetics and pharmacodynamics of rVIII-SingleChain, a novel recombinant single-chain factor VIII. *Thrombosis Research* 134, 125–131 (2014).

106. Schmidbauer, S. *et al.* Physicochemical characterisation of rVIII-SingleChain, a novel recombinant single-chain factor VIII. *Thrombosis Research* 136, 388–395 (2015).

107. Pipe, S. W., Montgomery, R. R., Pratt, K. P., Lenting, P. J. & Lillicrap, D. Life in the shadow of a dominant partner: the FVIII-VWF association and its clinical implications for hemophilia A. *Blood* 128, 2007–2016 (2016).

108. Krishnamoorthy, S. *et al.* Recombinant factor VIII Fc (rFVIIIFc) fusion protein reduces immunogenicity and induces tolerance in hemophilia A mice. *Cellular Immunology* 301, 30–39 (2016).

109. Jawa, V. *et al.* T-cell dependent immunogenicity of protein therapeutics: Preclinical assessment and mitigation. *Clinical Immunology* 149, 534–555 (2013).

110. Oldenburg, J. & Pavlova, A. Genetic risk factors for inhibitors to factors VIII and IX. *Haemophilia* 12 Suppl 6, 15–22 (2006).

111. Astermark, J. Inhibitor development: patient-determined risk factors. *Haemophilia* 16, 66–70 (2010).

112. Reipert, B. M., van Helden, Pauline M. W., Schwarz, H.-P. & Hausl, C. Mechanisms of action of immune tolerance induction against factor VIII in patients with congenital haemophilia A and factor VIII inhibitors. *British Journal of Haematology* 136, 12–25 (2007).

113. De Groot, Anne S. & Scott, D. W. Immunogenicity of protein therapeutics. *Trends in Immunology* 28, 482–490 (2007).

114. Wroblewska, A., Reipert, B. M., Pratt, K. P. & Voorberg, J. Dangerous liaisons: how the immune system deals with factor VIII. *Journal of Thrombosis and Haemostasis* 11, 47–55 (2013).

115. André, S. *et al.* A Cellular Viewpoint of Anti-FVIII Immune Response in Hemophilia A. *Clinic Rev Allerg Immunol* 37, 105–113 (2009).

116. Scandella, D. H. *et al.* In Hemophilia A and Autoantibody Inhibitor Patients: The Factor VIII A2 Domain and Light Chain Are Most Immunogenic. *Thrombosis Research* 101, 377–385 (2001).

117. Nguyen, P.-C. T. *et al.* High-resolution mapping of epitopes on the C2 domain of factor VIII by analysis of point mutants using surface plasmon resonance. *Blood* 123, 2732–2739 (2014).

118. Lubahn, B. C., Ware, J., Stafford, D. W. & Reisner, H. M. Identification of a F.VIII epitope recognized by a human hemophilic inhibitor. *Blood* 73, 497–499 (1989).

119. Lebreton, A. *et al.* Discontinuous epitopes on the C2 domain of coagulation Factor VIII mapped by computer-designed synthetic peptides. *British Journal of Haematology* 155, 487–497 (2011).

120. Gilles, J. G., Arnout, J., Vermylen, J. & Saint-Remy, J. M. Anti-factor VIII antibodies of hemophiliac patients are frequently directed towards nonfunctional determinants and do not exhibit isotypic restriction. *Blood* 82, 2452–2461 (1993).

121. Prescott, R. *et al.* The Inhibitor Antibody Response Is More Complex in Hemophilia A Patients Than in Most Nonhemophiliacs With Factor VIII Autoantibodies. *Blood* 89, 3663–3671 (1997).

122. Cannavo, A. *et al.* Nonneutralizing antibodies against factor VIII and risk of inhibitor development in severe hemophilia A. *Blood* 129, 1245–1250 (2017).

123. Algiman, M. *et al.* Natural antibodies to factor VIII (anti-hemophilic factor) in healthy individuals. *Proceedings of the National Academy of Sciences* 89, 3795–3799 (1992).

124. Hu, G.-L., Okita, D. K., Diethelm-Okita, B. M. & Conti-Fine, B. M. Recognition of coagulation factor VIII by CD4+ T cells of healthy humans. *J Thromb Haemost* 1, 2159–2166 (2003).

125. Ghosh, K. & Shetty, S. Immune Response to FVIII in Hemophilia A: An Overview of Risk Factors. *Clinic Rev Allerg Immunol* 37, 58–66 (2009).

126. Carcao, M., Re, W. & Ewenstein, B. The role of previously untreated patient studies in understanding the development of FVIII inhibitors. *Haemophilia* 22, 22–31 (2016).

127. Hu, G.-L., Okita, D. K. & Conti-Fine, B. M. T cell recognition of the A2 domain of coagulation factor VIII in hemophilia patients and healthy subjects. *J Thromb Haemost* 2, 1908–1917 (2004).

128. Scott, D. W. Inhibitors - cellular aspects and novel approaches for tolerance. *Haemophilia* 20, 80–86 (2014).

129. Van Helden, P. M. W., van Haren, S. D., Fijnvandraat, K., van den Berg, M. H. & Voorberg, J. Factor VIII-specific B cell responses in haemophilia A patients with inhibitors. *Haemophilia* 16, 35–43 (2010).

130. Hartholt, R. B., Peyron, I. & Voorberg, J. Hunting down factor VIII in the immunopeptidome. *Cellular Immunology* 301, 59–64 (2016).

131. Oldenburg, J. *et al.* Environmental and genetic factors influencing inhibitor development. *Seminars in Hematology* 41, 82–88 (2004).

132. Mueller, R. *et al.* Evaluation of the immuno-stimulatory potential of stopper extractables and leachables by using dendritic cells as readout. *Journal of pharmaceutical sciences* 98, 3548–3561 (2009).

133. Gouw, S. C., van den Berg, H. M., Le Cessie, S. & van der Bom, J. G. Treatment characteristics and the risk of inhibitor development: a multicenter cohort study among previously untreated patients with severe hemophilia A. *Journal of Thrombosis and Haemostasis* 5, 1383–1390 (2007).

134. Lillicrap, D., Fijnvandraat, K. & Santagostino, E. Inhibitors - genetic and environmental factors. *Haemophilia* 20, 87–93 (2014).

135. Kempton, C. L., Soucie, J. M. & Abshire, T. C. Incidence of inhibitors in a cohort of 838 males with hemophilia A previously treated with factor VIII concentrates. *Journal of Thrombosis and Haemostasis* 4, 2576–2581 (2006).

136. Astermark, J. *et al.* Polymorphisms in the TNFA gene and the risk of inhibitor development in patients with hemophilia A. *Blood* 108, 3739–3745 (2006).

137. Astermark, J., Oldenburg, J., Pavlova, A., Berntorp, E. & Lefvert, A.-K. Polymorphisms in the IL10 but not in the IL1beta and IL4 genes are associated with inhibitor development in patients with hemophilia A. *Blood* 107, 3167–3172 (2006).

138. Astermark, J., Wang, X., Oldenburg, J., Berntorp, E. & Lefvert, A.-K. Polymorphisms in the CTLA-4 gene and inhibitor development in patients with severe hemophilia A. *Journal of Thrombosis and Haemostasis* 5, 263–265 (2007).

139. Franchini, M. *et al.* Blood Group O Protects against Inhibitor Development in Severe Hemophilia A Patients. *Seminars in thrombosis and hemostasis* 43, 69–74 (2017).

140. Viel, K. R. *et al.* Inhibitors of Factor VIII in Black Patients with Hemophilia. *N Engl J Med* 361, 1618-1627 (2009).

141. Carpenter, S. L., Michael Soucie, J., Sterner, S. & Presley, R. Increased prevalence of inhibitors in Hispanic patients with severe haemophilia A enrolled in the Universal Data Collection database. *Haemophilia* 18, e260-e265 (2012).

142. Astermark, J. FVIII inhibitors: pathogenesis and avoidance. *Blood* 125, 2045–2051 (2015).

143. Brackmann, H. H. & Gormsen, J. Massive Factor-VIII Infusion In Haemophiliac With Factor-VIII Inhibitor, High Responder. *The Lancet,* 933 (1977).

144. Chang, Sher, Blanchette & Teitel. The impact of inhibitors on the cost of clotting factor replacement therapy in haemophilia A in Canada. *Haemophilia* 5, 247–252 (1999).

145. Ullman, M. & Hoots, W. K. Assessing the costs for clinical care of patients with high-responding factor VIII and IX inhibitors. *Haemophilia* 12 Suppl 6, 74-80 (2006).

146. Di Minno, M. N. D., Di Minno, G., Di Capua, M., Cerbone, A. M. & Coppola, A. Cost of care of haemophilia with inhibitors. *Haemophilia* 16, e190-e201 (2010).

147. Hay, C. R. M. & DiMichele, D. M. The principal results of the International Immune Tolerance Study: a randomized dose comparison. *Blood* 119, 1335–1344 (2012).

148. Valentino, L. A. *et al.* US Guidelines for immune tolerance induction in patients with haemophilia a and inhibitors. *Haemophilia* 21, 559–567 (2015).

149. Kempton, C. L. & Meeks, S. L. Toward optimal therapy for inhibitors in hemophilia. *Blood* 124, 3365–3372 (2014).

150. Minno, G. D., Santagostino, E., Pratt, K. & Königs, C. New predictive approaches for ITI treatment. *Haemophilia* 20, 27–43 (2014).

151. Mariani, G. & Kroner, B. Immune tolerance in hemophilia with factor VIII inhibitors: predictors of success. *Haematologica* 86, 1186–1193 (2001).

152. DiMichele, D. M. & Kroner, B. L. The North American Immune Tolerance Registry: Practices, Outcomes, Outcome Predictors. *Thrombosis and Haemostasis* 87, 52–57 (2002).

153. Coppola, A. *et al.* Factor VIII gene (F8) mutations as predictors of outcome in immune tolerance induction of hemophilia A patients with high-responding inhibitors. *Journal of Thrombosis and Haemostasis* 7, 1809–1815 (2009).

154. Waters, B. & Lillicrap, D. The molecular mechanisms of immunomodulation and tolerance induction to factor VIII. *Journal of Thrombosis and Haemostasis* 7, 1446–1456 (2009).

155. Gilles, J. G., Desqueper, B., Lenk, H., Vermylen, J. & Saint-Remy, J. M. Neutralizing antiidiotypic antibodies to factor VIII inhibitors after desensitization in patients with hemophilia A. *J. Clin. Invest.* 97, 1382–1388 (1996).

156. Pautard, B. *et al.* Successful immune tolerance induction by FVIII in hemophilia A patients with inhibitor may occur without deletion of FVIII-specific T cells. *Journal of Thrombosis and Haemostasis* 9, 1163–1170 (2011).

157. Mancuso, M. E. & Cannavò, A. Immune tolerance induction in hemophilia. *Clinical Investigation* 5, 321–335 (2015).

158. Jacquemin, M. G. *et al.* Mechanism and kinetics of factor VIII inactivation: study with an IgG4 monoclonal antibody derived from a hemophilia A patient with inhibitor. *Blood* 92, 496–506 (1998).

159. Whelan, S. F. J. *et al.* Distinct characteristics of antibody responses against factor VIII in healthy individuals and in different cohorts of hemophilia A patients. *Blood* 121, 1039–1048 (2013).

160. Reding, M. T. *et al.* Distribution of Th1- and Th2-induced Anti-factor VIII IgG Subclasses in Congenital and Acquired Hemophilia Patients. *Thromb Haemost* 88, 568–575 (2002).

161. Germain, R. The Biochemistry and Cell Biology of Antigen Processing and Presentation. *Annual review of immunology* 11, 403–450 (1993).

162. Georgescu, M. T., Lai, J. D., Hough, C. & Lillicrap, D. War and peace: Factor VIII and the adaptive immune response. *Cellular Immunology* 301, 2–7 (2016).

163. Lenschow, D. J., Walunas, T. L. & Bluestone, J. A. CD28/B7 system of T cell costimulation. *Annual review of immunology* 14, 233–258 (1996).

164. Wieczorek, M. *et al.* Major Histocompatibility Complex (MHC) Class I and MHC Class II Proteins: Conformational Plasticity in Antigen Presentation. *Frontiers in immunology* 8, 1–16 (2017).

165. Godkin, A. J. *et al.* Naturally Processed HLA Class II Peptides Reveal Highly Conserved Immunogenic Flanking Region Sequence Preferences That Reflect Antigen Processing Rather Than Peptide-MHC Interactions. *The Journal of Immunology* 166, 6720–6727 (2001).

166. Southwood, S. *et al.* Several Common HLA-DR Types Share Largely Overlapping Peptide Binding Repertoires. *Journal of Immunology* 160, 3363–3373 (1998).

167. Lippolis, J. D. *et al.* Analysis of MHC Class II Antigen Processing by Quantitation of Peptides that Constitute Nested Sets. *The Journal of Immunology* 169, 5089–5097 (2002).

168. Sadegh-Nasseri, S. & Kim, A. MHC Class II Auto-Antigen Presentation is Unconventional. *Frontiers in immunology* 6, 1–5 (2015).

169. Weaver, J. M. *et al.* Immunodominance of CD4 T Cells to Foreign Antigens Is Peptide Intrinsic and Independent of Molecular Context. Implications for Vaccine Design. *The Journal of Immunology* 181, 3039–3048 (2008).

170. Lazarski, C. A. *et al.* The Kinetic Stability of MHC Class II:Peptide Complexes Is a Key Parameter that Dictates Immunodominance. *Immunity* 23, 29–40 (2005).

171. Sturniolo, T. *et al.* Generation of tissue-specific and promiscuous HLA ligand databases using DNA microarrays and virtual HLA class II matrices. *Nature Biotechnology* 17, 555–561 (1999).

172. De Groot, A S, McMurry, J. & Moise, L. Prediction of immunogenicity: in silico paradigms, ex vivo and in vivo correlates. *Current Opinion in Pharmacology* 8, 620–626 (2008).

173. Moise, L. *et al.* Effect of HLA DR epitope de-immunization of Factor VIII in vitro and in vivo. *Clinical Immunology* 142, 320–331 (2012).

174. van Haren, Simon D. *et al.* Limited promiscuity of HLA-DRB1 presented peptides derived of blood coagulation factor VIII. *PLoS ONE* 8, 1-11 (2013).

175. Navarrete, A. *et al.* Splenic marginal zone antigen-presenting cells are critical for the primary allo-immune response to therapeutic factor VIII in hemophilia A. *Journal of Thrombosis and Haemostasis* 7, 1816–1823 (2009).

176. van Haren, Simon D., Wroblewska, A., Fischer, K., Voorberg, J. & Herczenik, E. Requirements for immune recognition and processing of factor VIII by antigen-presenting cells. *Blood Reviews* 26, 43–49 (2012).

177. Lacroix-Desmazes, S. *et al.* Dynamics of factor VIII interactions determine its immunologic fate in hemophilia A. *Blood* 112, 240–249 (2008).

178. Tangri, S. *et al.* Rationally Engineered Therapeutic Proteins with Reduced Immunogenicity. *The Journal of Immunology* 174, 3187–3196 (2005).

179. Weber, C. A. *et al.* T cell epitope: Friend or Foe? Immunogenicity of biologics in context. *Advanced Drug Delivery Reviews* 61, 965–976 (2009).

180. De Groot, Anne S. & Moise, L. Prediction of immunognicity for therapeutic proteins: State of the art. *Current Opinion in Drug Discovery & Development* 10, 1–9 (2007).

181. Davenport, M. P., Ho Shon, Ivan A. P. & Hill, Adrian V. S. An empirical method for the prediction of T-cell epitopes. *Immunogenetics* 42, 392–397 (1995).

182. Paul, S. *et al.* Evaluating the Immunogenicity of Protein Drugs by Applying In Vitro MHC Binding Data and the Immune Epitope Database and Analysis Resource. *Clinical and Developmental Immunology* 2013, 1–7 (2013).

183. National Institute of Allergy and Infectious Diseases. Immune Epitope Database and Analysis Resource (IEDB). Available at http://www.iedb.org/.

184. Sampei, Z. *et al.* Identification and Multidimensional Optimization of an Asymmetric Bispecific IgG Antibody Mimicking the Function of Factor VIII Cofactor Activity. *PLoS ONE* 8, 1-13 (2013).

185. Mufarrege, E. F. *et al.* De-immunized and Functional Therapeutic (DeFT) versions of a long lasting recombinant alpha interferon for antiviral therapy. *Clinical Immunology* 176, 31–41 (2017).

186. Steere, A. C. *et al.* Antibiotic-refractory Lyme arthritis is associated with HLA-DR molecules that bind a Borrelia burgdorferi peptide. *The Journal of experimental medicine* 203, 961–971 (2006).

187. Reding, M. T. *et al.* Sensitization of CD4+ T Cells to Coagulation Factor VIII: Response in Congenital and Acquired Hemophilia Patients and in Healthy Subjects. *Thromb Haemost* 84, 643–652 (2000).

188. Bouneaud, C., Kourilsky, P. & Bousso, P. Impact of negative selection on the T cell repertoire reactive to a self-peptide: a large fraction of T cell clones escapes clonal deletion. *Immunity* 13, 829–840 (2000).

189. Bluestone, J. A. & Abbas, A. K. Natural versus adaptive regulatory T cells. *Nat Rev Immunol* 3, 253–257 (2003).

190. Kamate, C., Lenting, P. J., van den Berg, H. M. & Mutis, T. Depletion of CD4+/CD25high regulatory T cells may enhance or uncover factor VIII-specific T-cell responses in healthy individuals. *Journal of Thrombosis and Haemostasis* 5, 611–613 (2007).

191. Depil, S. *et al.* Peptide-binding assays and HLA II transgenic Abeta degrees mice are consistent and complementary tools for identifying HLA II-restricted peptides. *Vaccine* 24, 2225–2229 (2006).

192. Shirai, M. *et al.* CTl Responses of HLA-A2.1-Transgenic Mice Specific for Hepatitis C Viral Peptides Predict Epitopes for CTL of Humans Carrying HLA-A2.1. *Journal of Immunology* 154, 2733–2742 (1995).

193. Man, S. *et al.* Definition of a human T cell epitope from influenza A non-structural protein 1 using HLA-A2.1 transgenic mice. *Int Immunol* 7, 597–605 (1995).

194. Traggiai, E. *et al.* Development of a Human Adaptive Immune System in Cord Blood Cell–Transplanted Mice. *Science* 304, 104-107 (2004).

195. Ishikawa, F. *et al.* Development of functional human blood and immune systems in NOD/SCID/IL2 receptor γ chain^{null} mice. *Blood* 106, 1565–1573 (2005).

196. Li, Y. *et al.* A novel Flt3-deficient HIS mouse model with selective enhancement of human DC development. *European journal of immunology* 46, 1291–1299 (2016).

197. Thermo Fisher Scientific. FreeStyle™ 293 Expression System. Available at https://www.thermofisher.com/de/de/home/references/protocols/cell-culture/transfection-protocol/freestyle-293-expression-system.html (2007). 10.04.2018.

198. Fischer, S. *et al.* Transient recombinant protein expression in a human amniocyte cell line: the CAP-T® cell system. *Biotechnology and bioengineering* 109, 2250–2261 (2012).

199. Wang, P. *et al.* A systematic assessment of MHC class II peptide binding predictions and evaluation of a consensus approach. *PLoS computational biology* 4, 1-10 (2008).

200. De Groot, Anne S. & Martin, W. Reducing risk, improving outcomes: Bioengineering less immunogenic protein therapeutics. *Clinical Immunology* 131, 189–201 (2009).

201. Anthony Marcello. DeFT: Immune Engineering Functional Therapeutics. Available at http://www.epivax.com/protein-engineering/deft-including-how-tregitope-can-be-used-in-a-deft-project/ (2010). 20.08.2017.

202. Graham, F. L., Smiley, J., Russell, W. C. & Nairn, R. Characteristics of a Human Cell Line Transformed by DNA from Human Adenovirus Type 5. *Journal of General Virology* 36, 59–72 (1977).

203. Quah, Ben J C, Warren, H. S. & Parish, C. R. Monitoring lymphocyte proliferation in vitro and in vivo with the intracellular fluorescent dye carboxyfluorescein diacetate succinimidyl ester. *Nat Protoc* 2, 2049–2056 (2007).

204. Miller, L. *et al.* Danger signal-dependent activation of human dendritic cells by plasma-derived factor VIII products. *Thromb Haemost* 114, 268–276 (2015).

205. Böhnlein, K. Master Thesis. Is FVIII in combination with other hemorrhage associated factors sufficient for DC maturation to rais an immune response against FVIII? Philipps-Universität Marburg, 2014.

206. Jonuleit, H. *et al.* Pro-inflammatory cytokines and prostaglandins induce maturation of potent immunostimulatory dendritic cells under fetal calf serum-free conditions. *Eur J Immunol* 27, 3135–3142 (1997).

207. Trepiakas, R. *et al.* Comparison of α-Type-1 polarizing and standard dendritic cell cytokine cocktail for maturation of therapeutic monocyte-derived dendritic cell preparations from cancer patients. *Vaccine* 26, 2824–2832 (2008).

208. Jeras, M., Bergant, M. & Repnik, U. In vitro preparation and functional assessment of human monocyte-derived dendritic cells—potential antigen-specific modulators of in vivo immune responses. *Transplant Immunology* 14, 231–244 (2005).

209. Schlienger, K., Craighead, N., Lee, K. P., Levine, B. L. & June, C. H. Efficent priming of protein antigen-specific human CD4+ T cells by monocyte-derived dendritic cells. *Blood* 96, 3490–3498 (2000).

210. Dauer, M. *et al.* Mature Dendritic Cells Derived from Human Monocytes Within 48 Hours: A Novel Strategy for Dendritic Cell Differentiation from Blood Precursors. *The Journal of Immunology* 170, 4069–4076 (2003).

211. Qadura, M. *et al.* Reduction of the immune response to factor VIII mediated through tolerogenic factor VIII presentation by immature dendritic cells. *Journal of Thrombosis and Haemostasis* 6, 2095–2104 (2008).

212. Pascolo, S. *et al.* HLA-A2.1–restricted Education and Cytolytic Activity of CD8+ T Lymphocytes from β2 Microglobulin (β2m) HLA-A2.1 Monochain Transgenic H-2Db β2m Double Knockout Mice. *Journal of Experimental Medicine* 185, 2043–2051 (1997).

213. Shultz, L. D., Brehm, M. A., Garcia-Martinez, J. V. & Greiner, D. L. Humanized mice for immune system investigation: progress, promise and challenges. *Nature reviews. Immunology* 12, 786–798 (2012).

214. Mackarehtschian, K. *et al.* Targeted Disruption of the flk2/flt3 Gene Leads to Deficiencies in Primitive Hematopoietic Progenitors. *Immunity* 3, 147–161 (1995).

215. Legrand, N. *et al.* Functional CD47/signal regulatory protein alpha (SIRPα) interaction is required for optimal human T- and natural killer- (NK) cell homeostasis in vivo. *Proceedings of the National Academy of Sciences of the United States of America* 108, 13224–13229 (2011).

216. Chen, Q., He, F., Kwang, J., Chan, J. K. Y. & Chen, J. GM-CSF and IL-4 stimulate antibody responses in humanized mice by promoting T, B, and dendritic cell maturation. *Journal of Immunology* 189, 5223–5229 (2012).

217. Aban, I. B. & George, B. Statistical considerations for preclinical studies. *Experimental neurology* 270, 82–87 (2015).

218. Nahm, F. S. Nonparametric statistical tests for the continuous data: the basic concept and the practical use. *Korean journal of anesthesiology* 69, 8–14 (2016).

219. Dayhoff, M. O., Schwartz, R. M. & Orcutt, B. C. A Model of Evolutionary Change in Proteins. *Atlas of Protein Sequence and Structure,* 345-352 (1978).

220. Nakamura, Y., Gojobori, T. & Ikemura, T. Codon usage tabulated from international DNA sequence databases: status for the year 2000. *Nucleic Acids Research* 28, 292 (2000).

221. Barrowcliffe, T. W., Raut, S., Sands, D. & Hubbard, A. R. Coagulation and Chromogenic Assays of Factor VIII Activity: General Aspects, Standardization, and Recommendations. *Semin Thromb Hemost* 28, 247–255 (2002).

222. Lang, T. & Depka, M. von. Diagnostische Möglichkeiten und Grenzen der Thrombelastometrie/-graphie. *Hämostaseologie* 3a, 20–29 (2006).

223. van Veen, J. J., Gatt, A. & Makris, M. Thrombin generation testing in routine clinical practice: are we there yet? *British Journal of Haematology* 142, 889–903 (2008).

224. McIlroy, D. & Gregoire, M. Optimizing dendritic cell-based anticancer immunotherapy: maturation state does have clinical impact. *Cancer Immunology, Immunotherapy* 52, 583–591 (2003).

225. Sarkar, R., Gao, G. P., Chirmule, N., Tazelaar, J. & Kazazian, H. H. Partial correction of murine hemophilia A with neo-antigenic murine factor VIII. *Human Gene Therapy* 11, 881–894 (2000).

226. Lind, P. *et al.* Novel Forms of B-Domain-Deleted Recombinant Factor VIII Molecules. *European Journal of Biochemistry* 232, 19–27 (1995).

227. Sandberg, H. *et al.* Structural and Functional Characterization of B-Domain Deleted Recombinant Factor VIII. *Seminars in Hematology* 38, 4–12 (2001).

228. van Haren, Simon D. *et al.* HLA-DR-presented peptide repertoires derived from human monocyte-derived dendritic cells pulsed with blood coagulation factor VIII. *Molecular & cellular proteomics : MCP* 10, M110.002246 (2011).

229. Peyron, I. *et al.* Comparative profiling of HLA-DR and HLA-DQ associated factor VIII peptides presented by monocyte-derived dendritic cells. *Haematologica* 103, 172–178 (2018).

230. Reding, M. T., Okita, D. K., Diethelm-Okita, B. M., Anderson, T. A. & Conti-Fine, B. M. Epitope repertoire of human CD4+ T cells on the A3 domain of coagulation factor VIII. *Thromb Haemost* 2, 1385–1394 (2004).

231. Jones, T. D. *et al.* Identification and removal of a promiscuous CD4+ T cell epitope from the C1 domain of factor VIII. *J Thromb Haemost* 3, 991–1000 (2005).

232. Reding, M. T., Okita, D. K., Diethelm-Okita, B. M., Anderson, T. A. & Conti-Fine, B. M. Human CD4+ T-cell epitope repertoire on the C2 domain of coagulation factor VIII. *Journal of Thrombosis and Haemostasis* 1, 1777–1784 (2003).

233. Gallwitz, M., Enoksson, M., Thorpe, M., Hellman, L. & Xu, W. The Extended Cleavage Specificity of Human Thrombin. *PLoS ONE* 7, 1-16 (2012).

234. Bellone, M., Karachunski, P. I., Ostlie, N., Lei, S. & Conti-Tronconi, B. M. Preferential pairing of T and B cells for production of antibodies without covalent association of T and B epitopes. *Eur J Immunol* 24, 799–804 (1994).

235. Healey, J. F. *et al.* Residues 484-508 Contain a Major Determinant of the Inhibitory Epitope in the A2 Domain of Human Factor VIII. *The Journal of biological chemistry* 270, 14505–14509 (1995).

236. Griffiths, A. E., Wang, W., Hagen, F. K. & Fay, P. J. Use of affinity-directed liquid chromatography-mass spectrometry to map the epitopes of a factor VIII inhibitor antibody fraction. *Journal of Thrombosis and Haemostasis* 9, 1534–1540 (2011).

237. Zhong, D., Saenko, E. L., Shima, M., Felch, M. & Scandella, D. Some Human Inhibitor Antibodies Interfere With Factor VIII Binding to Factor IX. *Blood* 92, 136–142 (1998).

238. Nogami, K. *et al.* Identification of a factor VIII peptide, residues 2315-2330, which neutralizes human factor VIII C2 inhibitor alloantibodies: requirement of Cys2326 and Glu2327 for maximum effect. *British Journal of Haematology* 107, 196–203 (1999).

239. Scandella, D. *et al.* Some Factor VIII Inhibitor Antibodies Recognize a Common Epitope Corresponding to C2 Domain Amino Acids 2248 Through 2312, Which Overlap a Phospholipid-Binding Site. *Blood* 86, 1811–1819 (1995).

240. Wölfel, J. *et al.* CAP-T cell expression system: a novel rapid and versatile human cell expression system for fast and high yield transient protein expression. *BMC proceedings* 5 Suppl 8, 1-2 (2011).

241. Schiedner, G. *et al.* Human Cell Lines for Production of Biopharmaceuticals in *Cells and Culture,* pp. 503–511.

242. D'Amici, G. M., Timperio, A. M., Gevi, F., Grazzini, G. & Zolla, L. Recombinant clotting factor VIII concentrates: Heterogeneity and high-purity evaluation. *Electrophoresis* 31, 2730–2739 (2010).

243. Sandberg, H. *et al.* Functional characteristics of the novel, human-derived recombinant FVIII protein product, human-cl rhFVIII. *Thrombosis Research* 130, 808–817 (2012).

244. Hartholt, R. B. *et al.* To serve and protect: The modulatory role of von Willebrand factor on factor VIII immunogenicity. *Blood Reviews* 31, 339–347 (2017).

245. Kosloski, M. P., Miclea, R. D. & Balu-iyer, S. V. Role of Glycosylation in Conformational Stability, Activity, Macromolecular Interaction and Immunogenicity of Recombinant Human Factor VIII. *AAPS J* 11, 424–431 (2009).

246. Hausl, C. High-dose factor VIII inhibits factor VIII-specific memory B cells in hemophilia A with factor VIII inhibitors. *Blood* 106, 3415–3422 (2005).

247. Bykovskaia, S. N. *et al.* Differentiation of Immunostimulatory Stem-Cell- and Monocyte-Derived Dendritic Cells Involves Maturation of Intracellular Compartments Responsible for Antigen Presentation and Secretion. *Stem Cells* 20, 380–393 (2002).

248. Langenkamp, A. *et al.* T cell priming by dendritic cells: thresholds for proliferation, differentiation and death and intraclonal functional diversification. *European journal of immunology* 32, 2046–2054 (2002).

249. Kotenko, S. V. IFN-λs. *Current Opinion in Immunology* 23, 583–590 (2011).

250. Lazear, H. M., Nice, T. J. & Diamond, M. S. Interferon-λ: Immune Functions at Barrier Surfaces and Beyond. *Immunity* 43, 15–28 (2015).

251. Qian, J., Borovok, M., Bi, L., Kazazian, Haig H. Jr. & Hoyer, L. W. Inhibitor Antibody Development and T Cell Response to Human Factor VIII in Murine Hemophilia A. *Thromb Haemost* 81, 240–244 (1999).

252. Chao, B. N. *et al.* Characterization of a genetically engineered mouse model of hemophilia A with complete deletion of the F8 gene. *Journal of Thrombosis and Haemostasis* 14, 346–355 (2016).

253. Hay, C. R. M. *et al.* Incidence of factor VIII inhibitors throughout life in severe hemophilia A in the United Kingdom. *Blood* 117, 6367–6370 (2011).

List of abbreviations

Abbreviation	Definition
2D-DIGE	Two-dimensional difference gel electrophoresis
2D-GE	Two-dimensional gel electrophoresis
A	Alanine
AC	Affinity chromatography
AEX	Anion exchange chromatography
APC	Allophycocyanin
aPCC	Activated prothrombin complex concentrate
APCs	Antigen-presenting cells
aPTT	Activated partial thromboplastin time
ASGPR	Asialoglycoprotein receptor
BDD	B domain-deleted
BHK	Baby hamster kidney
BRGSF-A2	BALB/c *Rag2*$^{-/-}$ *IL-2R*$\gamma_C^{-/-}$ *SIRP*α^{NOD} *Flk2*$^{-/-}$ *TgHLA-A2*
BRP	Biological reference preparation
BSA	Bovine serum albumin
Ca^{2+}	Divalent calcium ion
$CaCl_2$	Calcium chloride
CAP-T	Cevecs's Amniocyte Production
CD	Cluster of differentiation
CFDA-SE	Carboxyfluorescein diacetate succinimidyl ester
CFSE	Carboxyfluorescein succinimidyl ester
CHAPS	3-[(3-Cholamidopropyl)dimethylammonio]-1-Propanesulfonate
CHO	Chinese hamster ovary
Cl^-	Chloride ion
CLIP	Class II-associated invariant chain peptide
CO_2	Carbon dioxide
cRPMI	Complete RPMI medium
CTLA-4	Cytotoxic T-lymphocyte-associated protein 4
Cu^{2+}	Divalent copper ion
CV	Column volume
Cy	Cyanine
D	Aspartic acid

DC	Dendritic cell
dhfr	Dihydrofolate reductase
DMSO	Dimethyl sulfoxide
DNA	Deoxyribonucleic acid
DOE	Design of experiment
DTT	Dithiotthreitol
E	Glutamic acid
E16	Exon 16
EDTA	Ethylenediaminetetraacetic acid
EF-1α	Elongation factor-1 alpha
ELISA	Enzyme-linked Immunosorbent Assay
ELISpot	Enzyme-linked Immunospot Assay
F	Phenylalanine
$F8^{TKO}$	FVIII total knockout
FBS	Fetal Bovine Serum
FII	Factor II, Prothrombin
FIIa	Activated Factor II, Thrombin
FITC	Fluorescein isothiocyanate
FIX	Factor IX
FIXa	Activated Factor IX
Flk2	Fetal liver kinase-2
Flt3	Fms like tyrosine kinase 3
FPLC	Fast protein liquid chromatography
FSC	Forward scatter
FV	Factor V
FVa	Activated Factor V
FVII	Factor VII
FVIIa	Activated Factor VII
FVIII	Factor VIII
FVIII-19M	Factor VIII containing 19 amino acid exchanges
FVIII-6rs	Factor VIII containing six restriction sites
FVIIIa	Activated Factor VIII
FX	Factor X
FXa	Activated Factor X
FXI	Factor XI
FXIa	Activated Factor XI

FXII	Factor XII
FXIIa	Activated Factor XII
FXIII	Factor XIII
FXIIIa	Activated Factor XIII
G	Glycine
g	Gravitational force
GCSF	Granulocyte colony stimulation factor
GITR	Tumor necrosis factor receptor related protein
GM-CSF	Granulocyte-macrophage colony-stimulating factor
H	Histidine
H_2SO_4	Sulfuric acid
HC	Heavy chain
HEK	Human embryonic kidney
HEPES	4-(2-hydroxyethyl)-1-piperazineethanesulfonic acid
HIS	Human immune system
HLA	Human leukocyte antigen
HRP	Horseradish peroxidase
HSPG	Heparan-sulfate proteoglycans
I	Isoleucine
iDCs	Immature Dendritic cells
IEDB	Immune Epitope Database and Analysis Resource
IEF	Isoelectric focusing
IEX	Ion exchange chromatography
IFN	Interferon
IgG	Immunoglobulin G
IgM	Immunoglobulin M
IL	Interleukin
IL-2Rγ_c	IL-2 receptor gamma chain
IPG	Immobilized pH gradient
IRDye	Infrared dye
iTEM	Individual T cell Epitope Measure
ITI	Immune-tolerance-induction
K	Lysine
KO	Knockout
L	Leucine

LC	Light chain
LDL	Low-density lipoprotein
LDS	Lithium dodecyl sulfate
LPS	Lipopolysaccharides
LRP1	LDL receptor-related protein
M	Methionine
MACS	Magnetic Activated Cell Sorting
mDCs	Mature Dendritic cells
MFI	Mean fluorescence intensity
MHC	Major histocompatibility complex
MIP	Macrophage Inflammatory Protein
MMR	Macrophage mannose receptor
Mn^{2+}	Divalent manganese
MOPS	3-(N-morpholino) propane sulfonic acid
MW	Molecular weight
N	Asparagine
NaCl	Sodium chloride
Neg	Negative
NK	Natural killer
NOD	Non-obese diabetic
ns	Not significant
OVA	Ovalbumin
PAM	Point accepted mutation
PBMCs	Peripheral blood mononuclear cells
PBS	Phosphate-buffered saline
PE	Phycoerythrin
PEG	Polyethylene glycol
PerCP	Peridinin-chlorophyll-protein complex
pFVIII	Plasmatic Factor VIII
PGE_2	Prostaglandin E_2
pH	Potential of hydrogen
pI	Isoelectric point
PLA	Parallel line assay
PMTs	Photomultiplier tubes
Pos	Positive
PTPs	Previously treated patients

PUPs	Previously untreated patients
Q	Glutamine
R	Arginine
Rag2	Recombination activating gene 2
RBC	Red blood cell
rFVIII	Recombinant Factor VIII
ROTEM	Rotation thromboelastometry
S	Serine
SAEx	Strong anion exchange chromatography
SDS	Sodium dodecyl sulfate
SDS-PAGE	Sodium dodecyl sulfate polyacrylamide gel electrophoresis
SEC	Size exclusion chromatography
sgp	Soluble glycoprotein
SIRPα	Signal regulatory protein α
$SIRP\alpha^{NOD}$	Signal regulatory protein α from NOD mice
sR	Soluble receptor
SSC	Sideward scatter
SV40	Simian vacuolating virus 40
T	Threonine
TBSA	Tris-BSA
TCR	T cell receptor
TE	Tris-EDTA
TEM	Thromboelastometry
TF	Tissue factor
TFF	Tangential flow filtration
TGA	Thrombin Generation Assay
Th	T helper cell
TMB	Tetramethylbenzidine
TNF-α	Tumor necrosis factor alpha
TRANCE	TNF-related activation-induced cytokine
UV	Ultraviolet
V	Valine
vWF	Von Willebrand Factor
W	Tryptophan
w/o	without
Y	Tyrosine

List of units

Unit	Definition
%	Percent
°C	Degree Celsius
BU	Bethesda Unit
Da	Dalton
IU	International Unit
kg	Kilogram
L	Liter
M	Molar
m	Meter
m^2	Square meter
min	Minute
rpm	Rounds per minute
U	Unit
V	Volt
Vh	Volt hours

List of figures

List of tables

Acknowledgement

Meinem Doktorvater, Prof. Dr. Harald Kolmar, möchte ich dafür danken, dass ich meine externe Promotion so problemlos und ohne große Hürden durchführen konnte. Auch wenn persönliche Treffen in den letzten vier Jahren selten waren, haben mich die Gespräche jedes Mal ein Stück weitergebracht.

PD Dr. med. Dr. med. habil. Jörg Schüttrumpf möchte ich nicht nur für die Übernahme des Korreferats danken, sondern auch dafür, dass er mir die Möglichkeit gegeben hat bei der Biotest AG meine Doktorarbeit anzufertigen und für seine Betreuung in dieser Zeit.

Prof. Dr. Beatrix Süß und Prof. Dr. Siegfried Neumann danke ich, dass sie meine Prüfer waren.

Ein großer Dank geht an die vielen Leute bei Biotest, die mich in den letzten Jahren unterstützt haben. Allen voran sind dies Steffen Kistner und Jens Daufenbach, mit deren Hilfe in vielen langen Diskussionsrunden immer neue spannende Ideen entstanden sind, die mich immer weiter an mein Ziel geführt haben. Zudem möchte ich auch Matthias Germer, Nicolette Mamant und Tobias Röser danken, die mich bei der Lösung von Problemen unterstützt haben, die eine Promotion in der Industrie so mit sich bringt.

Bedanken möchte ich mich auch beim ganzen Laborteam IAB, die mich innerhalb und außerhalb des Labors immer unterstützt haben, mir die Geheimnisse der Gerinnung verraten haben und für jedes Problem ein offenes Ohr und meistens auch eine Lösung hatten. Mein ganz besonderer Dank gilt hier Katja Böhnlein und Andreas Ernst, die mich von Anfang bis Ende begleitet und unterstützt haben, immer eine helfende Hand hatten und die auch die stressigsten und schwierigsten Situationen mit einem Kaffee und einem Quarkbällchen wieder gerettet haben. Danke für eure Hilfe und Freundschaft!

Ebenfalls danken möchte ich Felix Mikus, dessen Zeit bei Biotest zwar kurz war, der mich aber in dieser Zeit vor allem mit seiner Arbeit, aber auch mit seinen Ideen und seiner positiven Art enorm unterstützt hat.

Special thanks go to EpiVax. Not only for providing the basis for my thesis but also for supporting me throughout the whole time. Thanks Annie De Groot, Eduardo Guillén and William Martin for all the brilliant ideas and the excellent analyses only you could provide.

Meinen Eltern danke ich für die Unterstützung die sie mir schon ein Leben lang geben und ohne die ich nicht so weit gekommen wäre. Ich danke meiner ganzen Familie dafür, dass sie immer für mich da ist und auch für ihr Verständnis, dass ich im vergangenen Jahr kaum ansprechbar war.

Timm, dir danke ich ganz besonders dafür, dass du diese Zeit mit mir zusammen gemeistert hast und dass du vor allem an besonders schlechten Tagen immer ein offenes Ohr hattest. Mir hat besonders dein Abstand zu meinem Fachgebiet immer sehr geholfen und mit nicht ganz ernst gemeinten Fragen wie „Es gibt auch Faktor XI? Warum bist du dann immer noch bei Faktor VIII?“ war die gute Laune auch schnell wiederhergestellt. Danke für deine Unterstützung!

A. Appendix

A.1. Additional figures

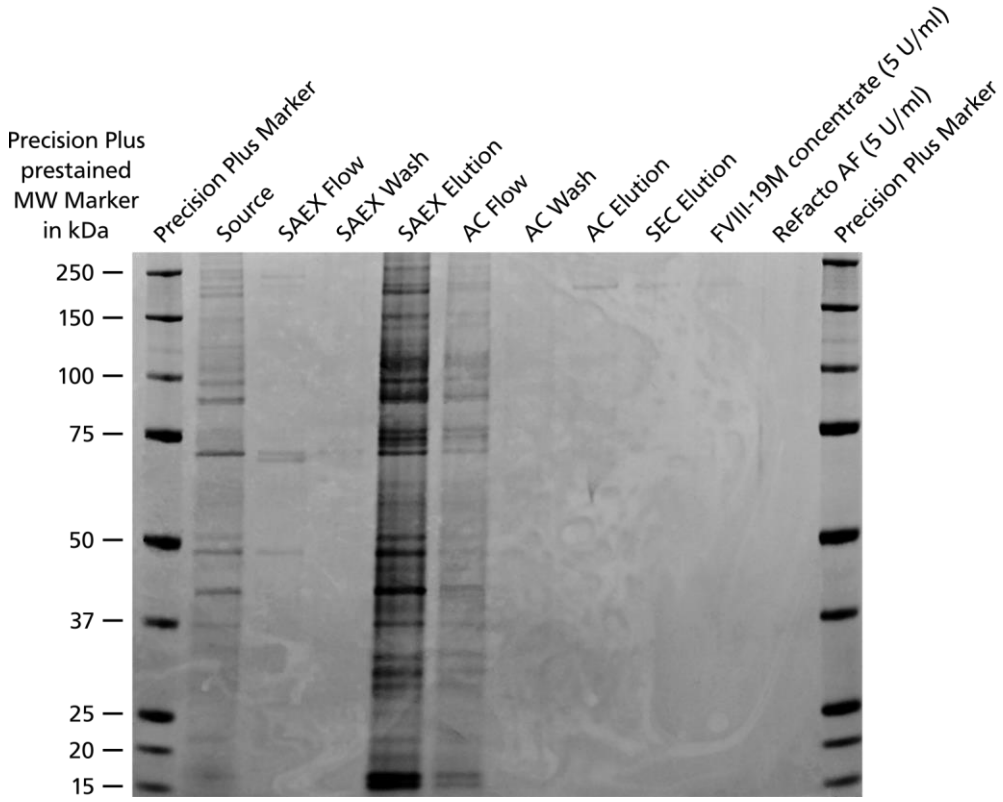

Figure A-1: SDS-PAGE of the second FVIII-19M purification developed with Imperial Protein Stain. The samples from the purification were not pre-diluted, except for the FVIII-19M concentrate and the reference ReFacto AF, which were set to 5 U/ml FVIII.

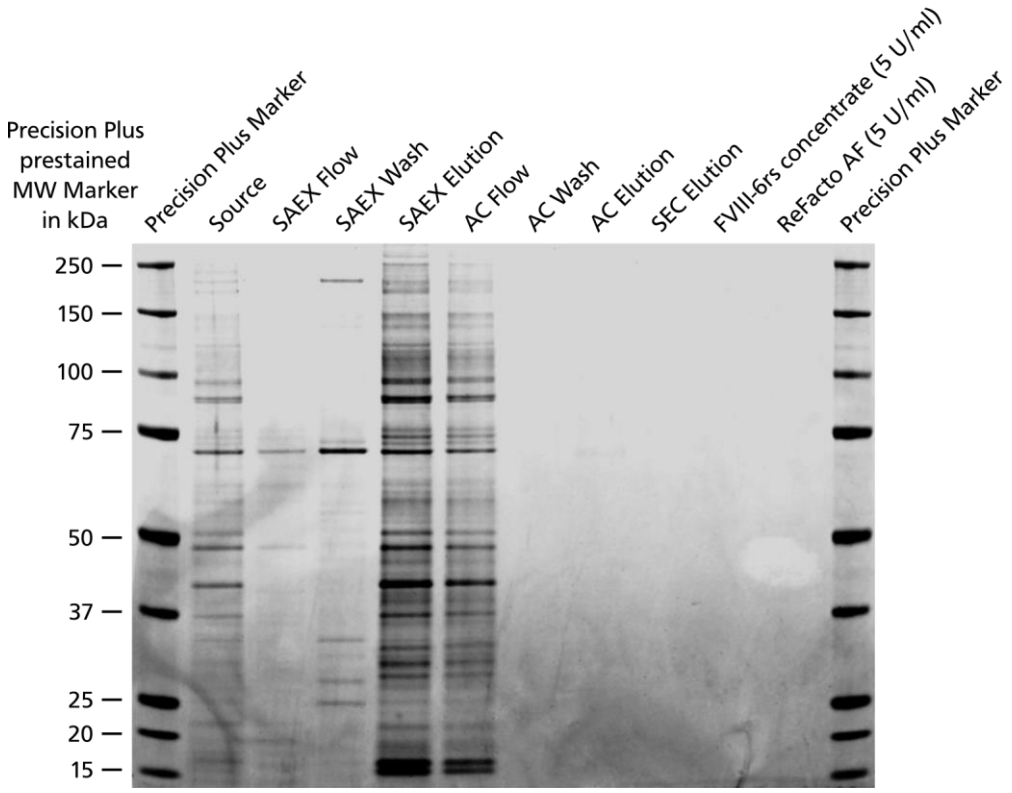

Figure A-2: SDS-PAGE of the second FVIII-6rs purification developed with Imperial Protein Stain. The samples from the purification were not pre-diluted, except for the FVIII-6rs concentrate and the reference ReFacto AF, which were set to 5 U/ml FVIII.

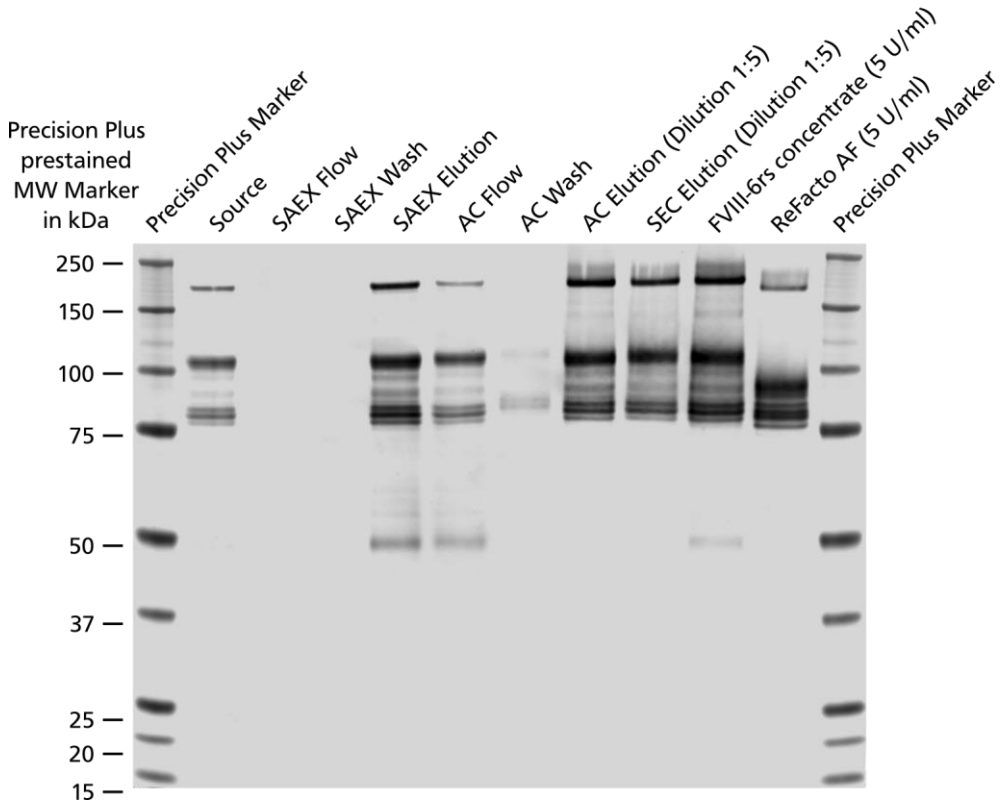

Figure A-3: Western Blot of the second FVIII-19M purification developed with a polyclonal sheep anti-human Factor VIII antibody and a donkey anti-sheep IgG IRDye 900CW. The samples from the purification were not pre-diluted, except for the elutions from the AC and the SEC, which were pre-diluted 1:5, and the FVIII-19M concentrate and the reference ReFacto AF, which were set to 5 U/ml FVIII. The upper band (≈ 200 kDa) represents single-chain FVIII, not processed by furin. The second band (≈ 110 kDa) represents the heavy chain and the following set of bands (≈ 80-90 kDa) are differently glycosylated forms of the light chain. The bands around 50 kDa represent degraded FVIII.

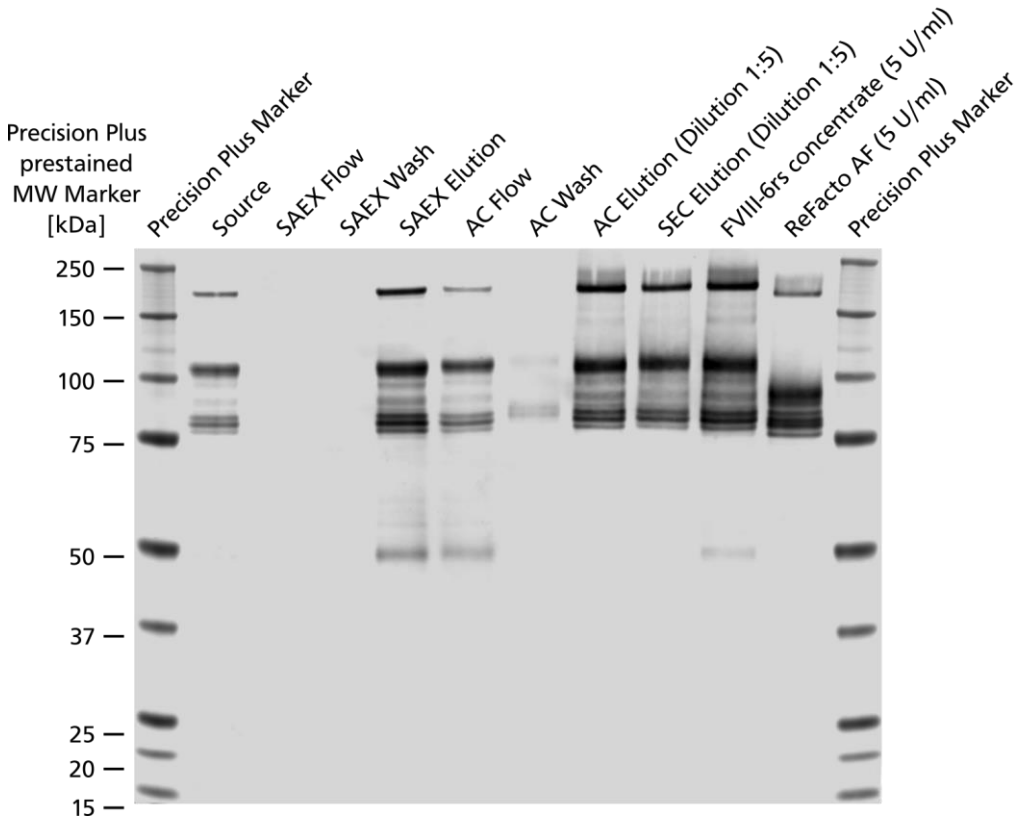

Figure A-4: Western Blot of the second FVIII-6rs purification developed with a polyclonal sheep anti-human Factor VIII antibody and a donkey anti-sheep IgG IRDye 800CW. The samples from the purification were not pre-diluted, except for the elutions from the AC and the SEC, which were pre-diluted 1:5 and the FVIII-6rs and the reference ReFacto AF, which were set to 5 U/ml FVIII. The upper band (≈ 200 kDa) represents single-chain FVIII, not processed by furin. The second band (≈ 110 kDa) represents the heavy chain and the following set of bands (≈ 80-90 kDa) are differently glycosylated forms of the light chain. The bands around 50 kDa represent degraded FVIII.

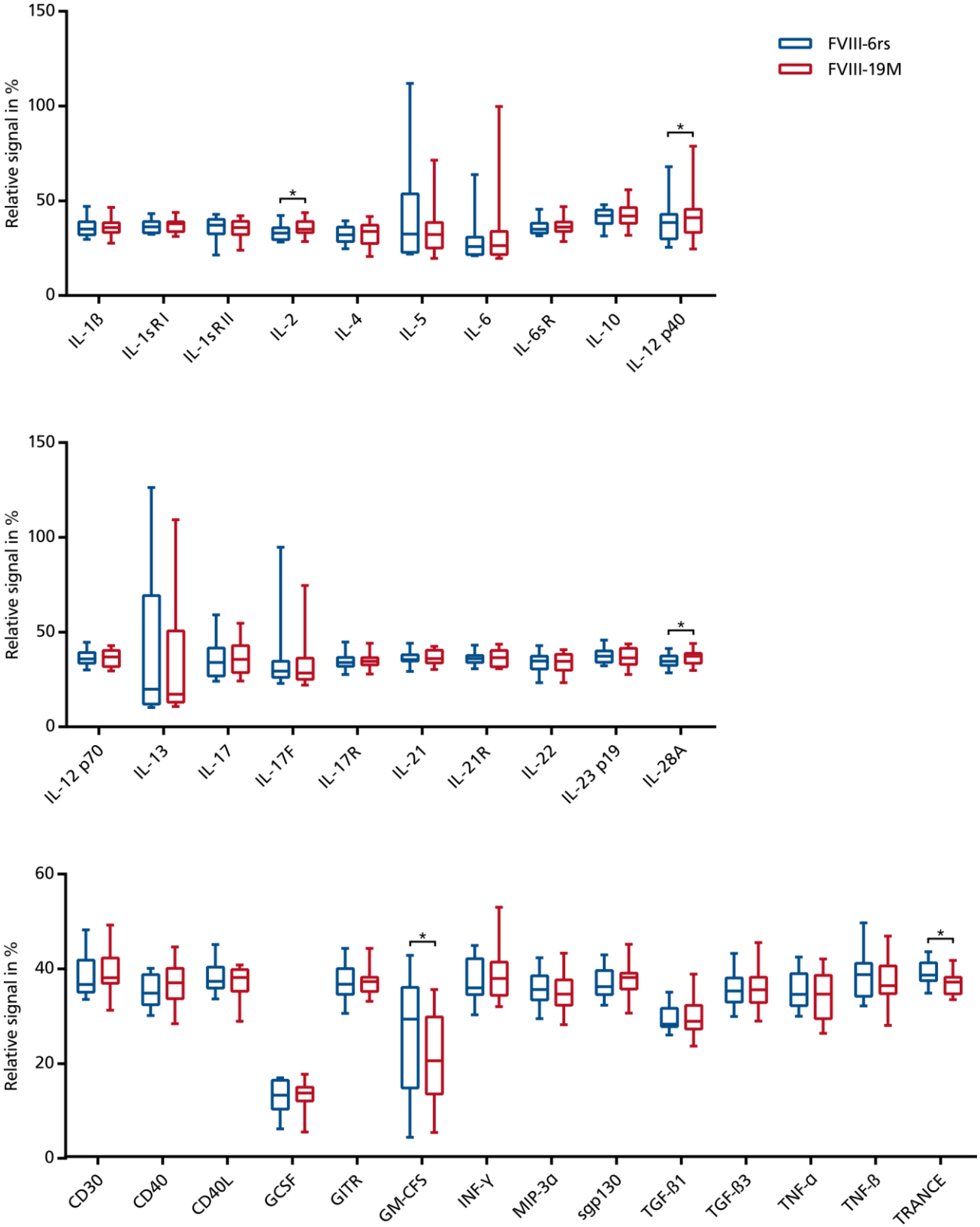

Figure A-5: Results of the cytokine arrays. The boxplots contain the cytokine signal values from all donors, except Donor #4, #13 and #14 for which no cytokine data were available. All cytokine values were calculated in relation to the control, which was a mixture of supernatant of all analyzed co-cultures. The statistical analysis was performed using the Wilcoxon test.

A.2. Additional data and statistical analyses

Table A-1: Statistical analysis of the specific activities of FVIII-19M and FVIII-6rs based on the chromogenic activities. The statistical analysis was performed using the Wilcoxon test with n = 4 per FVIII product.

Comparison	Significance	P value
FVIII-19M vs. FVIII-6rs	Not significant	0.875

Table A-2: Statistical analysis of the specific activities of FVIII-19M and FVIII-6rs based on clotting activities. The statistical analysis was performed using the Wilcoxon test with n = 4 per FVIII product.

Comparison	Significance	P value
FVIII-19M vs. FVIII-6rs	Not significant	0.125

Table A-3: Statistical analysis of the amounts of generated peak thrombin for ReFacto AF, Nuwiq, FVIII-19M and FVIII-6rs. The statistical analysis was performed using the Friedman test with n = 4 per FVIII product.

Comparison	Significance at 0.25 U/ml	Significance at 0.063 U/ml	Significance at 0.016 U/ml
ReFacto AF vs. Nuwiq	Not significant	Not significant	Not significant
ReFacto AF vs. FVIII-19M	*	Not significant	*
ReFacto AF vs. FVIII-6rs	Not significant	Not significant	Not significant
Nuwiq vs. FVIII-19M	Not significant	*	Not significant
Nuwiq vs. FVIII-6rs	Not significant	Not significant	Not significant
FVIII-19M vs. FVIII-6rs	Not significant	Not significant	Not significant

Table A-4: Statistical analysis of the area under the curve values for ReFacto AF, Nuwiq, FVIII-19M and FVIII-6rs. The statistical analysis was performed using the Friedman test with n = 4 per FVIII product.

Comparison	Significance at 0.25 U/ml	Significance at 0.063 U/ml	Significance at 0.016 U/ml
ReFacto AF vs. Nuwiq	Not significant	Not significant	Not significant
ReFacto AF vs. FVIII-19M	*	Not significant	*
ReFacto AF vs. FVIII-6rs	Not significant	Not significant	Not significant
Nuwiq vs. FVIII-19M	Not significant	*	Not significant
Nuwiq vs. FVIII-6rs	Not significant	Not significant	Not significant
FVIII-19M vs. FVIII-6rs	Not significant	Not significant	Not significant

Table A-5: Statistical analysis of the time to peak thrombin generation values for ReFacto AF, Nuwiq, FVIII-19M and FVIII-6rs. The statistical analysis was performed using the Friedman test with n = 4 per FVIII product.

Comparison	Significance at 0.25 U/ml	Significance at 0.063 U/ml	Significance at 0.016 U/ml
ReFacto AF vs. Nuwiq	Not significant	Not significant	Not significant
ReFacto AF vs. FVIII-19M	*	*	Not significant
ReFacto AF vs. FVIII-6rs	Not significant	Not significant	Not significant
Nuwiq vs. FVIII-19M	Not significant	Not significant	Not significant
Nuwiq vs. FVIII-6rs	Not significant	Not significant	Not significant
FVIII-19M vs. FVIII-6rs	Not significant	Not significant	*

Table A-6: Statistical analysis of the potency of ReFacto AF, Nuwiq, FVIII-19M and FVIII-6rs to bind to vWF. The statistical analysis was performed using the Friedman test with n = 4 per FVIII product.

Comparison	Significance
ReFacto AF vs. Nuwiq	Not significant
ReFacto AF vs. FVIII-19M	Not significant
ReFacto AF vs. FVIII-6rs	Not significant
Nuwiq vs. FVIII-19M	*
Nuwiq vs. FVIII-6rs	Not significant
FVIII-19M vs. FVIII-6rs	Not significant

Table A-7: Median of the MFIs of the differently stimulated DCs. The median was calculated from the response of three to five healthy donors per DC-stimulation condition.

DC stimulus	Added protein	Median MFI of HLA-DR expression	Median MFI of CD40 expression	Median MFI of CD80 expression	Median MFI of CD86 expression
No stimulus	No protein	32270	5563	497	3497
	OVA	52206	7170	441	4108
	ReFacto AF	33524	6180	471	3306
LPS	No protein	68797	11960	948	4723
	OVA	86346	13846	839	4022
	ReFacto AF	72388	10321	798	4285
IL-Mix	No protein	82535	12539	891	4896
	OVA	78339	13097	836	4834
	ReFacto AF	89960	11830	794	4708
IL-Mix (w/o IL-8)	No protein	73316	11748	972	4485
	OVA	66576	11172	969	4115
	ReFacto AF	71876	11244	923	4225

Table A-8: Statistical analysis of the MFI of the fluorochrome-coupled antibodies against different surface proteins on DCs. The table presents the statistical results for the MFI of anti-HLA-DR, anti-CD40, anti-CD80 and anti-CD86 antibodies at the different stimulation conditions. The statistical analysis was performed using the Kruskal-Wallis test with n = 3-5 per stimulation condition.

Comparison	Significance
iDCs vs. mDCs + LPS	Not significant
iDCs vs. mDCs + IL-Mix	Not significant
iDCs vs. mDCs + IL-Mix (w/o IL-8)	Not significant
mDCs + LPS vs. mDCs + IL-Mix	Not significant
mDCs + LPS vs. mDCs + IL-Mix (w/o IL-8)	Not significant
mDCs + IL-Mix vs. mDCs + IL-Mix (w/o IL-8)	Not significant
iDCs + OVA vs. mDCs + LPS + OVA	Not significant
iDCs + OVA vs. mDCs + IL-Mix + OVA	Not significant
iDCs + OVA vs. mDCs + IL-Mix (w/o IL-8) + OVA	Not significant
mDCs + LPS + OVA vs. mDCs + IL-Mix + OVA	Not significant
mDCs + LPS + OVA vs. mDCs + IL-Mix (w/o IL-8) + OVA	Not significant
mDCs + IL-Mix + OVA vs. mDCs + IL-Mix (w/o IL-8) + OVA	Not significant
iDCs + ReFacto AF vs. mDCs + LPS + ReFacto AF	Not significant
iDCs + ReFacto AF vs. mDCs + IL-Mix + ReFacto AF	Not significant
iDCs + ReFacto AF vs. mDCs + IL-Mix (w/o IL-8) + ReFacto AF	Not significant
mDCs + LPS + ReFacto AF vs. mDCs + IL-Mix + ReFacto AF	Not significant
mDCs + LPS + ReFacto AF vs. mDCs + IL-Mix (w/o IL-8) + ReFacto AF	Not significant
mDCs + IL-Mix + ReFacto AF vs. mDCs + IL-Mix (w/o IL-8) + ReFacto AF	Not significant
iDCs vs. mDCs + OVA	Not significant
iDCs vs. mDCs + ReFacto AF	Not significant
mDCs + OVA vs. mDCs + ReFacto AF	Not significant
mDCs + LPS vs. mDCs + LPS + OVA	Not significant
mDCs + LPS vs. mDCs + LPS + ReFacto AF	Not significant
mDCS + LPS + OVA vs. mDCs + LPS + ReFacto AF	Not significant
mDCs + IL-Mix vs. mDCs + IL-Mix + OVA	Not significant
mDCs + IL-Mix vs. mDCs + IL-Mix + ReFacto AF	Not significant
mDCS + IL-Mix + OVA vs. mDCs + IL-Mix + ReFacto AF	Not significant
mDCs + IL-Mix (w/o IL-8) vs. mDCs + IL-Mix (w/o IL-8)+ OVA	Not significant
mDCs + IL-Mix (w/o IL-8) vs. mDCs + IL-Mix (w/o IL-8) + ReFacto AF	Not significant
mDCS + IL-Mix (w/o IL-8) + OVA vs. mDCs + IL-Mix (w/o IL-8) + ReFacto AF	Not significant

Table A-9: Statistical analysis of the viability of differently stimulated DCs. The statistical analysis was performed using the Kruskal-Wallis test with n = 3-5 per stimulation condition.

Comparison	Significance
iDCs vs. mDCs + LPS	Not significant
iDCs vs. mDCs + IL-Mix	Not significant
iDCs vs. mDCs + IL-Mix (w/o IL-8)	Not significant
mDCs + LPS vs. mDCs + IL-Mix	Not significant
mDCs + LPS vs. mDCs + IL-Mix (w/o IL-8)	Not significant
mDCs + IL-Mix vs. mDCs + IL-Mix (w/o IL-8)	Not significant
iDCs + OVA vs. mDCs + LPS + OVA	Not significant
iDCs + OVA vs. mDCs + IL-Mix + OVA	Not significant
iDCs + OVA vs. mDCs + IL-Mix (w/o IL-8) + OVA	Not significant
mDCs + LPS + OVA vs. mDCs + IL-Mix + OVA	Not significant
mDCs + LPS + OVA vs. mDCs + IL-Mix (w/o IL-8) + OVA	Not significant
mDCs + IL-Mix + OVA vs. mDCs + IL-Mix (w/o IL-8) + OVA	Not significant
iDCs + ReFacto AF vs. mDCs + LPS + ReFacto AF	Not significant
iDCs + ReFacto AF vs. mDCs + IL-Mix + ReFacto AF	Not significant
iDCs + ReFacto AF vs. mDCs + IL-Mix (w/o IL-8) + ReFacto AF	Not significant
mDCs + LPS + ReFacto AF vs. mDCs + IL-Mix + ReFacto AF	Not significant
mDCs + LPS + ReFacto AF vs. mDCs + IL-Mix (w/o IL-8) + ReFacto AF	Not significant
mDCs + IL-Mix + ReFacto AF vs. mDCs + IL-Mix (w/o IL-8) + ReFacto AF	Not significant
iDCs vs. mDCs + OVA	Not significant
iDCs vs. mDCs + ReFacto AF	Not significant
mDCs + OVA vs. mDCs + ReFacto AF	Not significant
mDCs + LPS vs. mDCs + LPS + OVA	Not significant
mDCs + LPS vs. mDCs + LPS + ReFacto AF	Not significant
mDCs + LPS + OVA vs. mDCs + LPS + ReFacto AF	Not significant
mDCs + IL-Mix vs. mDCs + IL-Mix + OVA	Not significant
mDCs + IL-Mix vs. mDCs + IL-Mix + ReFacto AF	Not significant
mDCs + IL-Mix + OVA vs. mDCs + IL-Mix + ReFacto AF	Not significant
mDCs + IL-Mix (w/o IL-8) vs. mDCs + IL-Mix (w/o IL-8)+ OVA	Not significant
mDCs + IL-Mix (w/o IL-8) vs. mDCs + IL-Mix (w/o IL-8) + ReFacto AF	Not significant
mDCs + IL-Mix (w/o IL-8) + OVA vs. mDCs + IL-Mix (w/o IL-8) + ReFacto AF	Not significant

Table A-10: Statistical analysis of the proliferation of $CD4^+$ T cells, $CD4^+CD25^+$ T cells as well as $CD4^+CD25^-$ T cells in response to differently stimulated DCs. The statistical analysis was performed using the Kruskal-Wallis test with n = 3-6 per DC stimulation condition.

Comparison	Significance
T cells + iDCs vs. T cells + mDCs + LPS	Not significant
T cells + iDCs vs. T cells + mDCs + IL-Mix	Not significant
T cells + iDCs vs. T cells + mDCs + IL-Mix (w/o IL-8)	Not significant
T cells + mDCs + LPS vs. T cells + mDCs + IL-Mix	Not significant
T cells + mDCs + LPS vs. T cells + mDCs + IL-Mix (w/o IL-8)	Not significant
T cells + mDCs + IL-Mix vs. T cells + mDCs + IL-Mix (w/o IL-8)	Not significant
T cells + iDCs + OVA vs. T cells + mDCs + LPS + OVA	Not significant
T cells + iDCs + OVA vs. T cells + mDCs + IL-Mix + OVA	Not significant
T cells + iDCs + OVA vs. T cells + mDCs + IL-Mix (w/o IL-8) + OVA	Not significant
T cells + mDCs + LPS + OVA vs. T cells + mDCs + IL-Mix + OVA	Not significant
T cells + mDCs + LPS + OVA vs. T cells + mDCs + IL-Mix (w/o IL-8) + OVA	Not significant
T cells + mDCs + IL-Mix + OVA vs. T cells + mDCs + IL-Mix (w/o IL-8) + OVA	Not significant
T cells + iDCs + ReFacto AF vs. T cells + mDCs + LPS + ReFacto AF	Not significant
T cells + iDCs + ReFacto AF vs. T cells + mDCs + IL-Mix + ReFacto AF	Not significant
T cells + iDCs + ReFacto AF vs. T cells + mDCs + IL-Mix (w/o IL-8) + ReFacto AF	Not significant
T cells + mDCs + LPS + ReFacto AF vs. T cells + mDCs + IL-Mix + ReFacto AF	Not significant
T cells + mDCs + LPS + ReFacto AF vs. T cells + mDCs + IL-Mix (w/o IL-8) + ReFacto AF	Not significant
T cells + mDCs + IL-Mix + ReFacto AF vs. T cells + mDCs + IL-Mix (w/o IL-8) + ReFacto AF	Not significant
T cells + iDCs vs. T cells + mDCs + OVA	Not significant
T cells + iDCs vs. T cells + mDCs + ReFacto AF	Not significant
T cells + mDCs + OVA vs. T cells + mDCs + ReFacto AF	Not significant
T cells + mDCs + LPS vs. T cells + mDCs + LPS + OVA	Not significant
T cells + mDCs + LPS vs. T cells + mDCs + LPS + ReFacto AF	Not significant
T cells + mDCS + LPS + OVA vs. T cells + mDCs + LPS + ReFacto AF	Not significant
T cells + mDCs + IL-Mix vs. T cells + mDCs + IL-Mix + OVA	Not significant
T cells + mDCs + IL-Mix vs. T cells + mDCs + IL-Mix + ReFacto AF	Not significant
T cells + mDCS + IL-Mix + OVA vs. T cells + mDCs + IL-Mix + ReFacto AF	Not significant
T cells + mDCs + IL-Mix (w/o IL-8) vs. T cells + mDCs + IL-Mix (w/o IL-8)+ OVA	Not significant

T cells + mDCs + IL-Mix (w/o IL-8) vs. T cells + mDCs + IL-Mix (w/o IL-8) + ReFacto AF	Not significant
T cells + mDCs + IL-Mix (w/o IL-8) + OVA vs. T cells + mDCs + IL-Mix (w/o IL-8) + ReFacto AF	Not significant

Table A-11: Amount of proliferating $CD4^+$ T cells for each stimulation after 9 days of co-cultivation. The amount was calculated on all viable $CD4^+$ T cells.

Donor #	**Proliferating $CD4^+$ T cells stimulated with**			
	DCs + IL-Mix	DCs + IL-Mix + FVIII-19M	DCs + IL-Mix + FVIII-6rs	DCs + IL-Mix + ReFacto AF
1	17.6 %	29.0 %	30.5 %	n/a
2	22.4 %	27.5 %	36.1 %	30.7 %
3	41.8 %	54.4 %	52.0 %	54.7 %
4	54.3 %	14.7 %	5.56 %	61.5 %
5	35.5 %	52.9 %	64.8 %	61.2 %
6	11.2 %	5.83 %	18.1 %	12.1 %
7	34.0 %	29.3 %	23.3 %	43.2 %
8	29.8 %	54.8 %	89.5 %	43.9 %
9	70.6 %	69.5 %	84.9 %	n/a
10	69.6 %	22.5 %	78.2 %	77.3 %
11	7.80 %	8.96 %	18.0 %	13.2 %
12	16.6 %	11.4 %	17.3 %	27.1 %
13	17.9 %	3.51 %	27.7 %	18.7 %
14	21.2 %	17.0 %	21.3 %	34.1 %
15	6.48 %	4.76 %	1.22 %	8.08 %
16	2.46 %	3.78 %	6.75 %	3.48 %
17	5.43 %	7.98 %	4.66 %	7.22 %
18	17.5 %	5.38 %	3.55 %	n/a
19	67.3 %	48.4 %	38.5 %	n/a
20	19.3 %	11.0 %	15.5 %	13.3 %
21	17.9 %	4.40 %	6.40 %	9.84 %
22	15.1 %	11.8 %	14.5 %	n/a
23	6.87 %	5.05 %	4.24 %	6.12 %

Table A-12: Amount of viable CD4⁺ T cells for each stimulation after 9 days of co-cultivation. The amount was calculated on all detected events.

Donor #	Viable CD4⁺ T cells stimulated with			
	DCs + IL-Mix	DCs + IL-Mix + FVIII-19M	DCs + IL-Mix + FVIII-6rs	DCs + IL-Mix + ReFacto AF
1	65.2 %	61.2 %	64.7 %	n/a
2	61.5 %	52.7 %	40.4 %	63.4 %
3	61.6 %	62.4 %	50.7 %	59.6 %
4	25.9 %	8.34 %	0.72 %	21.6 %
5	21.2 %	12.8 %	2.64 %	19.4 %
6	26.4 %	24.7 %	1.38 %	26.7 %
7	40.9 %	36.0 %	33.9 %	42.8 %
8	28.1 %	34.3 %	59.2 %	25.9 %
9	48.4 %	50.4 %	44.2 %	n/a
10	42.4 %	21.5 %	34.6 %	43.7 %
11	59.6 %	55.7 %	30.6 %	57.2 %
12	38.8 %	23.0 %	18.2 %	40.5 %
13	44.6 %	29.4 %	1.92 %	42.8 %
14	25.2 %	20.2 %	1.92 %	42.8 %
15	62.0 %	49.6 %	12.3 %	50.9 %
16	37.0 %	23.3 %	5.93 %	37.4 %
17	16.4 %	14.4 %	6.87 %	16.5 %
18	13.9 %	6.51 %	5.91 %	n/a
19	36.0 %	28.7 %	11.9 %	n/a
20	44.0 %	41.2 %	21.6 %	41.3 %
21	12.5 %	4.32 %	1.25 %	3.76 %
22	n/a	8.32 %	7.86 %	n/a
23	16.4 %	11.7 %	6.61 %	12.9 %

Table A-13: Statistical analysis of the difference in proliferation of CD4⁺ T cells to FVIII-19M and FVIII-6rs. Either 17 or 11 healthy donors were analyzed. The statistical analysis was performed using the Wilcoxon test.

Comparison	Group size	Significance	P value
T cells + DCs + IL-Mix + FVIII-6rs vs. T cells + DCs + IL-Mix + FVIII-19M	17	*	0.0267
T cells + DCs + IL-Mix + FVIII-6rs vs. T cells + DCs + IL-Mix + FVIII-19M	10	*	0.0371

Table A-14: Statistical analysis of the difference in secreted cytokines in co-cultures with DCs stimulated with FVIII-19M and FVIII-6rs. All cytokine values were calculated in relation to the control, which was a mixture of supernatant of all analyzed co-cultures. No cytokine data were available for Donor #4, #13 and #14. The statistical analysis was performed using the Wilcoxon test.

Cytokine	Median relative cytokine signal in % of co-culture with FVIII-6rs stimulated DCs	Median relative cytokine signal in % of co-culture with FVIII-19M stimulated DCs	Significance	P value
IL-1β	35.1	35.9	Not significant	0.5830
IL-1sRI	36.3	37.9	Not significant	> 0.9999
IL-1sRII	37.2	35.8	Not significant	0.2166
IL-2	33.0	35.0	*	0.0134
IL-4	32.1	33.8	Not significant	> 0.9999
IL-5	32.5	32.2	Not significant	0.5830
IL-6	25.9	26.3	Not significant	0.3575
IL-6sR	35.0	36.2	Not significant	0.9032
IL-10	42.2	42.0	Not significant	0.6698
IL-12 p40	38.6	41.1	*	0.0419
IL-12 p70	35.8	36.9	Not significant	0.9515
IL-13	19.9	17.2	Not significant	0.8077
IL-17	34.0	35.7	Not significant	0.1937
IL-17F	29.4	28.4	Not significant	0.8552
IL-17R	33.9	34.6	Not significant	0.5830
IL-21	35.5	36.0	Not significant	0.7148
IL-21R	36.0	36.5	Not significant	0.5416
IL-22	34.8	34.6	Not significant	0.9032
IL-23 p19	37.2	36.4	Not significant	0.7148
IL-28A	34.6	37.3	*	0.0353
CD30	36.4	37.8	Not significant	0.4631
CD40	34.5	36.7	Not significant	0.1040
CD40L	37.0	37.8	Not significant	0.2676
GCSF	13.0	13.5	Not significant	0.6698
GITR	36.4	36.9	Not significant	0.6698
GM-CSF	29.0	20.3	*	0.0494
IFN-γ	35.7	37.6	Not significant	0.1040
MIP-3α	35.3	34.3	Not significant	0.7609
sgp130	35.9	37.8	Not significant	0.9515
TGF-β1	28.0	28.6	Not significant	0.8077

TGF-β3	35.0	35.2	Not significant	0.5416
TNF-α	34.3	34.3	Not significant	0.1937
TNF-β	38.5	36.1	Not significant	0.4631
TRANCE	38.3	36.8	*	0.0107

Table A-15: Statistical analysis of the antibody titers of E16 FVIII KO mice immunized with different FVIII products or FVIII Formulation Buffer. Either eight or ten mice were analyzed per stimulus. The statistical analysis was performed using the Kruskal-Wallis test.

Comparison	Significance
PBS vs. ReFacto AF	Not significant
PBS vs. FVIII-6rs	Not significant
PBS vs. FVIII-19M	Not significant
ReFacto AF vs. FVIII-6rs	Not significant
ReFacto AF vs. FVIII-19M	Not significant
FVIII-6rs vs. FVIII-19M	Not significant

Table A-16: Statistical analysis of the difference in proliferation of $CD4^+$ T cells of E16 FVIII KO mice upon restimulation with FVIII or PBS. Either eight or ten mice were analyzed per stimulus. The statistical analysis was performed using the Wilcoxon test.

Mice immunized with	Comparison restimulation	Significance	P value
FVIII Formulation Buffer	T cells + PBS vs. T cells + ReFacto AF	Not significant	0.8438
ReFacto AF	T cells + PBS vs. T cells + ReFacto AF	*	0.0371
FVIII-6rs	T cells + PBS vs. T cells + FVIII-6rs	*	0.0195
FVIII-19M	T cells + PBS vs. T cells + FVIII-19M	Not significant	0.3828

Table A-17: Statistical analysis of the difference in proliferation of $CD4^+$ T cells of BRGSF mice upon restimulation with FVIII or medium. Three to five mice were analyzed per stimulus. The statistical analysis was performed using the Wilcoxon test.

Mice immunized with	Comparison restimulation	Significance	P value
ReFacto AF	T cells + Medium vs. T cells + ReFacto AF	Not significant	0.625
FVIII-6rs	T cells + Medium vs. T cells + FVIII-6rs	Not significant	0.125
FVIII-19M	T cells + Medium vs. T cells + FVIII-19M	Not significant	0.25